No. FHWA-RD-77-28

AMENTAL STUDIES IN THE LONGITUDINAL CONTROL OF AUTOMATED GROUND VEHICLES

December 1976
Final Report

Document is available to the public through
the National Technical Information Service,
Springfield, Virginia 22161

Prepared for
FEDERAL HIGHWAY ADMINISTRATION
Offices of Research & Development
Washington, D. C. 20590

NOTICE

This document is disseminated under the sponsorship of the Department of Transportation in the interest of information exchange. The United States Government assumes no liability for its contents or use thereof.

The contents of this report reflect the views of the contracting organization, which is responsible for the facts and the accuracy of the data presented herein. The contents do not necessarily reflect the official views or policy of the Department of Transportation. This report does not constitute a standard, specification, or regulation.

The United States Government does not endorse products or manufacturers. Trade or manufacturers' names appear herein only because they are considered essential to the object of this document.

Technical Report Documentation Page

1. Report No.	2. Government Accession No.	3. Recipient's Catalog No.
FHWA-RD-77-28		

4. Title and Subtitle	5. Report Date
Fundamental Studies in the Longitudinal Control of Automated Ground Vehicles	December 1976
	6. Performing Organization Code: RF 4302
7. Author(s): R.E. Fenton, K.W. Olson, R.J. Mayhan, G.M. Takasaki	8. Performing Organization Report No.: RF 4302 A1-1
9. Performing Organization Name and Address: Transportation Control Laboratory, Department of Electrical Engineering, The Ohio State University, Columbus, Ohio 43210	10. Work Unit No. (TRAIS)
	11. Contract or Grant No.: DOT-FH-11-8874
12. Sponsoring Agency Name and Address: Office of Research and Development, Federal Highway Administration, Department of Transportation, Washington, D.C. 20590	13. Type of Report and Period Covered: Final Report, Aug. 1975 - Dec. 1976
	14. Sponsoring Agency Code

15. Supplementary Notes

FHWA Contract Manager: Fred Okano (HRS-32)

16. Abstract

Four essential aspects of the longitudinal control of vehicles in an automated, individual-vehicle system are considered here: a) Sector-level control; b) Communications between each controlled vehicle and the sector computer; c) The development of techniques for obtaining extremely accurate estimates of a vehicle's state; and d) The control of each individual vehicle. The emphasis was on the design, development and testing of hardware subsystems essential for implementing these facets in the context of high-speed (to 93 ft/sec or 28 m/s), small time-headway (1-2 sec) operation.

The accomplishments over the second year of a two-year study include: a) The development and field evaluation of techniques for obtaining accurate estimates of vehicle position and instantaneous speed -- ± .05 ft in 10 ft (± .015m in 3.05m) and ± 0.7 ft/sec (± 0.21 m/s), respectively for one of the three approaches evaluated; b) The development of validated models for both the propulsion and braking dynamics of a typical U.S. sedan; c) The design and field testing of a vehicle controller which provided good tracking and a comfortable ride; and d) The specification of both minimal and realistic requirements for sector-level communications.

17. Key Words	18. Distribution Statement
Automatic highway, dual-mode, automatic longitudinal control, information source, sector communications, sector computer.	This document is available to the public through the National Technical Information Service, Springfield, Virginia, 22161

19. Security Classif. (of this report)	20. Security Classif. (of this page)	21. No. of Pages	22. Price
Unclassified	Unclassified	192	

FUNDAMENTAL STUDIES IN THE LONGITUDINAL CONTROL OF AUTOMATED GROUND VEHICLES

EXECUTIVE SUMMARY

The achievement of safe and efficient longitudinal control is probably the most significant technical problem associated with individual automated-vehicle, transport systems such as the automatic highway and automated guideway transit.

One general control structure would involve a central controller to oversee network operations with this including the coordination of sector-level computers--each of which would supervise and control the vehicles operating in its assigned sector. Four essential facets of operations at this sector level are:

a) The specification and/or generation of vehicle command states;

b) Communications between sector control and each controlled vehicle;

c) The determination of the state of each vehicle; and

d) The control of each individual vehicle.

The research reported here was performed during the second year of a two-year study, and it deals with the design, development and testing of hardware systems essential for implementing these facets in the context of high-speed (to 93 ft/sec), small time-headway (1-2 sec) operation.

Within this framework, the principal accomplishments over the second year of this study include:

a) The development and field evaluation of a technique, which involves the use of laterally positioned, current-carrying wires embedded in the roadway, for measuring vehicle position to within ±0.06 ft over the speed range 0-100 ft/sec;

b) The development and laboratory testing of an approach employing audio frequencies and helically wound transmission lines for providing continuous absolute position information, within an accuracy of ±0.17 ft, to a string of moving vehicles;

c) The use of a vehicle-borne radar and scattering enhancement plates embedded under the roadway surface to provide both an accurate position signal (e.g., a maximum position error of .05 ft in a 10 ft-distance), and an estimate of instantaneous velocity which is within ±.5 ft/sec of the true value under all expected operating conditions over the speed range 0-100 ft/sec;

d) The specification of both the propulsion- and braking dynamics of a "typical" U.S. passenger sedan, and a corresponding design of a vehicle controller for nonemergency operations; and

e) The demonstration of controller performance on a roadway where position information was obtained from embedded current-carrying conductors and a vehicle-borne interpolator (This demonstration was successful in that a comfortable ride ($|J| < 1.6$ ft/sec^3), an insensitivity to adverse environmental effects, and fairly good position control (±2 ft tracking errors) were achieved).

Secondary accomplishments include:

a) The specification of three general approaches to sector-level control, and the selection of one for further detailed study;

b) The specification of both the minimal information transmission requirements for a sector computer-to-vehicle link, and the greatly increased requirements when safety factors are given a paramont importance; and

c) The specification of the accuracies to be expected, in measuring both position and instantaneous velocity, with a fifth wheel.

Future efforts will be focused on the development of a 4-mile sector wherein vehicles would be controlled via a sector computer located at roadside.

TABLE OF CONTENTS

Chapter (Cont.)

Appendices (Cont.)

LIST OF FIGURES

Figures (Cont.)

Figure

Figures (Cont.)

Figure

Figures (Cont.)

Figure

Figures (Cont.)

Figure

LIST OF TABLES

METRIC CONVERSION FACTORS

Approximate Conversions to Metric Measures

Symbol	When You Know	Multiply by	To Find	Symbol
	LENGTH			
in	inches	*2.5	centimeters	cm
ft	feet	30	centimeters	cm
yd	yerds	0.9	meters	m
mi	miles	1.6	kilometers	km
	AREA			
in^2	square inches	6.5	square centimeters	cm^2
ft^2	square feet	0.09	square meters	m^2
yd^2	square yards	0.8	square meters	m^2
mi^2	square miles	2.6	squere kilometers	km^2
	ecres	0.4	hectares	ha
	MASS (weight)			
oz	ounces	28	grams	g
lb	pounds	0.45	kilograms	kg
	short tons (2000 lb)	0.9	tonnes	t
	VOLUME			
tsp	teespoons	5	milliliters	ml
Tbsp	tablespoons	15	milliliters	ml
fl oz	fluid ounces	30	milliliters	ml
c	cups	0.24	liters	l
pt	pints	0.47	liters	l
qt	querts	0.95	liters	l
gal	gallons	3.8	liters	l
ft^3	cubic feet	0.03	cubic meters	m^3
yd^3	cubic yards	0.76	cubic meters	m^3
	TEMPERATURE (exact)			
°F	Fahrenheit tempereture	5/9 (after subtracting 32)	Celsius temperature	°C

*1 in = 2.54 (exactly). For other exact conversions and more detailed tables, see NBS Misc. Publ. 286, Units of Weights and Measures, Price $2.25, SD Catalog No. C13.10:286.

Approximate Conversions from Metric Measures

Symbol	When You Know	Multiply by	To Find	Symbol
	LENGTH			
mm	millimeters	0.04	inches	in
cm	centimeters	0.4	inches	in
m	meters	3.3	feet	ft
m	meters	1.1	yards	yd
km	kilometers	0.6	miles	mi
	AREA			
cm^2	squere centimeters	0.16	square inches	in^2
m^2	square meters	1.2	square yards	yd^2
km^2	square kilometers	0.4	square miles	mi^2
ha	hectares (10,000 m^2)	2.5	acres	
	MASS (weight)			
g	grams	0.035	ounces	oz
kg	kilograms	2.2	pounds	lb
t	tonnes (1000 kg)	1.1	short tons	
	VOLUME			
ml	milliliters	0.03	fluid ounces	fl oz
l	liters	2.1	pints	pt
l	liters	1.06	quarts	qt
l	liters	0.26	gallons	gal
m^3	cubic meters	35	cubic feet	ft^3
m^3	cubic meters	1.3	cubic yards	yd^3
	TEMPERATURE (exact)			
°C	Celsius temperature	9/5 (then add 32)	Fahrenheit temperature	°F

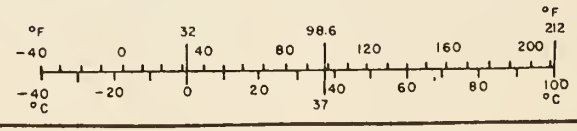

CHAPTER I

INTRODUCTION

A. Introduction

An examination of traffic conditions today--congested roadways, vehicle-related noise and pollution, a large number of accidents and fatalities, and poor service to large numbers of our population--indicates the need for improvement in our transportation system. Unfortunately, these conditions will be worse in the next few decades for it is widely predicted that both the number of vehicles and the miles traveled per vehicle will greatly increase. If one would look further ahead to the turn of the century, he would see vast sprawling supercities, with populations characterized by adequate incomes, longer life spans, and increased amounts of leisure time. One predictable result is greatly increased travel. The resulting traffic situation could be chaotic, unless some dramatic improvements are instituted beforehand.

The solution to both the current and the anticipated future problems will be a combination of many approaches including perhaps the following: improved high-speed rail systems; VTOL aircraft for short-distance trips; new and innovative mass transit systems; and the automation of various facets of individual ground transport. Here, the focus will be on the latter, wherein the suggested systems have generally fallen into three categories:

1) Captive vehicle systems for use in restricted geographical areas;
2) Dual-mode systems for general coverage of urban areas; and
3) Dual-mode systems for intercity automated highways.

The potential advantages associated with each category are well known and will only be briefly summarized here. The first offers transportation to all citizens in a limited area--such as a downtown business district--and the partial or complete elimination of privately owned vehicles from that area with an attendant reduction in noise, air pollution, and congestion. The feasibility of this type of system is currently being evaluated via the operational captive-vehicle network at Morgantown, West Virginia.[1]

The general class of dual-mode systems offers the prospects of high flow capacities, enhanced vehicle safety, door-to-door movement in either a public conveyance, such as dial-a-bus, or in a privately owned vehicle, and extended mobility to the poor, the aged, and the infirm. The U.S. Department of Transportation had planned to develop a prototype dual-mode system by the early 1980's;[2] however, these plans are currently inactive.

The initial studies on the automated highway were initiated in the late 1950's by General Motors Corporation,[3] and subsequently much effort was expended, both here and abroad, by various industrial organizations, government laboratories, and academic institutions.[4-13] One ongoing effort is a cost-benefit analysis of various automated highway concepts by CALSPAN Corporation under the sponsorship of the Federal Highway Administration.[14]

An automated highway system would probably be first considered for an already congested network (e.g., the Northeast Corridor) because of its prospects for substantially increasing both flow capacity and highway safety.

B. Dual-Mode System Concept

The general dual-mode concept involves a roadway complex which consists of both automated and nonautomated roads. Various main arteries would probably be equipped for automation while various secondary streets/roads would not be

equipped. Ultimately, it would be expected that public vehicles and both individual private vehicles and commercial traffic would use the system; however, it seems likely that initially only mass transit vehicles would be employed.

An individual vehicle would enter the system at a special entrance point where it would first undergo a rapid automatic checkout, and the driver would indicate his destination. If it "passed" the checkout, the vehicle would move to an entrance ramp from which it would be automatically merged into the traffic stream. However, if it "failed" the vehicle would not be allowed to merge into the traffic stream; instead, it would be rejected and guided to a nearby service facility for repair.

The traffic stream velocity would be fixed by a central traffic controller and would be dependent on weather, roadway conditions, the state of the traffic stream, etc. Once in the traffic stream, the vehicle would remain under automatic control until the driver's preselected exit were reached. Then the vehicle would be guided off the roadway onto an exit ramp, and control would be returned to the driver.

In the event of vehicle disability, the vehicle would be ejected from the main traffic stream. If it were controllable, it would be routed to the nearest emergency exit. If it were not, the use of one lane would be lost until the vehicle could be moved off the roadway. Hence, it would be temporarily necessary to direct the mainstream vehicles around the disabled one. Clearly, some provision must be made for clearing the roadway as quickly as possible.

C. Dual-Mode Control Hierarchy

The control required for the automated part of a dual-mode system is comprised of two intimately related facets. The first, macro-control, embodies the entire hierarchy of control which is necessary for system coordination. This is, of course, the "systems" level of control, and it includes such

operations as vehicle scheduling and routing, the determination and specification of traffic speeds, and system response to abnormal and emergency situations. The second facet, micro-control, is explicitly concerned with individual vehicle position regulation and maneuvering and encompasses both vehicle lateral control and longitudinal control.

One general control hierarchy is shown in Fig. 1, where a central computer is shown as overseeing network operations. This task includes the coordination of individual sector computers--one of which is assigned to supervise and control the vehicles operating in each network sector. Depending upon the size and complexity of a network, it might be desirable to have an additional level(s) of control in this hierarchy (i.e., a central computer to oversee network operations and to coordinate individual regional computers--each of which would, in turn, supervise several sector-level computers).

Note from Fig. 2 that a sector-level, control configuration would be comprised of four basic elements;

i) A sector computer;

ii) A communication link for achieving both computer-to-vehicle and vehicle-to-computer transmissions;

iii) An information source for directly providing the computer with state information on each vehicle;

iv) An information source embedded in, or located nearby, the guideway and intended to supply state information to each controlled vehicle.

With this general configuration, the sector computer would have two independent indications of the state of each vehicle--one from the guideway-to-sector computer information source and one transmitted from the vehicle.

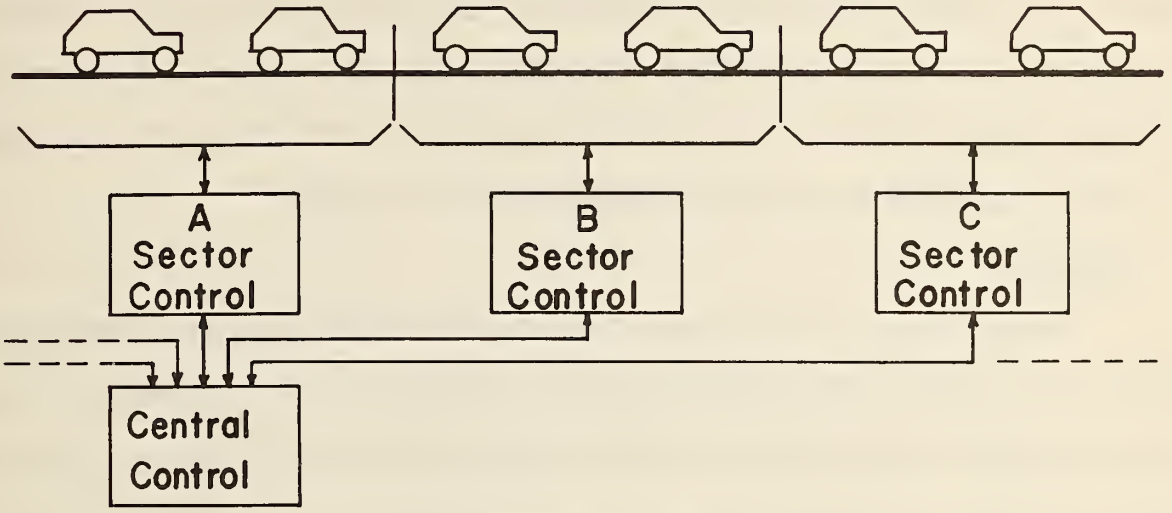

Fig. 1 One network control configuration.

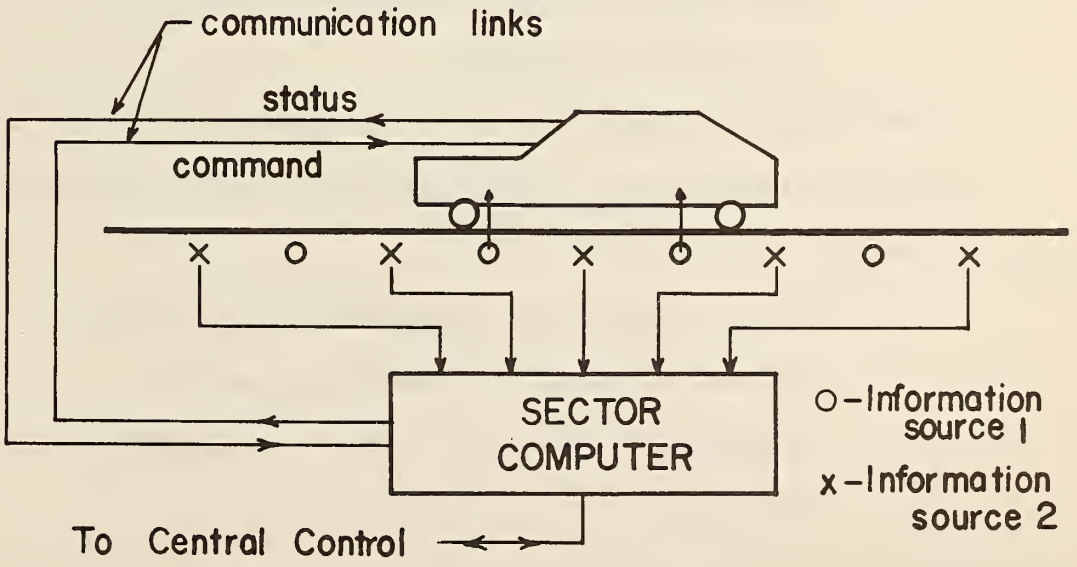

Fig. 2 The basic elements of a sector-level control configuration.

This would provide desired redundancy. Further, if the information received were of sufficient accuracy and timeliness, the system could be designed for a quick response to an anomalous situation. It may be noted that the configuration of Fig. 2 could be employed in conjunction with either a synchronous, an asynchronous, or a quasi-synchronous control strategy.

D. Overview

During the past two years, the Ohio State University has investigated various facets of sector-level longitudinal control with an emphasis on high-speed (up to 88 ft/sec) operation at time headways as small as 1 sec.* During the first year, the principal focus was directed toward:

i) A laboratory study of practically implementable information source configurations; and

ii) The identification of vehicle longitudinal dynamics, the design of a vehicle controller based on those dynamics, and a field-test evaluation of the designed controller.

A detailed description of these efforts is contained in Reference 16.

During the second year of this investigation, the primary focus was on the following:

i) Field and laboratory evaluations of 3 selected information source configurations, and the implementation of two of these in a field-test facility;

---

* In a previous study, a reference system/vehicle-controller combination for automatic lateral control was designed and tested under full-scale conditions. This effort was quite successful and demonstrated that excellent automatic lateral control could be achieved.[15]

ii) The identification of a vehicle's braking dynamics, the development of a refined model of vehicle propulsion system/roadway-interface dynamics, and the design of a vehicle controller for use with one developed information source configuration; and

iii) Full-scale testing and evaluation of an information source/vehicle-controller combination.

A secondary focus was an overview of:

i) Sector-computer operations; and

ii) Sector computer-to-controlled vehicle communications.

A fairly intensive survey of the accomplishments during this year are contained in the following chapters, and various detailed findings are included in the attached appendices.

CHAPTER II

ON SECTOR COMPUTER OPERATIONS

A. Introduction

As a first step toward specifying the requirements of a sector-level computer, three general approaches to sector-level computer operations are examined. In this analysis, it is assumed that the trajectory of each vehicle in a sector is specified by a higher-level control (e.g., a regional controller) and communicated to the sector computer. Subsequently, the latter would provide each controlled vehicle with appropriate longitudinal reference information (e.g., its desired position and desired speed versus time).*

The approaches considered are defined as follows:

Approach #1. All permitted trajectories (position ($X_c(t)$) and speed ($V_c(t)$) would be stored in memory at sector level, and these would be recalled from memory as required and transmitted to each controlled vehicle.

Approach #2. All allowed acceleration (A_c) trajectories would be stored in memory. When a specified position/velocity trajectory were required, the corresponding A_c trajectory would be recalled from memory and processed at the sector level to provide the required V_c and X_c information. The latter would be transmitted to a controlled vehicle.

---

* In a subsequent study, it may be desirable to consider the case where each vehicle's trajectory is specified at the sector level. This would result in a requirement for more computer processing capability at the sector level than is specified here.

Approach #3. All permitted A_c trajectories would be stored onboard each vehicle, and the required processing to obtain V_c and X_c would be accomplished onboard.

This listing is not intended to be all-inclusive and other approaches, which are possibly more suitable, can readily be defined.

B. Sector Configuration

In this preliminary analysis, there was no convincing reason for selecting a sector composed of complex geometrics--especially since reasonable estimates of various parameters could be obtained from a relatively simple configuration.

The selected geometrics are shown in Fig. 3. These consist of a single, mainline lane of one-way traffic and a merging lane from which vehicles can merge onto the mainline. For reasons of convenience, it will be assumed that the sector shown in Fig. 3 is characterized by the parameters listed in Table I. These are probably typical of what might be expected in practice and, at the very least, correspond to those tentatively selected for a planned OSU facility at East Liberty, Ohio.

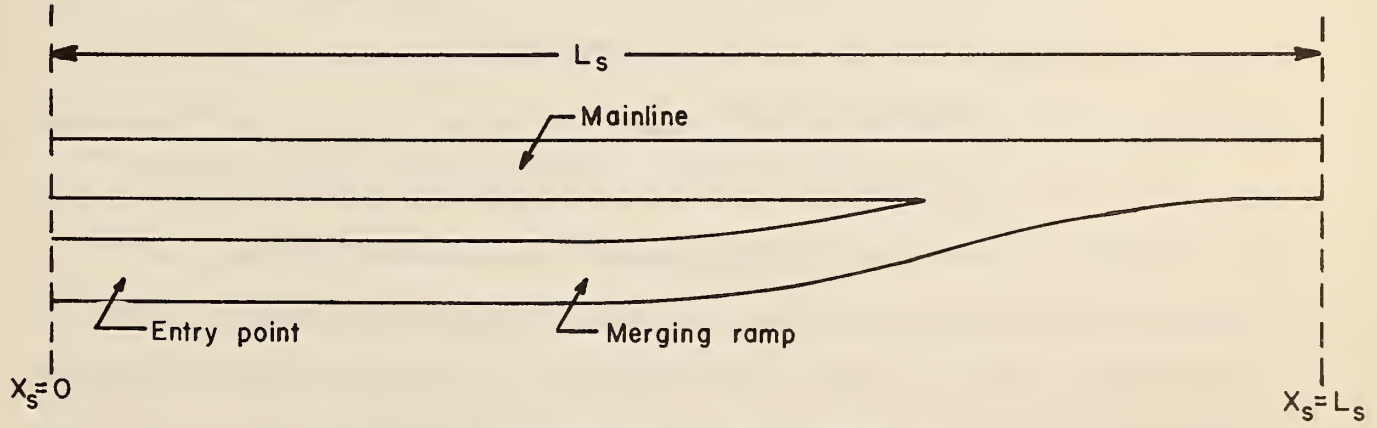

Fig. 3 A simple sector configuration.

The symbol X_s is used to represent a longitudinal position within a sector. Thus, as shown in Fig. 3, $X_s = 0$ corresponds to the beginning of a sector and $X_s = L_s$ to the end.

TABLE I

BASIC PARAMETERS

Quantity	Symbol	Value
Sector Length	L_s	3280 ft
Communication Interval	T_c	100 m sec
Maximum Speed	V_{max}	93 ft/sec
Maneuvering Acceleration	a_o	3.22 ft/sec^2
Design Time Headway	H_t	1 sec
Position Quantization	ΔX	0.05 ft

C. Required Command Trajectories

It presently appears as if trajectories for the following would be necessary:

i) Constant-speed operation.

ii) Mainline maneuvering (moveup-moveback).

iii) Mainline speed changes.

iv) System entry (merging operations).

v) Emergency braking.

vi) System startup (after a shutdown of mainline traffic).

The parameters associated with each operation are listed in Table II. For example, constant-speed operation would be at one of four speeds--30, 45, 60, or 88 ft/sec. These, and the other selections specified in this table, are believed to be typical of what would be required in practice.

The command sent to a vehicle, for example Vehicle i, is represented via the following notation:

$X_{Ci}(KT)$ = The command position of Vehicle i at t = KT.

$V_{ci}(KT)$ = The command speed of Vehicle i at t = KT.

$A_{ci}(KT)$ = The command acceleration of Vehicle i at t = KT.

The state of that vehicle is represented by

$X_i(KT)$ = The position of Vehicle i at t = KT.

$V_i(KT)$ = The speed of Vehicle i at t = KT.

$A_i(KT)$ = The acceleration of Vehicle i at t = KT.

D. Approach 1

a) Computer Architecture

Consider the computer architecture shown in Fig. 4. It is comprised of the following primary parts:

i) A central processing unit (CPU);

ii) Address registers;

iii) Multiplexing (MUX) units;

iv) A permanent memory (ROM); and

v) Output devices.

There would be two general inputs to the CPU--one comprising the command information for each vehicle in the sector, and the second, status information from both each vehicle and Information Source 2. The former would be employed to select an addressing sequence for each vehicle which would be used to obtain, via a multiplexer, the corresponding $V_c(t)$ and $X_c(t)$ from the permanent memory.* Note that this information would be sent to two locations--to the appropriate controlled vehicle via a communication link and back to the CPU for checking purposes.

---

* The sequence for a given vehicle would be changed if it were subsequently necessary to modify the specified operation.

TABLE II

PERMITTED OPERATIONS

Operation	Symbols	Parameter Range
Constant Speed	V_s	30 ft/sec 45 ft/sec 60 ft/sec 88 ft/sec.
Mainline Maneuvering (a_o = 3.22 ft/sec^2)	V_s, $-\Delta V_{r1}$ $+\Delta V_{r2}$ (See Fig. 3)	30 ft/sec, -7.5 ft/sec +7.5 ft/sec 45 ft/sec, -7.5 ft/sec +12 ft/sec 60 ft/sec, -12 ft/sec +12 ft/sec 88 ft/sec, -14 ft/sec + 5 ft/sec.
Mainline Speed Changes	V_{so}, V_{sf}	30 ft/sec, 45 ft/sec 45 ft/sec, 30 ft/sec 45 ft/sec, 60 ft/sec 60 ft/sec, 45 ft/sec 60 ft/sec, 88 ft/sec 88 ft/sec, 60 ft/sec.
System Entry (Vehicle initially stationary)	V(0) = 0, V_s	30 ft/sec 45 ft/sec 60 ft/sec 88 ft/sec.
Emergency Braking	V(t), a_E	0-93 ft/sec, 6.43 ft/sec^2 0-93 ft/sec, 12.86 ft/sec^2.
System Startup	V(0) = 0, V_s	Same as for System entry.

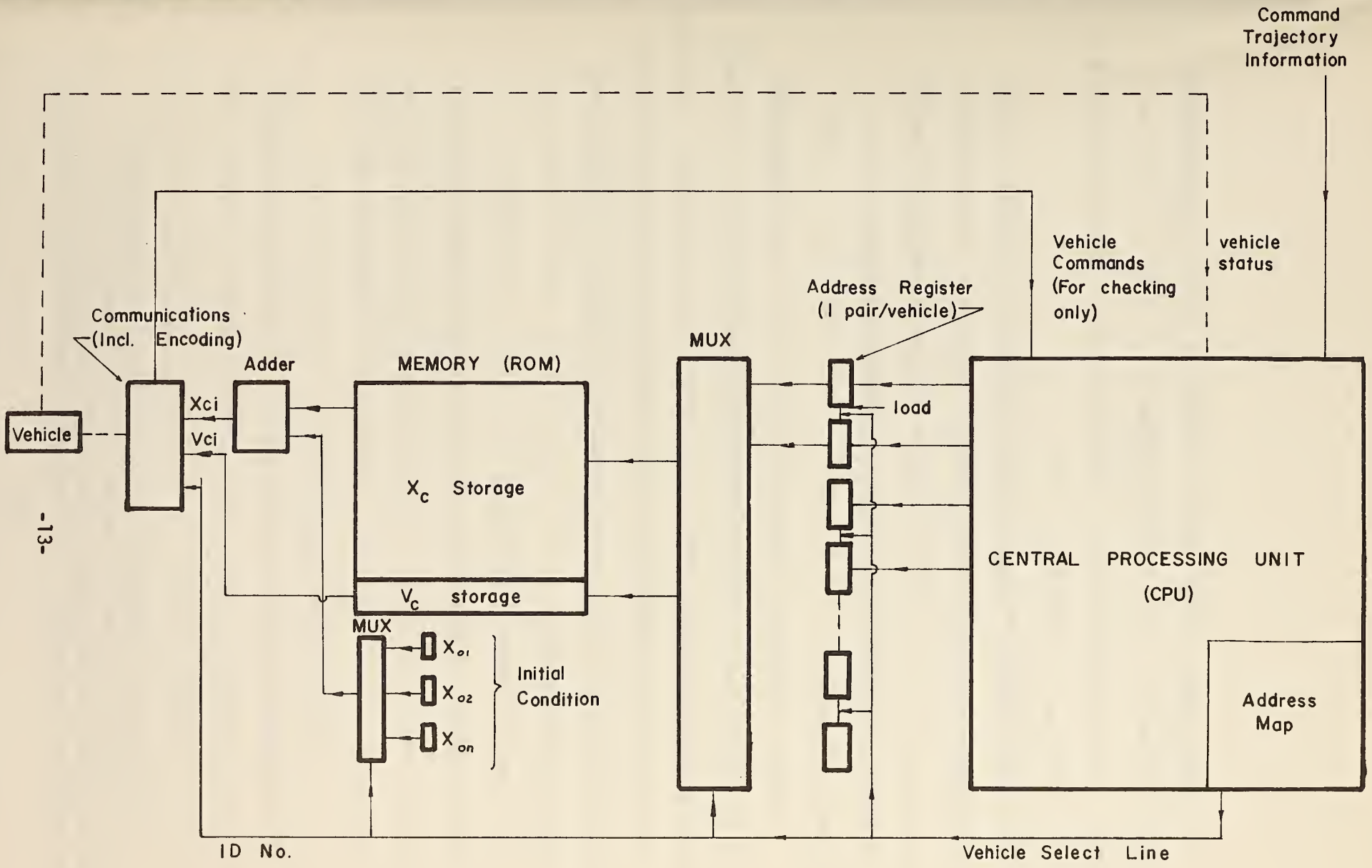

Fig. 4 Computer architecture for Approach 1.

The second input, vehicle status information, would be compared with the command information so that large deviations in a vehicle's state could be detected. It is estimated that up to 90% of the CPU's "active" processing time would be focused on this task.

The sector-computer "output," which is shown at the extreme left of Fig. 4, consists of an ID number, V_{ci} and X_{ci}. These would be encoded and communicated to the ith vehicle--a process which would be repeated every T_c secs.* A similar signal would also be sent to every other vehicle in the sector every T_c seconds.

In essence, without any further discussion of the architecture shown here, all required X_c and V_c trajectories are permanently stored so that "table lookup" may be employed together with a limited amount of sector-level processing.

It should be noted that no provision for redundant operations, and thus enhanced reliability, has been made. Clearly, this would be an essential feature of any operational unit.

b) Permanent Memory Requirements

Next consider the specification of the permanent memory required if all individual vehicle position and velocity trajectories were either stored for "table lookup" or available with a near-minimum of processing per Fig. 4.

i) Constant-Speed Operation

The information required for operation at a specified fixed speed is determined via the procedure shown in the following example.

---

* Alternatively, the complete trajectory could be transmitted to each vehicle before it entered the sector. A vehicle would follow its assigned trajectory unless a modification were subsequently transmitted. This would be necessary, for example, if an emergency condition were to develop.

Example 1

L_S = 3280 ft. T_C = 0.1 sec.

V_S = 30 ft/sec.

T_S = 3280/30 = 109.3 secs.

N_S = T_S/0.1 = 1093 words.

Here T_S is the time required for a vehicle, traveling at 30 ft/sec, to traverse a sector, and N_S is the corresponding number of times two-way communications between that vehicle and sector control occur.

The results of computations for the four specified speeds are given in Table III, from which it should be noted that the total requirement is 2742 words.

ii) Mainline Maneuvering

A typical moveup trajectory is shown in Fig. 5. In general, the corresponding maneuver would encompass two of more sectors, and can be initiated or terminated at any point within those sectors. Thus, if a strict "lookup" procedure were employed, one would store each allowed trajectory for every possible (V_S, X_S) combination. As the number of identifiable X's in a sector is $L_S/\Delta X$ = 65,600, the number of trajectories to be stored would clearly be excessive. This number can be reduced by two orders of magnitude via a nominal amount of sector-level processing.

Consider a moveup operation which is to be initiated when a vehicle, traveling at a speed V_S, enters a sector. Per Fig. 5, the required speed trajectory would be

$$\begin{aligned} V_C(t) &= V_S + a_o t && 0 \le t < \Delta V_r/a_o \\ V_C(t) &= V_S + \Delta V_r && \Delta V_r/a_o \le t < \gamma \\ V_C(t) &= (V_S + \Delta V_r) - a_o t && \gamma \le t < \gamma + \Delta V_r/a_o \end{aligned} \qquad (2\text{-}1)$$

TABLE III

INFORMATION REQUIREMENTS--

CONSTANT-SPEED OPERATION

V_s (ft/sec)	T_s (secs)	N_s (words)
30	109.3	1093
45	72.9	729
60	54.7	547
88	37.3	373

Σ = 2742 words.

where γ is the time the vehicle is to begin decelerating back to mainline speed.*

The corresponding required position trajectory would be

$$X_c(t) = X_s + V_s t + \tfrac{1}{2} a_o t^2 \qquad 0 \leq t < \Delta V_r / a_o.$$

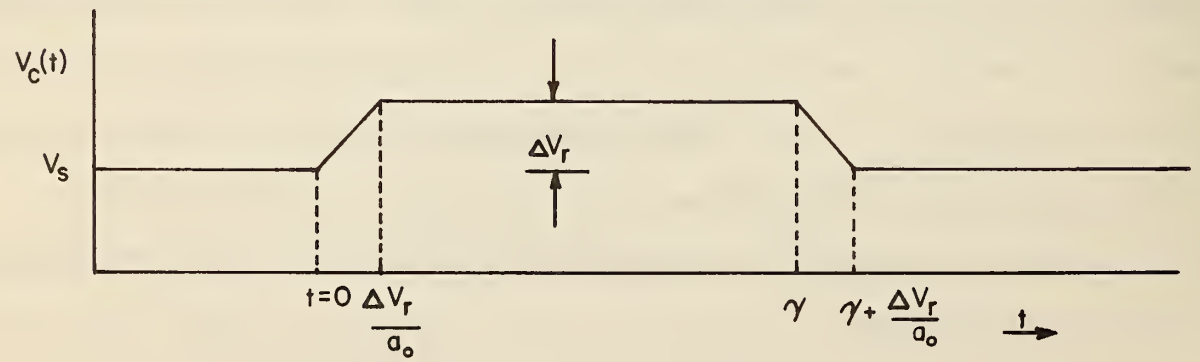

Fig. 5 Typical moveup velocity trajectory.

---

* For convenience, the subscript i (e.g., $V_{ci}(t)$) is deleted in this analysis.

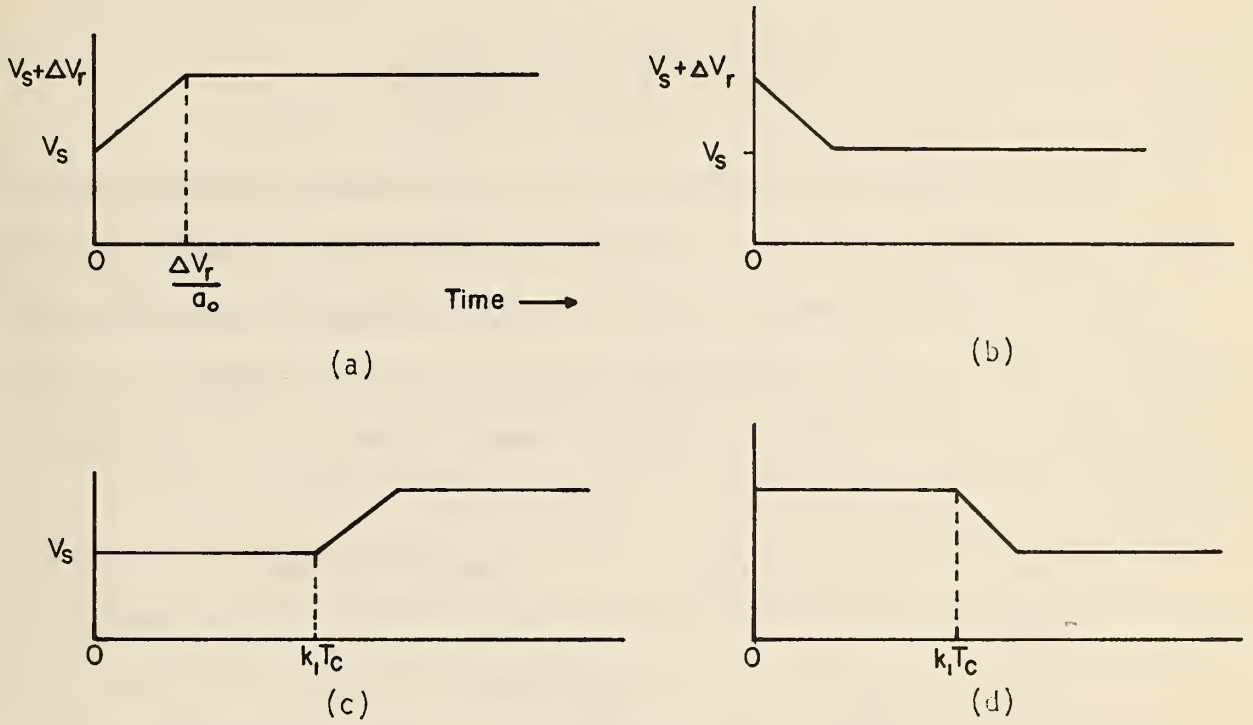

Fig. 6 Trajectories employed in moveup/moveback maneuvers.

$$X_c(t) = X_s + (V_s + \Delta V_r)t \qquad \Delta V_r/a_o \leq t < \gamma$$
$$X_c(t) = X_s + (V_s + \Delta V_r)t - \tfrac{1}{2}a_o t^2 \qquad \gamma \leq t < \gamma + \Delta V_r/a_o \qquad (2\text{-}2)$$

Here, as the vehicle enters the sector at $t = 0$, $X_s = 0$.

The corresponding discrete versions of these speed and position command trajectories are obtained by evaluating (2-1) and (2-2) for $t = 0, T_c, 2Tc,$ ....etc. The results are as follows:

Time	Command Speed	Command Position
(K)	$V_c(KT_c)$	$X_c(KT_c)$
0	V_s	$X_c(0) = 0$
1	$V_s + a_oT_c$	$X_c(T_c) = X_1$
2	$V_s + a_o2T_c$	$X_c(2T_c) = X_2$

. . . . . .

Here, a shorthand notation has been used for the command positions.

$$K = 1 \qquad X_c(T_c) = V_s T_c + \tfrac{1}{2} a_o T_c^2 \triangleq X_1$$

$$K = 2 \qquad X_c(2T_c) = V_s(2T_c) + \tfrac{1}{2} a_o 4T_c^2 \triangleq X_2 \text{ etc.}$$

Next consider a case where a vehicle, traveling at a fixed mainline speed, is K_1 time units "into" a sector. At this time $t = K_1 T_c$, it is desired to initiate the moveup operation specified above (Compare Figs. 6(a) and (b) with Figs. 6(c) and (d)). The required speed and position commands could be formed from (2-1) and (2-2), and thus the above listing, in the following manner:

Time (K)	Command Speed	Command Position
0	V_s	$X_c(0) = 0$
1	V_s	$X_c(T_c) = V_s T_c$
2	V_s	$X_c(2T_c) = 2V_s T_c$
.	.	.
.	.	.
.	.	.
K_1	V_s	$X_c(K_1 T_c) = K_1 V_s T_c$
$K_1 + 1$	$V_s + a_o T_c$	$X_c[(K_1 + 1)T_c] = K_1 V_s T_c + X_1$
$K_1 + 2$	$V_s + a_o 2T_c$	$X_c[(K_1 + 2)T_c] = K_1 V_s T_c + X_2$
.	.	.
.	.	.
.	.	. etc.

Note that the same command position notation X_1, X_2, ... etc. as previously used has been employed here.

It should be apparant that this type of processing can be employed with all moveup/moveback maneuvers, emergency braking, and speed changes.

A second aspect of such maneuvers is the required maneuvering distance. Per Fenton et al[17], the total distance required for an n-slot moveup is

$$D = nH_tV_s + \frac{nH_tV_s^2}{\Delta V_r} + \frac{V_s\Delta V_r}{a_o} \qquad (2\text{-}3)$$

where H_t = desired time headway (This would be the time equivalent of 1 slot in a synchronous system), and n = number of slots of moveup. The distance required for a moveback maneuver of n slots is

$$D = -nH_tV_s + \frac{nH_tV_s^2}{\Delta V_r} + \frac{V_s\Delta V_r}{a_o} . \qquad (2\text{-}4)$$

If an improper value of ΔV_r were selected with a given V_s, the specified trapezoidal trajectory would not result. If it were necessary to employ such a trajectory, as is assumed here, one would be restricted in his choice of ΔV_r.

Consider two moveup trajectories--one of which is a valid choice and a second of which violates the constraint of a trapezoidal trajectory.

Example 2 (A 1-slot moveup)

Conditions

V_s = 60 ft/sec; ΔV_r = 12 ft/sec, and a_o = 3.22 ft/sec^2.

Computations

Acceleration phase

$\Delta V_r/a_o$ = 12/3.22 = 3.73 sec.

Words required = 3.73/0.1 = 38 words

Constant-speed phase

Moveup speed = 60 + 12 = 72 ft/sec.

Time to traverse a sector = $L_s/(V_s + \Delta V_r)$ = 45.6 sec.

Words required = 45.6/0.1 = 456

Deceleration phase

$-\Delta V_r/-a_o$ = 3.73 sec.

Words required = 3.73/0.1 = 38 words.

Total words required

$$38 + 456 + 38 = 532 \text{ words.}$$

Next the required moveup distance must be checked. Per Eqn. (2-3), for a 1-slot moveup and H_t = 1 sec,

$$D = 60 + 3600/12 + 60 \times 12/3.22 = 583.6 \text{ ft.}$$

For the specified trajectory, one has the distance traveled during the acceleration phase, the constant-speed phase and the deceleration phase. These should, of course, sum to the distance required for a 1-slot moveup. Thus

$$D = 2[V_s \frac{\Delta V_r}{a_o} + \tfrac{1}{2}a_o t_1^2] + (V_s + \Delta V_r)T$$

or

$$583.6 = [2 \times 246.2] + 72T.$$

Since $T = \gamma - \Delta V_r/a_o$, which is the time spent at speed $V_s + \Delta V_r$, is greater than 0, the desired type of trajectory would result.

Example 3 (A nonpermitted moveup maneuver)

Conditions

V_s = 60 ft/sec; ΔV_r = 14 ft/sec; and a_o = 3.22 ft/sec^2.

Computations

Per Eqn. (2-3) for a 1 slot moveup with H_t = 1 sec.,

$$D = 60 + 3600/14 + 60 \times 14/3.22 = 578 \text{ ft.}$$

This distance as calculated via Eqn. (2-2) is 587.4 + 72T ft. Clearly,

$$578 \neq 587.4 + 72T$$

unless $T < 0$. Thus no time would be spent at the maneuvering speed and a trapezoidal trajectory would not result.

The results of a series of computations are shown in Table IV. It is noted that the choices of ΔV_r employed here were chosen arbitrarily and some storage could be saved by employing fewer values of ΔV_r.* The total number of words required for those selected is 5346.

---

*One reasonable choice of online speeds might be 22, 44, 66 and 88 ft/sec. With this choice, perhaps only 1 or 2 ΔV_r's might be employed.

TABLE IV

INFORMATION REQUIREMENTS--

ONLINE MANEUVERING

V_s (ft/sec)	ΔV_r (ft/sec)	$V_s + \Delta V_r$ (ft/sec)	t_1 (sec)	$X(t_1)$ (ft)	D (ft)	Words Required
30	-7.5	22.5	2.33	61.2	159.9	1506
	+7.5	37.5	2.33	78.6	219.9	923
45	-7.5	37.5	2.33	96.1	329.8	48
	+12.0	57.0	3.73	190.2	381.4	651
60	-12.0	48.0	3.73	201.42	463.6	759
	+12.0	72.0	3.73	246.2	583.6	532
88	-14.0	76.0	4.35	352.5	848.	530
	+5.0	93.0	2.15	196.6	1773.	397
						Σ = 5346

iii) Mainline speed changes

This is almost a subset of the previous case, and if V_s and ΔV_r were chosen carefully this case would be incorporated into Table IV. However, this was not the case here, and Table V was prepared via an analysis of Figs. 4(c) and (d). The total number of words required is 362.

iv) System entry

In a previous study[17], it was determined that an initially stationary off-line vehicle could be satisfactorily merged into a high-speed (88 ft/sec) traffic stream with a merging time of 30 sec. With this information, one can readily prepare Table VI, wherein it is noted that the required words total 1200.

It is important to note that precisely these same trajectories could be employed for a startup maneuver (after system shutdown); thus, the latter need not be considered separately.

v) Emergency braking

Let a vehicle be in the state

$$V_i(KT) = V_e$$

$$X_i(KT) = X_s$$

when it is commanded to emergency brake at a constant rate a_e. The corresponding position command trajectory is

$$X_c(t) = X_s + V_e t - \tfrac{1}{2} a_e t^2 \qquad (2\text{-}5)$$

As in the maneuvering case, one can set

$$X_s = 0$$

and only store

$$V_e t - \tfrac{1}{2} a_e t^2$$

which is valid for a specified V_e. It can be applied to a vehicle in the state (V_e, $X_s \geq 0$) by adding X_s via simple processing. Thus, a trajectory need only

TABLE V

INFORMATION REQUIREMENTS--

MAINLINE SPEED CHANGES

$V_s(0)$ (ft/sec)	$V_s(t_f)$ (ft/sec)	$\Delta V_r/a_o$ (sec)	Words
30	45	4.658	47
45	30	4.658	47
	60	4.658	47
60	45	4.658	47
	88	8.696	87
88	60	8.696	87

Σ = 362 words

be stored for each possible value of V_e and a_e. The possible velocity values are specified as 5-93 ft/sec in 0.5 ft/sec steps, and a_e as 6.43 ft/sec^2 and 12.86 ft/sec^2. The information associated with a given speed and braking rate is computed as per Example 4.

TABLE VI

INFORMATION REQUIREMENTS

SYSTEM ENTRY (Merging Operations)

Initial Speed	V_s (ft/sec)	T_m (sec)	Words
0	30	30	300
0	45	"	300
0	60	"	300
0	88	"	300

Σ = 1200 words

Example 4

For convenience, braking operations are assumed to begin at t = 0 when the vehicle just enters the sector. Let V_e = 88 ft/sec and a_e = 12.86 ft/sec^2. The command velocity is

$$V_c(t) = 88 - 12.86t,$$

and the vehicle is stopped at a time (t_s) such that

$$0 = 88 - 12.86t_s$$

or

$$t_s = 88/12.86 = 6.82 \text{ sec.}$$

$$N_s = 6.82/0.1 = 69 \text{ words.}$$

The results of computations for all permitted speed-braking rate combinations are shown in Table VII. The total words required are 20,288--a number which is much larger than desired.

It seems expedient to determine if additional sector-level processing could be employed to reduce this number. Rewriting Eqn. (2-5), there results

$$X_c(t) - X_s + \tfrac{1}{2}a_e t^2 = V_e t.$$

Clearly, the term $\tfrac{1}{2}a_e t^2$ is common to all trajectories for a given a_e, although the total time required is different for each V_e. Thus consider storing both $X_c(t) - X_s$ (with $X_s = 0$) and $\tfrac{1}{2}a_e t^2$ for the highest speed case.

TABLE VII

INFORMATION REQUIREMENTS--

EMERGENCY BRAKING

$V(t_e)$ (ft/sec)	a_e (ft/sec^2)	N_s (words)
0-93	6.43	13488
0-93	12.86	6800

Σ = 20,288 words

The function $V_e t$ is a ramp with slope V_e. The longest braking time expected is 14.2 sec corresponds to V_e = 93 ft/sec and a_e = 6.43 ft/sec^2. Let tu(t) be stored for 14.2 sec, and consider the following processing sequence for a vehicle in the initial state (V_e, $X_s \geq 0$).

a) Specify (V_e, $X_s \geq 0$)

b) Remove $u(\tau)$ from storage (τ is a dummy time variable and $u(\tau)$ is a unit-step function).

c) Let $\tau = t - t_k$, where t_k is the time the vehicle under consideration is to begin decelerating. Form $(t - t_k)u(t - t_k)$

d) Multiply by V_e

e) Add X_s to $V_e(t - t_k)[(t - t_k)u(t - t_k)]$

f) Remove $\frac{1}{2}a_e\tau^2\, u(\tau)$ from storage

g) Let $\tau = t - t_k$ to form $\frac{1}{2}a_e(t - t_k)^2u(t - t_k)$

h) Sum to obtain the desired position command signal

$$X_c = X_s + V_e(t - t_k)u(t - t_k) - \tfrac{1}{2}a_e(t - t_k)^2u(t - t_k)^*$$

---

* An additional processing capability would be added to Fig. 4 if these operations were to be performed.

TABLE VIII

INFORMATION REQUIREMENTS--

EMERGENCY BRAKING

(Modified Approach)

Function	a_e (ft/sec^2)	Max Time (sec)	Words req'd.
$tu(t)$	-	14.2	142
$\frac{1}{2}a_e t^2$	6.43	14.2	142
$\frac{1}{2}a_e t^2$	12.86	7.1	71

Σ = 355 words.

The permanent word storage associated with this approach is listed in Table VIII. Such an approach, if it could be implemented simply with a negligible amount of online processing, would be extremely attractive as only 355 words of permanent storage would be required.

vi) Information Requirements--Summary

The total word requirement for the case under consideration is summarized in Table IX. In essence, if the complete braking trajectories were stored, the requirement is some 30,000 words whereas if the modified approach were used, the requirement would be approximately 10,000 words.*

TABLE IX

SUMMARY OF

INFORMATION STORAGE REQUIREMENTS

Function	Words
Constant Speed	2742
Online Maneuvering	5346
Mainline Speed Changes	362
Merging Operations	1200
Emergency Braking	20,288
Emergency Braking (modified)	355

Σ = 29,919 words

Σ = 9986 words

* If 10,000 words were stored, a 14-bit address word would be required in Fig. 4.

vii) Estimate of required wordlength

An estimate of the required word length may be obtained using the parameters listed in Table I. In general, each word would be comprised of four components corresponding to bits for vehicle identification, position, velocity and error detection and/or correction.

1) Identification Bits

$$\frac{L_s}{(V_s)_{max}} = \frac{3280}{88} = 37.2 \text{ veh/sector.}$$

As $2^6 = 64$, 6 ID bits would be required.

2) Position resolution

$$\frac{L_s}{\Delta X} = 65{,}600$$

As $2^{17} = 131, 072$, 17 bits would be required to achieve this resolution.

3) Velocity resolution

For $\Delta V = 0.1$ ft/sec and $V \in [0, 93]$ one would require

$$2^n > 930$$

or 10 bits.

4) Error detection/correction

It is estimated that 8 bits would be required.

The estimated word length is thus 6 + 17 + 10 + 8 = 41 bits. As this would be excessive, especially if an error detecting/correcting code were employed to transmit information to each vehicle, one would probably reduce this length via the dropping of nonsignificant bits and the elimination of redundant information from the command signals.

vii) Approach 1--Summary

Per the preliminary analysis given here, this approach is clearly a feasible one. The primary advantage is that accurate trajectories are stored and thus directly available to the CPU.

The disadvantages are:

a) The supervision of the sector-level processing might tend to be unduly complex.

b) A large amount of data must be communicated to each controlled vehicle.

c) The probability of errors in the encoding/communication/decoding process could be higher than desired.

This approach would be more attractive if appropriate coding were employed to reduce the data transmission requirements.*

E. Approach 2

a) Computer Architecture

In the second approach, all allowed acceleration trajectories are stored in memory. When a given position/velocity trajectory is required, the corresponding A_c trajectory is recalled from memory and processed to provide the required V_c and X_c information. The latter is transmitted to a controlled vehicle.

The required computer operations may be accomplished via the architecture shown in Fig. 7. Here, as in Approach 1, there would be two general inputs to the CPU--one comprising command information for each vehicle in the

---

* In the analysis presented, no provision was made for redundancy and thus enhanced reliability. Such provision would result in a more complex configuration than was considered.

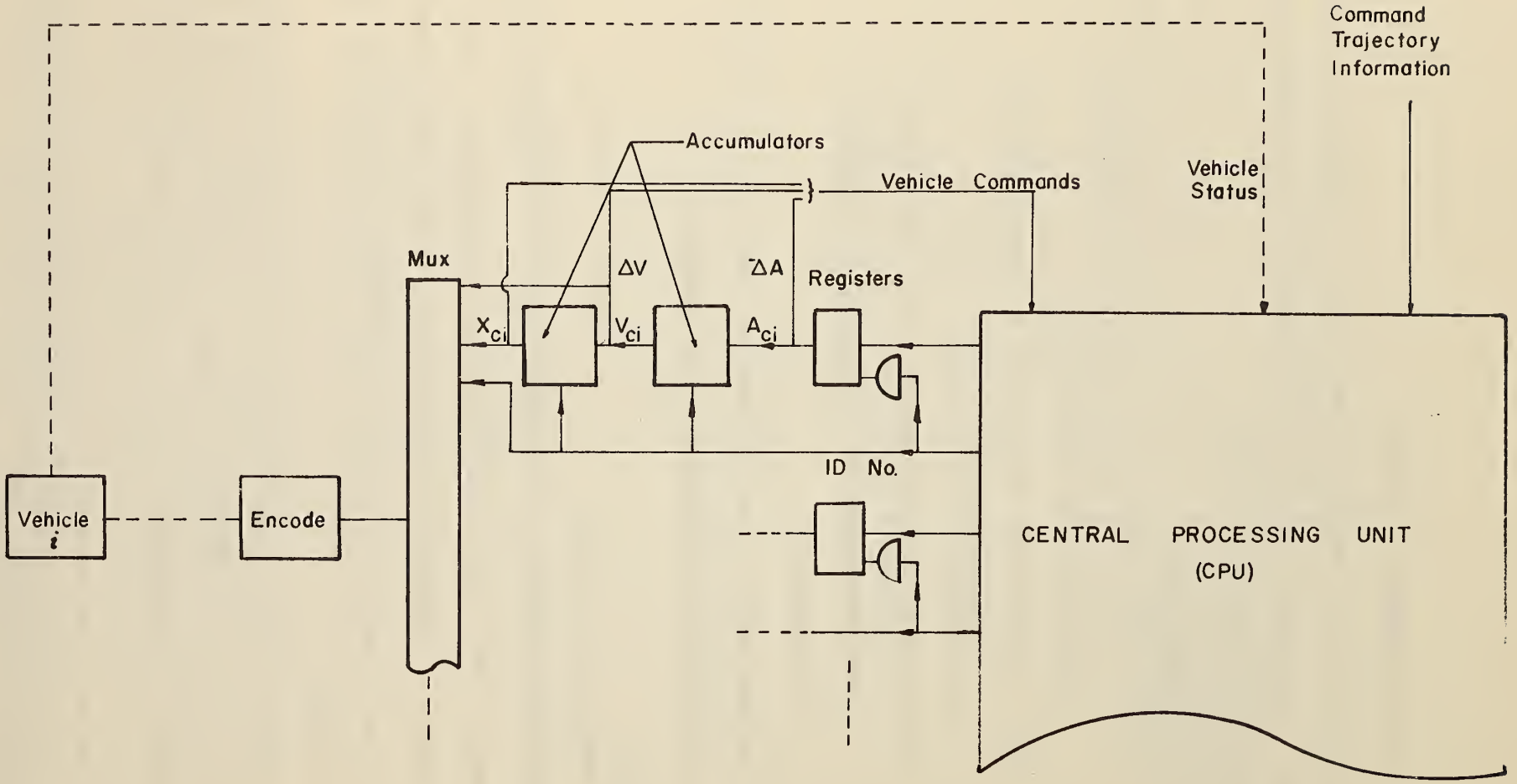

Fig. 7 Computer architecture for Approach 2.

sector, and the second, status information pertaining to each vehicle. The former would be employed to select an acceleration trajectory for each vehicle, which together with that vehicle's ID number, would be the CPU "output."

The operations required to generate command position and velocity trajectories for a given vehicle, say Vehicle i, are also shown in Fig. 7. In each communication interval, which is of duration T_c, an updated acceleration command A_c would be processed, via two accumulators, to provide V_{ci} and X_{ci}. These signals would be inserted into a multiplexer, which would be synchronized via the vehicle ID number, encoded and transmitted to the ith vehicle.* In addition, they would be fedback to the CPU for checking purposes. Similar operations would be required for every other controlled vehicle; thus, if n_1 were the maximum number of vehicles in a sector, n_1 registers and $2n_1$ accumulators would be required.

Here, no provision for redundancy and thus enhanced reliability has been made. Clearly, this would be an essential part of any operational unit.

b) Considerations Associated with Acceleration Quantization

One primary parameter is the acceleration quantization level (ΔA_c) and this, together with the time per event T_{CK}, determines both the velocity quantization level (ΔV_c) and the position quantization level (ΔX_c). These levels are related via

$$\Delta V_c = \Delta A_c \, T_{CK}$$

and

$$\Delta X_c = \tfrac{1}{2}\Delta A_c \, T_{CK}^2$$

One would like to make both ΔA_c and T_{CK} very small numbers so as to have extremely accurate quantized representations of both $V_c(t)$ and $X_c(t)$. For example, if $\Delta A_c = 0.1$ ft/sec^2 and $T_{CK} = 0.01$ sec, Then

---

* An alternative approach involves the generation of the complete trajectory, and its transmission to a vehicle prior to that vehicle's entry into the sector.

$$\Delta V_c = .001 \text{ ft/sec}$$

and

$$\Delta X_c = 5 \times 10^{-6} \text{ ft.}$$

With such levels, the quantized functions $\hat{V}_c(t)$ and $\hat{X}_c(t)$ would be practically the same as their continuous counterparts $V_c(t)$ and $X_c(t)$, and the quantization errors would be negligible. The word lengths for these choices are 17 bits for velocity and 30 for position (A velocity range of 0-93 ft/sec and a position range of 0-3280 ft was assumed here). These lengths are excessively large--especially in the context of communicating information, via an error detecting/correcting code to each vehicle. Thus, in practice, it would probably be expedient to either round off or truncate the lowest-order bits. Thus, for example, if command velocity were to be resolved to within .05 ft, the required word lengths could be reduced to 9 and 17 bits respectively. Further reductions in the lengths could be obtained by using the redundancy inherent in V_c and X_c so that only a significant "critical" part of each word would need to be transmitted.

Clearly, the word lengths could be substantially reduced by increasing ΔA_c and T_{CK}. However, if ΔA_c were large (e.g., $\Delta A_c \geq 4$ ft/sec^2), a substantial command jerk would be present when A_c changed. This could result in a jerky and uncomfortable ride (The ride quality would, of course, also depend on such factors as vehicle controller design and the inherent jerk-limiting properties of the vehicle).

Thus, the choice of quantization levels is, in part, dictated by somewhat opposing requirements--a large value of ΔA_c to reduce the required word length and facilitate reliable communications versus a small ΔA_c for a comfortable ride.

c) Permanent Memory Requirements

Next consider the amount of permanent memory required if all acceleration trajectories are stored for table "lookup." In essence, one must have an acceleration-versus-time profile corresponding to each of the trajectories specified in Section C.

i) Constant Speed

In this case, $A_c = 0$ for all t_1 and thus only a single word need be stored. It would also be necessary to store the desired stream speed, as this would be added as an initial condition to the "velocity" accumulator output. Alternatively, one could store a single word, which would consist of $A_c = 0$ and V_c = constant, for each of the four desired stream speeds.

ii) Online Maneuvering

Typical maneuvering trajectories are shown in Fig. 6, from which it should be noted that the required acceleration trajectory is a piecewise-constant function. Initially, a vehicle would be in a constant-speed mode characterized by

$$A_c(t) = 0 \qquad V_s = V_{s1}.$$

Subsequently, the following three-word command would be applied

$$A_c(t) = a_o$$

$$A_c(t) = 0$$

$$A_c(t) = -a_o.$$

Upon completion of the maneuver, the command would again be

$$A_c(t) = 0 \qquad V_s = V_{s1}.$$

Eight maneuvering situations have been specified (See Table II), and thus eight 3-word trajectories would be required. Each word would contain $A_c(t)$ and the time it was to be applied.

iii) Mainline Speed Changes

This case is quite similar to the previous one. Prior to the initiation of a mainline speed change, the command would be

$$A_c(t) = 0, \quad V_c(t) = V_{s1} \text{ (Constant)}$$

The subsequent command would involve

$$A_c(t) = a_o$$

for the necessary amount of time followed by operation at the new stream speed

$$A_c(t) = 0, \quad V_c(t) = V_{s2} \text{ (Constant)}.$$

Seven speed-changing situations were defined in Table II; thus, there would be a requirement for no more than 7 words. Each word would contain $A_c(t)$, and the time interval over which it was to be commanded.

As the same acceleration values, a_o and $-a_o$ would be used in both maneuvering operations and for mainline speed changes, one could achieve some modest word saving by choosing ΔV_r (See Table II) so that some portions of the maneuvering and speed-changing trajectories were common.

iv) System Entry

In a study of merging operations[17], it was specified that the following trajectory was one satisfactory choice:

$$A_c(t) = 2K_1 + 6K_2t \quad [0, T_m].$$

Here, K_1 and K_2 are determined by constraints imposed at $t = T_m$, the time at which a merging vehicle is inserted into mainstream traffic.

Both the word size and the number of words required are dependent upon the quantization level ΔA_c. For example, consider the case where the terminal constraints are $V_c(T_m) = 88$ ft/sec, $A_c(T_m) = 1.6$ ft/sec^2 and $T_m = 30$ sec. For these values,

$$A_c(t) = 4.264 - 0.088t \quad t \in [0, 30].$$

This function is shown in Fig. 8, together with quantized functions corresponding to ΔA_c = 0.2 ft/sec^2, and 0.8 ft/sec^2. Fourteen words are required for the former and 3 for the latter. If one makes a conservative choice of ΔA_c = 0.2 ft/sec^2, some 20 words would be required for the merging operations defined in Table II.

Each of these words would consist of two parts--one to define the desired acceleration and a second to define the time that acceleration would be applied. As the range of command accelerations is encompassed in -13 to 8 ft/sec^2, 7 "acceleration" bits would be required. It would appear that 9 "time" bits, corresponding to a maximum time of 51.2 sec, would be sufficient. Thus, a 16-bit word could be employed.

v) Emergency Operations

As two emergency braking values were selected, one would require only two words--provided the words were properly processed and transmitted to a vehicle.*

d) Approach 2--Summary

A summary of the estimated storage requirements for Approach 2 is shown in Table X, from which it should be noted that only 57 words would be required. A conservative word size would be 16 bits, if the quantization level were selected as 0.2 ft/sec^2.

Per the preliminary analysis presented here, this approach appears feasible and includes the following advantages:

i) The permanent storage requirements are minimal; and

ii) Extremely accurate trajectories, which can be used to obtain estimates of both $V_c(t)$ and $X_c(t)$, can readily be stored.

---

* As the time duration of a braking trajectory depends on a vehicle's initial speed, this must be considered in the generation of $\hat{V}_c(t)$ and $\hat{X}_c(t)$.

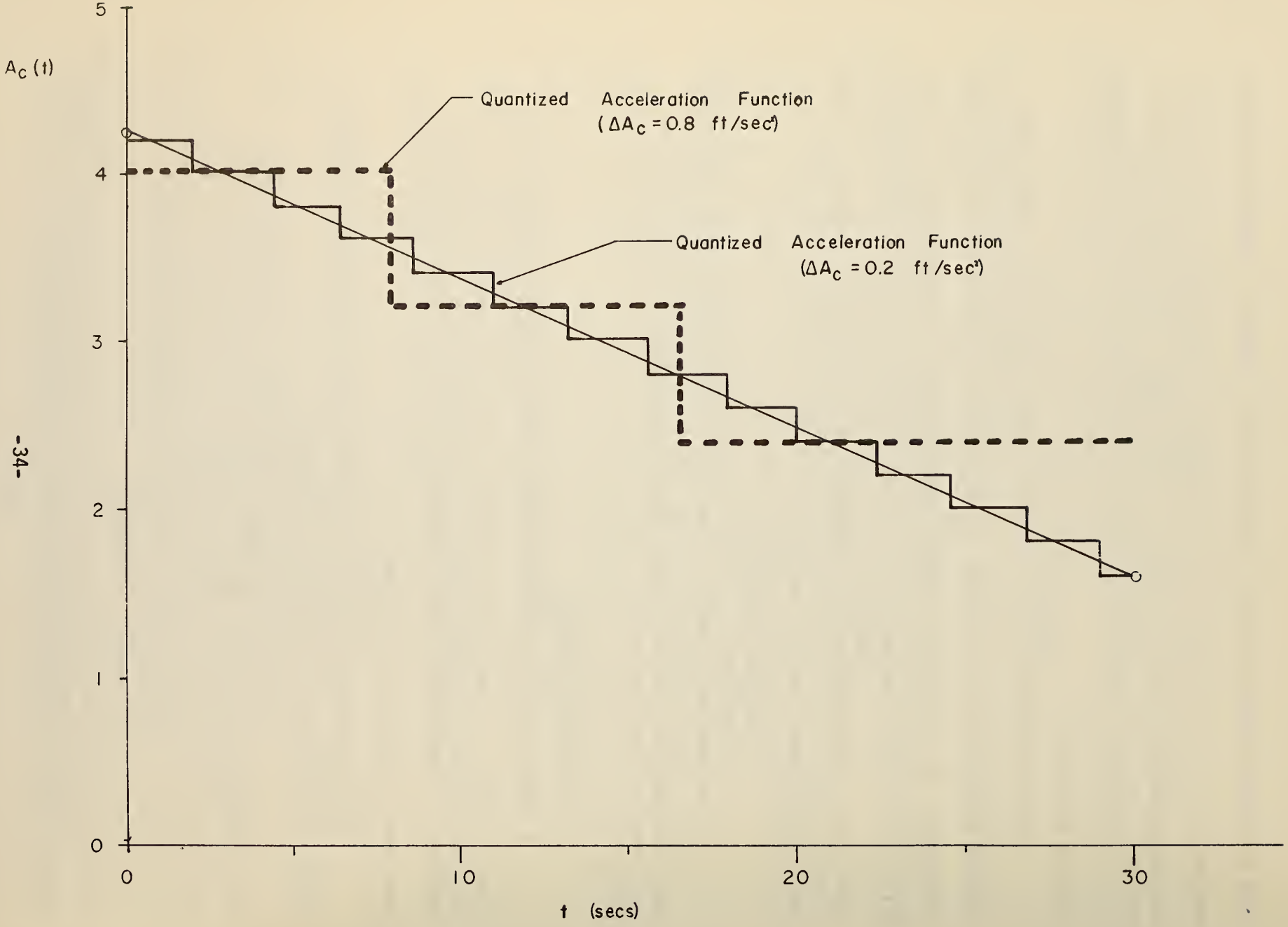

Fig. 8 Quantization of a command-acceleration merging trajectory.

TABLE X

SUMMARY OF
INFORMATION STORAGE REQUIREMENTS
(Approach II)

Function	Trajectories	Words
Constant Speed	4	4
Online Maneuvering	8	24
Mainline Speed Changes	7	7
Merging Operations	4	20
Emergency Braking	2	2

Σ = 57 words.

The disadvantages are

i) A substantial amount of sector-level processing is required;

ii) The probability of an error in either V_c or X_c might be increased via this processing;

iii) A large amount of data (The same as in Approach 1) must be communicated to each vehicle; and

iv) The probability of errors (The same as in Approach 1) in the encoding/communication/decoding process could be higher than desired.

This approach would be quite attractive if the probability of a sector-level processing error were negligibly small, and if efficient coding were employed to reduce the data transmission requirements.

F. Approach 3

a) Computer Architecture

In the third approach, all allowed acceleration trajectories would be stored in memory at the sector level and onboard each controlled vehicle.

When a specific position/velocity trajectory were required, the corresponding A_c would be recalled from memory, at both the sector level and onboard the controlled vehicle, and processed to provide the required X_c and V_c information. Thus, this information would be available at both locations. Some redundancy is involved here; however, the availability of two independent computations of $\hat{V}_c$ and $\hat{X}_c$ could be beneficial in terms of system reliability.

The required sector computer operations could be accomplished via the architecture shown in Fig. 9. Here, as in the previous approaches, there would be two inputs to the CPU--one comprising command information for each vehicle in the sector, and the second status information from each vehicle. The former would be employed to select an acceleration for each vehicle, which together with that vehicle's ID number, would be the CPU "output." This acceleration would be processed, as shown, to provide $\hat{X}_c$ and $\hat{V}_c$ for comparison with true vehicle position and speed. Note that the signal transmitted to a controlled vehicle would consist of a command selection and an ID number.

b) Approach 3--Summary

The same advantages as associated with Approach 2 are present here; in addition, a minimal amount of command information would be transmitted,* the probability of errors in the encoding/communication/decoding process would be much less than for Approaches 1 and 2, and V_c and X_c would be available in an almost continuous form onboard each controlled vehicle.

The disadvantages include the following:

a) A substantial amount of sector-level processing would be required;

b) A substantial amount of processing would be required onboard each vehicle; and

---

* This matter is considered in detail in Chapter III.

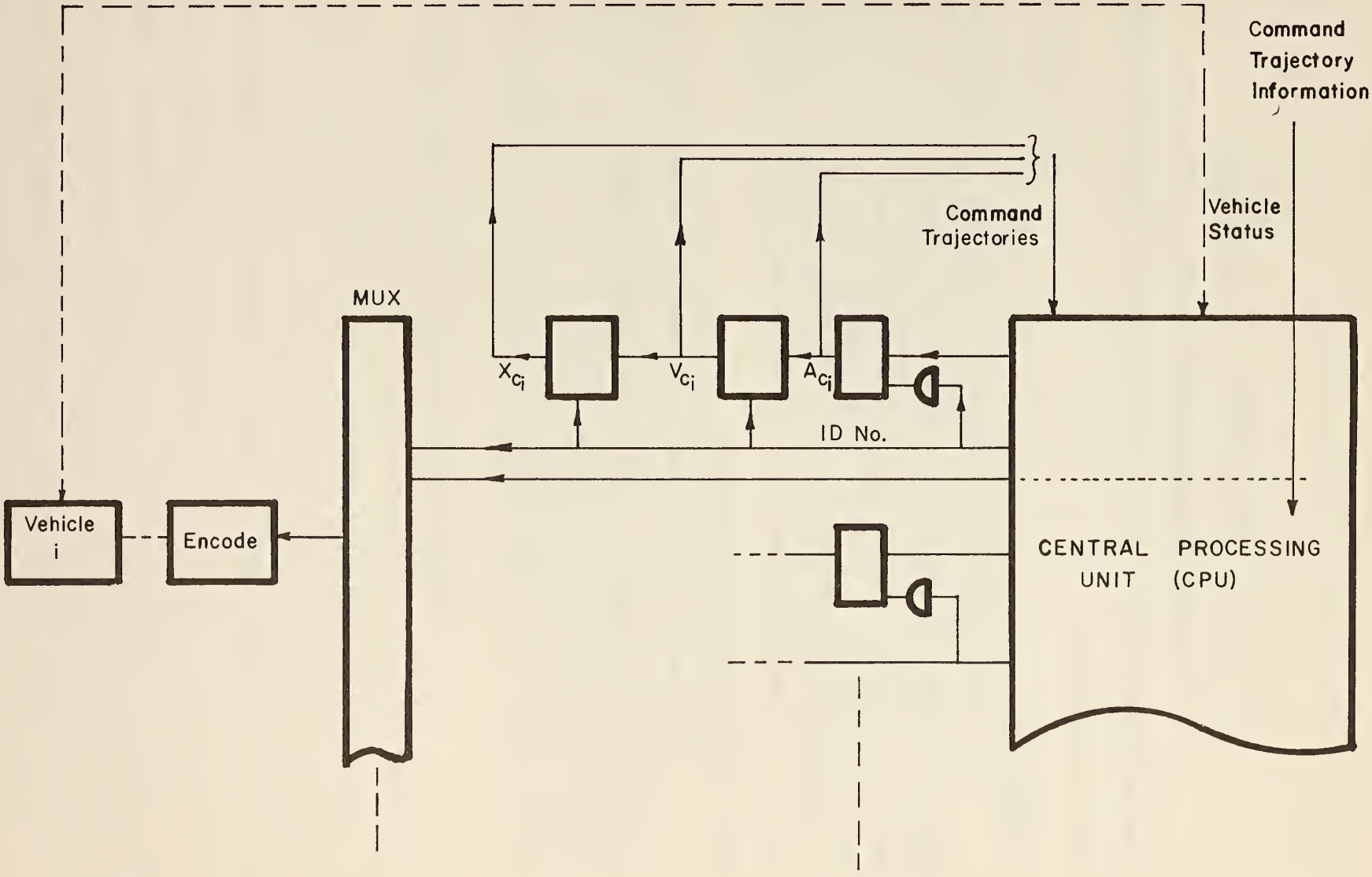

Fig. 9 Computer architecture for Approach 3.

c) The probability of an error in either V_c or X_c could be substantial.

As two estimates of both X_c and V_c would be available, the latter problem should be resolvable.

G. Conclusions

Three general approaches to sector-level computer operations have been examined, and their advantages and disadvantages enumerated. This was done primarily to provide a source document for further research efforts, and does not, at least at this time, particularily emphasize any given approach. In essence, all three appproaches offer particular advantages, and each is worthy of more detailed investigation.

It should be noted that a number of other approaches may be formulated by utilizing various aspects of the three presented. Ideally, one would like to obtain the most beneficial aspects of each and eliminate some of the unwanted aspects. The "cost" involved would probably be increased complexity.

CHAPTER III

ON SECTOR-LEVEL COMMUNICATIONS

A. Introduction

Relatively little effort has been devoted to studying the communication aspects of individual-vehicle, automated ground transport. However, much relevant work, which was focused on other applications, has been accomplished as may be noted in a recent state-of-the-art survey.[18] In particular, some useful experimental results, which were obtained in a high-speed rail context, are available.[19-21]

The work reported here is a continuation of an earlier effort,[16] and it is focused on communications between a sector-level computer and the individual vehicles under its supervision and/or control. The emphasis is on Approach 3 (which is defined in Fig. 9), as this approach should result in a minimal or near-minimal amount of transmitted information.

B. Minimal Required Information Transmission Rates

Consider the sector-level structure shown in Fig. 2, and note that the computer is the source of command information ($X_c(t)$, $V_c(t)$ and $A_c(t)$) and the controlled vehicle(s) is a source of status information ($X(t)$, $V(t)$, $A(t)$ and other data). The information content of these sources is largely dependent on the operating policies of a particular sector realization, and is thus strongly influenced by technical and economic constraints and safety considerations. For communication-analysis purposes, the policy adopted may be described by an "a priori probability structure." One reasonable structure, which is not unique, is defined by the following assumptions:

1) All possible command trajectories would be predetermined, and their number would be manageably small.

2) Each vehicle would be assigned a trajectory prior to entering the sector, and each normative trajectory is equally likely to be assigned.

3) Each vehicle would be assigned an identification number (ID), and the possible assignments would be equally likely.

4) Every T_c sec each vehicle in the sector would receive an indication as to whether or not emergency operations should be initiated.

5) Under normative conditions, the vehicle/controller dynamics would be known (e.g., the dynamics specified in Chapter V), and thus a vehicle's response to $(X_c(t), V_c(t), A_c(t))$ would also be known.

6) The status information would be quantized and the probability density functions (p.d.f.) for both X(t) and V(t) are known, discrete and uniform for all normative conditions.*

7) A(t) and some other status variables (e.g., oil pressure and water temperature) would be quantized into two levels--one indicating normal operation and the other a failure.

---

*The uncertainty in X(t) and V(t) as caused by random disturbances, measurement errors, parameter variations, etc. is described in terms of these p.d.f.'s. In normal situations, X(t) and V(t) would be the outputs of a low-pass system, and thus would be approximately normally distributed over some range. However, the use of a uniform distribution is convenient, and results in a conservative estimate of source information content.

8) The probability of a failure occurring within a given time interval is very small (<< 1 failure/ 10 hrs).

In three of these assumptions, equally likely (or a uniform p.d.f.) conditions are assumed. Since this condition results in a maximum source entropy (maximum average information content), the resulting information rates would be greater than the minimum values.

Consider the calculation of the source entropies for a sector in which the traffic flow is saturated (a worst-case communication condition). The average information (I_{c1}) sent from the sector computer, in an H/V_{sm} time interval, to a vehicle prior to its entering the sector would be

$$I_{c1} = -P_{nor} \log_2 \frac{P_{nor}}{N_T} - P_{em_1} \log_2 P_{em_1} - P_{em_2} \log_2 P_{em_2} - \log_2 \frac{1}{N_v} \text{ (bits)}.$$

Since $\frac{P_{nor}}{N_T}$ is the probability of occurrence of each normative command, the first term, which is comprised of N_T identical terms (i.e., $-\frac{P_{nor}}{N_T} \log_2 \frac{P_{nor}}{N_T}$), corresponds to the source entropy associated with commands for normal operation. The second and third terms are associated with emergency operation, and since $\frac{1}{N_v}$ is the probability of each ID assignment, the fourth term is associated with ID selection. (All symbols employed in this analysis are defined in Table XI). The average information (I_{c2}) sent in an interval $\frac{T_c}{N_v}$ to each vehicle already in the sector would be

$$I_{c2} = -P_{nor} \log_2 P_{nor} - P_{em_1} \log_2 P_{em_1} - P_{em_2} \log_2 P_{em_2} \text{ (bits)}.$$

Thus, a minimal average information rate (C_c) for the command link is

$$C_c = \frac{V_{sm}}{H} I_{c1} + \frac{N_v}{T_c} I_{c2} \text{ (bits/sec)}.$$

The condition that $P_{em_1} <<< P_{nor}$ and $P_{em_2} <<< P_{nor}$ (i.e., $P_{nor} \doteq 1$) means that vehicles receive no information while in the sector. This is reasonable since Subchannel 2 is included for safety purposes (i.e., to transmit an emergency signal and the

need for this has a probability close to 0). Under this condition $I_{c2} \doteq 0$ and

$$C_c \doteq \frac{V_{sm}}{H}[\log_2 N_T + \log_2 N_v]. \qquad (3\text{-}1)$$

A similar analysis may be conducted to obtain a minimal average

TABLE XI

DEFINITION OF SYMBOLS

Symbol	Definition	Typical Value*
L_s	Sector length	3520 ft
V_{sm}	Maximum stream speed	88 ft/sec
T_c	Frame time interval (i.e., the interval in which each vehicle is addressed once)	0.1 sec
H	Slot size	88 ft
N_v	Maximum permitted number of vehicles in the sector	40 ft
N_T	Number of permitted normative trajectories	16
P_{em_i}	Probability that an emergency occurs within a given T_c interval and emergency command i (i = 1, 2) is selected	$\doteq 0$
P_{nor}	Probability that normal sector operation is continued within a given T_c interval ($P_{nor} = 1 - P_{em}$)	$\doteq 1$
C_{sn}	Average information rate as transmitted from a "normal" vehicle	-
C_{sf}	Average information rate as transmitted from a "failed" vehicle	-
P_n	Probability of normal vehicle operation at time t	-
P_f	Probability of a vehicle failure at time t	-
r_v	The range of possible speeds at time t	4 ft/sec
r_x	The range of possible positions at time t	2 ft

* These values are specified for illustrative purposes only.

TABLE XI(Cont.)

Symbol	Definition	Typical Value*
q_v	Velocity quantization level	0.5 ft/sec
q_x	Position quantization level	0.5 ft
B_v	Effective power spectrum bandwidth of the random velocity deviations	2.5 Hz
B_x	Effective power spectrum bandwidth of the random position deviations	1.0 Hz
a_d	Component of vehicle acceleration due to a disturbance force	-
$\hat{X}(t)$	An estimate of $X(t)$	-
$\hat{V}(t)$	An estimate of $V(t)$	-
r_{A_c}	The range of possible A_c	-20 ft/sec^2 to 10 ft/sec^2
r_{V_c}	The range of possible V_c	0-100 ft/sec
q_{A_c}	Quantization step-size of A_c	2 ft/sec^2
q_{V_c}	Quantization step-size of $V_c (= q_{A_c} T_c)$	0.2 ft/sec
q_{X_c}	Quantization step-size of $X_c (= \frac{1}{2} q_{A_c} T_c^2)$	0.01 ft
ε	Allowance for overshoot	2 ft/sec

information rate (C_s) for the status link with the following result:

$$C_s = \frac{N_v}{T_c} (P_n \log_2 P_n + P_f \log_2 P_f) + N_v (P_n C_{sn} + P_f C_{sf}).$$

The quantity C_{sf} is difficult to specify since the state $(X(t), V(t))$ of a failed vehicle is probably a nonlinear, nonstationary process; however, since one would expect $P_n >>> P_f$, then

$$C_s \doteq N_v C_{sn}.$$

C_{sn} is largely determined by the distributions of $\hat{X}$ and $\hat{V}$* (See Fig. 10).

---

* Hereafter, $\hat{X}$ and $\hat{V}$ will represent estimates of X and V.

These distributions are not statistically independent since X and V are linearly related; however, since X and V would be quantized independently, and possibly contaminated by independent sources of measurement noise, the correlation between $\hat{X}$ and $\hat{V}$ would be less than one. For simplicity, $\hat{X}$ and $\hat{V}$ are assumed to be statistically independent; thus, the resulting calculated C_{sn} would be an upper bound on the true value.

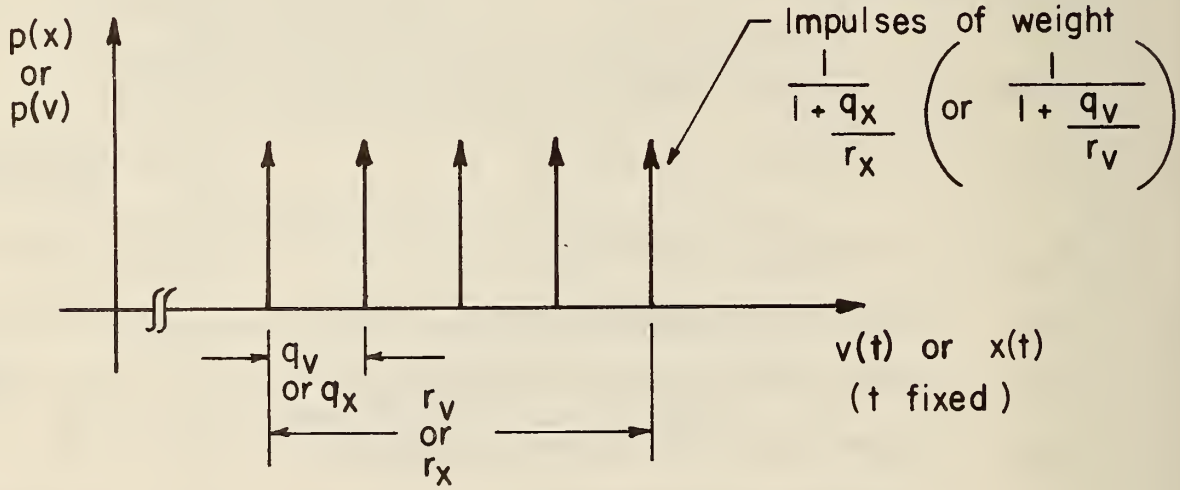

Fig. 10. A typical probability density function.

Note: The mean of this distribution is the deterministic response to $X_c(t)$, and would not in general, equal $X_c(t)$.

The entropies of the other status variables (e.g., acceleration and engine temperature) also affect C_{sn}; however, their effect is negligibly small as a result of Assumptions 7 and 8.

Using an approach specified by Schwartz,[22]

$$C_{sn} = B_v \log_2 \left(1 + \frac{r_v}{q_v}\right) + B_x \log_2 \left(1 + \frac{r_x}{q_x}\right) \quad \text{(bits/sec)}. \qquad (3\text{-}2)$$

The quantities B_v and B_x, which are defined in Table XI, could be approximated from the frequency-response characteristics of the vehicle's longitudinal control system.*

An indication of the magnitudes of both C_c and C_{sn} may be obtained using Eqns. (3-1) and (3-2) and the parameter values given in Table X. The result is

$$C_c \doteq 10 \text{ bits/sec}$$

and

$$C_s \doteq 400 \text{ bits/sec}.$$

These values are rather small and are a reflection of the rates required if it were possible to transmit all source information in the most efficient manner. In practice, one would have much higher rates because of coding constraints, safety requirements, and a need for the detection and/or correction of errors in transmitted signals.

This analysis is based on one set of assumptions regarding sector operation, and is, of course, not unique in that another set could have been employed. However, in general, it appears that the utilization of a "reasonable" set would result in the elimination of considerable redundancy from the transmitted information and minimal bit-rates.

---

* A conservative selection of B_v and B_x would be the 20db below-peak frequency response of $\frac{v}{a_d}(j\omega)$ and $\frac{x}{a_d}(j\omega)$, respectively. Here $a_d(j\omega)$ is that component of acceleration due to a disturbance force.

C. Encoding of the Command and Status Information

Both the command and status information must be encoded* for transmission, and the requirements of this process result in larger bit-rates than the minimal ones specified in the previous section. In that section, the word bit refers to a measure of information content, or entropy. Hereafter, it will be synonymous with "binit, or binary digit."

a) Command Link

This link would consist of two subchannels. Identification and command information would be transmitted, on Subchannel 1, to a vehicle prior to its entering the sector, and command information would be transmitted on Subchannel 2 to each of the vehicles already in the sector. The latter information would include an indication as to whether emergency operation should be initiated and lateral guidance information (It should be noted that the latter was not included in the analysis of the previous section).

An 11-bit code word is formulated for Subchannel 1 in Table XII and, as a vehicle would enter the sector every second (for H/V_{sm} =1 sec) under saturated flow conditions, the minimal required bit-rate would be 11 bits/sec.

A 3-bit code word is formulated for Subchannel 2 in Table XIII. Since the sector computer would communicate with a maximum of 40 vehicles within each T_c = .1 sec, the corresponding bit-rate would be 1200 bits/sec. Thus, the total bit rate for the command link would be 1211 bits/sec.

b) Status Link

Before specifying the status link bit-rate, the emergency detection mechanisms should be defined. Here, it is assumed that an emergency could be detected in any of the following ways:

* Here, only binary, or 2-symbol, communication is discussed. Using more than 2 symbols could result in better performance; however, more complex transceivers would be required.

TABLE XII

FORMULATION OF MINIMAL CODE WORD

FOR

SUBCHANNEL 1

Source	Information	Number of bits
Vehicle ID No.	1 of 40 different numbers	6
Command Selection	1 of 18 different commands	5
		Σ = 11 bits/word

TABLE XIII

FORMULATION OF MINIMAL CODE WORD

FOR

SUBCHANNEL 2 (1)

Source	Information	Number of bits
Longitudinal Command	1. Maintain normal trajectory	
	2. Brake at -0.2g	
	3. Brake at -0.4g	2
Lateral Command (2)	1. Guide left	
	2. Guide right	1
		Σ = 3 bits/word

Note: (1) Here the vehicle ID No. is not considered as part of the information word; however, it may be necessary to include it for communication and system synchronization.

(2) The number of bits required for lateral command information is dependent upon the means employed for realizing lateral control. For some choices, a third command "maintain present course" would be required and thus 2 bits would be needed.

i) The sector computer processes X(t) and V(t), as received from each vehicle, and determines if either the position or velocity deviations exceed decision thresholds (e.g., ± 1.5 ft for position and ± 2.5 ft/sec for velocity).

ii) Several types of failures would be detected onboard a vehicle, and the corresponding information (1 or 2 bits) is communicated to the sector computer.

iii) If A(t), as measured onboard a vehicle, exceeds threshold bounds (e.g. $|0.2g|$),* an emergency "flag" is set in the status word.

The last condition is especially important as it eliminates the need to transmit A(t). It is not necessary to transmit higher-order bits of position and velocity as is illustrated in the following example.

Consider the velocity-versus-time plot shown in Fig. 11. Here V_c = 88 ft/sec and the decision threshold is specified as ±2.5 ft/sec. At $t = (K_1 - 1)T_c$, it is assumed that an emergency isn't detected; therefore

$$85.5 \leq V[(K_1 - 1)T_c] \leq 90.5 \qquad \text{(ft/sec)}.$$

If the acceleration thresholds (± 0.2g) are not surpassed in the next T_c sec, then

$$84.86 \leq V(K_1 T_c) \leq 91.15 \qquad \text{(ft/sec)}$$

as is shown in the figure.

If q_v = 0.5 ft/sec, then it would be necessary to transmit only the low order 4 bits of the total velocity word, since each quantization level with the interval [84.86, 91.15] could be uniquely identified by these 4 bits. A similar analysis may be conducted for the position variable.

These ideas have been used in the construction of the status word and, as is shown in Table XIV; a 9-bit word results. Since each of a maximum of 40 vehicles communicates with the sector computer every 0.1 sec, the minimal required bit-rate would be 3600 bits/sec.

---

* This criterion would not be employed in system entry operations where $|a| > 0.2g$.

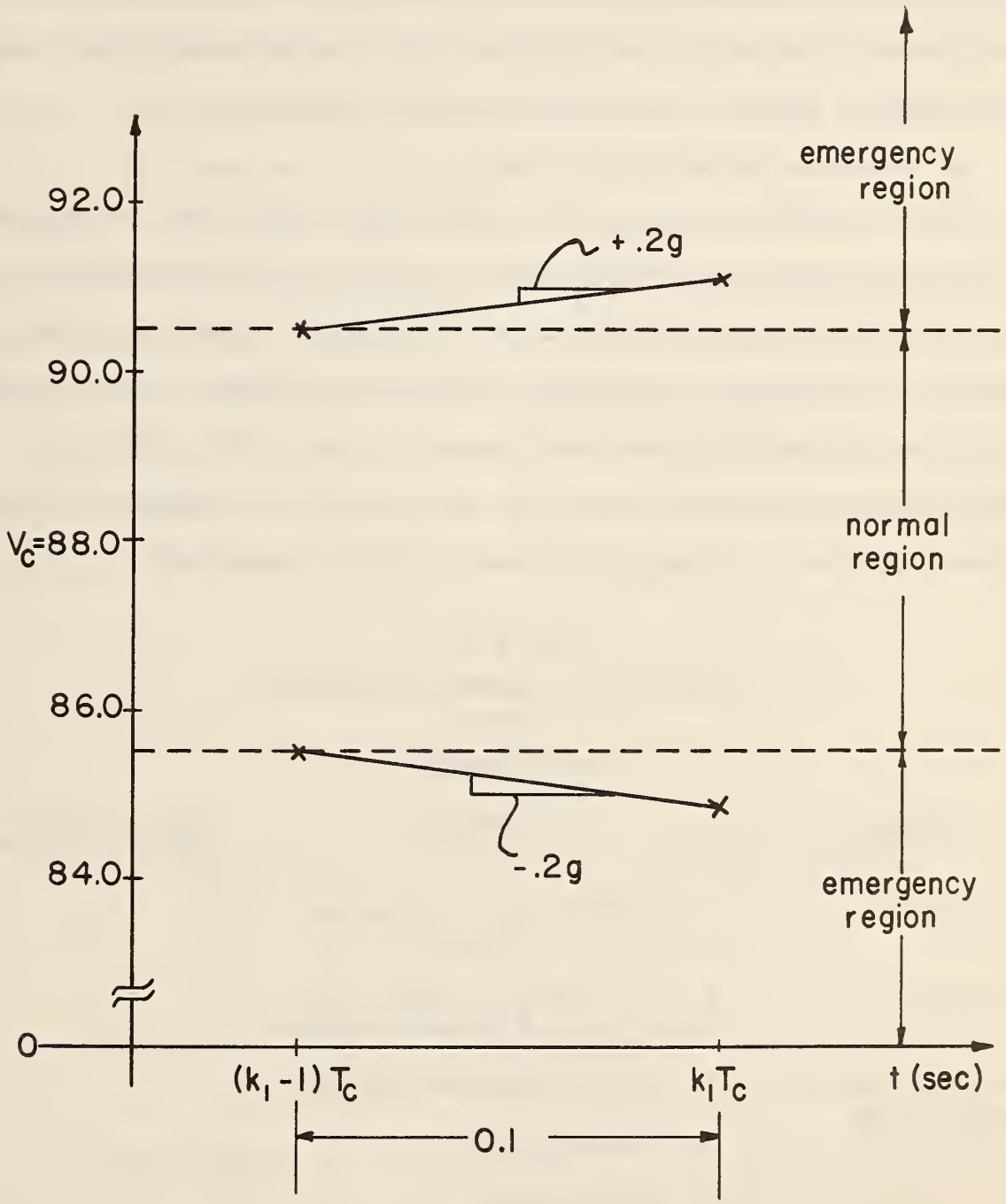

Fig. 11 The worst-case failure if the acceleration bounds are <u>not</u> exceeded.

Note that the practical bit-rates for both links are much larger than the corresponding information rates given in Section B. Much of this difference is attributed to the safety specification that the sector computer must communicate with each vehicle at least once in each T_c interval.

c) Encoding for Approaches 1 and 2

It is worthwhile to compare the above results with those obtained when both the command information (X_c, V_c and A_c) and the status information are not transmitted in reduced form (e.g., as in Approaches 1 and 2). In this comparison, the parameters specified in Table XI are employed. The step-sizes q_{A_c}, q_{V_c} and q_{X_c} specified there were chosen to eliminate the effects of command quantization noise. (Since this was the case for Approach 3, it seems reasonable to make it so here for purposes of a fair comparison).

TABLE XIV
FORMULATION OF MINIMAL CODE WORD
FOR
STATUS CHANNEL

Source	Information	Number of bits
Position	1 of 8 levels (4 ft quantized into 0.5 ft increments)	3
Velocity	1 of 16 levels (8 ft/sec quantized into 0.5 ft/sec increments)	4
Acceleration and other status information	1. Continuing normal operation	
	2. Pending failure	
	3. Loss of power	
	4. Acceleration bounds exceeded	2
		Σ = 9 bits/word

Note: Here the Vehicle ID No. is not considered as part of the information word; however, it may be necessary to include it for communication system synchronization.

The bit-rate for Subchannel 1 of the command link would be 6 bits/sec as the required word would only contain vehicle identification information. The minimal required word length for Subchannel 2 is 33 bits as is shown in Table XV. Since commands must be transmitted to a maximum of 40 vehicles within each 0.1 sec interval, the required bit-rate would be 13,200 bits/sec.

The word length for the status link is 23 bits as is shown in Table XVI, and since the sector computer must receive commands from a maximum of 40 vehicles within each 0.1 sec, the corresponding bit-rate is 9200 bits/sec.

The total required bit-rate is some 23,000 bits/sec as compared to 5000 bits/sec for Approach 3.* Clearly, the channel bandwidths may be significantly reduced by effectively utilizing a priori knowledge.

TABLE XV
FORMULATION OF NOMINAL CODE WORD
FOR
SUBCHANNEL 2

Source	Information	Number of bits
X_c	1 of $(1 + \frac{L_s}{q_{X_c}})$ levels	19
V_c	1 of $(1 + \frac{r_{V_c}}{q_{V_c}})$ levels	9
A_c	1 of $(1 + \frac{r_{A_c}}{q_{A_c}})$ levels	4
Lateral Guidance	1. Guide left	
	2. Guide right	1
		Σ= 33 bits.

* Note that additional bits may be necessary for synchronization and error-detection and/or correction.

TABLE XVI

FORMULATION OF NOMINAL CODE WORD

FOR

STATUS LINK

Source	Information	Number of bits
X	1 of $(1 + \frac{L_s}{q_{X_c}})$ levels	13
V	1 of $(1 + \frac{rV_c + \varepsilon}{q_{V_c}})$ levels	8
Acceleration and other status information	(Same as before)	2
		Σ = 23 bits/word.

D. Coding for Error-Detection and -Correction

Parity bits may be added to an information word for the detection and/or correction of errors due to channel noise. Various types of codes have been developed for this purpose; here, only the cyclic block codes will be discussed because, as a class, these appear to be the most powerful, well-developed and easily implemented choice.*

First, consider the random-error-correcting** capabilities of these codes as a function of the number of parity bits. The following assumptions, which appear realistic, are made to simplify this comparison:

1. The number of information bits transmitted per unit time is fixed;
2. There are k information bits per word (Here, k = 9, corresponding to the status word derived in Section C).

---

* A detailed exposition of this class is contained in Peterson and Weldon.[23]

** A random-bit error is one which occurs independently of all other errors.

3. The binary symbols are equiprobable and have equal energy.
4. The channel noise is additive (no fading), normally distributed and white.
5. The signals are detected via noncoherent, frequency-shift keying.
6. The average received signal power is fixed (i.e., it is independent of bit frequency).

In view of Assumptions 1, 2 and 6, the addition of parity bits would result in a decrease in the energy per bit. Thus prior to decoding, the probability of an error occurring within a code word would be increased by two mechanisms--the bit-error probability would be increased due to a decrease in signal-to-noise ratio, and the number of bits per word would be increased. However, after the decoding process, the word error probability would usually be less than it would be if no parity bits are used.

The random-error-correcting properties of several (n, k) codes, which are among the most powerful known for this purpose, are compared in Table XVII. Here, the following symbols are employed:

n = the total number of bits per word;

d_o* = the BCH bound[23] on the minimum Hamming distance;

E = the average signal energy per bit;

N_o = the power spectral density of the noise;

P_e = the probability of a bit error ($P_e = \frac{1}{2}e^{-\frac{E}{2N_o}}$)

P_c = the probability of obtaining the correct code word after decoding.

---

* If a (BCH) code is characterized by d_o, then it can correct all combinations of t_o or fewer errors, where $d_o = 2t_o + 1$.

** The equation is valid for noncoherent detection of a frequency-shift keyed signal in a non-fading channel.

TABLE XVII

COMPARISON OF SEVERAL RANDOM-ERROR CORRECTING CODES

(n, k)	d_o	$\frac{E}{N_o}$ (dB)	P_e	$1 - P_c$ (approximate upper bound)
(9, 9)	0	14.2	1.0×10^{-6}	9×10^{-6}
(15, 9)	4	12.0	1.9×10^{-4}	3.8×10^{-6}
(21, 9)	6	10.5	1.8×10^{-3}	7.5×10^{-6}
(31, 9)	12	8.8	1.1×10^{-2}	1.0×10^{-6}

Note that P_c is only moderately improved if parity bits are used. Further, as the decoding process would require a special-purpose computer,[23] the use of these codes may not be feasible.

A more effective means of reducing $1 - P_c$ would be to increase E/N_o. For example, if no parity bits were employed and E_o/N_o = 20db, then $1 - P_c \doteq 10^{-21}$. This would, of course, correspond to the virtual elimination of random errors.

In practice, spurious, nonstationary and sustained disturbances, or burst noise, would tend to cause groups of bit errors (burst errors).* In these cases, increasing E/N_o may not be adequate since the instantaneous noise power could be unpredictably large. Here, codes designed for error-detection and burst-error-correction could substantially improve communication system performance.

Let t_w, the time required to transmit one code word, be fixed (i.e., it is independent of n). All burst errors of length b, which would be due to noise bursts of duration $\frac{bt_w}{n}$, would require at least 2b parity bits for

---

* A burst error of length b is a sequence of b bits of which at least the first and last are in error.

correction. Several superior burst-error-correcting codes are shown in Table XVIII. For example, a (15, 9) code could correct one error less than or equal to 3 in length in a single code word.

Noise bursts of duration greater than $\frac{bt_w}{n}$ would result in uncorrectable burst errors; however, all burst errors of up to duration (n - k) and most of those greater than (n - k), would be detectable.* For example, one well-designed (15, 9) code would detect all errors of length less than or equal to 6, 96.8% of all burst errors of length 7, and 98.4% of those of length 8 or greater. Thus, in most practical cases, the probability of an undetected error could be made negligible. In practice, the duration of noise bursts would, at times, probably exceed $t_w/2$; hence, to avoid false corrections, cyclic codes should be used for error detection only.

The decoding circuits associated with error detection and burst error correction, unlike those for random error correction, are simple and inexpensive. Some typical circuits can be found in Peterson and Weldon.[23]

TABLE XVIII

THE PERFORMANCE OF SOME BURST-ERROR CORRECTING CODES

(n, k)	Burst-Correcting Ability b	$\frac{b}{n}$
(15, 9)	3	.20
(19, 9)	5	.26
(21, 9)	6	.29
(25, 9)	8	.32

Note: $\frac{b}{n} < 0.5$, and the upper bound may be approached only by choosing n - k large.

* Any cyclic code with n - k parity bits could detect a burst error of length n - k or less; also the fraction of bursts of length b > n - k that could be undetected is $2^{-(n-k-1)}$ for b = n - k + 1, and $2^{-(n-k)}$ for b > n - k + 1. Thus, the only burst errors that could be undetected are those which transform one code word into another.

E. Synchronization

Synchronization between transmitter and receiver is essential to the operation of a clocked communication system. In the application of interest here, one channel could be shared by many separate transmitters and receivers through time-division multiplexing and the loss of synchronization could have serious consequences. For example, if the transceiver in one vehicle were out of synchronization with the system, it could interfere with communications between the other vehicles and the sector computer.

Synchronization is also important for control purposes as it provides the time reference for the vehicles' trajectories. A value for X_c, however precise, has little meaning if the corresponding time, at which it is applicable, is not known. Thus, a reliable time reference is as necessary as a reliable position reference.

The following synchronization levels are listed in order of decreasing time ambiguity:

1. Carrier synchronization (This would be required if coherent detection methods were employed);
2. Bit synchronization to mark the beginning of each bit.
3. Word synchronization to denote the beginning of each code word.
4. Frame synchronization to define the time interval (T_c) in which all vehicles were addressed at least once.

Theoretically, each of the lower synchronization levels (1 - 3) could be derived from a higher one. However, in practice, it is easier to achieve and and maintain total synchronization by using separate methods for some or all of the lower levels.

The following methods have been discussed in detail by Stiffler:[24]

1. The use of separate time and/or frequency channels (synchronization at any of the levels listed could be achieved in this manner);
2. The application of maximum-likelihood techniques on the information portion of the signal to achieve carrier and bit synchronization; and
3. Special coding methods (prefix, comma, and comma-free methods) to achieve word and frame synchronization.

Since the achieving of synchronization is especially critical in a vehicle-control application, some combination of these methods would probably be employed in practice.

F. Conclusions

If the a priori probability structure, which was described in Section B, were acceptable, then the required channel capacity would be some 5,000 to 10,000 bits/sec depending upon the number of parity bits employed.

Also, a large signal-to-noise ratio should be a primary design goal, as $\frac{E}{N_0} > 20$ dB could result in a virtual elimination of random errors.

Burst errors could be effectively detected and/or corrected via the use of a cyclic block code. Ultimately, it may be more practical to simply detect errors and not correct them.

Finally, the importance of synchronization in sector communications and control should not be underestimated--particularly in the application of interest here.

CHAPTER IV

INFORMATION SOURCES FOR LONGITUDINAL CONTROL

A. Introduction

There are two types of information sources for vehicle longitudinal control shown in Fig. 2--one to provide state information to each controlled vehicle, and a second to provide such information directly to the sector computer. Hereafter, these sources are defined as Information Source 1 and Information Source 2, respectively.

The following general requirements should be satisfied by both types of sources:

i) The signal available at the receiver (either onboard each vehicle or at the sector computer) should have a large signal-to-noise ratio;

ii) This signal should be available in an unambiguous form over the expected range of state deviations--both in the lateral and longitudinal directions;

iii) The signal characteristics should be essentially unaffected by the environment; and

iv) The source must be highly reliable so that the probability of a failure is extremely low.

In addition, it was considered highly desirable to obtain highly accurate measures of vehicle position (< 0.2 ft error) and "instantaneous" velocity (± 1.0 ft/sec) so that precise control could be achieved under small time-headway conditions.

B. Information Source 1

The primary purpose of an Information Source 1 configuration is to provide sufficient information so that satisfactory individual vehicle control can be achieved in both normative and emergency situations. To achieve this, it would be desirable to have the following quantities available:

i) X_c, X and/or $X_c - X = \Delta X$;

ii) V_c, V and/or $V_c - V = \Delta V$; and

iii) A_c, A and/or $A_c - A_c = \Delta A$.

Each vehicle would receive its command state from the sector computer, and it's actual state (X, V and A) from the information source. However, there is presently no efficient, accurate and economical approach for determining A--at least from information received from a roadway-based reference. Therefore, the configurations to be discussed will not involve the acquisition of this quantity.*

During a previous study,[16] three roadway-based configurations were suggested for use as (or in conjunction with) an Information Source 1. The results of detailed experimental studies of each of these are discussed here.

C. Information Source 1--A Crossed-Wire Approach

One approach to the measurement of vehicle position is shown in Fig. 12. Here, widely spaced position-reference markers, hereafter referred to as absolute position markers, would be employed to provide an accurate measure of a vehicle's absolute position when that vehicle passed over a given marker. This would be achieved by employing the detected signal to zero a vehicle-borne counter. Intermediate position markers would be located between the absolute

---

* This does not preclude the onboard measurement of A, and its use as a control/feedback variable.

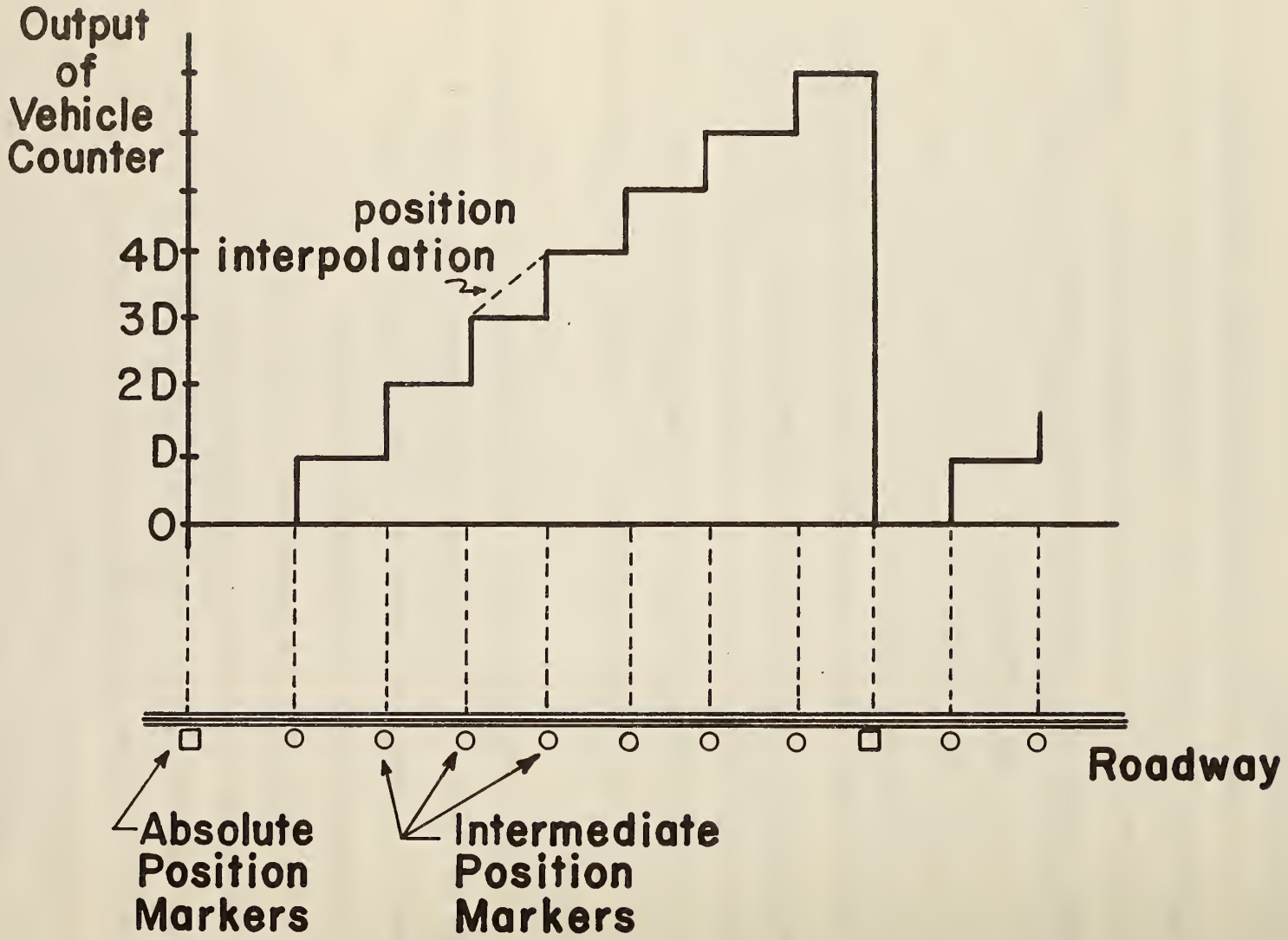

Fig. 12 A discrete element, information source with position interpolation.

markers, and the vehicle counter would be advanced as it passed each such marker. The distance traversed between each marker pair could readily be estimated; thus, a continuous estimate of X would be available.

It was previously noted[16] that magnets could be successfully employed for absolute position markers because of their high reliability, good reported position resolution (within ±1 in), insensitivity to environmental factors, and low-noise properties. The use of current-carrying wires for intermediate position markers would result in both these and the following advantages:

i) Superior position resolution (within ±1/16 in);

ii) Multiple-frequency excitation for coding purposes; and

iii) Dual use as an information source and a communication channel.

a) A Crossed-Wire Configuration--Theory

Consider the spatially periodic, wire configuration shown in Fig. 13.* Note that the magnetic flux, which results from current flowing in this wire, reverses direction each half period (i.e., for each 1 ft of longitudinal travel). It is relatively simple to sense this reversal and thereby determine the position of each lateral wire.

A sensor configuration, which has been used successfully, consists of two vehicle-borne, vertically mounted coils spaced 6 in apart, as is shown in Fig. 14. The leading coil is used to sense the phase of the field relative to the phase sensed by the reference coil.

---

* This configuration has been imbedded in a 2209-ft section of asphalt berm strip adjacent to the FHWA Skid Calibration Pad at the Transportation Research Center of Ohio as is described in Appendix A.

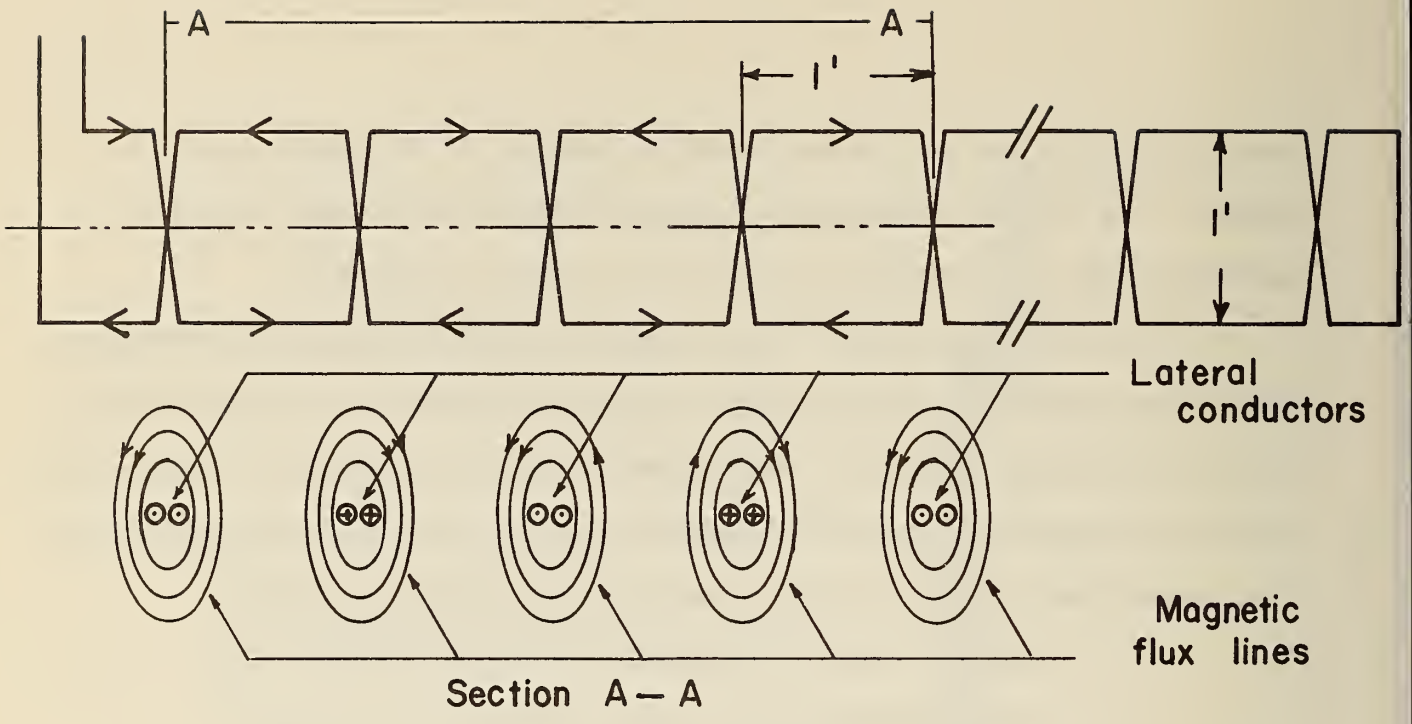

Fig. 13 Top view of a spatially periodic wire configuration.

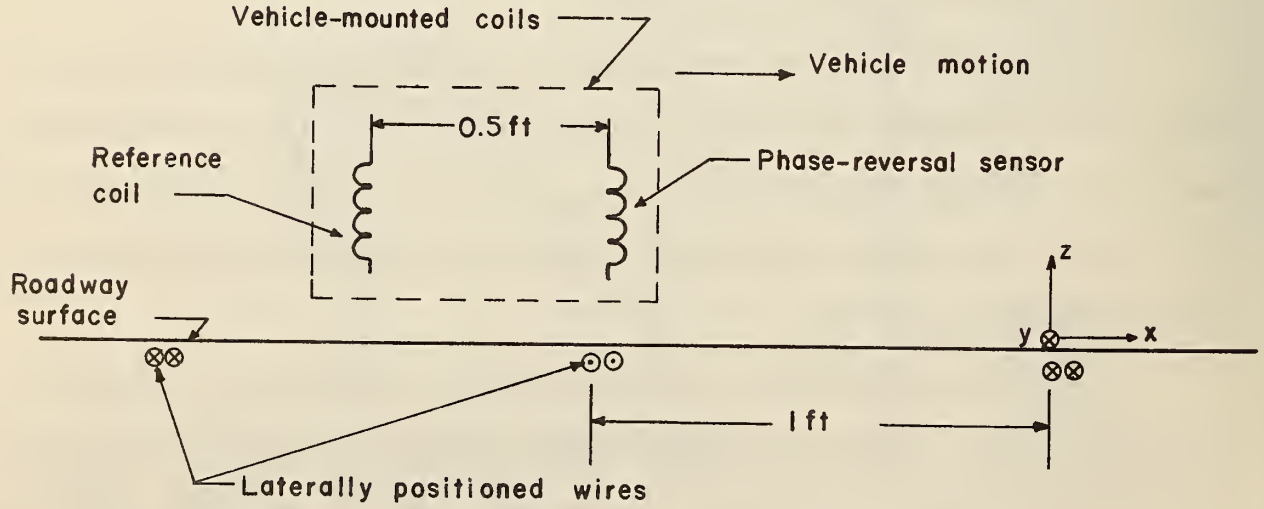

Fig. 14 The relationship of two vertically mounted, sensing coils to the laterally positioned wires.

Assume that at a given instant, both coils are between two laterally positioned wires. The fluxes linking these coils would therefore be in phase. As the lead coil approaches and passes a wire, the flux linking this coil would decrease in magnitude, go to zero over the wire, and then increase in magnitude but with a phase opposite to that linking the reference coil.

The signal processing required is achieved as shown in the block diagram of Fig. 15. The voltages induced in the sensing coils are amplified, filtered to attenuate undesired frequency components, and multiplied. When the two voltages are in phase, the multiplier output is

$$(A \cos \omega t)(B \cos \omega t) = \frac{AB}{2} [\cos 2\omega t + 1]$$

The cos $2\omega t$ term is attenuated by the low-pass filter following the multiplier leaving the constant $+AB/2$ and additive ripple at 2ω rad/sec.

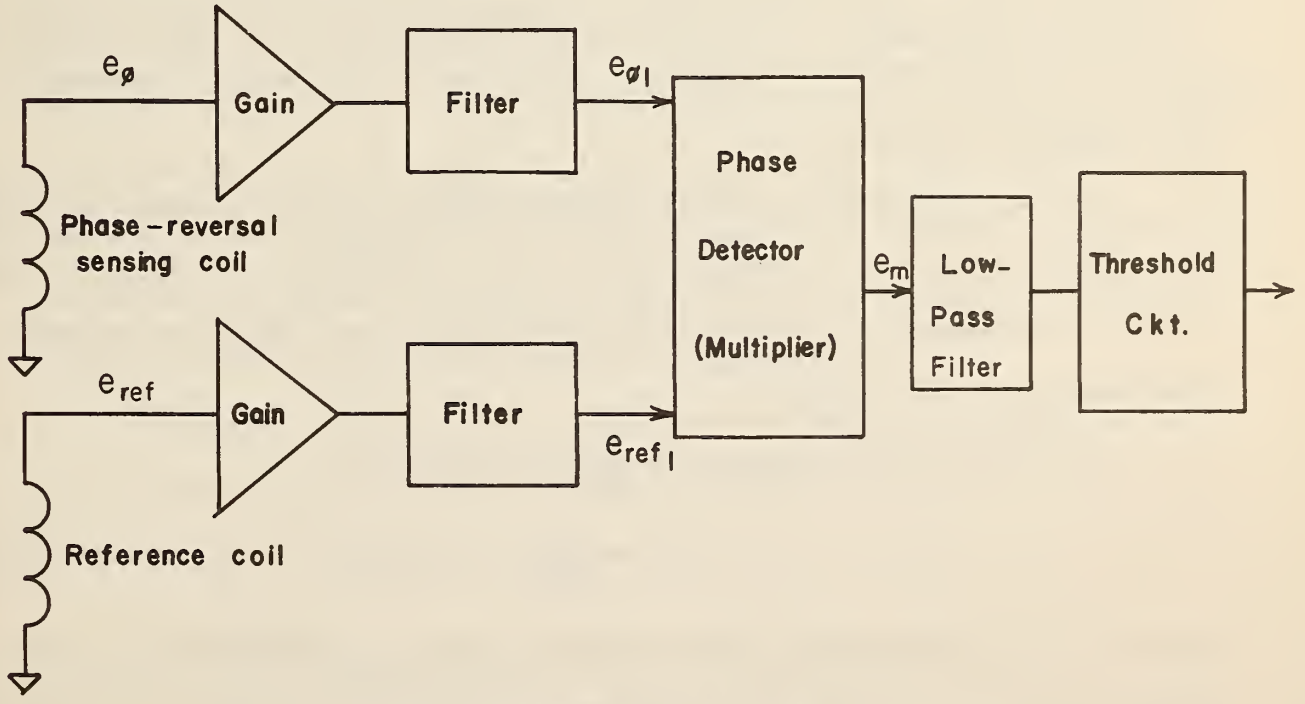

Fig. 15 A block diagram of the signal processing employed with the "crossed-wire" approach.

When the phase of the voltage in the lead coil reverses relative to that of the reference, the multiplier output becomes

$$[A \cos (\omega t + 180^0)][B \cos \omega t] = - \frac{AB}{2}[\cos 2\omega t + 1].$$

In this case, the output of the low-pass filter is -AB/2 with additive ripple at frequency 2ω rad/sec.

Thus, when the phase-reversal sensing coil crosses a lateral wire, the low-pass filter output changes from a positive to a negative polarity. The threshold circuit responds to the zero crossing of this change by changing its binary state (This advances a vehicle-borne counter per Fig. 12).

Since the spacing between lateral wires is twice that between the two sensing coils, the reference coil crosses the lateral wire when the phase-reversal sensing coil is midway between wire crossings, causing the sensor voltages to be in phase once again. The response of the threshold circuit to the resulting negative-to-positive transition of its input is ignored by all suceeding circuitry.

In this discussion, relative motion effects in the field-sensing process were ignored; however, the motion of the sensor relative to the magnetic field induces a component of voltage in the phase-sensing coil which can degrade the accuracy of the sensor.

The voltage (e) induced in a coil of N turns is

$$e = N \frac{d\phi}{dt} \quad \text{(volts)} \tag{4-1}$$

where ϕ = flux linking the coil in webers. This flux distribution may be modeled by

$$\phi = F(x, y, z)I \tag{4-2}$$

where I = current in amperes, and F(x, y, z) is a function uniquely determined

by the geometry of the current-carrying wire configuration, and x, y, and z are the coordinates of the sensing point relative to an origin of coordinates located as shown in Fig. 14. Because of the complexity of the configuration employed, it is simpler to determine F experimentally rather than analytically.

Upon substituting (4-2) into (4-1), there results

$$e = N\left[F(x, y, z)\frac{dI}{dt} + I\frac{\partial F}{\partial x}\frac{dx}{dt} + I\frac{\partial F}{\partial y}\frac{dy}{dt} + I\frac{\partial F}{\partial z}\frac{dz}{dt}\right] \qquad (4\text{-}3)$$

The last two terms (i.e., the voltage components due to lateral velocity and vertical velocity) can be neglected since both $\partial F/\partial y$ and $\partial F/\partial z$ are very small over practical ranges of y and z; therefore, only the first two terms need be considered.

Based on empirical measurements with z = 0.34 ft, y = 0 and N = 400, F(x, 0, 0.34) was as observed to be as shown in Fig. 16. This function is characterized by a substantial peak magnitude and a nonnegligible rate of change with respect to x. Thus, the first term in (4-3), which is the voltage induced due to the time-changing current in the wire, is not negligible provided the current frequency is sufficiently high. It is this term which varies in magnitude and phase in accordance with the earlier discussion and should therefore be considered as the desired voltage component.

The second term in (4-3) is due to the longitudinal velocity of the vehicle, and it is proportional to both V and $\partial F/\partial x$. Note from Fig. 16 that the derivative, in the region of a wire crossing, is constant and

$$\left|\partial F/\partial X\right|_{\text{wire crossing}} \doteq 1.59 \times 10^{-9} \quad \text{weber/amp/ft.}$$

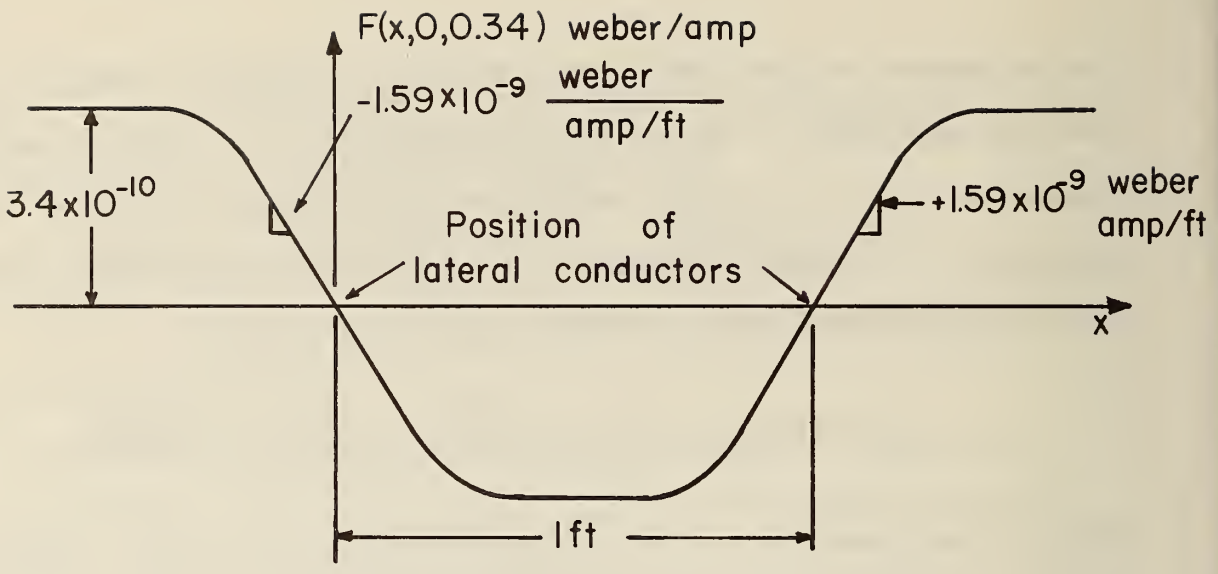

Fig. 16 An empirically determined choice for F(x, 0, .34).

If the current were specified as

$$I = I_m \sin \omega t,$$

then, in the vicinity of a crossed wire (located at x = 0 for convenience), the voltage (e_ϕ) induced in the phase-reversal sensing coil would be

$$e_\phi = 1.59 \times 10^{-9} \times NI_m \omega \cos \omega t + 1.59 \times 10^{-9} NI_m V \sin \omega t \qquad (4\text{-}4)$$

The units of x and V are ft and ft/sec, respectively.

The waveform associated with the first term is shown in Fig. 17(a) while that associated with the second is shown in 17(b).

Clearly, the net induced voltage is not zero at the wire crossing. The extent to which this unwanted component degrades the position measurement will be discussed after a consideration of the voltage induced in the reference coil.

Consider the voltage induced in the reference coil when it is located midway between two laterally positioned wires (see Fig. 14). The function $F(x, 0, 0.34) = 3.4 \times 10^{-10}$ weber/amp, both at and near this point (see Fig. 16), and $\partial F/\partial x \doteq 0$. The voltage induced in the N-turn reference coil is thus

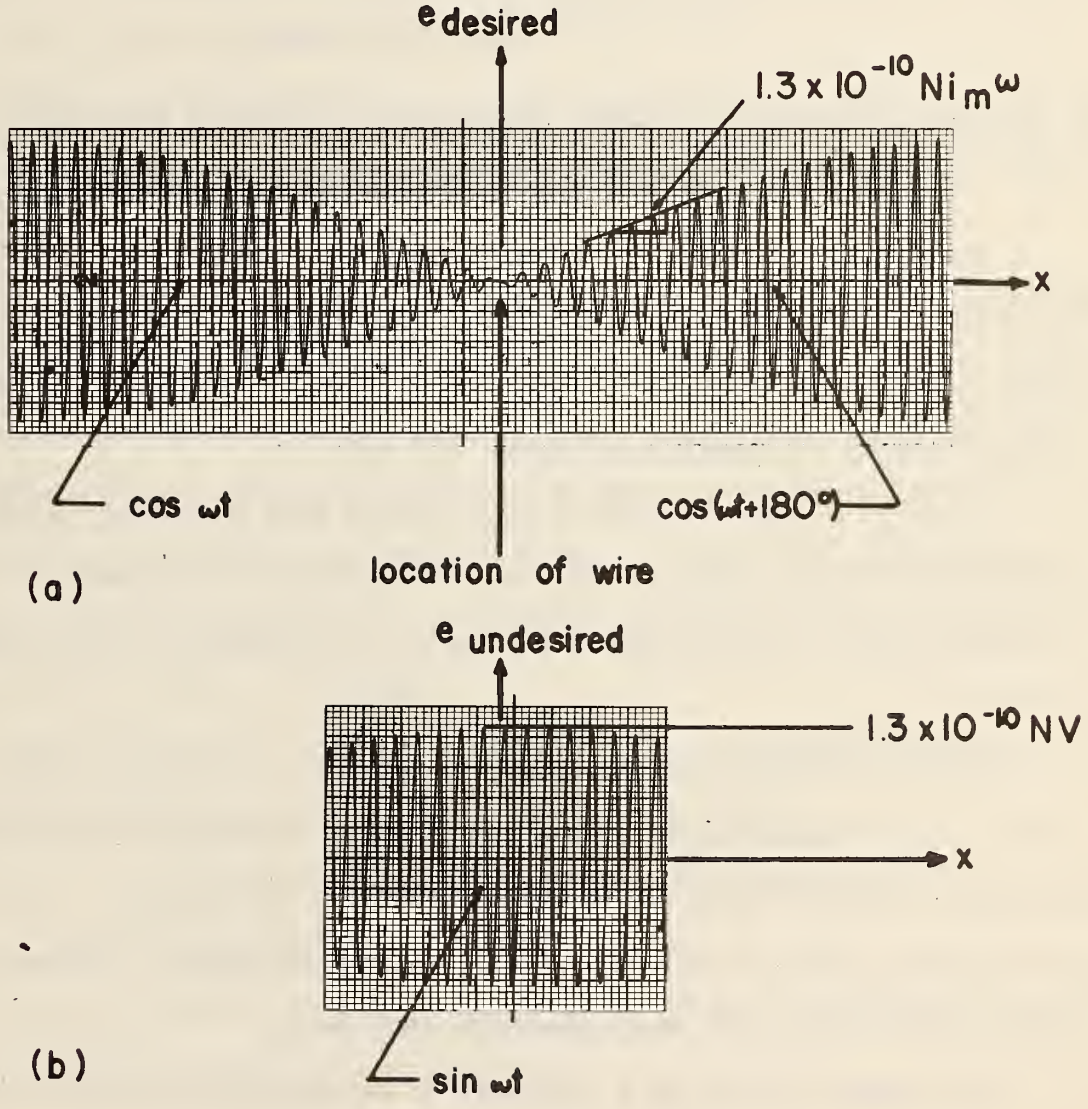

Fig. 17 Voltages induced in the phase-reversal sensing coil.

$$e_{ref} = 3.4 \times 10^{-10} NI_m \omega \cos \omega t.$$

As shown in Fig. 15, this quantity and e_ϕ (as given by (4-4)) are multiplied to give

$$e_m = 2.7 \times 10^{-19} N^2 \omega^2 I_m^2 (1 + \cos 2\omega t)x$$
$$+ 2.7 \times 10^{-19} N^2 \omega V I_m^2 \sin 2\omega t.$$

If the low-pass filter completely eliminated the terms at frequency 2ω, then

$$e_m = 2.7 \times 10^{-19} N^2 \omega^2 I_m^2 x.$$

However, to limit the delay caused by a first-order, low-pass filter to that which would cause an error of approximately 1/64" at 100 ft/sec, the filter time constant must be no more than 15 μsec or, equivalently, the filter corner frequency (f_c) must be at least 10.6 kHz.

Clearly, ω must be sufficiently greater than ω_c so that appreciable attenuation of the 2ω rad/sec component is achieved. For example if f = 50 kHz, a filter with f_c = 10.6 kHz would attenuate the resulting 100 kHz component by 19.5 db.

The net effect of the residual sin $2\omega t$ term in the input to the threshold circuit, is an indication of a wire crossing approximately 4×10^{-4} inches before the actual crossing (Here, it is assumed that V = 100 ft/sec). For all practical purposes, this is negligible. If the wire-excitation frequency were greater than 50 kHz, this error would be even less.

The upper limit on this frequency is determined by practical considerations such as increased signal attenuation at higher frequencies. A choice of f = 50 kHz has been a satisfactory choice in practice.

b) Experimental Results

The crossed-wire information source was evaluated using an instrumented test vehicle and current-carrying wires (f = 50 kHz) placed laterally across a roadway. The vehicle-borne equipment included a light-emitting diode and a

photo-transistor pair,mounted adjacent to a sensing-coil configuration so that the emitted beam could be interrupted by an optically opaque rod projecting vertically upward from the test track. The frequency response of the optical system was sufficiently high that its delay contributed less than .02 in error for a vehicle speed of 100 ft/sec.

Tests were conducted over a speed range from 29.4 to 88 ft/sec.* The measured error (e_x) is plotted versus V in Fig. 18, and it should be noted the errors are within a ±1/16 in band over the specified speed range.

It is difficult to correlate these results with the predicted errors due to motion as the latter are so small (e.g., 4×10^{-4} ft for V = 100 ft/sec); however, as the measured errors are not much greater than the uncertainty associated with the measuring technique employed, it seems reasonable to attribute them to unavoidable experimental error. In any event, these errors are so small as to be negligible and an extremely accurate, discrete measure of vehicle position may be obtained.

The wire-crossing information can be used to obtain an estimate of V(t) wherein there would be two sources of estimation error:

1) The uncertainty due to position quantization; and

2) The number of missed counts (c).

Since the wire spacing was 1 ft., the distance error in T sec would be $1 + c$, and the velocity estimation error would be

$$\frac{1 + c}{T} \qquad \text{(ft/sec)}.$$

The probability of a missed count appears to be exceeding small, and this expression reduces to 1/T.

---

*These and other tests were conducted by Michael Heslop and will be discussed in detail in both a forthcoming Master of Science thesis and a TCL working paper.

Negative indicates delayed distance from wire.

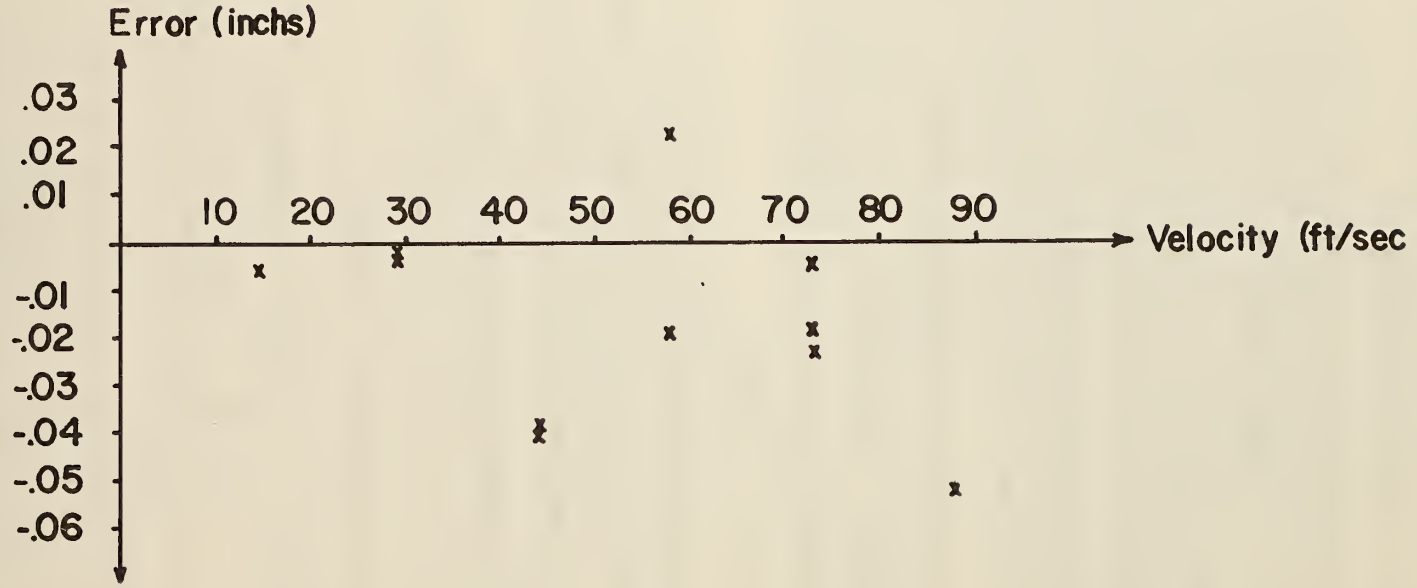

Fig. 18 Measured position error.

For T > 1 sec, this error would be small and thus an excellent measure of "average" velocity would be obtained. However, for T small, (e.g., T ≅ 0.1 sec), a large error could result. This approach would therefore not be satisfactory for the measurement of "instantaneous" speed.

c) A Vehicle State Estimator

Consider the achieving of position interpolation between intermediate position markers (see Fig. 12) and the estimation of V and A. This could be done by using unprocessed vehicle state information; however, as such information is often contaminated with undesired errors (e.g. bias errors, calibration errors, noise, etc.), it is generally desirable to employ some effective means of processing so as to achieve improved interpolation and/or state estimation.

Two commonly employed approaches, Kalman filtering[25] and adaptive filtering,[26] were not considered here as these generally result in complex processors, which presently appear to be unnecessary for a vehicle control application. Instead, a simpler approach, based on the concept of conditional feedback,[27] wherein the signal errors are attenuated without affecting the desired quantities, is employed.

Assume that the following measurement devices are available:

1) A wire-detector and -counter to provide a measure of $X + e_X$;
2) A tachometer to provide $V + e_V$; and
3) An accelerometer to provide $A + e_A$.

The terms e_X, e_V, and e_A are errors in the measurement of position, velocity and acceleration, respectively. The six quantities specified have the following important properties:

1) X, V, and A are obviously related; i.e. $A = pV = p^2X$;

2) The measurement of $X + e_X$ is made at discrete intervals and thus is available in a sampled form (The sampling frequency is $\frac{\overline{V}}{D}$ where D is the nominal wire spacing and $\overline{V}$ is the average vehicle speed between adjacent wires);

3) The mean of e_X is zero for the sources of this error--detector noise, motion-induced voltage, inaccurate wire placement, etc.--would not result in an offset error.*, **

4) The signal e_Y would be composed of both slowly varying and high-frequency components (These would result from tachometer miscalibration, variations in tire-rolling radius, wheel slippage, and high-frequency noise which is invariably present).

5) The signal e_A would also be composed of both slowly varying and high-frequency components, as the accelerometer output would be significantly influenced by gravitational forces and vehicle motions and/or vibrations.

These observations were utilized in the design, via the conditional feedback concept, of one possible state estimator (See Fig. 19). The estimator's inputs

---

* The mean of e_X is actually dependent on V; however, for the speed range of interest, it is less than 0.01 ft and thus is assumed negligible.

** It is assumed that the probability of a miscount is negligible.

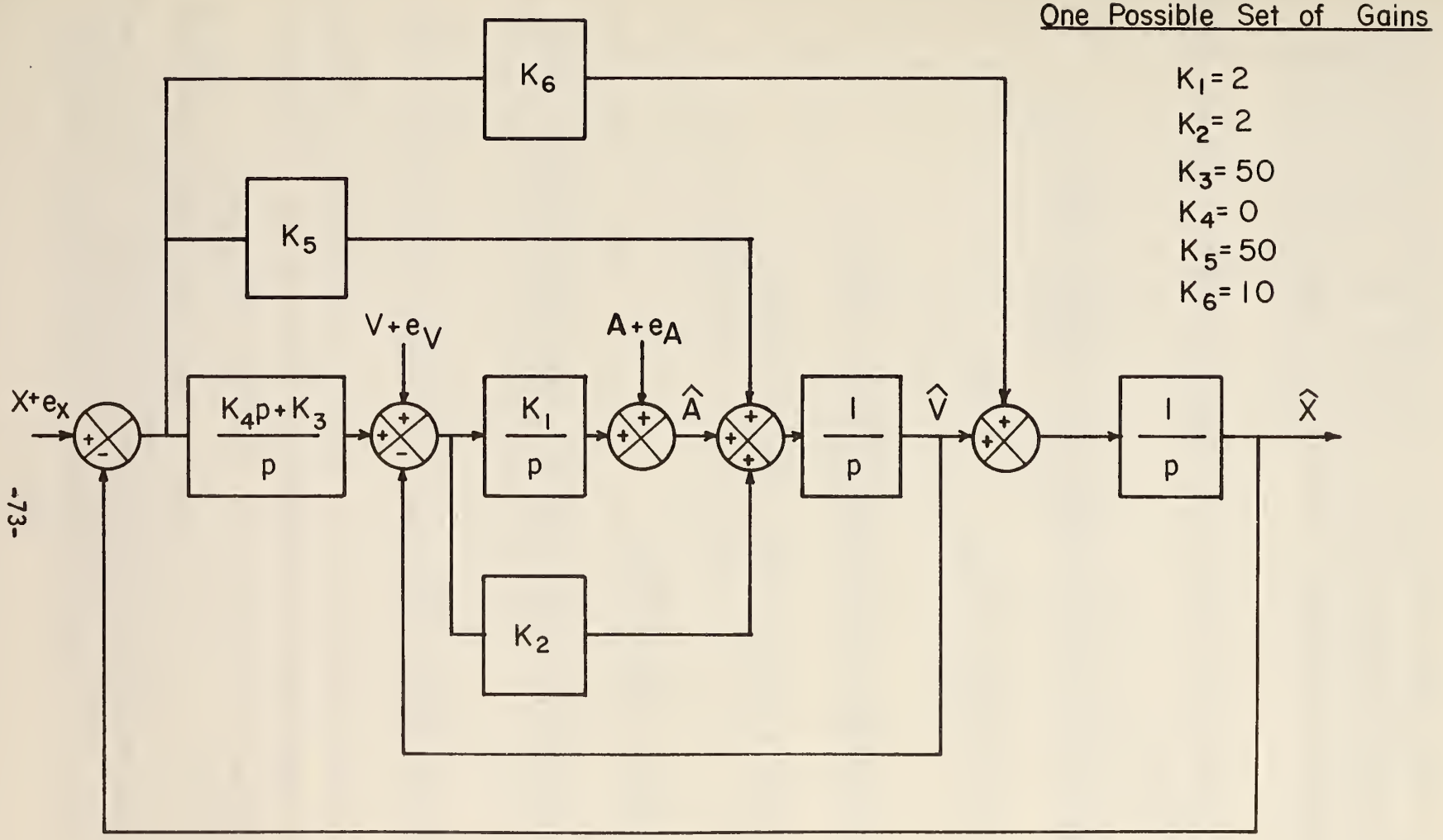

Fig. 19 A theoretical block diagram of the state estimator.

are $X + e_X$, $V + e_V$, and $A + e_A$, and its outputs are continuous estimates of position ($\hat{X}$), velocity ($\hat{V}$) and acceleration ($\hat{A}$). For the present, $X + e_X$ is assumed to be continuous; the effects of sampling are discussed later.

These estimates are given by the following equations, which are readily derived from Fig. 19:

$$\hat{A} = A + \frac{p^4 + (K_2 + K_6)\, p^3 + (K_2K_4 + K_2K_6 + K_5)\, p^2 + K_2K_3\, p}{\Delta} e_A$$

$$+ \frac{K_1p^3 + K_1K_6p^2 + K_1K_3p}{\Delta} e_V + \frac{K_1K_4p^3}{\Delta} e_X;$$

$$\hat{V} = V + \frac{p^3 + K_6p^2}{\Delta} e_A + \frac{K_2p^3 + (K_1 + K_2K_6)\, p^2 + K_1K_6p}{\Delta} e_V$$

$$+ \frac{(K_2K_4 + K_5)\, p^3 + (K_1K_4 + K_2K_3)\, p^2 + K_1K_3p}{\Delta} e_X;$$

$$\hat{X} = X + \frac{p^2}{\Delta} e_A + \frac{K_2p^2 + K_1p}{\Delta} e_V$$

$$+ \frac{K_6p^3 + (K_2K_4 + K_2K_6 + K_5)\, p^2 + (K_1K_4 + K_2K_3 + K_1K_6)\, P + K_1K_3}{\Delta} e_X,$$

where

$$\Delta = p^4 + (K_2 + K_6)p^3 + (K_2K_4 + K_2K_6 + K_5 + K_1)p^2 + (K_1K_4 + K_2K_3 + K_1K_6)p + K_1K_3.$$

Note that the desired quantities (X, V, and A) are unaffected by the estimator, while the measurement errors are attenuated by either low-pass, high-pass, or band-pass functions.

The gains (K_i, $i = 1,\ldots, 6$) should be judiciously chosen to minimize effects of measurement errors, and to insure stable behavior. For the specific measurement devices used here, the gain values shown in Fig. 19 result in

low-noise and essentially unbiased* position and velocity estimates, and an unbiased acceleration estimate.** Note that high-frequency components of e_A would be present in $\hat{A}$; thus, low-pass filtering of $\hat{A}$ should be included as part of the vehicle controller.

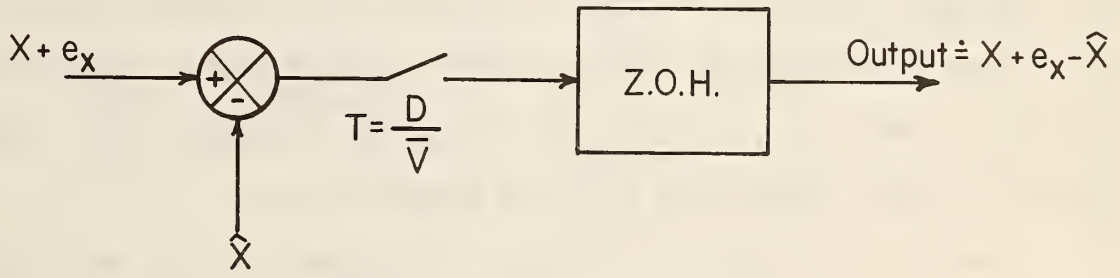

Fig. 20 Reconstruction of $X + e_X - \hat{X}$.

As noted previously, $X + e_X$ would be available in discrete form. A continuous position error $X + e_X - \hat{X}$ may be obtained by using a sample-and-hold device as shown in Fig. 20. The modified estimator would be stable for $\frac{\bar{V}}{D}$ sufficiently large (i.e. the additional phase lag introduced by the zero-order hold does not result in a phase margin $\leq 0^0$). For example, if the gains were chosen as in Fig. 19, the estimator would be unstable for $\frac{\bar{V}}{D} \lesssim 5$ Hz. For small $\frac{\bar{V}}{D}$'s, some circuit modification would be necessary; one possibility is discussed shortly.

---

* In steady-state operation, the expected values of $\hat{X}$, $\hat{V}$, and $\hat{A}$ are X, V, and A respectively, and $X - \hat{X}$, $V - \hat{V}$, and $A - \hat{A}$ are bounded; i.e., they are not accumulative.

** The K_i's could have been chosen to be "optimum" is some statistical sense. However, this would require a detailed statistical description of the errors, which is difficult (if not impractical) to obtain. At present, it suffices to employ K_i's which are merely adequate.

The circuit, shown in Fig. 21, is one physical realization of the theoretical state estimator of Fig. 19. The inputs are a pulse from the threshold circuit shown in Fig. 15, $V + e_V$, and $A + e_A$, and the outputs are $\hat{A}$, $\hat{V}$ and $\hat{\hat{X}}$. The latter is an interpolation of the distance between adjacent laterally positioned wires; i.e., $\hat{X} = \hat{\hat{X}}$ + the stair-step output of the wire-counter.

For $\frac{\overline{V}}{D} > 10$ Hz (e.g., D = 1 ft; V > 10 ft/sec) the circuit operation would be nearly identical to that of the theoretical estimator shown in Fig. 19, except that D is subtracted from the position output when a wire-crossing is detected. Then, $X + e_X - \hat{X}$ $(= D - \hat{\hat{X}})$ is sampled and held; after a negligible delay ($\doteq$ 50 μsec), Integrator A is also reset to $X + e_X - \hat{X}$.

For $\frac{\overline{V}}{D} < 10$ Hz (e.g., D = 1 ft; V < 10 ft/sec), S_1, S_2, and S_3 are opened, and Integrator B is reset to zero to maintain overall stability. In this mode, $\hat{V}(t)$ would not be unbiased, and $\hat{X}(t)$ ($\hat{\hat{X}}$ + the wire count) could contain small corrective steps at the instants of wire-crossings. If these steps were small ($\dot{<}$ .05 ft), and vehicles were not required to operate at 0 < V < 10 ft/sec for prolonged time periods, this should not be a problem. The potential accuracy ($X - \hat{X} < .05$ ft and $V - \hat{V} < 1.0$ ft/sec) and utility of these signals in constant-speed situations will be evaluated in full-scale experiments scheduled for 1977.

It should be noted that a similar circuit, using only two inputs, $X+e_x$ and $V+e_v$, has been employed in full-scale, vehicle-controller tests in which current-excited, crossed wires were the absolute position reference. In contrast to the circuit of Fig. 21 which provides $\hat{\hat{X}}$, $\hat{V}$ and $\hat{A}$, this circuit provided only $\hat{\hat{X}}$.

---

* A portion of this circuit (Fig. 21) was employed in the "phantom-signal" controller tests which are described in Chapter VI.

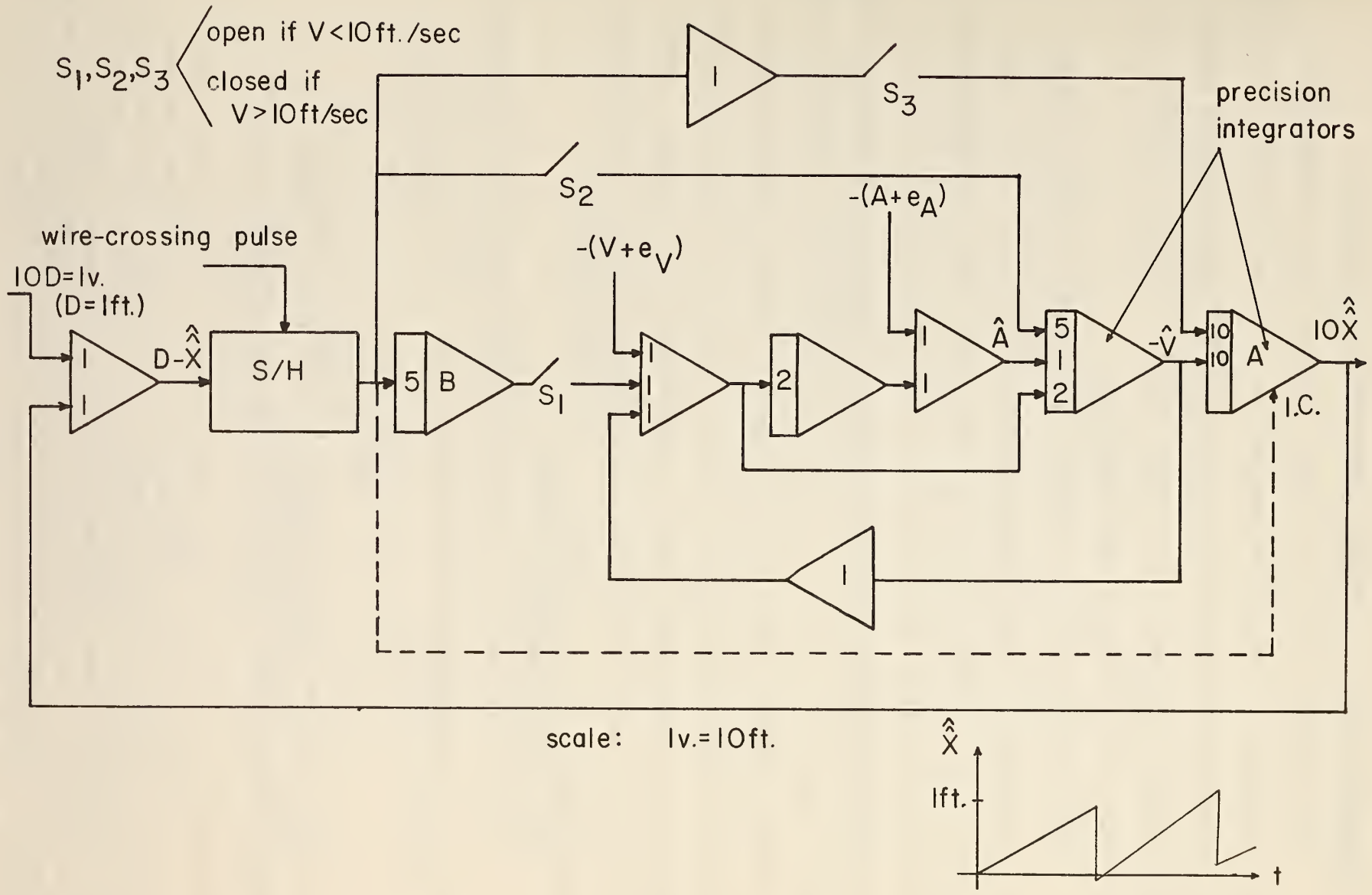

Fig. 21 One possible realization of the state estimator.

D. Information Source 1--A Helical Transmission-Line Approach

Each controlled vehicle can obtain continuous state information via helical transmission lines either embedded in, or located alongside, a roadway. This approach was introduced in an earlier report;[16] here, following the more detailed account in Appendix B, the basic theory is presented together with the results from an intensive laboratory study.

The spatially periodic, stationary, phase-difference (θ_d) waveform shown in Fig. 22 can be obtained by properly exciting two helically wound transmission lines, detecting the field near those lines with two probes, and processing the detected signal (See Fig. 23). The wave period, P_e, is the "effective pitch length of the lines" and is a function of the individual pitch lengths P_1 and P_2. A vehicle can use the information in this waveform to obtain a continuous position signal. Thus, a "coarse" position indication would be obtained by counting the sudden 360^0 phase changes and a "fine" indication by measuring the linear phase difference between each pair of changes. In the context of the previous discussion, the former may be viewed as discrete stationary markers.*

a) Position Uncertainty

The position uncertainty associated with this approach is proportional to the error in the phase-difference measurement. In the error-free case,

$$X_T = \frac{\theta_T}{360} P_e$$

where X_T is the true position and θ_T is the true phase-difference. If the measured phase-difference (θ_m) were in error (i.e., $\theta_m = \theta_T \pm \theta_e$) then,

---

* A moving waveform can be achieved if one transmission line were excited at a slightly different frequency from the other. Then, the waveform would move longitudinally along the roadway at a speed $v = \Delta f \, P_e$, where Δf is the frequency difference. Each vehicle would be commanded to track a certain phase-difference value and all vehicles would move in synchronism under normal operation. As this approach is less versatile than the stationary one in that changes in intervehicular spacing are more difficult to achieve, it will not be considered further.

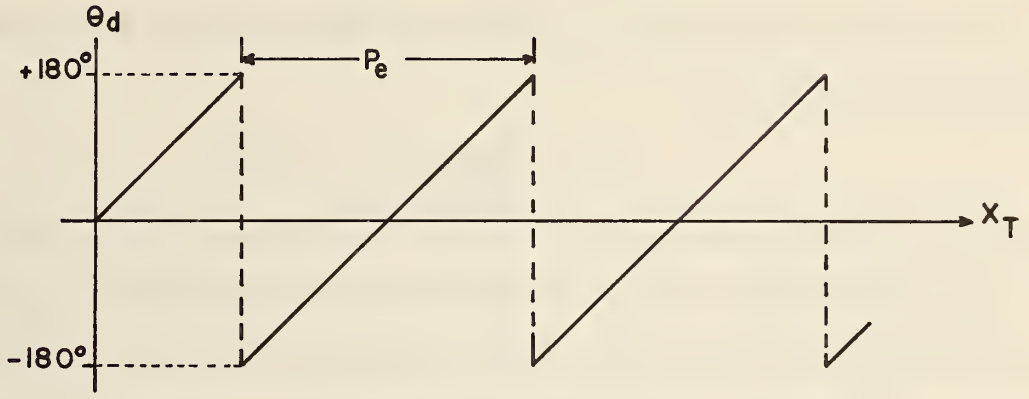

Fig. 22 Theoretical phase-difference versus the longitudinal coordinate.

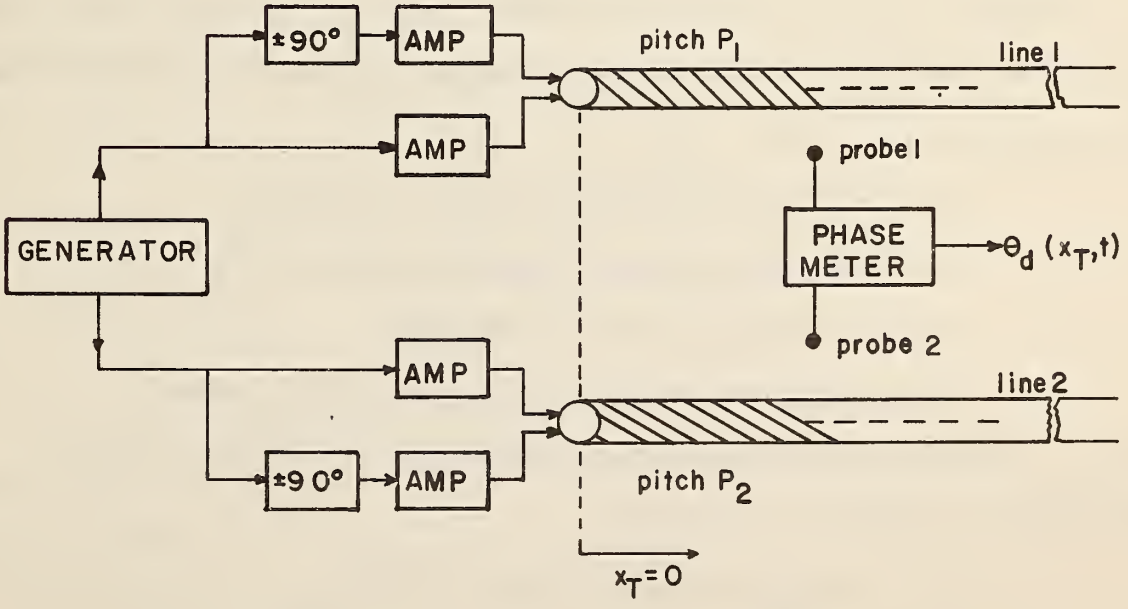

Fig. 23 Proposed longitudinal information source using two helically wound transmission lines.

$$X = X_T \pm X_e = \frac{\theta_T}{360} P_e \pm \frac{\theta_e}{360} P_e$$

Thus, the position uncertainty, X_e, would be directly related to the phase-difference error (θ_e) via

$$X_e = \frac{\theta_e}{360} P_e. \qquad (4\text{-}5)$$

Note that for a greater choice of P_e, θ_e must be decreased for a given X_e.

The phase-difference error is comprised of two components; θ_{e1} which arises from obvious factors (noise, meter inaccuracy, etc) and θ_{e2} which is due to lateral and vertical motions of the signal-detecting probes (See Fig. 23). The latter is a function of the isolation between each probe and the "other" transmission line. The derivation of the equations governing this error is given in Appendix B along with their experimental verification. An upper bound on θ_{e2} (i.e., θ_{e2_m}) was obtained and will be used in the following analysis.

Consider Fig. 24, where it is assumed that the lines are placed below the vehicle (the lines could be side-mounted but the maximum achievable separation would be less). With

$\pm\Delta z$ = the maximum lateral motion of the vehicle

$\pm\Delta y$ = the maximum vertical motion of the vehicle

y_o = the nominal height of the probes

d = the separation of the lines and of the probes,*

then $\theta_{e_{2_m}}$ results when the probes are at positions (1) in Fig. 24 as is demonstrated in Appendix B from which,

$$\theta_{e_{2_m}} \leq \sin^{-1} \left(\frac{r}{a}\right)^2 + \sin^{-1} \left(\frac{r}{b}\right)^2,$$

---

* If the probe and line separations are not equal due to construction factors, this would be accounted for via a larger Δz.

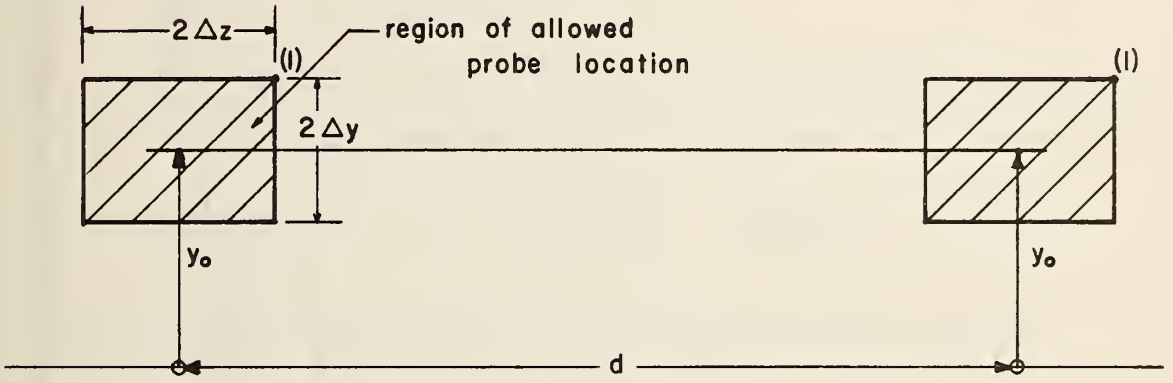

Fig. 24 Line placement and the region of allowed probe location.

where

$$r^2 = (y_0 + \Delta y)^2 + (\Delta z)^2$$
$$a^2 = (d - \Delta z)^2 + (y_0 + \Delta y)^2$$
$$b^2 = (d + \Delta z)^2 + (y_0 + \Delta y)^2.$$

A plot of $\theta_{e_{2_m}}$ vs.d for two extreme cases--y_0 = 4", Δy = 3", and Δz = 4", and y_0 = 8", Δy = 6", and Δz = 8"--is shown in Fig. 25.

This can be used with Eqn. (4-5) to determine the necessary effective pitch and allowable tolerance on the vehicle lateral and vertical deviations.

For example, to achieve a ±2" tolerance on Δy with P_e = 5 ft, then $\theta_e < 12^o$. If such factors as noise, meter inaccuracy etc. result in no more than 5^o of error, then $\theta_{e_2} \leq 7^o$. Note from Fig. 25, that

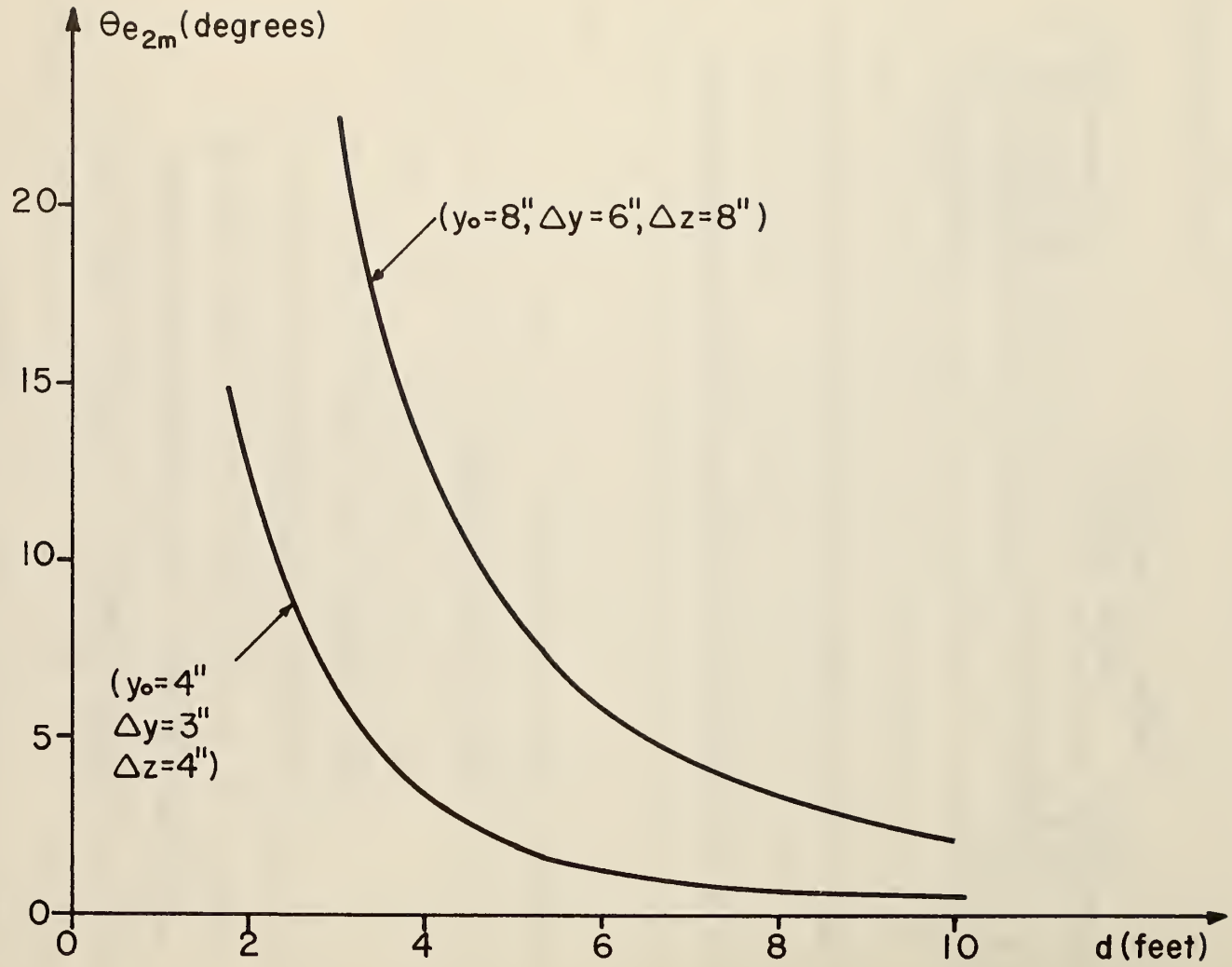

Fig. 25 Upper bound on the phase-difference error versus line separation.

d must be greater than 3 ft for the small-tolerance case and at least 5.5 ft for the looser tolerances.

b) Velocity Estimation

An estimate of vehicle velocity may be obtained by counting the number of 360^{o} phase transpositions in an interval of T sec and employing

$$\hat{V} = \frac{nP_e}{T} . \quad \text{(ft/sec)}$$

Under constant-speed conditions, the estimation error would be

$$\frac{\pm P_e}{T} ,$$

and, as $1 \leq P_e \leq 10$ (ft), it would be unacceptably large for small T.

A more desirable technique would be to employ the approach depicted in Fig. 26. When a measurement were desired, a timer would be initiated and activated over T sec during which time n transpositions would be counted. In addition, the fraction of pitch length (f_1) traveled before the first transposition and the fraction (f_2) traveled after the n^{th} transposition would be measured. The total distance traveled would be

$$(n-1)P_e + f_1P_e + f_2P_e .$$

Under constant-speed conditions, an assumption of no missed counts, and with $\pm\theta_e$, the phase errors in measuring f_1 and f_2, the maximum velocity uncertainty would be

$$\pm \frac{2\theta_e P_e}{360\ T} .$$

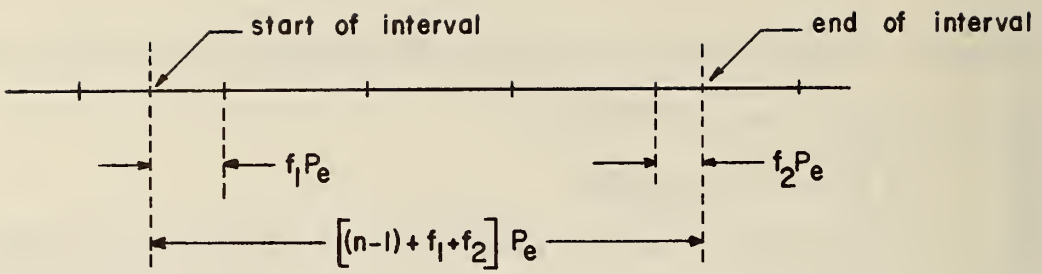

Fig. 26 Interval for velocity estimation (elapsed time T).

With parameter choices of P_e = 1 ft, T = .1 sec and $\theta_e = 12^o$, this maximum uncertainty would be 0.67 ft/sec. If it were necessary to use a larger P_e, a corresponding reduction in θ_e would be required to maintain the same uncertainty.

c) On the Choice of Line Parameters

It is impractical to completely "specific" the optimum helical line configuration (P_1, P_2, P_e, d) at this time, as this specification would depend upon other facets of the longitudinal control system. This would include the specification of tolerances on the permitted lateral and vertical motions of the vehicle, the allowable longitudinal position deviations, and the physical form of the roadway. With these data, the necessary design equations are available to then specify the optimum line geometry.

At the completion of this study, it was discovered that a flat "helical line" appears to possess properties as good as, if not better than, the helical line. If so, a major cost factor (that of the manufacturing and installing of the helical lines) will be circumvented. A variety of flat-line configurations will be evaluated under the continuation contract to ascertain a desirable shape for such lines.

E. Information Source 1--Scattering Enhancement Plates

a) Theory and Review

A third approach for obtaining almost continuous position and velocity information is via a Doppler radar in conjunction with enhancement plates embedded in, or mounted alongside, a roadway. This approach was previously described,[16,28] and low-speed test results were presented.

In essence, energy is directed at a roadway surface by a vehicle-borne Doppler radar, and part of this energy is reflected back. When no plates are present, nonspecular reflection occurs, and the returned signal is contaminated with both amplitude modulation (AM) and frequency modulation (FM). This results in errors in the position estimate. When the plates are present (Fig. 27), specular reflection occurs such that the returned signal contains little or no unwanted modulation, and an almost ideal Doppler signal

$$e(t) = E_0 \cos \left[\frac{2\pi}{\lambda/(2 \cos \alpha_p)} X_T(t)\right]$$

results. Here, λ is the wavelength of the radiation, $X_T(t)$ is the instantaneous position of the vehicle relative to some reference point, and α_p is the tilt angle of the enhancement plates. The amplitude, E_0, is essentially constant due to the regularity of both the reflectors and their spacing. In addition, the signal is enhanced if all returning rays are forced to constructively interfere. This is achieved by spacing the plates at intervals of $n\lambda/(2 \cos \alpha_p)$, where n is an integer.*

Since the phase of e(t) is proportional to $X_T(t)$, the latter could be determined within an uncertainty of $\pm\lambda/(2 \cos \alpha_p)$ by counting the number of 360^0 phase changes (This uncertainty could be halved if 180^0 phase changes were counted). For example, one change would occur every 0.65 in (1.64 cm) if $\alpha_p = 30^0$ and an X-band (10.5 GHz) radar were used.

*E_0 is a maximum for n = 1, however, this would require employing a maximum number of plates.

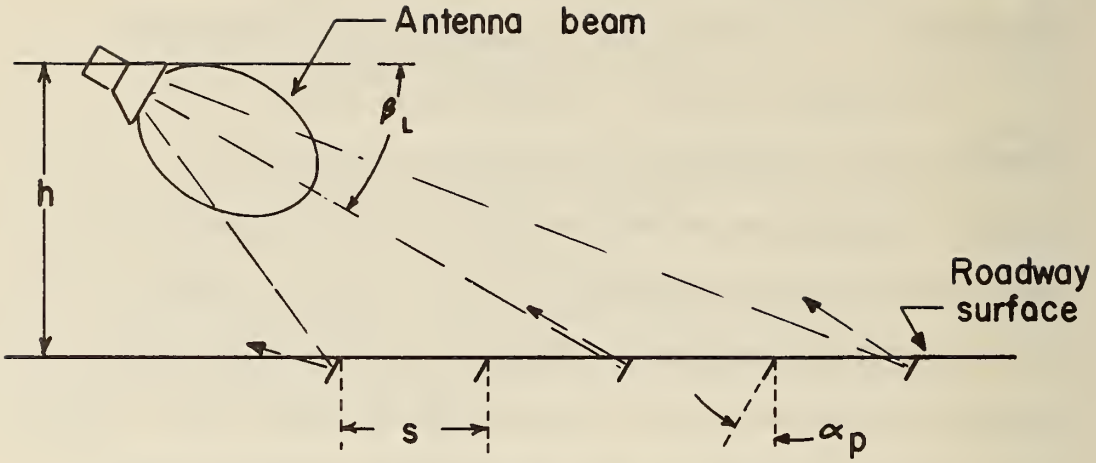

Fig. 27 Behavior of vehicle-mounted Doppler radar with enhancement plates.

b) Experimental Studies

Both laboratory tests and field tests were performed during the period covered by this report. The latter were performed at the skid calibration pad at TRCO. Here, as is depicted in Appendix A, 370 aluminum plates (2 in x 5/16 in) were positioned, with $\alpha_p = 30^0$, in a 2-in wide wooden structure embedded directly below an asphalt-surface roadway. The plate spacing was 0.65 in (1.64 cm), and the 20-ft structure was covered with an epoxy sealant. An X-band (10.5 GHz) radar, with an 18^0 (3 db) beamwidth horn, was mounted on a test vehicle such that h = 1 ft and $\beta_L \doteq 30^0$. Here h is the antenna height above the roadway and β_L is the "look angle" (See Fig. 27).

The results of low-speed tests ($0 \leq V \leq 5$ ft/sec) over this section of track were consistent with those from the laboratory; i.e., both a substantial increase ($\doteq$ 15 db) in backscattered energy and an almost ideal detected signal with no appreciable AM or FM resulted with the use of the plates. In addition, due to the slight curvature of the epoxy covering, water did not accumulate over the plates, and no loss of signal resulted when the tests were repeated under extremely wet conditions.

Four months later, high-speed tests were conducted. However, during this delay, the covering had cracked, and some sections of the wooden structure had absorbed considerable moisture. A severe signal attenuation was encountered over those sections. Thus, in practice, weatherproofing would be necessary for plates installed below the ground. If side-mounted plates were employed, the problem should not be as severe as good drainage should be easily achieved.

Additional tests were conducted with the plates located above the asphalt surface.* Here, a test vehicle was driven over the plates, and the detected signal was processed, via a counter, to indicate the number of 360^0 phase reversals. Two laterally positioned, current-carrying wires were used to define the beginning and end of a specified distance of some 6 feet, and a wire-crossing detector (similar to that discussed in Section C) was employed to activate the counter only over this distance. The vehicle was automatically steered, via the use of a wire-reference system, to insure that the radar antenna was always above the plates.

In the first series of tests, $\alpha_p = 20^0$, $\lambda/(2 \cos \alpha_p) = 0.6$ in (1.52 cm), and tests were conducted for speeds ranging from 7.3 to 88 ft/sec and β_L = 15, 20, 30, and 40 deg.

---

* In view of previous findings, the results obtained here should be the same as those obtained with buried plates.

One typical low-speed result is shown in Fig. 28 with e(t) in (a), the processed counter input in (b), and the processed wire-crossing, detected signal in (c) (The latter specifies the counting interval). Note that the returned signal over the plates was much stronger ($\doteq$ 15 db) than that over asphalt, and also that it was virtually free of both amplitude and frequency modulation. The presence of such modulation results in a loss of counts as can be seen from the processed "asphalt" returns of (b). The number of phase reversals counted over the specified distance was 121, and, as 121 plates were contained herein, a precise measure of distance traveled was obtained.

The same results* were obtained from each test in this series: i.e.,

i) The returned signal over the plates was much stronger ($\doteq$ 15 db) than that over the asphalt, and it was virtually free of both AM and FM; and

ii) The number of phase-reversal counts was constant at 121.

In a second series of tests, the effectiveness of $\beta_L < 15^0$ and $\beta_L > 4.0$ was evaluated. Consistent counts were not obtained, and it appears β_L should be maintained in the range between $15\text{-}40^0$ to eliminate the need for a precise mounting of the radar and/or a JANUS configuration to account for vehicle pitch.[16]

The effect of removing plates (for possible reduction of construction costs) were examined in a third series of test runs. Here, one of each two plates was removed and then 3 of each 4. The procedure was identical to that previously described and tests were conducted for various combinations of V and β_L within $7.3 < V < 88$ ft/sec and $15^0 \leq \beta_L \leq 40^0$.

---

* It was not possible to present similar data for a high-speed test because of the limited frequency response of the strip-chart recorder employed.

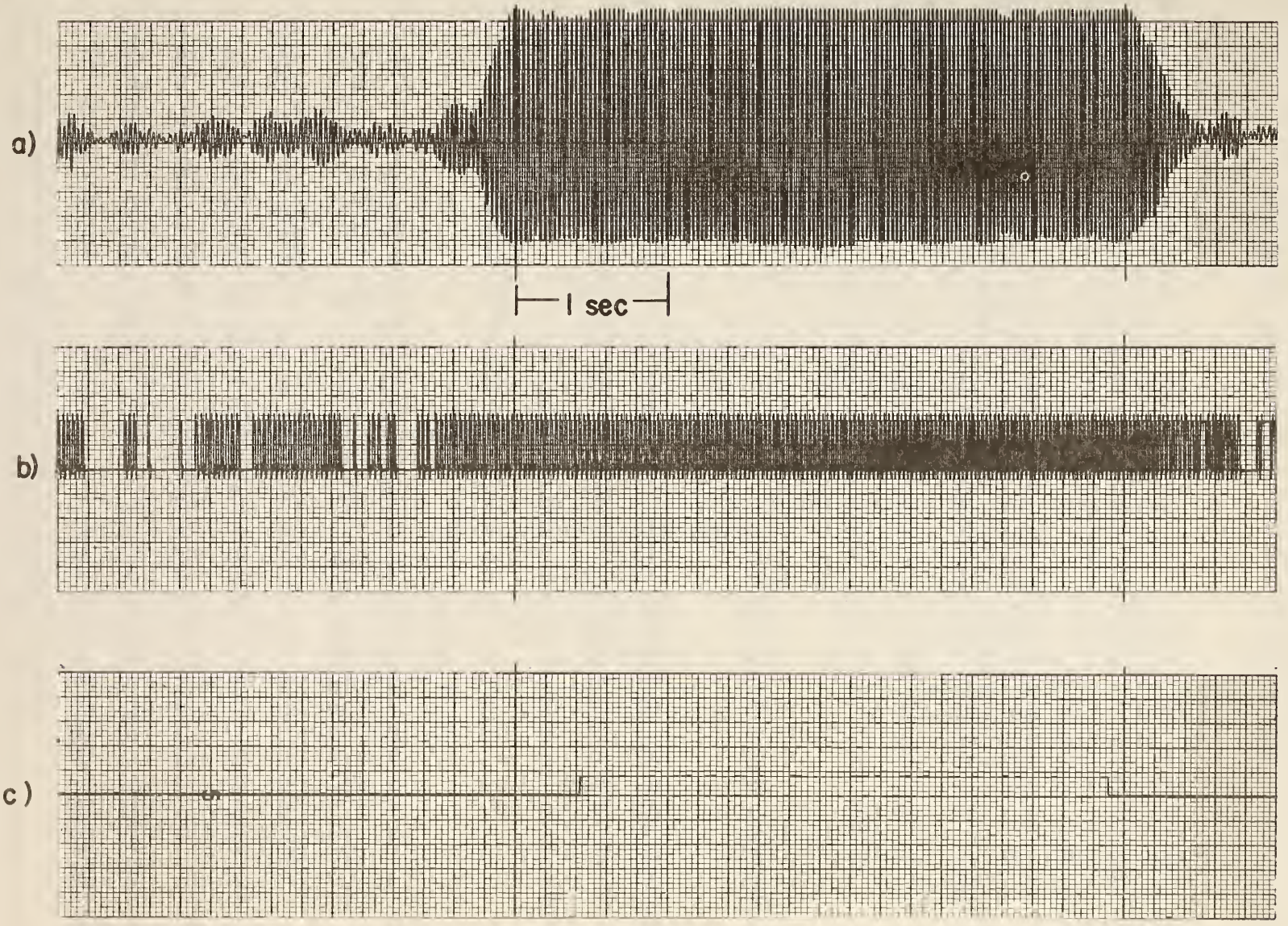

Fig. 28 Low-speed, full-scale test data for Doppler radar with enhancement plates.

Excellent results, a strong modulation-free signal and a consistent count of 121*, were obtained over the entire speed range and

$$20^0 \leq \beta_L \leq 30^0$$

Thus, the allowed variation in β_L was reduced. If more than 3 out of 4 plates were removed (e.g., 7 out of 8), consistent results could not be obtained for any (V, β_L) combination.

In a fourth series of tests $\alpha_p = 45^0$, with all other conditions remaining the same. The results were consistent with those reported here.

c) Sources of Position Estimation Error

In the ideal cause, one would have N counts for a distance X and

$$X = Nq.$$

In practice, the estimate would be

$$\hat{X} = X \pm \delta X$$

where the position estimation error (δX) would be dependent upon three factors:

1) The uncertainty in position due to quantization in units of $q = \lambda/(2 \cos \alpha_p)$;
2) The error due to the number (c) of missed (or added) counts; and
3) The error due to random variations in λ and/or α_p and thus in q.

The contribution due to the first is q; and that due to the second, cq. The quantity c is difficult to estimate since no counts were missed or added in the experiments performed to date. As a strong signal is received from the plates, the signal-to-noise ratio is large, and the probability of a missed count should be very small.

---

* Note the system does not "count plates" but simply counts units of $\lambda/(2 \cos \alpha_p)$ provided an approximately ideal signal of sufficient strength is received.

The contribution from the third factor would be $N\delta q$, where δq is the variation in q due to variations in λ and/or α_p. As variations in α_p would be distributed about a fixed average value, the effects should cancel over any appreciable number of counts. Thus, δq should be influenced mainly by variations in λ.

The composite δx is thus

$$\delta x = q + cq + N\delta q,$$

and the normalized error over a distance $X = Nq$ is

$$\frac{\delta x}{Nq} = \frac{c + 1}{N} + \frac{\delta q}{q}$$

Consider a typical case wherein a 10.5 GHz radar with a frequency stability of .1% (a common specification) is employed; $\alpha_p = 30^0$, and the measurement interval is 1.3 ft. Here, q = 0.65 in, N = 24 and δq = .00065 (due to changes in λ only), and

$$\frac{\delta x}{Nq} = .043$$

This error would be substantially decreased as X were increased; e.g., for X = 13 ft and N = 240, $\frac{\delta x}{Nq} = .0052$ (If 180^0 phase reversals were counted, these errors would be halved).

If an incorrect count (c = 1) were to occur, the errors would increase to .084 and .093, respectively. In addition, if the α_p variations did not, on the average, cancel these errors would be .094 and .019, respectively, for maximum variations of $\pm 1^0$. These errors would be an unrealistic worst-case, i.e.--these could be eliminated via a scale-factor change.

d) Estimation of Instantaneous Velocity

The precise position estimates available from this approach may be employed to obtain excellent estimates of a vehicle's instantaneous velocity provided an accurate time reference were available. One feasible approach is shown in Fig. 29. Here, the processed Doppler signal would be the input to an auxiliary counter, which would be triggered "on" for an interval T by the time reference. The counter output (N) would thus be proportional to the average vehicle velocity over that interval. The later would be obtained via

$$V = \left(\frac{\lambda}{2 \cos \alpha_p}\right) \frac{N}{T} .$$

In a constant-speed situation, the velocity estimation error would be

$$\begin{matrix} + \\ - \end{matrix} \left(\frac{\lambda}{2 \cos \alpha_p}\right) \frac{1}{T} ,$$

assuming that no counts were missed per the previous discussion on position error.

This error is independent of velocity and dependent on λ, α_p and T. In practice, one should employ a very high-frequency radar (i.e., X-band or greater) so as to obtain a source/sensor configuration of a reasonable size. A practical choice would be a 10.5 GH_z radar (λ = 1.13in) and, per the previous discussion, a reasonable plate setting would be $\alpha_p = 30^o$. Then the measurement accuracy would be

$$\pm \frac{\lambda}{2 \cos \alpha_p} \frac{1}{T} = \pm 0.0544 \frac{1}{T} .$$

This quantity is plotted versus T in Fig. 30.

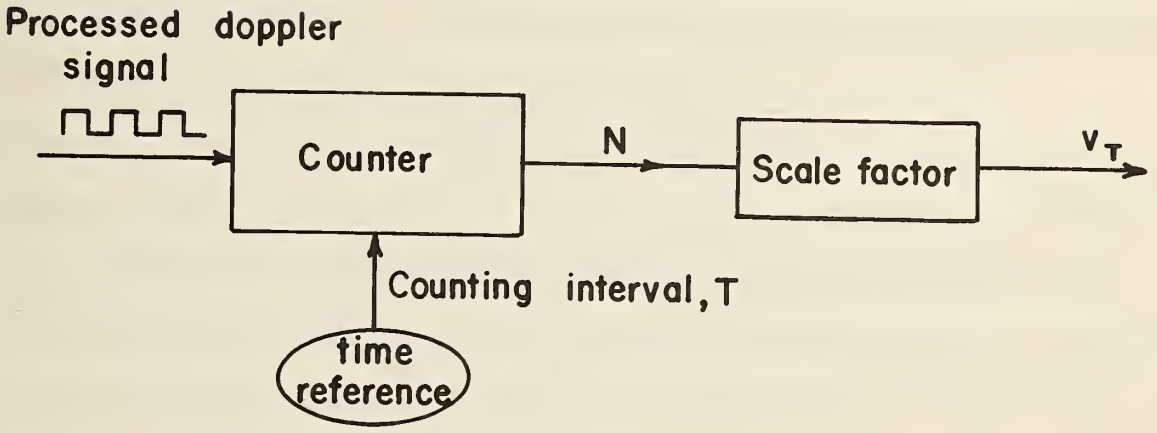

Fig. 29 One realization of velocity measurement.

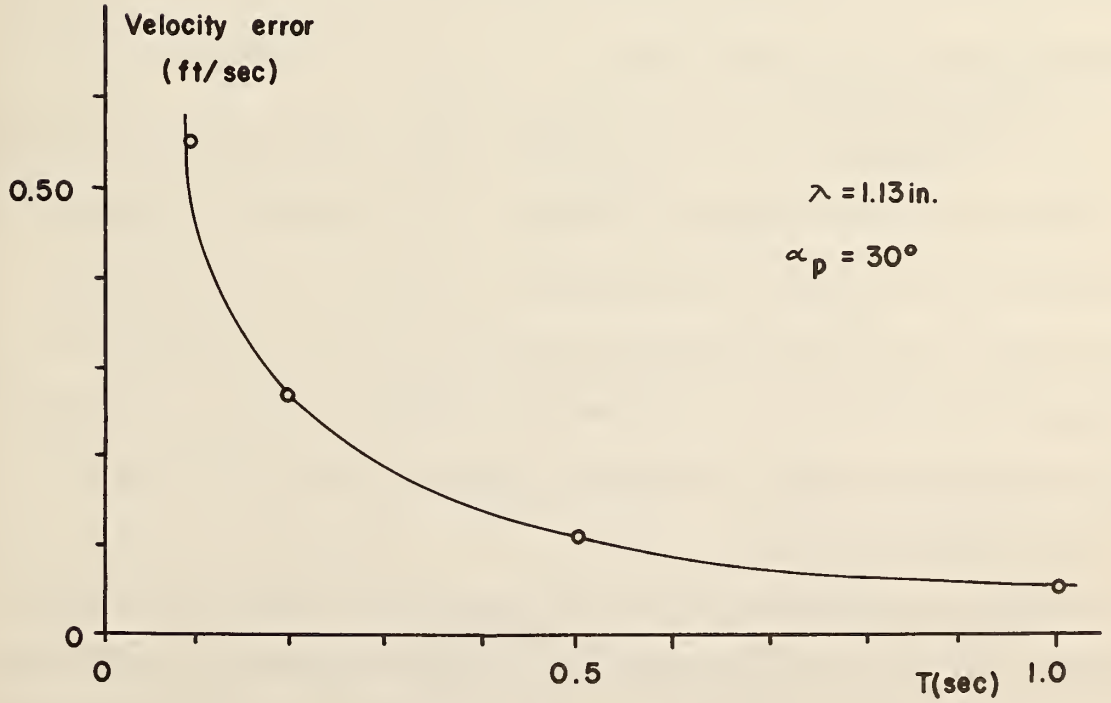

Fig. 30 Maximum measured error versus T--
constant-speed case.

To obtain velocity with an accuracy of some ±0.5 ft/sec, one must select $T \leq 0.1$ sec. Alternatively, one could count 180° phase changes for which the measurement accuracy would be

$$\pm \frac{\lambda}{2 \cos \alpha_p} \frac{1}{T} = \pm 0.0272 \frac{1}{T}$$

and select $T \leq 0.05$ sec.

In a constant acceleration (deceleration) situation, the average speed over the interval would be measured and not the true speed at the end of the interval. This results in an error of $\frac{AT}{2}$ as is discussed in Section F.

No experimental tests of this, or other suggested techniques, for estimating velocity were conducted during the past year.

F. Information Source 1--A Fifth Wheel

A fourth approach for obtaining position state information involved the use of a commercially manufactured fifth wheel.* This was not considered as a viable candidate for eventual implementation; instead, it was tested so that its accuracy as a position-measuring device could be established. This information would be useful, as it is sometimes necessary to use a fifth wheel in field evaluations of vehicle controllers because an installed information source is not always available.

This wheel was connected to the rear bumper of a 1969 Plymouth sedan and evaluated under both constant-speed and constant-acceleration conditions. The former encompassed 11 trials at each of 4 speeds (20, 40, 60 and 80 ft/sec)

---

* This unit was manufactured by Laboratory Equipment Corp., Mooresville, Indiana.

for a tire pressure (P_T) of 22 psi (The lower limit specified by the manufacturer, and 5 trials at each of these speeds for P_T = 35 psi (The upper limit specified). The latter involved tests with P_T = 22 psi and 35 psi. Those conducted with the lower pressure encompassed 12 trials for each of two speed-deceleration conditions--V_0 = 20 ft/sec, A_c = 5 ft/sec^2 and V_0 = 60 ft/sec, A_c = -5 ft/sec^2. The other tests included 5 trials for each of the same conditions. Data were collected only when the vehicle was operating either at a steady speed or at a constant acceleration/deceleration rate so that the replications, for a given condition, were conducted under nearly identical conditions. For example, the measurement interval for a deceleration test was selected as shown in Fig. 31.

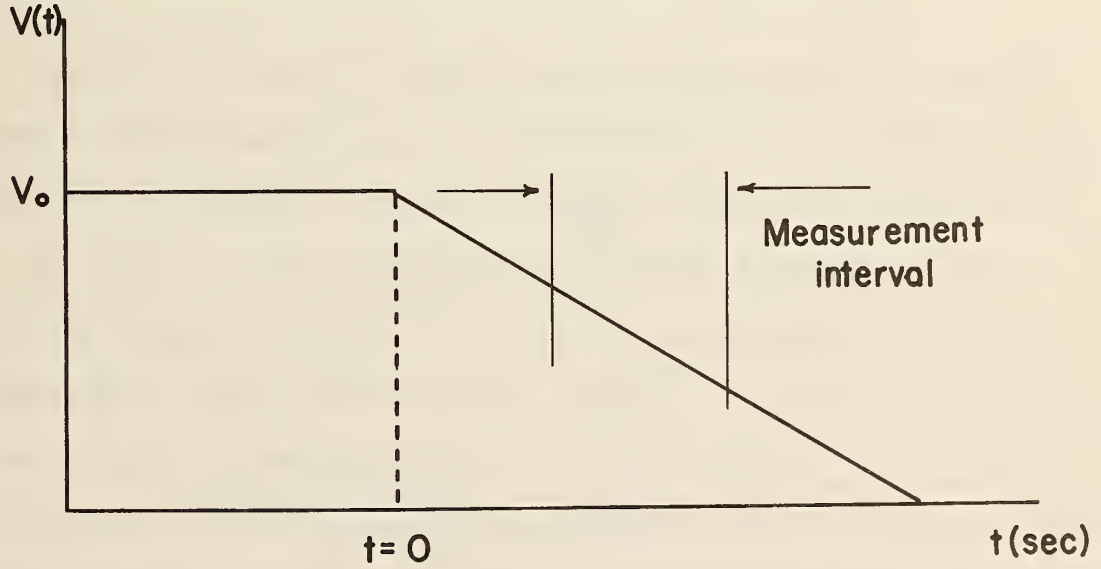

Fig. 31 Measurement interval during a constant deceleration test.

This interval was selected as 100 ft, and it was delineated via the laterally positioned, current-carrying wires described in Section C. These wires were laid on a fairly rough section of asphalt pavement.

The distance traveled, as measured by the fifth wheel, was obtained as follows:

A circular gear with N_T teeth was attached to the fifth-wheel axis. As the vehicle moved, this wheel rotated and these teeth passed a pickup unit wherein the passage of each tooth was counted. This count was initiated at the beginning of the measurement interval and terminated at its end. The measured distance (D) was obtained via

$$D = N\left(\frac{2\pi R}{N_T}\right) \tag{4-6}$$

where R is the effective radius of the 5th wheel*
and N is the total number of counts in an interval T.

The results from the constant-speed tests are shown in Table XIX where the mean count (μ) and standard deviation (σ) are shown for each condition. (These counts may easily be related to measured distance via Eqn. (4-6) with R = 1.0833 ft (for P_T = 22 psi) and N_T = 120). For P_T = 22 psi, the maximum range of the means was only 0.06%, and the maximum standard deviation was a low 3.21 at 80 ft/sec. In terms of distance, the latter corresponds to a distance error of ±.18 ft in 100 ft. In the high-pressure case, the mean range was greater (0.27%); however, $(\sigma)_{max}$ was only 2.24 corresponding to a distance error of ±0.13 ft in 100 ft. In essence for a given tire pressure, extremely consistent and accurate results were obtained; however, the results varied slightly with pressure--being some 0.33% lower for the greater pressure.

---

* This effective radius is a function of P_T and the tire-roadway interface. It can be specified by a simple calibration procedure involving (4-6) and a measurement of N from a field test over a known distance.

TABLE XIX

FIFTH-WHEEL DATA FROM CONSTANT-SPEED TESTS

P_T (psi)		V_o (ft/sec) 20	40	60	80
22	μ	1762.45	1763.36	1763.54	1762.55
	σ	0.69	1.12	2.75	3.21
35	μ	1755.20	1757.40	1756.20	1760.00
	σ	0.84	2.30	0.87	2.24

TABLE XX

FIFTH-WHEEL DATA

FROM

CONSTANT-ACCELERATION/DECELERATION TESTS

P_T	V_o, A_c	V_o = 20 ft/sec, A_c = 5 ft/sec^2	V_o = 60 ft/sec, A_c = -5 ft/sec^2
22	μ	1762.36	1766.00
	σ	0.92	2.10
35	μ	1755.2	1758.2
	σ	1.3	1.30

The results from the constant acceleration/deceleration tests are shown in Table XX. For a given P_T, these are extremely consistent both within this test and across the constant-speed case. This is evident from a comparison of the data in the previous table with that presented here. Also, note that the results for P_T = 35 psi are again generally lower than those for P_T = 22 psi.

The nonzero variance, for a given test condition, was probably caused by the bouncing of the fifth wheel and a corresponding incorrect count.

Clearly, the fifth wheel may be used to obtain an accurate measure of X provided the distance involved is not great. As the error would tend to be cumulative, an error of 0.18 ft in 100 ft could correspond to an error as large as 1.8 ft in 1000 ft. In a vehicle controller application, where tracking errors (ΔX) of 0.5 ft are expected, such an error could cause a considerable offset in the estimation of ΔX. In such situations, a fifth-wheel estimate of X should be used very carefully and only over relatively short distances.*

A measure of "instantaneous" velocity may be obtained using an approach similar to that described in Fig. 29. In a constant-speed situation, there would be two sources of estimation error:

1) The uncertainty associated with position measurement; and

2) The uncertainty due to position quantization.

A conservative choice for the former is, from the collected data,

$$\frac{12}{1763} D_T$$

---

* The fifth-wheel estimate of X could be used in conjunction with other unbiased position estimates (e.g., that obtained from crossed wires) to eliminate cumulative errors.

where D_T is the distance traveled in T sec. Since the spacing between counts was $\frac{2\pi R}{N_T}$, the total distance error in T sec would be

$$\pm \frac{12}{1763} D_T \pm \frac{2\pi R}{N_T}$$

with a corresponding worst-case velocity estimation error

$$\Delta V^1 = \pm \frac{12}{1763} V \pm \frac{2\pi R}{N_T} \frac{1}{T} \cdot \qquad \text{(ft/sec)}$$

The maximum deviation would occur at the maximum expected speed which is assumed to be 100 ft/sec. Then,

$$(\Delta V^1)_{max} = 1.25 \text{ ft/sec.}$$

(Here, it is assumed that P_T = 22 psi and the fifth wheel is calibrated, i.e., $17.63 \frac{2\pi R}{N_T} = 1$).

Next consider the situation where a vehicle is decelerating (accelerating) at a constant rate over at least T sec as is depicted in Fig. 32. Under ideal conditions, the measured velocity at t + T would be

$$\overline{V} = \frac{V(t) + V(t + T)}{2},$$

which is $\frac{AT}{2}$ units too large (for $V(t) > V(t + \tau)$). Thus, under nonideal conditions, the worst-case velocity estimation error would be

$$\Delta V^1 = \pm \frac{12}{1763} V \pm \frac{2\pi R}{N_T} \frac{1}{T} \pm \frac{AT}{2} \qquad \text{(ft/sec)}$$

The maximum error would occur when the vehicle were decelerating at a maximum permitted rate. For A = 12.88 ft/sec^2 and the parameters previously employed,

$$(\Delta V^1)_{max} = 1.89 \text{ ft/sec}^2.$$

If this were too high, a lower value could be achieved by increasing N_T and insuring that the percentage of missed counts remained the same.

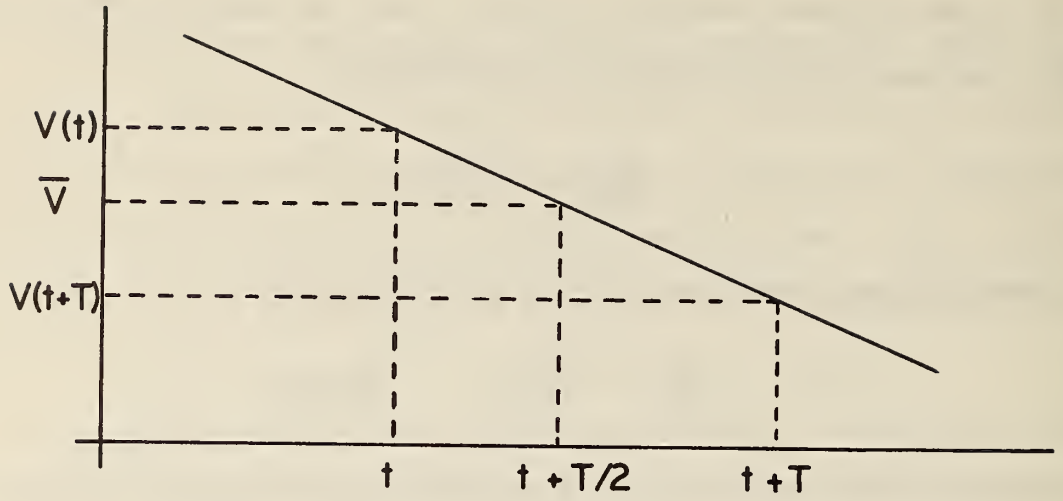

Fig. 32 Measurement interval for a vehicle decelerating at a constant rate.

In essence, the commercially available fifth wheel which was tested here, can be used to obtain an accurate estimate, within ±1.89 ft/sec of the true value, of "instantaneous" velocity in all expected operational situations at the critical high speeds 80-100 ft/sec which are of great interest. This estimate would be within ±1.42 ft/sec provided A were limited to ±3.22 ft/sec^2.

Clearly this fifth wheel, which is a typical commercial model, can be used with confidence as a source of state information for vehicle controller tests--provided its limitations are properly considered.

Beyond the merits of the specific wheel studies, it has been suggested that an "internally mounted" fifth wheel be employed to provide state information in an operational situation. Based on the results presented here, this could, with a proper design, result in excellent position estimates (especially if an unbiased updating measure were also provided) and velocity estimates with an accuracy of some ±1 ft/sec.

G. Information Source 2

In theory, Information Source 2, which would be intended to provide information directly from the roadway to the sector computer, would not be needed as all necessary functions could be handled by the roadway-to-vehicle/sector-computer combination. However, it would be highly desirable to have such an information source for purposes of redundancy.

During both the first and second years of this study, various approaches toward the realization of an adequate configuration were considered--some of which were listed previously.[16] In essence, none of the suggested approaches would result in vehicle state information to the same precision as that obtainable from the Information Source 1 configurations discussed here. This is an area in which much future effort should be expended.

H. Conclusions

Four approaches for providing individual vehicles with longitudinal state information have been evaluated and their performance limitations specified.

a) Crossed-Wire Configuration

This configuration could be effectively used to define intermediate position markers with marker intervals in the range of 1 to 100 or more feet. The measured position at a wire crossing, per the results presented here, would be within 0.0052 ft of the true position for speeds from 0-80 ft/sec (and probably for higher speeds as well). However, the velocity estimates derived from the crossings would not be a sufficiently accurate measure of a vehicle's "instantaneous" velocity.

The latter could be obtained by using a conditional feedback approach wherein the signals from the crossed wires, a tachometer and an accelerometer would be employed.*

b) Helical-Line Configuration

Properly excited helical transmission lines could be employed to both define the IPM's and provide a distance interpolation between these markers. The position measurement accuracy, per laboratory tests only, is some .17 ft for the particular parameters considered in Section D--a result which should be speed independent. Various approaches for obtaining a velocity estimate from these lines were considered. If P_e were small and a reasonable accuracy were present in the phase measurement, "instantaneous" velocity could be estimated to an accuracy of some 0.9 ft/sec provided $|A| < 3.22$ ft/sec.

A potential problem with the use of these lines involves the difficulties associated with their manufacture and roadway installation. These may be overcome by using planar lines which, after preliminary tests, appear to possess the same signal characteristics as the circular lines.

---

* This approach was employed in a series of field tests of a crossed-wire configuration (with 1 ft between each wire pair)/vehicle controller combination.

c) Scattering Enhancement Plates

These plates can be used to provide both an accurate position signal (e.g., a maximum position error of ±.05 ft in a 10-ft distance) and an estimate of instantaneous velocity which is within ±0.7 ft/sec, provided $|A| < 3.22$ ft/sec^2, over the speed range 0-100 ft/sec.
Thus, they could be used for both position interpolation between IPM's, and to provide an accurate velocity estimate to compare with a threshold value for emergency detection purposes.

d) A Fifth Wheel

When a permanently installed information source is not available, the fifth wheel evaluated (a standard commercial model) can be used as an accurate source of state information. Distance estimates obtained over a 100-ft interval were accurate to within ±.34 ft, and instantaneous velocity estimates should be accurate to within ±1.4 ft/sec for speeds from 0-100 ft/sec, provided $|A| < 3.22$ ft/sec.^{2} For $|A| \leq 12.88$ ft/sec^2, the latter should be accurate to within ±1.9 ft/sec.

Based on these results, an "internally mounted" fifth wheel could be employed to provide state information in an operational system. With a proper design, position estimation errors within

±.1 ft for a 100-ft interval, and velocity estimates within ±1 ft/sec of the true value should be achievable.

None of the approaches specified for an Information Source 2 would result in vehicle state information to the same precision as that available from the configurations listed above. This is an area in which much future effort should be expended.

Chapter V

ON THE IDENTIFICATION OF VEHICLE DYNAMICS

A. Introduction

In the design of a vehicle longitudinal controller, both braking and propulsion aspects must be considered. For realism, one must employ a valid model of both the braking and the propulsion roadway-interface dynamics. Otherwise, the desired performance characteristics, which would be incorporated into the design, would probably not be achieved by the corresponding physical implementation. Here these dynamics, which were obtained from full-scale tests, are specified for a U.S. passenger sedan.

B. A Model of Braking/Roadway-Interface Dynamics

The relationship between a brake actuating signal (V_i) and a vehicle's speed is dependent on such factors as the condition of the brakes, the properties of the tire/road interface, and the vehicle's deceleration rate. This relationship is nonlinear and quite complex. As the goal of the effort reported here is the design of a closed-loop braking system, it is probably not necessary to employ such a complex model, and a much simpler one, involving an input-output relationship for an expected range of vehicle speeds and deceleration rates, could be adequate.

One simple model is shown in Fig. 33. Its parameters K_B, α, β, δ and τ are assumed to be a function of condition (i.e., a fixed command deceleration rate (A_c) from an initial speed (V_o)), thus partially accounting for the nonlinearities in the braking dynamics. This model was selected after an examination of data obtained from braking tests.

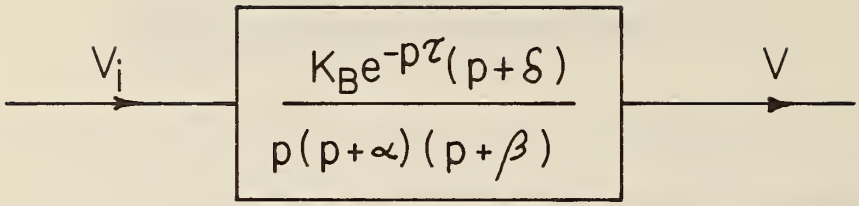

Fig. 33 A simple model of braking/roadway-interface dynamics.

The model parameters were specified for a 1969 Plymouth sedan by matching braking responses (ΔV vs.t), obtained under full-scale conditions from the configuration of Fig. 34, to the responses of a corresponding analog simulation model.* Three typical results are shown in Fig. 35 where both model and full-scale responses for the input command

$$V_c(t) = V_o \qquad t \leq 0$$

$$V_c(t) = V_o - 14.5t \qquad 0 < t \leq V_o/14.5$$

are shown for three initial speeds--20, 60, and 90 ft/sec. The following observations were made from both these and other responses obtained from different braking situations:

1) The response changes with V_o(e.g., the time at which the peak value (ΔV_m) occurs increases with increasing V_o);
2) The magnitude of the response does not increase linearly with increasing A_c; and
3) The form of the response changes with V_o and/or A_c.

---

* This presentation is a summary of the more complete treatment contained in Appendix C.

Thus, the braking dynamics are a nonlinear function of, at least, V_o and A_c; however, τ appears to be nearly constant at some 150 m sec.

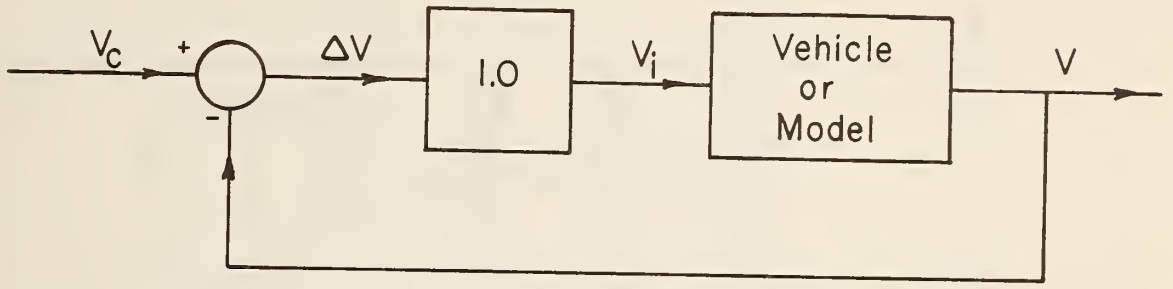

Fig. 34 Closed-loop system employed in the parameter-identification process.

The composite results are shown in Table XXI where V/V_i is defined for 20 $(V_o - A_c)$ combinations. The nonlinearity of the braking dynamics is at least partly shown here. Thus, if the model (and the braking dynamics) were linear, the quantity $\frac{K_B\delta}{\alpha\beta}$ would be invariant with respect to both V_o and A_c. Instead, as is shown in Fig. 36 where $K_B\delta/\alpha\beta$ is plotted versus V_o with A_c as a parameter, this quantity varies over a range from 2.63 to 1.25.

A considerable amount of variability was presented in the recorded responses. Thus, while ΔV_m = 8.5 ft/sec in Fig. 35(c), it ranged from 7.6 to 10.5 in other tests conducted under identical conditions. This variability is easily accounted by specifying a range of K_B for a given $(V_o - A_c)$ combination. The observed changes in K_B were some ±20% of the values specified in Table XX; thus, in designing a closed-loop braking system, one should design for an insensitivity to changes of at least this magnitude.

The model predictions correlated reasonably well with data obtained under both wet- and dry-road conditions; however, in some situations, generally those involving large deceleration commands and a very wet road surface, poor

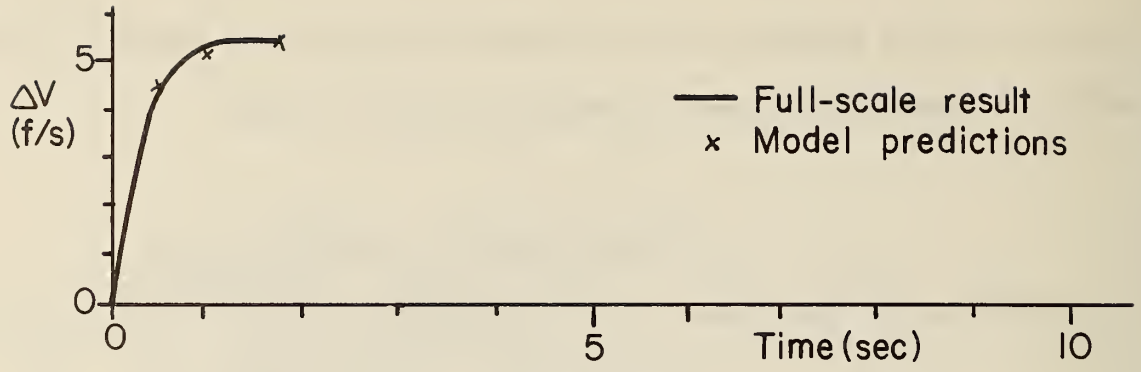

a) V_0 = 20 ft/sec.

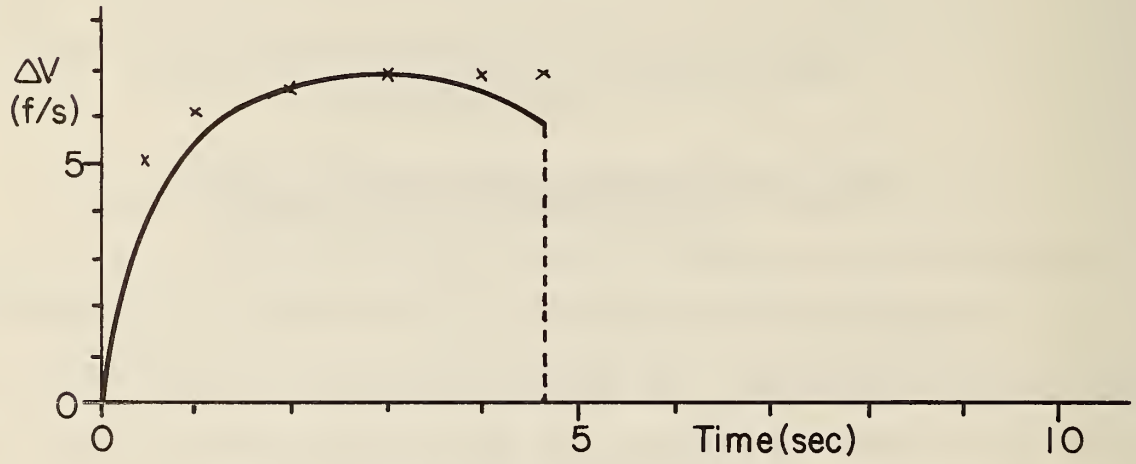

b) V_0 = 60 ft/sec.

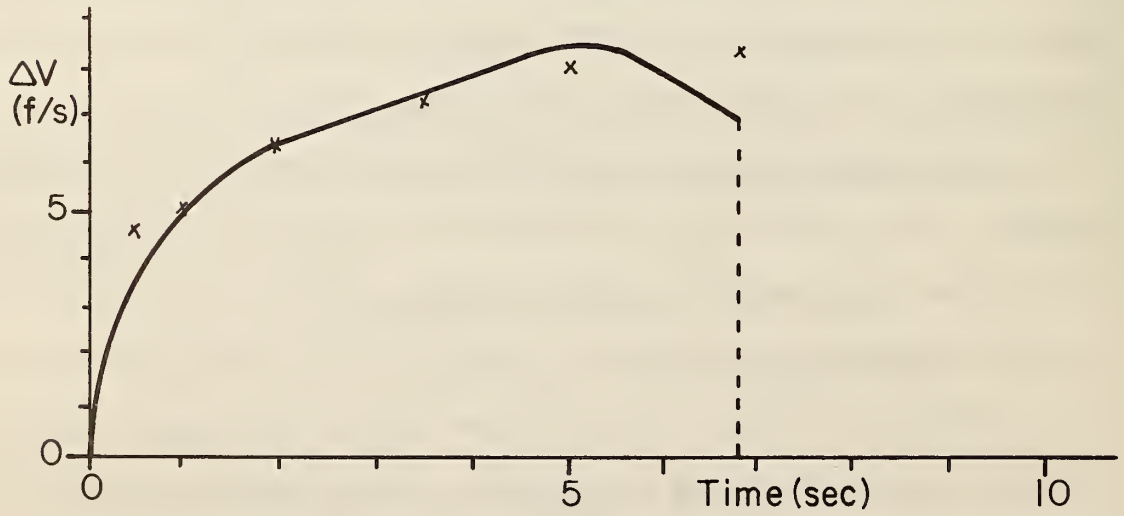

c) V_0 = 90 ft/sec.

Fig. 35 Comparison of vehicle response and model response for 3 selected initial speeds and A_c = 14.5 ft/sec^2 (Dry-pavement conditions).

A_c (ft/sec^2) \ V_o (ft/sec)	20	40	60	80	90
6.44	$\frac{18.045(p+1.75)}{p(p+3)(p+4)}$	$\frac{16.0\,(p+1.75)}{p(p+3)(p+4)}$	$\frac{15.57(p+1)}{p(p+2.5)(p+3.5)}$	$\frac{11.25(p+.5)}{p(p+1.5)(p+3)}$	$\frac{11.25(p+.5)}{p(p+1.5)(p+3)}$
9.66	$\frac{18.045(p+1.75)}{p(p+3)(p+4)}$	$\frac{13.82(p+1.75)}{p(p+3)(p+4)}$	$\frac{14.71(p+1)}{p(p+2.5)(p+3.5)}$	$\frac{12.15(p+.5)}{p(p+1.5)(p+3)}$	$\frac{12.15(p+.5)}{p(p+1.5)(p+3)}$
12.88	$\frac{18.045(p+1.75)}{p(p+3)(p+4)}$	$\frac{15.5(p+1.75)}{p(p+3)(p+4)}$	$\frac{16.1(p+1)}{p(p+2.5)(p+3.5)}$	$\frac{13.45(p+.5)}{p(p+1.5)(p+3)}$	$\frac{13.45(p+.5)}{p(p+1.5)(p+3)}$
14.50	$\frac{18.045(p+1.75)}{p(p+3)(p+4)}$	$\frac{15.5(p+1.75)}{p(p+3)(p+4)}$	$\frac{14.3(p+1.75)}{p(p+3)(p+4)}$	$\frac{15(p+.5)}{p(p+1.5)(p+3)}$	$\frac{15(p+.5)}{p(p+1.5)(p+3)}$

NOTE: $\tau \doteq 150$ m sec for all conditions.

TABLE XXI

MODEL PARAMETERS FOR $\frac{V_w}{V_i} = \frac{K_\beta(p+\delta)}{p(p+\alpha)(p+\beta)}$

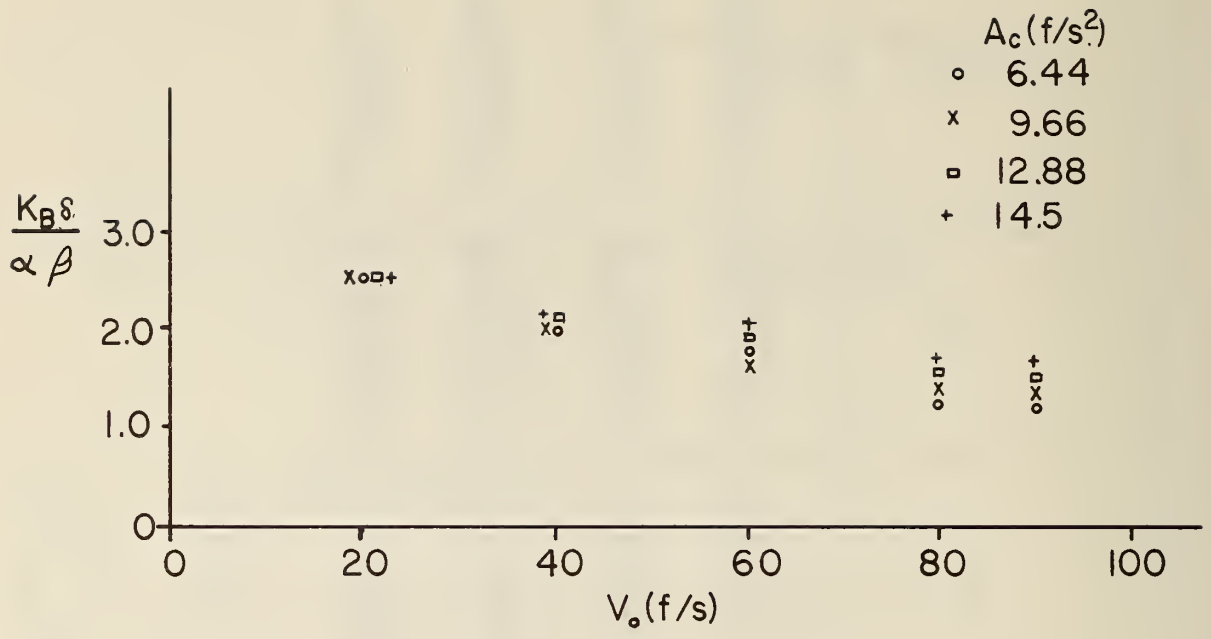

Fig. 36 $\frac{K_B\delta}{\alpha\beta}$ vs. V_o with A_c as a parameter.

correlation was obtained. This is shown in Fig. 37 where ΔV vs. t is shown for V_o = 40 ft/sec and A_c = 12.88 ft/sec. Note that wheel lock occurred, and the braking system responded in an antiskid mode. The resulting response was highly oscillatory, and quite different from the predicted response. If a more efficient antiskid mode (one that would have resulted in minimal amplitude oscillations and a more comfortable stop) had been employed, the model response would have been a fair approximation of the full-scale response. Thus, if the large oscillations of Fig. 37 were greatly reduced, the response shown in Fig. 38 would result. This response compares favorably with the model response which is also shown.

C. On Braking Controller Design

The model specified here results in predicted responses which are reasonable approximations to corresponding full-scale responses over the speed and acceleration ranges of interest. Thus, it should be useful in the design

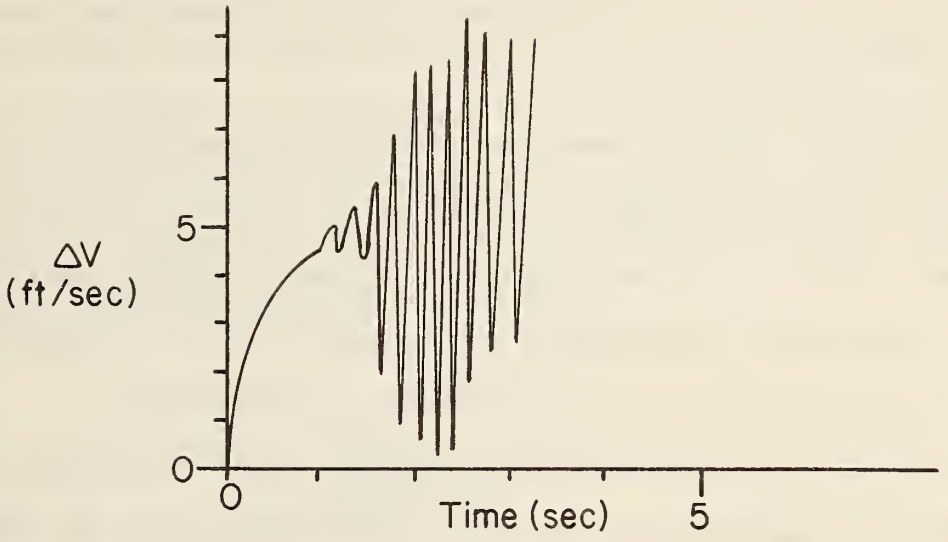

Fig. 37 Vehicle response for V_o = 40 ft/sec, A_c = 12.88 ft/sec^2 and wet-pavement conditions.

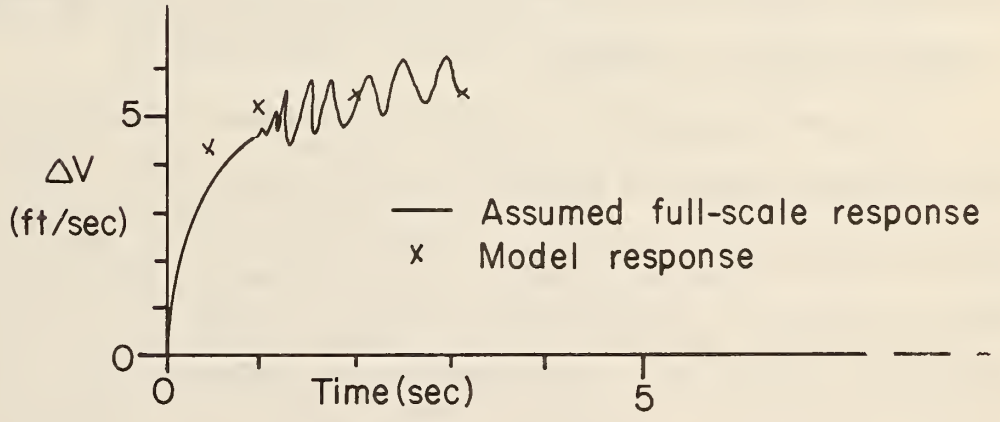

Fig. 38 Assumed full-scale response with an efficient anti-skid mode. (V_o = 40 ft/sec, A_c = 12.88 ft/sec^2 and wet-pavement conditions).

of a braking controller; however, in view of the variability of the recorded responses, which can be modelled by changing K_B from the value specified for each V_o - A_c combination, the controller should be designed for insensitivity to a highly variable braking gain.

An efficient anti-skid mode should be incorporated into the design so that adequate braking performance at rates up to 12.88 - 14.5 ft/sec^2 could be achieved on both dry and wet pavement. The specified model could be employed in this part of the design, as it should provide a reasonable approximation to the response in a well-controlled, anti-skid mode.

It should be emphasized that the specified model was selected because of its simplicity and potential for use in the braking-controller design process. Another model, with more accurate predictive properties, may be specified; however, it would probably be characterized by a fairly complex, nonlinear differential equation and be more difficult to use in this process.

D. Vehicle Propulsion Dynamics

In a previous study,[16] the propulsion/roadway interface dynamics of a 1969 Plymouth sedan were specified and subsequently used in the design of a vehicle longitudinal controller. During the past year, it was desired to test this controller in conjunction with the "crossed-wire" information source discussed in Chapter IV. This controller was implemented on a 1965 Plymouth,* as it was equipped for automatic steering which was necessary to keep the vehicle over the crossed wires.

During a full-scale evaluation of this controller/information source combination, it was observed that the vehicle response was inferior to that obtained from a simulation model of the vehicle model/controller combination.

---

* The 1969 Plymouth is not presently instrumented for automatic steering.

This was due to the inadequacy of the model which was not valid for the 1965 Plymouth. It thus became necessary to develop a model for this vehicle so that a more effective controller could be designed.

Consider the model shown in Fig. 39. This relatively complex, velocity-dependent model* is one possible simplification of a more complex model in which such phenomena as a transport delay in the fuel-air system, lags associated with the propulsion system-drivetrain combination, the nonlinear effects of slipping tires, and the variety of forces which act, linearly and nonlinearly, on a moving vehicle, are explicity included.

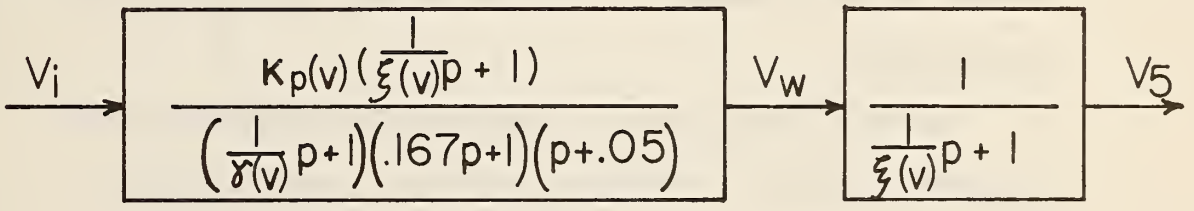

Fig. 39 A velocity-dependent model of vehicle propulsion system/roadway interface dynamics.

The model input is V_i which, in practice, would be the input to an actuator controlling the throttle-valve position. The quantity V_w is the driven-wheel velocity as measured via an onboard tachometer;** and V is vehicle velocity with respect to an inertial frame of reference. (This was obtained via a fifth wheel; i.e., it was assumed that $V_5 = V$). Three velocity-dependent functions $K_p(V)$, $\gamma(V)$ and $\xi(V)$ are included. The first two are associated with nonlinear effects in the propulsion-drivetrain combination and the third

---

* This model is more complex than that previously specified for a 1969 Plymouth.[16] The additional complexity was necessary to provide a good match between model response and full-scale responses.

** This is not to be confused with V_T which was previously defined as the velocity measurement obtained from a nondriven (braked) wheel.

with the tire-roadway interface. Average values of the latter,* which were specified in a previous study, are shown in Fig. 40.

The quantities $K_p(V)$ and $\xi(V)$ were determined via a model-matching approach, in which the following procedure was employed:

> The command input, $V_c = 2t$ (ft/sec), was applied to the controller/vehicle system shown in Fig. 41, while the vehicle was initially traveling at a fixed speed, and the signal e(t), which is defined in this figure, was recorded. This procedure was repeated several times at that speed to verify that a true response indication was obtained. This was done for eleven initial speeds: 0, 5, 10, 20, 30, 40, 50, 60, 70, 80, and 90 ft/sec.
>
> The full-scale tests were subsequently replicated using an analog computer. The system model was excited with the same command, and the response e(t) was matched with that obtained in the corresponding full-scale test by appropriately adjusting Υ and K_p. Thus, these quantities were assigned values for each selected speed.

Typical full-scale and model responses are compared in Fig. 42. Three comparisons are shown, corresponding to initial speeds of 20, 40, and 80 ft/sec. Note that good correlation exists in each case.

The composite results $K_p(V)$ vs. V and $\Upsilon(V)$ vs. V are specified in Figs. 43 and 44, respectively. Note that both quantities change substantially with V (as does $\xi(V)$, which was shown in Fig. 40). These results are generally

---

* In the model for the 1969 Plymouth, a lower bound on $\xi(V)$ was employed to allow for a worst-case phase lag. Since $\xi(V)$ is now included as a zero (phase lead) in $\frac{V_w}{V_i}$, a lower bound would not result in a worst-case condition.

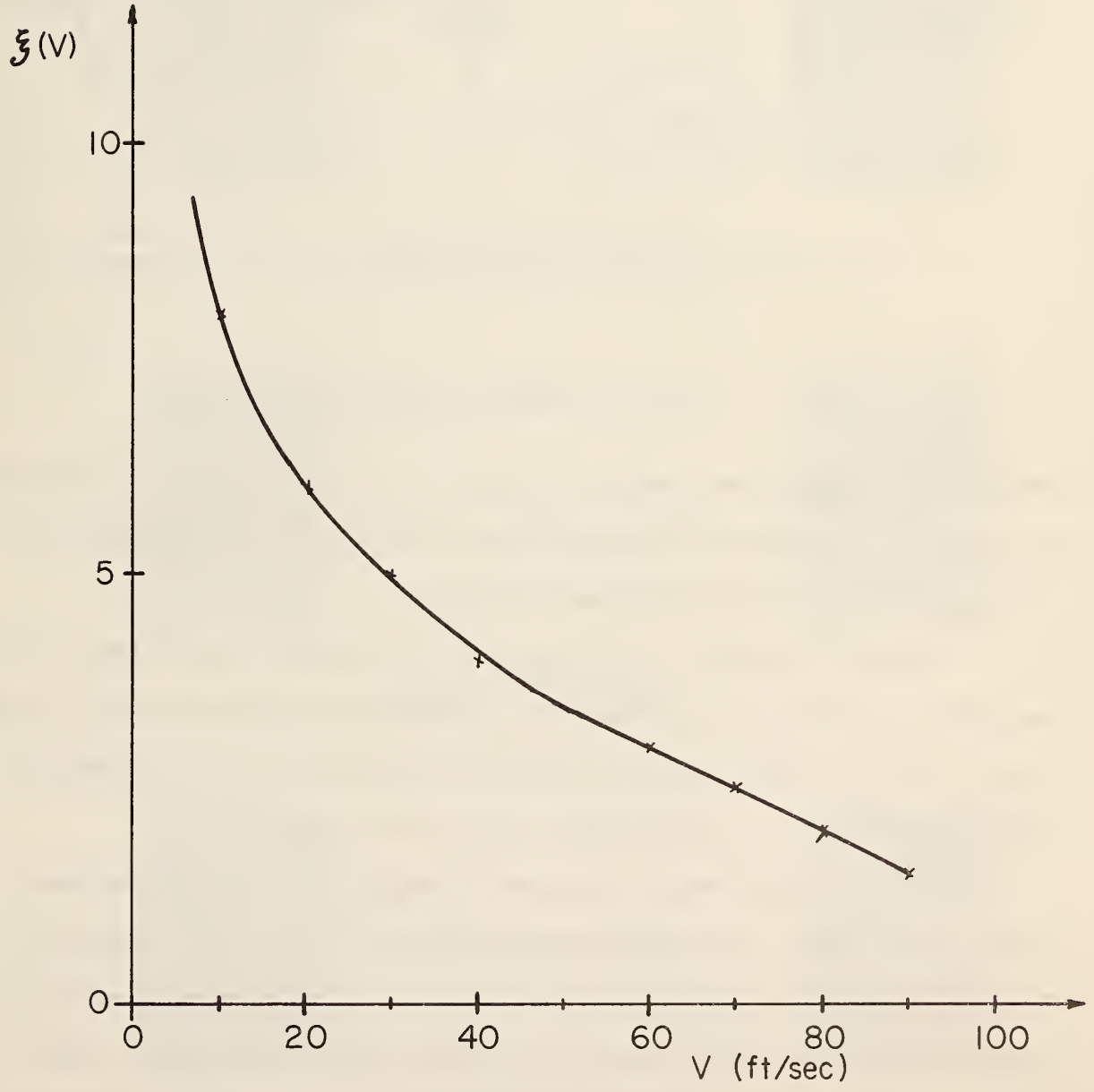

Fig. 40 $\xi(V)$ versus V (obtained from Reference 16).

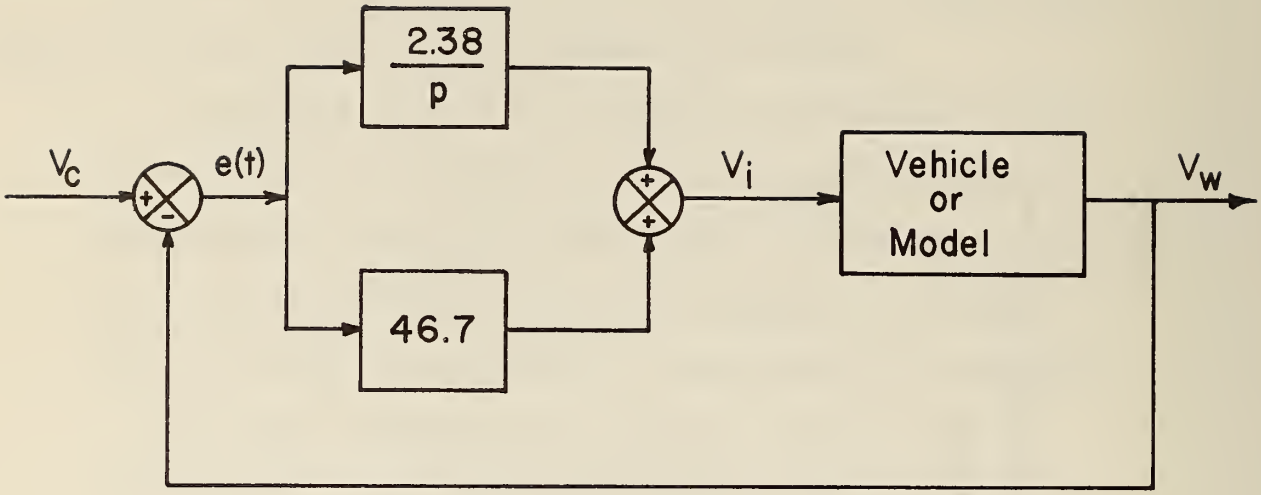

Fig. 41 Velocity controller used for modeling.

consistent with those previously specified for a 1969 Plymouth, and emphasize the need for accounting for nonlinearities when dealing with rubber-tired vehicles driven by internal combustion engines.

This model was used in the design of the position controller, which is described in Chapter VI. Although this controller resulted in small tracking errors, the full-scale responses deviated somewhat from the corresponding model responses as is subsequently discussed in detail.

These deviations may be overcome by employing a more complex model. Such a model, which is currently being evaluated (Nov. 1976), is shown in Fig. 45. Note that $K_p = K_p(V, V_i)$ and $\gamma = \gamma(V, \omega_e, \omega_t)$ where ω_e is the engine speed, and ω_t is the torque-converter turbine speed. With such a model, one should be better able to predict various phenomena (e.g., the existance of a low-speed limit cycle) which result from the nonlinearities inherent in the vehicle dynamics.

Model responses

Vehicle responses

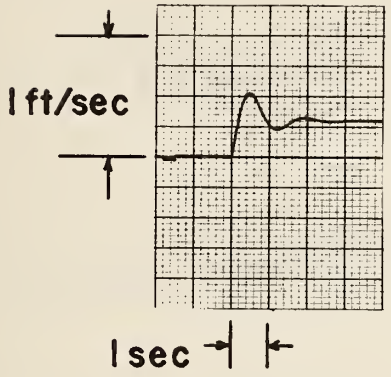

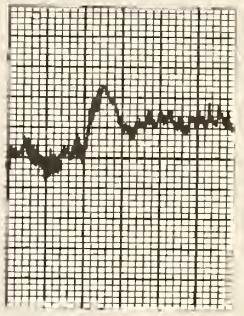

(a) V = 20 ft/sec

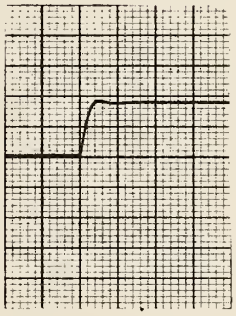

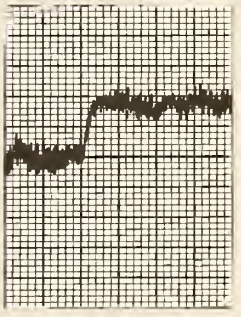

(b) V = 40 ft/sec

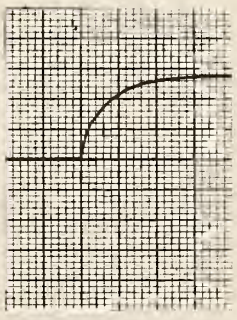

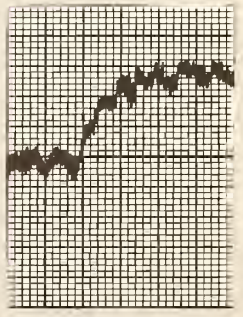

(c) V = 80 ft/sec

Fig. 42 Comparison of model and vehicle responses.

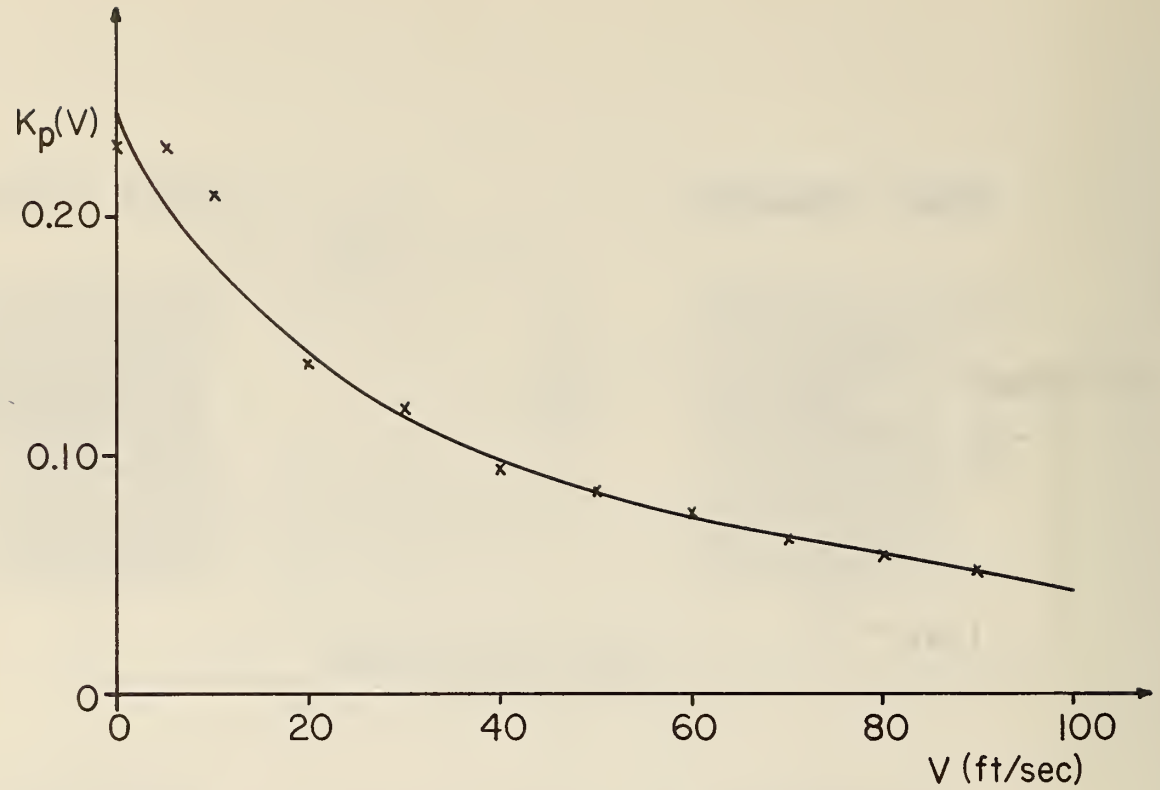

Fig. 43 $K_p(V)$ versus V.

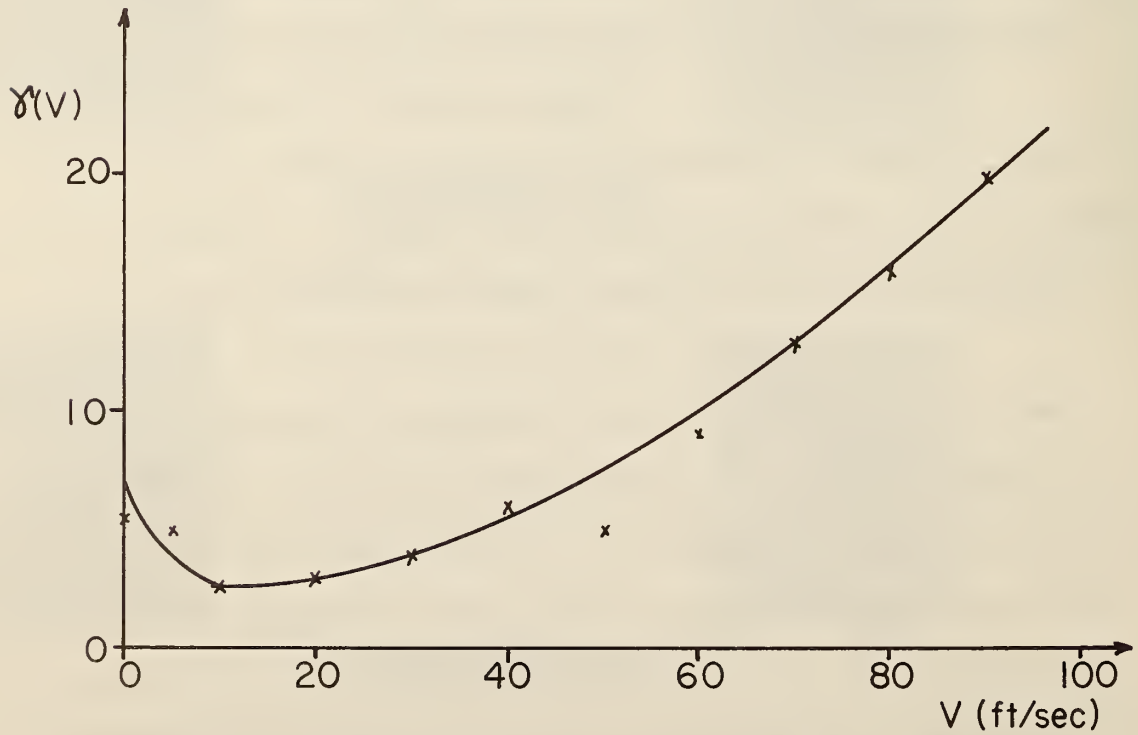

Fig. 44 $\gamma(V)$ versus V.

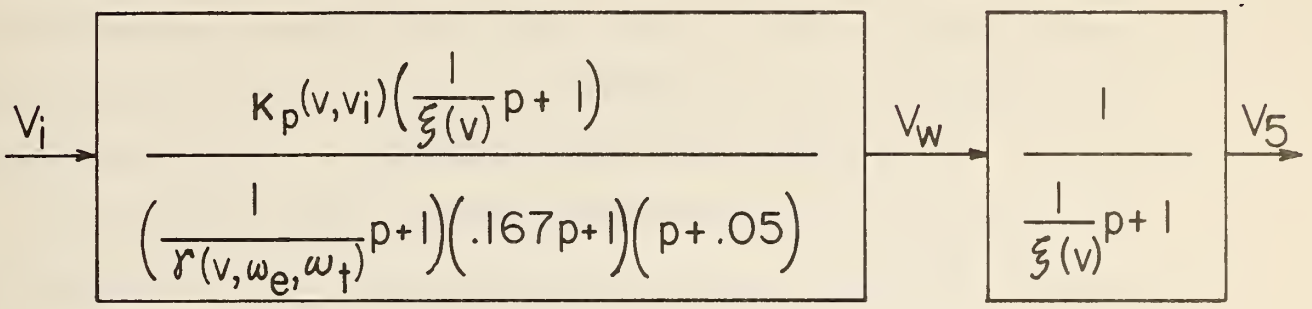

Fig. 45 A more complex model.

CHAPTER VI

A VEHICLE LONGITUDINAL CONTROLLER--
DESIGN AND EVALUATION

A. Introduction

A longitudinal control system for an individual vehicle must be designed so that the following general requirements are satisfied:

i) Physical realizability--any required response must be within the capabilities of the vehicle;

ii) Passenger ride comfort ($|Jerk| < 1.6$ ft/sec^3 in online operations);

iii) A small vehicle-position error (< 1 ft) under all input conditions;

iv) Minimal effects from disturbance inputs;

v) A minimal ramp length for entry merging maneuvers; and

vi) A quick and accurate response to an emergency command input.

These were previously discussed in detail,[16] and a preferred controller type specified. This was a position controller, as good control of a vehicle's position would result in correspondingly good control of both its acceleration and velocity.

Consider the position controller shown in Fig. 46. It is characterized by command inputs $X_c(t)$, $V_c(t)$ and $A_c(t)$, a disturbance input and a single output $X(t)$. In view of the discussion in Chapter IV, longitudinal state

information should be available to each vehicle in either a continuous or near-continuous form. Therefore, the controller should be designed to respond to such inputs.

Previously, a controller with excellent performance characteristics was designed for a 1969 Plymouth sedan and evaluated under field conditions.[16] Here, a fifth wheel was employed to measure the required state variables. In the studies of the past year, it was desired to evaluate this controller in conjunction with the crossed-wire information source and a state estimator similar to that discussed in Chapter IV. A 1965 Plymouth was employed as it was instrumented for automatic steering (This was necessary to maintain the vehicle over the crossed wires). The previously designed controller, when installed in this vehicle, did not result in satisfactory performance, and it was necessary to design the controller discussed here.

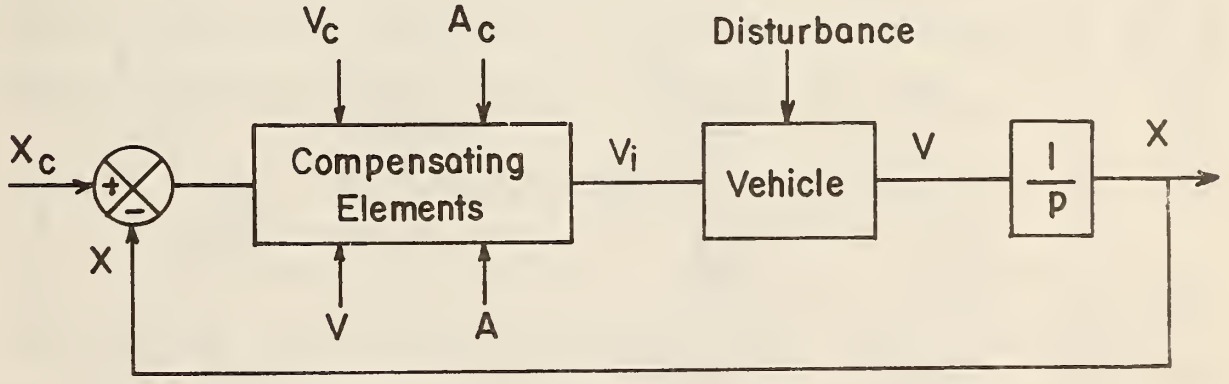

Fig. 46 General position controller.

B. Controller Design

The controller shown in Fig. 47 was selected for reasons of simplicity, the availability of all required feedback variables and inputs, and its general ease of implementation.

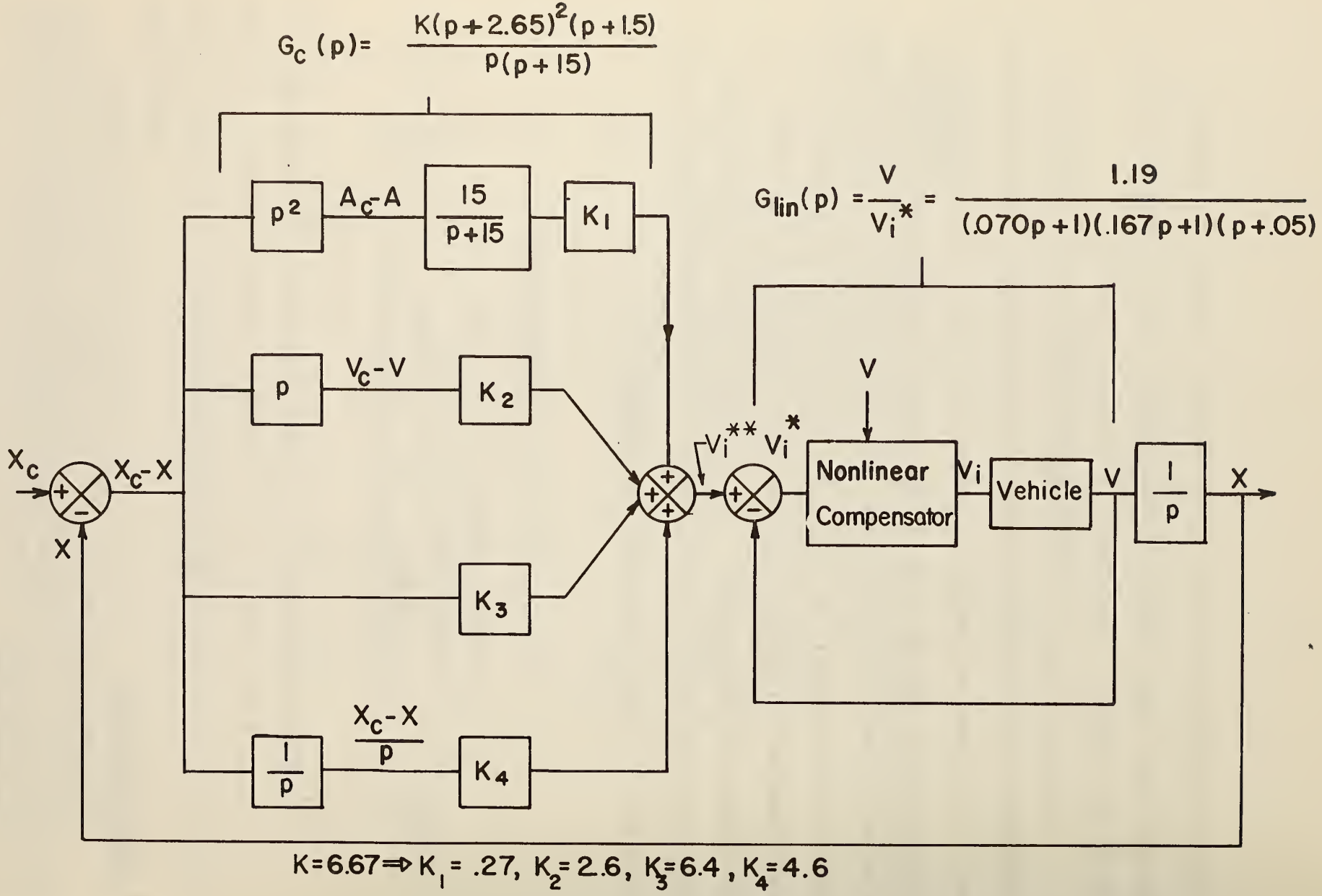

Fig. 47 A vehicle longitudinal control system.

The inputs are X_c, V_c and A_c, and X, V, and A are employed for control purposes. The latter three would be available as estimates: $\hat{X}$, $\hat{V}$ and $\hat{A}$, respectively. If an appropriate state estimator were used (See Chapter IV, Section C), $\hat{X}$ and $\hat{V}$ would be unbiased and relatively noisefree, and

$$\hat{X} \doteq X \text{ and } \hat{V} \doteq V.$$

As $\hat{A}$ would contain a substantial amount of high-frequency noise (e.g., that due to vehicle vibration), the function $(\frac{15}{p + 15})$ was selected to appropriately filter $A_c - \hat{A}$. Then, one may assume

$$\hat{A} \doteq A$$

with no appreciable effect on the controller design.

The composite linear compensator $G_c(p)$ was selected to insure small position errors to both ramp- and parabolic-position commands. The nonlinear compensator, which is detailed in Fig. 48, was selected to nullify the velocity-dependencies of γ and K_p which were specified in the previous chapter. The piecewise-linear approximations for $\frac{1}{K_p}$ and $\frac{1}{\gamma}$ shown in Figs. 49 and 50 were employed, and the resulting linearized propulsion model was

$$G_{1in}(p) = \frac{V}{V_i^*} \doteq \frac{1.19}{(0.07p + 1)(0.167p + 1)(p + 0.05)} .$$

Internal velocity feedback was used to speedup the response of this linearized model, and to reduce the effects of model inaccuracies at low frequencies (0.1 rad/sec). The resulting transfer function was

$$\frac{X}{V_i^{**}} = \left(\frac{1}{p}\right)\left(\frac{G_{1in}(p)}{1 + G_{1in}(p)}\right) = \frac{102}{p(p + 15)(p + 2.65)^2} ,$$

where V_i^{**} is defined in Fig. 47.

The selection of

$$G_c(p) = \frac{K(p + 2.65)^2 (p + 1.5)}{p(p + 15)^2} ,$$

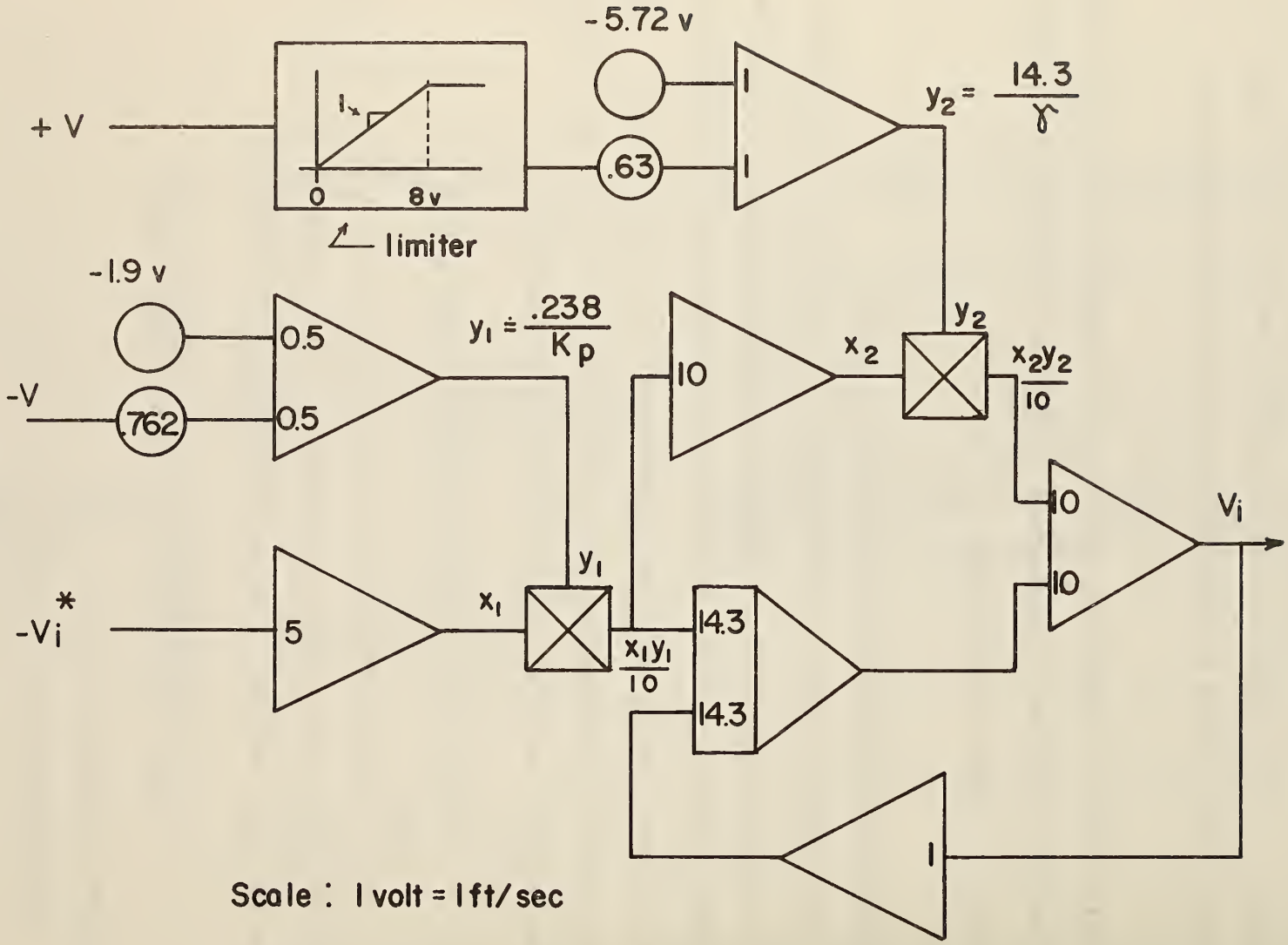

Fig. 48 A nonlinear compensator.

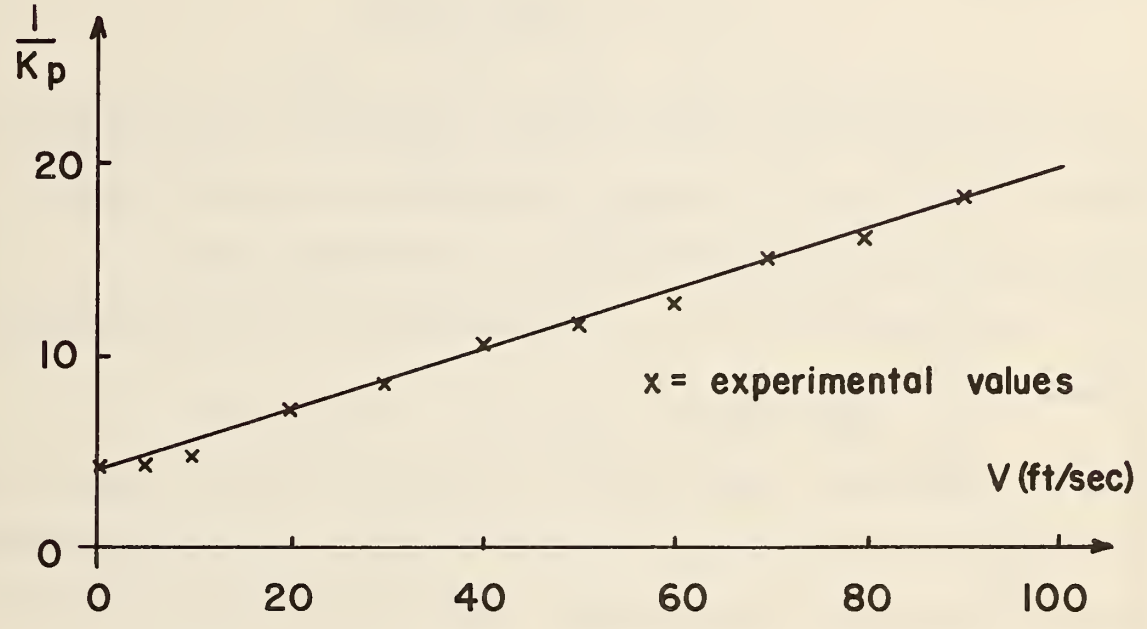

Fig. 49 A linear approximation of $\frac{1}{K_p}$.

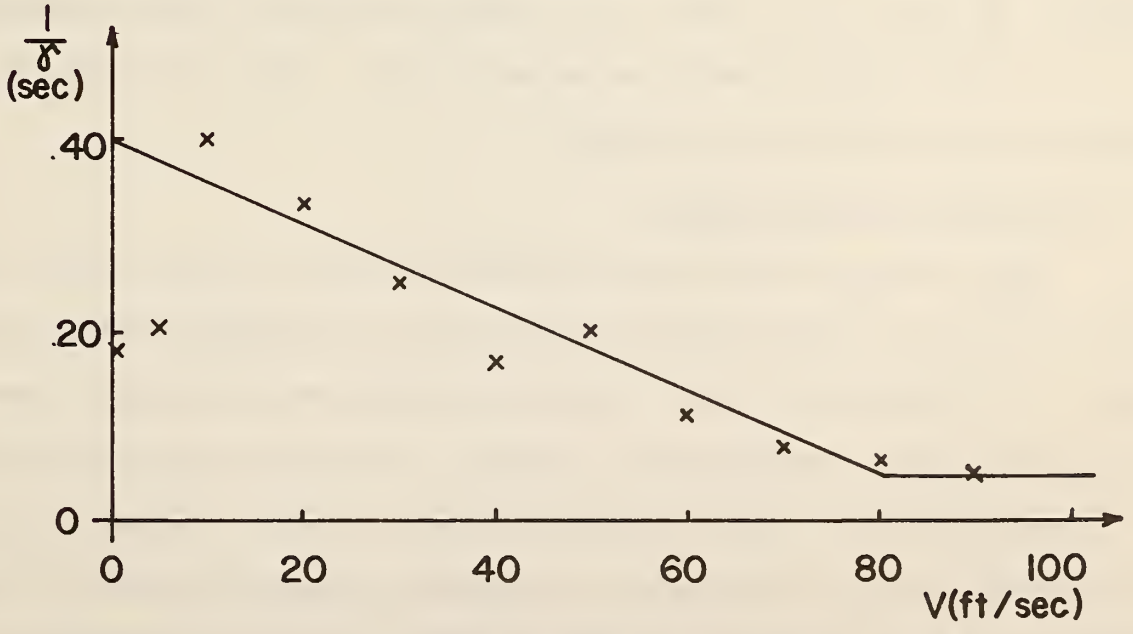

Fig. 50 A piecewise linear approximation of $\frac{1}{\gamma}$.

resulted in the root loci shown in Fig. 51, where the open-loop transfer function was

$$G_o(p) = \frac{102K\,(p + 1.5)}{p^2\,(p + 15)^2}\,.$$

Note that K = 6.67 would result in adequate damping and a fast-responding system. As this is a Type 2 system, the steady-state position error to a ramp-position (constant-speed) command is theoretically zero.

The response (X_e - X) of a simulation model to the move-up, maneuvering command

$$X_c(t) = X(0) + V(0)t + t^2, \qquad (0 < t < 5)$$

which was applied to a vehicle initially moving at a constant speed, is shown in Fig. 52(a). The response peak is 0.45 ft, and X_c - X quickly approached zero after the maneuver was completed. Note that this response should be speed independent.

The response to a disturbance input, equivalent to a sudden 44 ft/sec headwind, is shown in Fig. 52(b). The response deviation reached a maximum of .25 ft and thereafter rapidly decreased to zero. Thus, this design is relatively insensitive to such inputs.

C. Full-Scale Tests and Results

The simulation studies were followed by partial full-scale tests, which were conducted on a high-speed test track using an instrumented 1965 Plymouth sedan. The longitudinal control functions--braking and acceleration--were accomplished using electrohydraulic actuators. An analog computer consisting of 22 operational amplifiers, 15 potentiometers, and other necessary components was installed over the back seat. The computing elements were used for command generation, state estimation and data collection. Controller compensation was

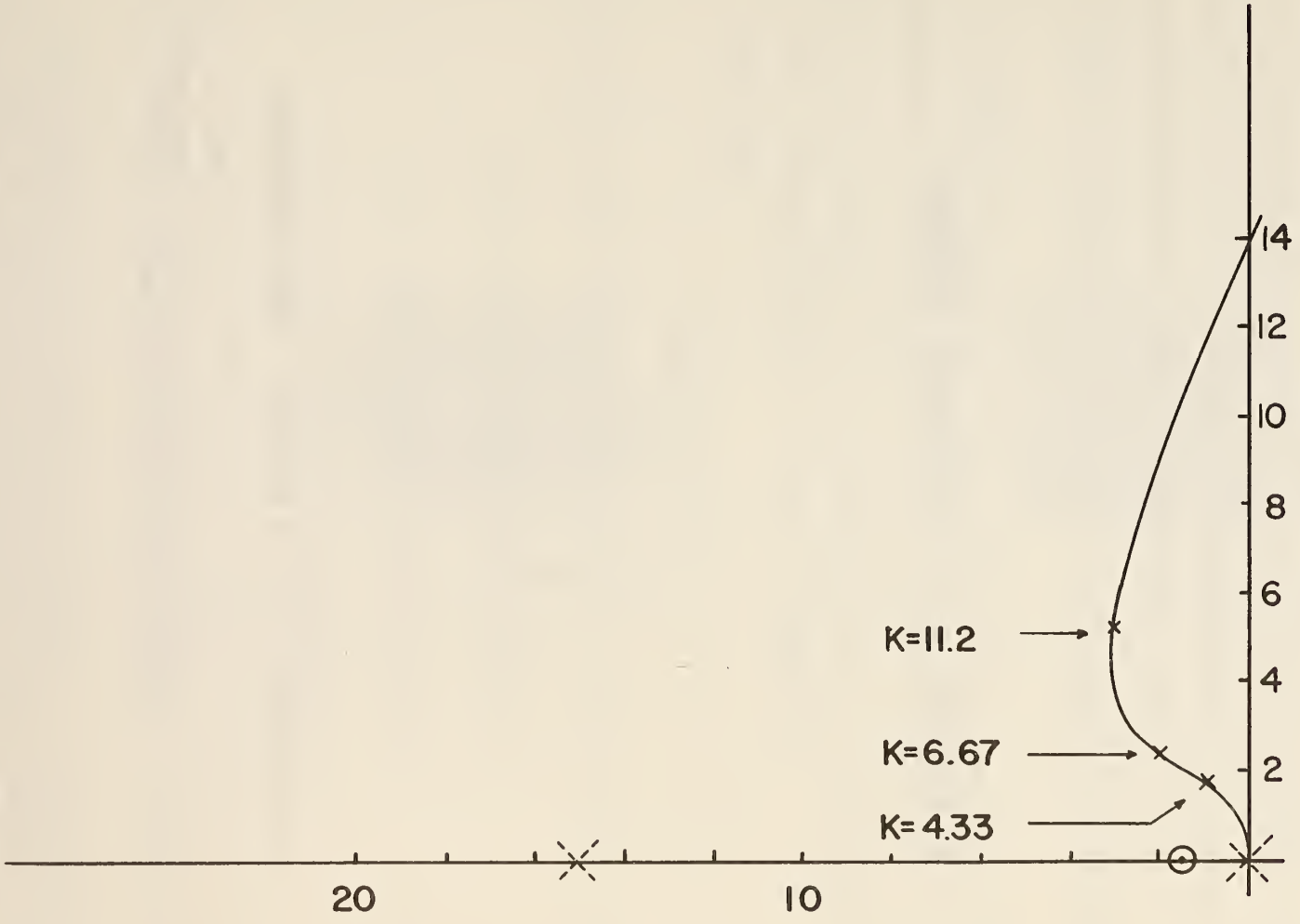

Fig. 51 Root-locus plot corresponding to $G_o(p) = \frac{102K\ (p + 1.5)}{p^2\ (p + 15)^2}$.

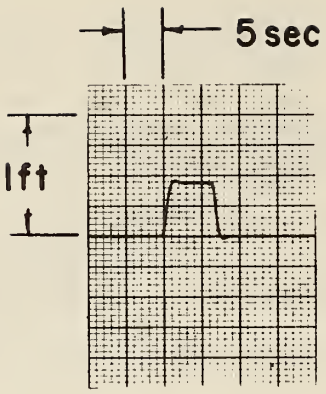

(a) Response to a maneuvering command.

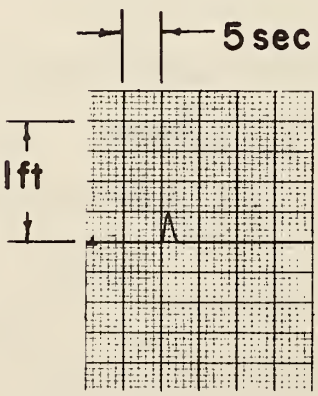

(b) Response to a 44 ft/sec step headwind.

Fig. 52 Simulation responses (X_C - X) to a maneuvering command and a disturbance input.

accomplished via a circuit, which was separate from the computer. All collected data were recorded on a 6-channel, strip-chart recorder located next to the driving position. The acceleration and velocity were measured by an accelerometer and a fifth-wheel tachometer, respectively.

All of the roadway-based equipment required for a complete full-scale test was not available, and thus the command quantities (X_c, V_c and A_c) were generated onboard the controlled vehicle and the estimates, ($\hat{X}$, $\hat{V}$ and $\hat{A}$) were obtained by appropriate processing of V_5 and A_{ACC}, the accelerometer output.

One practical processor is shown in Fig. 53. The estimator portion of this processor is essentially equivalent to the state estimator of Fig. 21 with S_1, S_2, and S_3 opened, and the command portion is an analog equivalent of the digital command generator discussed in Appendix D.*

If one sets

$$V_5 = V + e_V$$

and

$$A_{ACC} = A + e_A,$$

then the state estimates ($\hat{X}$, $\hat{V}$, and $\hat{A}$) are easily derived from Fig. 53 as

$$\hat{A} = A + \frac{2p}{p^2 + 2p + 2} e_V + \frac{p^2 + 2p}{p^2 + 2p + 2} e_A ;$$

$$\hat{V} = V + \frac{2p + 2}{p^2 + 2p + 2} e_V + \frac{p}{p^2 + 2p + 2} e_A ;$$

$$\hat{X} = X + \frac{2p + 2}{p(p^2 + 2p + 2)} e_V + \frac{1}{p^2 + 2p + 2} e_A .$$

Note that X, V, and A are unaffected by the circuit. Per the discussion in Chapter IV, Section C, e_V and e_A would contain both bias (or slowly-varying)

---

* One objective of this study was to determine a suitable value for the command sampling interval T_S; thus, an analog command generator was used since it would have been difficult to vary T_S in a digital one. However, in an operational system, a digital command generator would be employed to satisfy accuracy requirements.

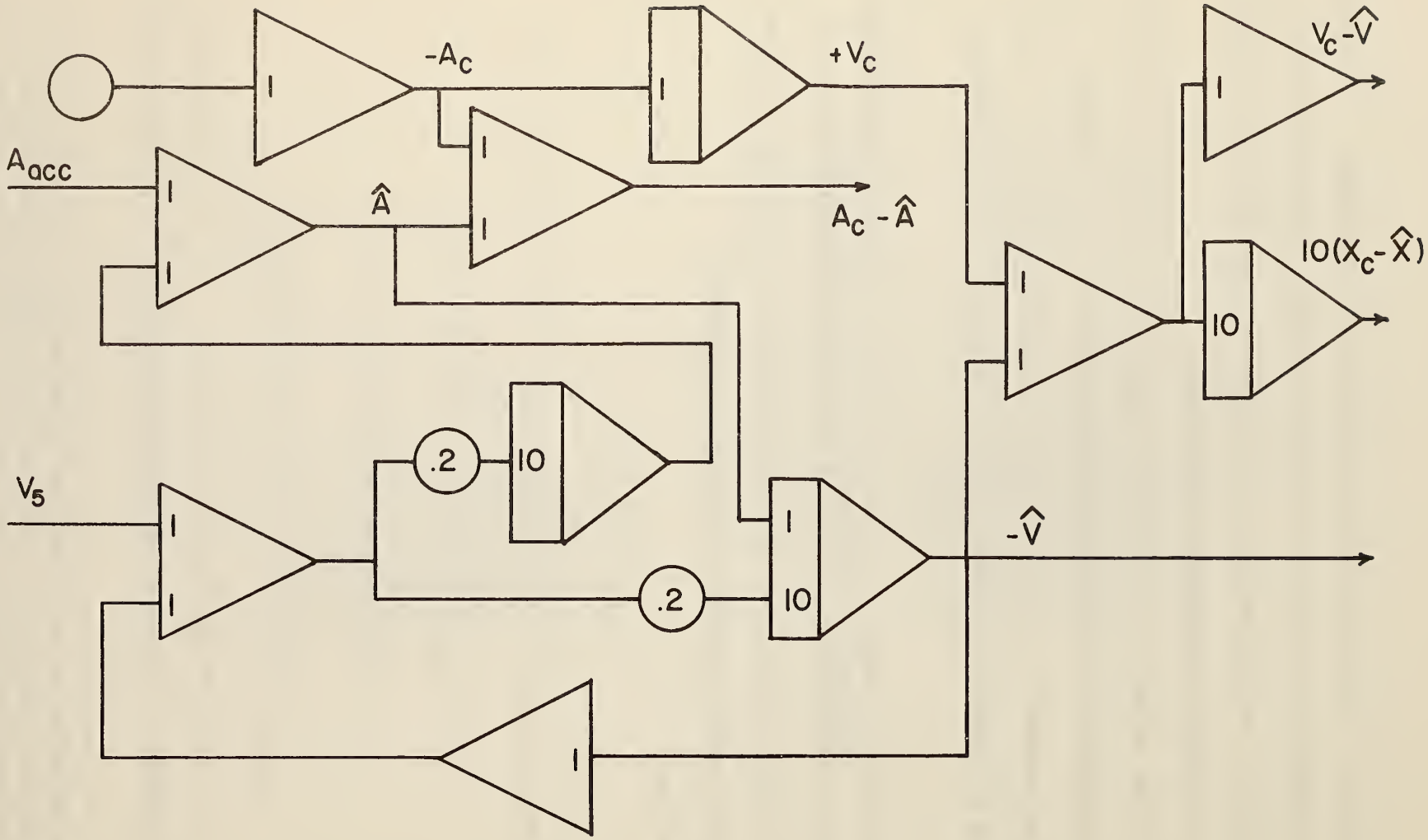

A_{acc}= acceleration indication from a accelerometer.

V_5 = velocity indication from a fifth-wheel tachometer.

Scale: 1.0 ft = 0.1 v

Fig. 53 The command generator and state estimator.

and high-frequency components; thus, according to the preceding equations, $\hat{A}$ would be an unbiased (but noisy) estimate of A. Although $\hat{V}$ and $\hat{X}$ are relatively noise-free (The high-frequency components due to e_V and e_A are greatly attenuated), $\hat{V}$ could contain a small bias error introduced through e_V, and hence, the error in $\hat{X}(= \frac{\hat{V}}{p})$ could accumulate slowly in time.

In an operational system, all vehicles would obtain position information from an absolute marker (e.g., a crossed wire or a magnet) at frequent intervals, and such errors, which are highly undesirable, would be reduced toward zero and have no long-term effect. In an experimental situation, in which the goal was to measure the response of an individual vehicle to various inputs, these errors could be large; however, if they were compared against a command signal generated onboard a vehicle (See Fig. 53), there would be little effect on the recorded responses (e.g., $\Delta V = V_C - \hat{V}$ and $\Delta X = X_C - \hat{X}$).

The signal-processor outputs are the inputs to the controller circuit shown in Fig. 54. This circuit is one realization of the controller design presented in the previous section. Here, sample-and-hold devices are used since X_C, V_C, and A_C would only be available at discrete times if a digital-command generator were used (This would, of course, be the case in an operational system). For this controller, no noticeable deterioration in system performance was observed if the sampling interval T_S were 0.1 sec or less. For $T_S > 0.2$ sec, the responses were under damped (or unstable), and the ride was generally uncomfortable. Thus, T_S was chosen to be 0.1 sec.

The experimental procedure was as follows: At t = 0, the command trajectory shown in Fig. 55(a) was initiated, and as the vehicle responded, V_C, $\hat{V}$, $X_C - \hat{X}$, and V_i were recorded. This was repeated several times to verify that the response was consistent.

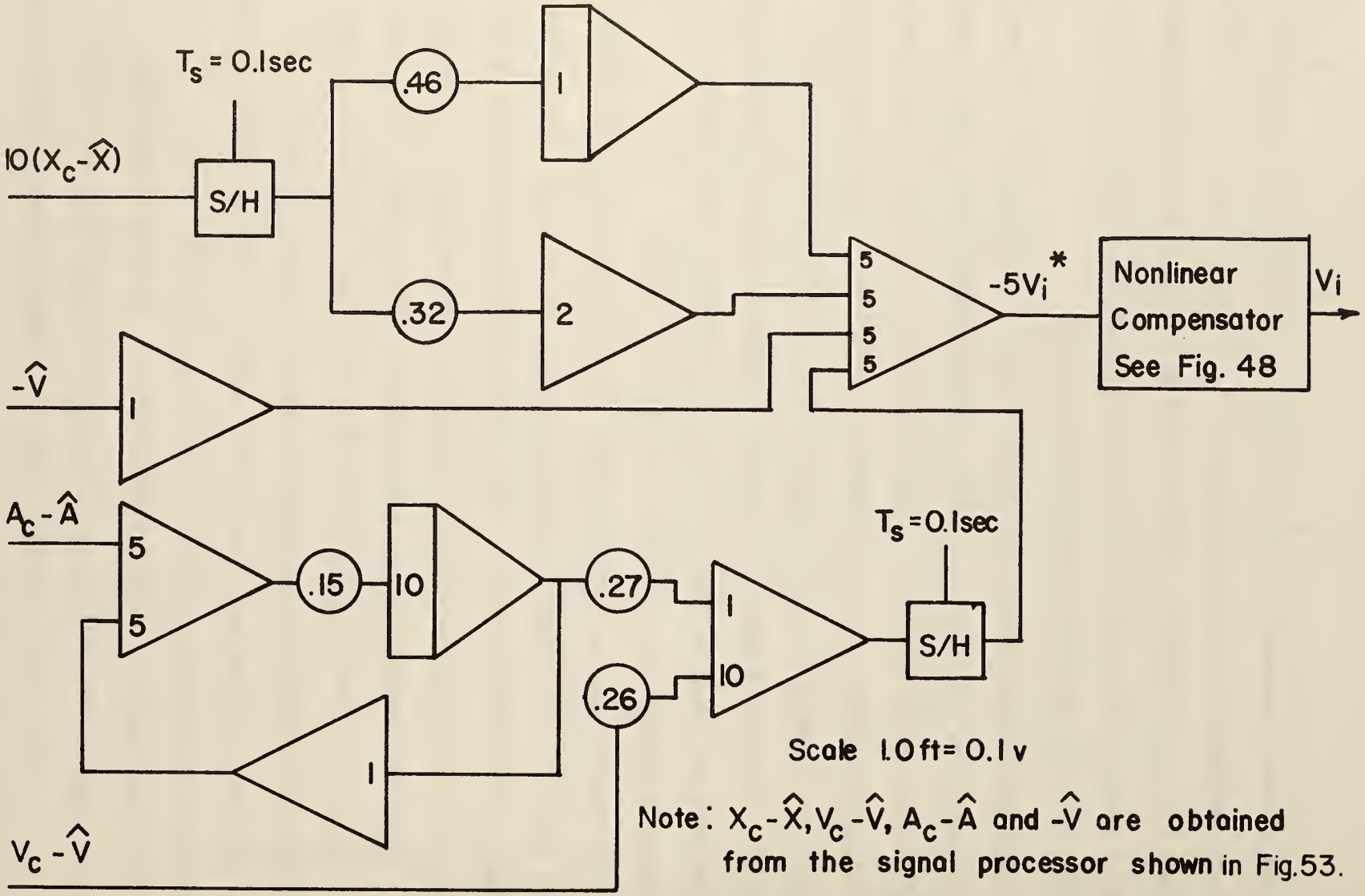

Fig. 54 The vehicle longitudinal controller.

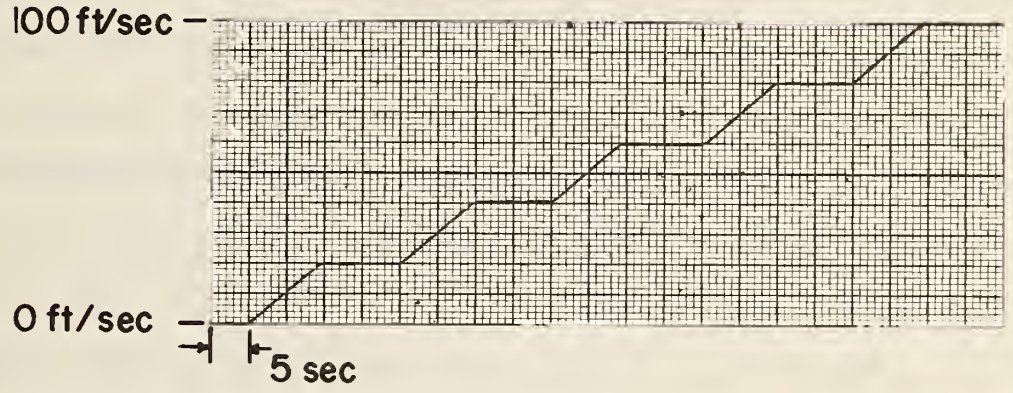

(a) V_c

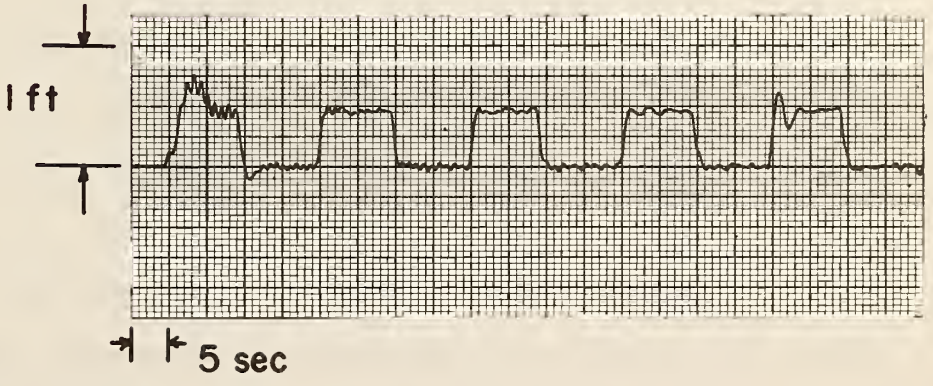

(b) $X_c - \hat{X}$

Fig. 55 Full-scale response ($X_c - \hat{X}$) maneuvering command.

A typical response ($X_c - \hat{X}$) is shown in Fig. 55(b). Note that the steady-state error was essentially zero during constant-speed operation, and was less than 0.5 ft when $A_c = 2.0$ ft/sec^2. The responses at the midspeeds appeared to match the theoretical response (See Fig. 52(a)) fairly well. However, high-frequency (1 Hz) oscillations were present at low-speeds, and a relatively large overshoot was noticed at high speeds. If the model had been sufficiently accurate, this should not have occurred; thus, it appears that a more complex model is necessary.

One such model, which is currently being studied, is shown in Fig. 45. A modified controller, based on this improved model, will be evaluated using the approach specified here (with the signal processor shown in Fig. 53). Eventually, the command generator (Appendix D)/ state estimator (Fig. 21)/ controller combination will be evaluated in complete full-scale tests in which the crossed-wires will provide an absolute position reference.

CHAPTER VII

SUMMARY AND CONCLUSIONS

A. Summary and Conclusions

The achievement of safe and efficient longitudinal control is probably the most significant technical problem associated with individual automated-vehicle, transport systems such as the automatic highway and automated guideway transit.

One general control structure would involve a central controller to oversee network operations with this including the coordination of sector-level computers--each of which would supervise and control the vehicles operating in its assigned sector. Four essential facets of operations at this sector level are:

a) The specification and/or generation of vehicle command states;

b) Communications between sector control and each controlled vehicle;

c) The determination of the state of each vehicle; and

d) The control of each individual vehicle.

The research reported here was performed during the second year of a two-year study, and it deals with the design, development and testing of hardware systems essential for implementing these facets in the context of high-speed (to 93 ft/sec), small time-headway (1-2 sec) operation.

The primary emphasis was focused on:

1) The development of three promising information source configurations for providing each vehicle in a sector with a continuous and accurate measure of its state;
2) The specification of realistic longitudinal control systems which employ continuous (or near-continuous) inputs under both normal and emergency situations; and
3) The demonstrating, under field conditions, of a vehicle controller/information-source combination in various operational situations at speeds up to 88 ft/sec.

The secondary emphases were on: An examination of three general approaches to sector-computer operations; An overview of sector computer-to-controlled vehicle communications; the identification of both the propulsion and braking dynamics of a typical U.S. sedan; and the evaluation of a fifth wheel as an information source.

The first configuration for providing a controlled vehicle with state information involved the use of current-carrying conductors located, at 1-ft intervals, along a roadway. Signals from these conductors were detected and processed onboard a vehicle to obtain a discrete estimate of vehicle position, to an accuracy of better than ±.06 ft, as it passed each conductor. This could be achieved for conductor spacings from 1 to several hundred feet. A position interpolator with an equivalent accuracy was implemented to provide position information between conductors. However, the velocity estimates, derived from measurements of position of the wire crossings, were not a sufficiently accurate measure of a vehicle's "instantaneous" velocity.

The second configuration, which involves a vehicle's continuous acquisition of position information, was comprised of two helically wound, transmission structures embedded in, or alongside, a roadway. The absolute position-measurement accuracy, per laboratory tests only, was 0.17 ft for "practical" line parameters -- a result which is speed independent. Various approaches for obtaining a velocity estimate from these lines were considered. If P_e were small and a reasonable accuracy were present in the phase measurement, "instantaneous" velocity could be estimated to an accuracy of some 0.9 ft/sec provided $|A| < 3.22$ ft/sec.

The third configuration, a vehicle-borne radar and scattering enhancement plates embedded under the roadway surface, resulted in both an accurate position signal (e.g., a maximum position error of .05 ft in a 10-ft distance) and an estimate of instantaneous velocity which is within ±0.7 ft/sec of the true value of the speed range 0-100 ft/sec provided $|A| < 3.22$ ft/sec^2.

In essence, all three configurations, either singly or in combination, appear quite promising for use in a high-performance system.

In many previous efforts on vehicle longitudinal control designs, simple linear models of vehicle dynamics were employed. Such models are not realistic for rubber-tired vehicles traveling at moderate to high speeds, and thus the designs presented were of limited value. Here, continuing the efforts of the first year, an empirical, nonlinear model of vehicle longitudinal dynamics was developed and employed in the design of a vehicle longitudinal control system.

This system was demonstrated on a roadway where position information was obtained from embedded current-carrying conductors and an interpolator onboard the vehicle. The demonstration was successful in that a comfortable ride ($|J| < 1.6$ ft/sec^3), an insensitivity to adverse environmental effects,

and fairly good position control (±2 ft tracking accuracy) were achieved. Superior performance, especially improved tracking accuracy, will be achieved in a modified design.

B. Future Efforts

Future efforts will be focused on the development of a complete 4-mile sector wherein vehicles would be under the control of a roadside, sector-level computer. During the next year, this will involve the field installation of at least one of the three evaluated information sources, and the specification of the required computer and communications equipment. Subsequently, these items will be designed, implemented and installed in this sector so that complete sector-level operations may be achieved and evaluated under realistic normative and emergency conditions.

When completed, this facility will provide a unique capability for the evaluation of most aspects of sector-level operations--information sources, vehicle controllers, computer hardware/software, etc. This will be an important step toward the demonstration of the technological feasibility of the automated highway.

APPENDIX A

INSTRUMENTATION INSTALLED AT THE TRANSPORTATION RESEARCH CENTER OF OHIO

In order to evaluate several realizations of an Information Source 1 under field conditions, a small, instrumented test facility was required. A 3300-ft section of asphalt roadway, which is adjacent to the FHWA skid-calibration facility at the Transportation Research Center of Ohio (TRCO), was available for this purpose, and 2209 ft of this section were instrumented as shown in Fig. A-1. Approximately 500 ft of noninstrumented contiguous roadway are always available for making a low-speed entry onto the instrumented roadway. When necessary, a high-speed entry can be obtained by using the figure "8" loop which is incorporated into the adjacent vehicle dynamics area.

The completed installations consists of two separate units--a crossed-wire configuration and radar scattering-enhancement plates--which are sealed below the roadway surface. The former consists of 5 wires installed in the slots shown in Fig. A-2(a). Two wires each form a spatial square wave (See Fig. A-2 (b)) which are located in the square slots along with two linear wires, and the fifth wire is located in the single linear slot.

A crossed-wire configuration is obtained by exciting either (or both) of the square-wire configurations with an alternating current. As the lateral wires are 1-ft apart, the minimum marker interval is 1 ft; however, it should be clear that other intervals, which are multiples of 1 ft, could readily be obtained from this configuration. The single linear wire is used for an automatic steering reference; ultimately it, and the linear conductors in the square slots, will be evaluated for communications usage as well.

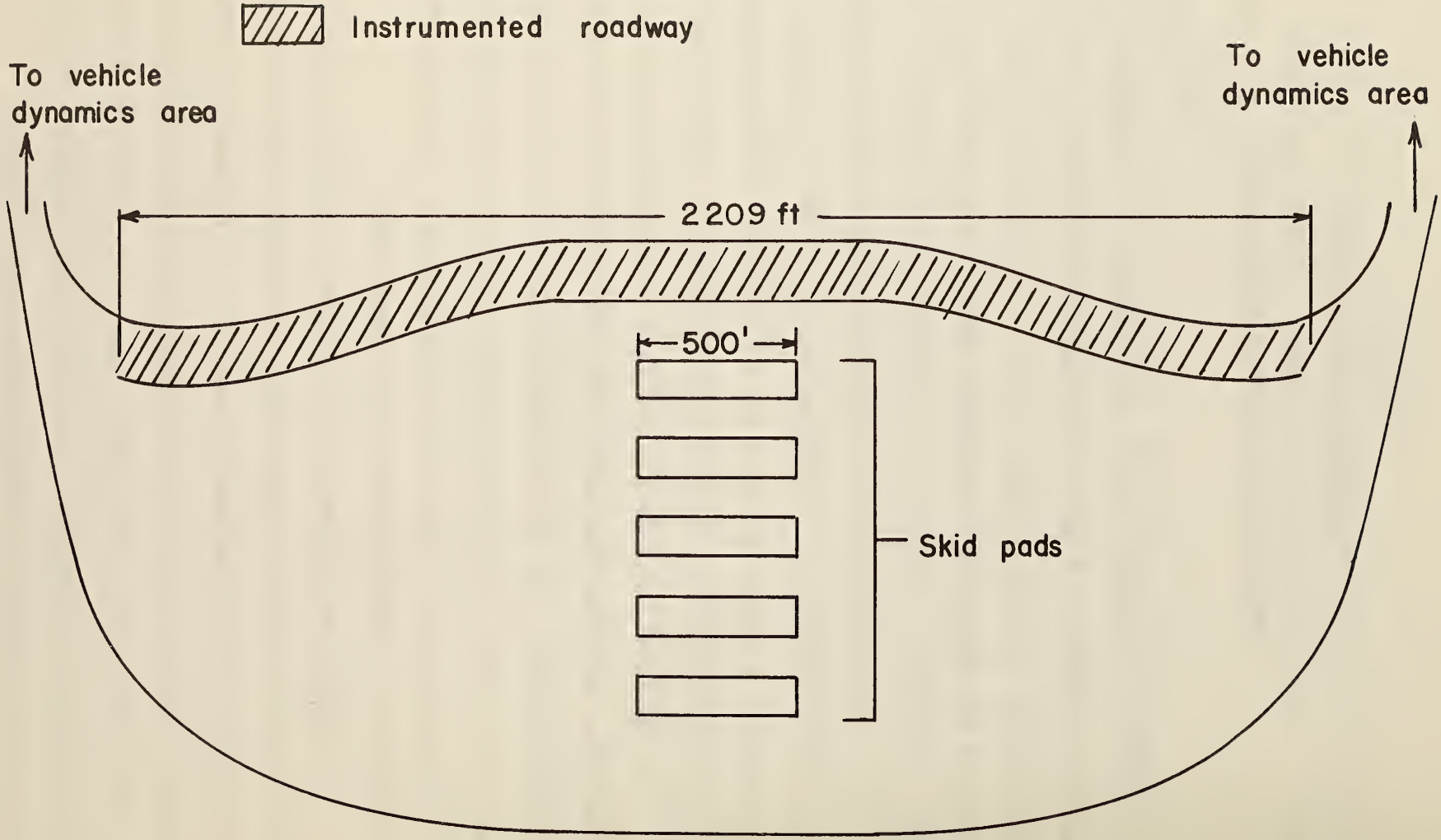

Fig. A-1 Instrumented section of roadway.

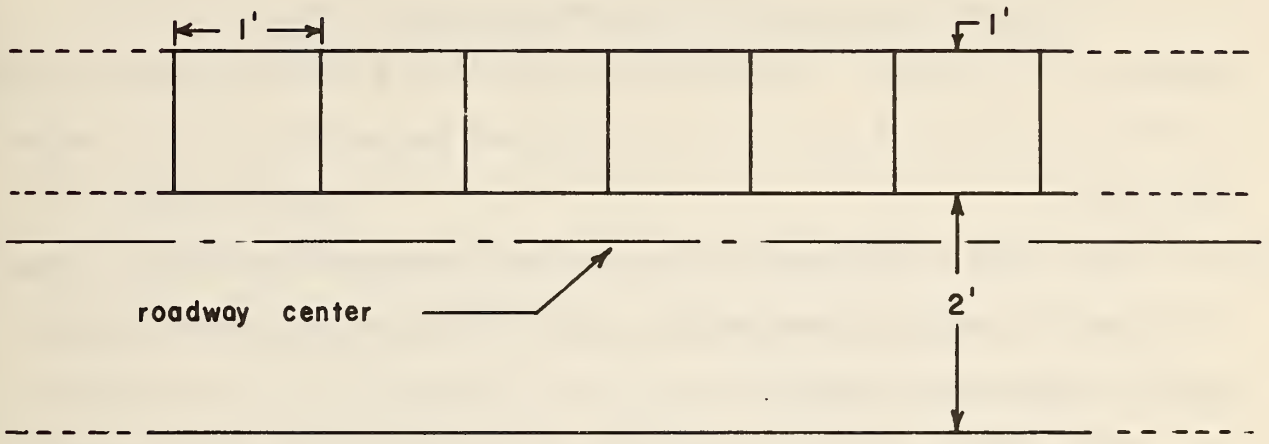

a) Slots cut into roadway surface (top view)

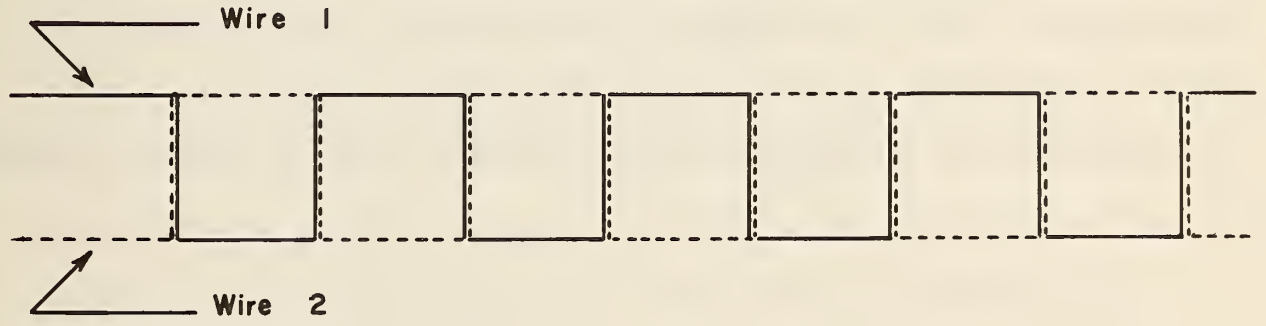

b) Spatial square waves of wire

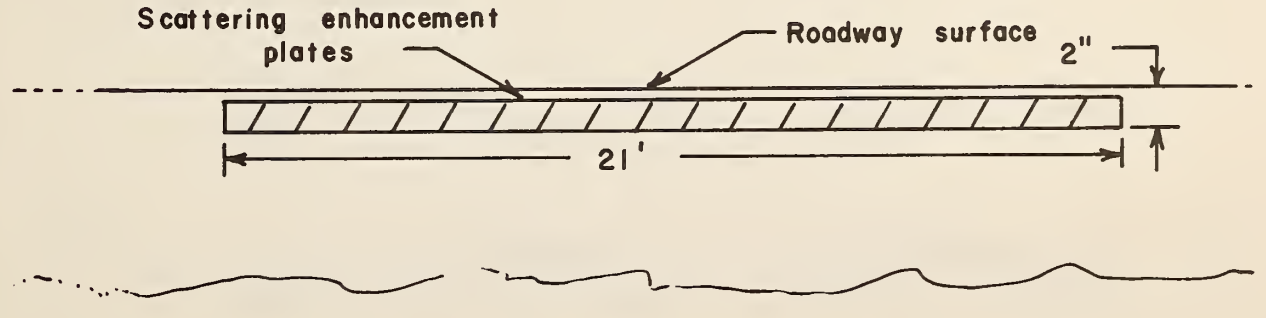

c) Plates for use with Doppler Speedometer

Fig. A-2 Installations under the roadway surface.

A 21-ft section of scattering enhancement plates was installed as depicted in Fig. A-2(c). The plates were mounted in a wooden structure (.167 ft x .167 ft x 21 ft) with $\alpha_p = 30$, and positioned approximately 0.25 in below the surface.

If it were necessary to evaluate helically wound transmission lines in a vertically-mounted configuration, then light wooden support structures would be installed at roadside.

Other instrumentation was installed at TRCO under a previous contract. This consisted of two linear conductors, which were installed over a 3-mile distance in a precut slot between the 80 and 100 mph lanes on the 8-mile high-speed test track. Two miles are straight roadway, while the third consists of a transition and curve with a 2500-ft radius of curvature. This instrumentation was previously used in an intensive study of automatic steering.[15]

APPENDIX B

HELICAL TRANSMISSION LINES AS AN INFORMATION SOURCE

A. Ideal Operation

Two properly deployed helical transmission lines can be used to provide state information to ground vehicles. The operation of these lines may be understood by first considering the magnetic field $\vec{H}$ in the vicinity of a single line. Toward this end, consider the two parallel wires, excited by currents, I, shown in Fig. B-1. At the observation point O, the components of $\vec{H}$ (H_x and H_y) are

$$H_x = \frac{Iy}{2\pi r_2^2} - \frac{Iy}{2\pi r_1^2} \tag{B-1}$$

and

$$H_y = \frac{I(x + h/2)}{2\pi r_1^2} - \frac{I(x - h/2)}{2\pi r_2^2} \tag{B-2}$$

where $r_1^2 = (x + h/2)^2 + y^2$, $r_2^2 = (x - h/2)^2 + y^2$, and h, x, and y are defined in Fig. B-1.* In polar coordinates, the equivalent components are

$$H_r = H_x \cos\phi + H_y \sin\phi$$

and

$$H_\phi = -H_x \sin\phi + H_y \cos\phi.$$

These can be expressed as

$$H_r = \frac{Ih \sin\phi}{4\pi r^2}\left[\frac{1}{1 + (h/r)\cos\phi + (h/2r)^2} + \frac{1}{1 - (h/r)\cos\phi + (h/2r)^2}\right]$$

and

$$H_\phi = \frac{I}{2\pi r^2}\left[\frac{r + (h/2)\cos\phi}{1 + (h/r)\cos\phi + (h/2r)^2} - \frac{r - (h/2)\cos\phi}{1 - (h/r)\cos\phi + (h/2r)^2}\right].$$

---

* In order to comform to the conventional (r, ϕ, z) and (x, y, z) coordinate-system representation, z will be used for the longitudinal variable as opposed to x which was used in the text of the report. The text equations are obtained by replacing z by x and x by z.

If $h/r \ll 1$, then

$$H_r \doteq \frac{I}{2\pi} \frac{h \sin \phi}{r^2}$$

and

$$H_\phi \doteq - \frac{I}{2\pi} \frac{h \cos \phi}{r^2} ,$$

so that

$$\vec{H} = \frac{Ih}{2\pi r^2} [\sin \phi \, \hat{r} - \cos \phi \, \hat{\phi}]. \qquad \text{(B-3)}$$

Here, $\hat{r}$ and $\hat{\phi}$ are unit vectors as shown in Fig. B-1.

Consider now the cross-sectional view of 4 parallel wires, excited by currents I_1 and I_2, as shown in Fig. B-2. The resultant magnetic field can be obtained by superimposing the fields of each line pair. The result is (for $h/r \ll 1$)

$$\vec{H} = \frac{h}{2\pi r^2} [(I_1 \sin \phi - I_2 \cos \phi)\hat{r} - (I_1 \cos \phi + I_2 \sin \phi)\hat{\phi}].$$

If I_1 and I_2 were the phasors

$$I_1 = I_o \, e^{jo}$$

and

$$I_2 = I_o \, e^{\pm j \, \pi/2},$$

then $\vec{H}$ would be

$$\vec{H} = \frac{I_o h}{2\pi r^2} [(\sin \phi \mp j \cos \phi)\hat{r} - (\cos \phi \pm j \sin \phi)\hat{\phi}].$$

The upper sign corresponds to the + 90° shift on I_2 and the lower to the -90° shift (This convention will be adhered to throughout this appendix). Since

$$\sin \phi \mp j \cos \phi = \mp j e^{\pm j\phi}$$

and

$$\cos \phi \pm j \sin \phi = e^{\pm j\phi},$$

$\vec{H}$ can be written as

$$\vec{H} = \frac{I_o h}{2\pi r^2} [\mp j\hat{r} - \hat{\phi}] \, e^{\pm j\phi}. \qquad \text{(B-4)}$$

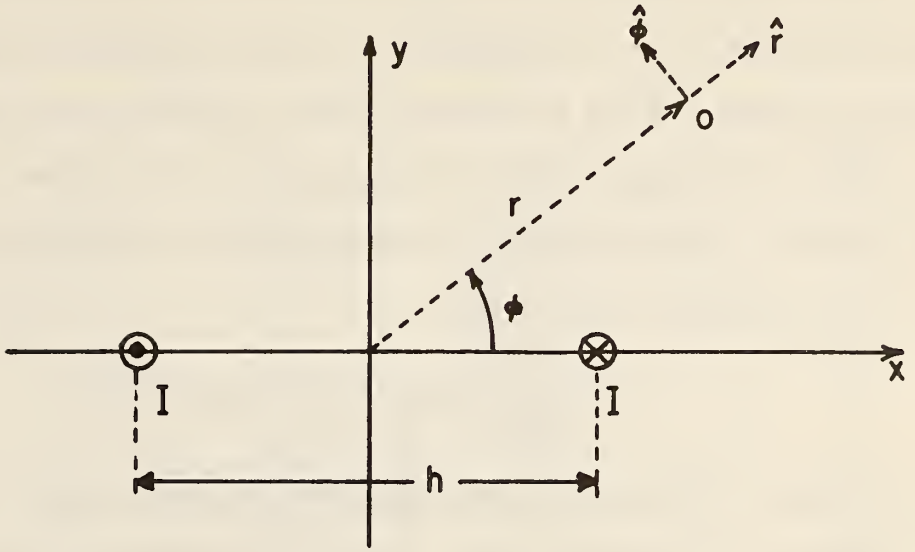

Fig. B-1 Two parallel wires with current I.

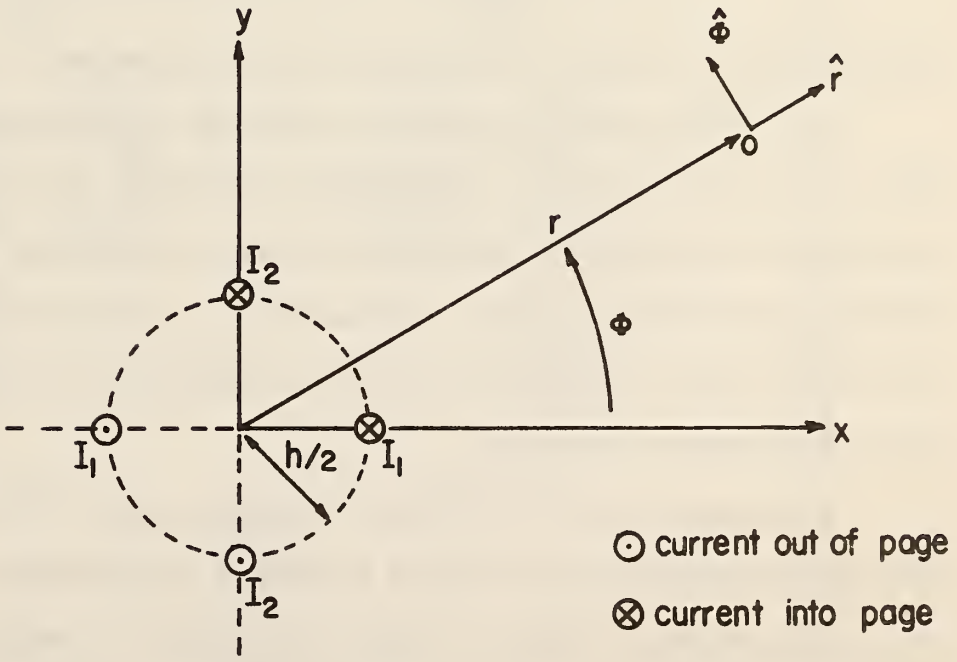

Fig. B-2 Four parallel wires with currents I_1 and I_2.

The expressions for the magnetic field of a helically wound line (of pitch length P), as a function of z, can be obtained as follows: Consider a cross-sectional view of the line at various positions along the z axis. The views would be rotated, relative to that of Fig. B-2, either in the clockwise direction for a left-hand pitch or counter clockwise for a right-hand pitch. Thus, if one assumes $r << P$, then

$$\vec{H} = \frac{I_o h}{2\pi r^2} [\mp j\hat{r} - \hat{\phi}] \, e^{\pm j\phi} \, e^{\mp j(2\pi/P)z} \qquad (B\text{-}5)$$

for a RH pitch. The corresponding expression for a LH pitch is identical if P is allowed to be negative. Here it was assumed that no phase change due to the propagation constant, β, results. Thus, the frequency of excitation, f, must be sufficiently low so that $\lambda >> P$, where $\lambda = \frac{2\pi f}{c_\ell}$, and c_ℓ is the velocity of propagation of the line. In rectangular coordinates, (B-5) is

$$\vec{H} = \frac{I_o h}{2\pi r^2} [\mp j\hat{x} - \hat{y}] \, e^{\pm j2\phi} \, e^{\mp j(2\pi/P)z} \, . \qquad (B\text{-}6)$$

This form would be useful if H_x and/or H_y were detected.

If a probe were positioned at a constant cross-sectional point ($r = r_o$ and $\phi = \phi_o$) and moved in the longitudinal direction, any component (H_r, H_ϕ, H_x or H_y) of the detected signal would undergo a continuous phase-shift--totaling 360^0 for every P distance moved. For motion in a given direction ($\pm z$), this phase shift would be positive or negative depending on the method of excitation and/or the sense of the pitch.

A reference must be available to measure phase. This could be obtained from another helically-wound line.* A proposed configuration is shown in Fig. B-3, where arbitrary pitches P_1 and P_2 are shown. The method of line excitation

---

* Actually, any transmission line could be used. The superior noise-rejection capability of the helical structure makes it a strong candidate. In addition, if similar structures are used for both lines then any effect of β on the phase difference (however slight) would cancel.

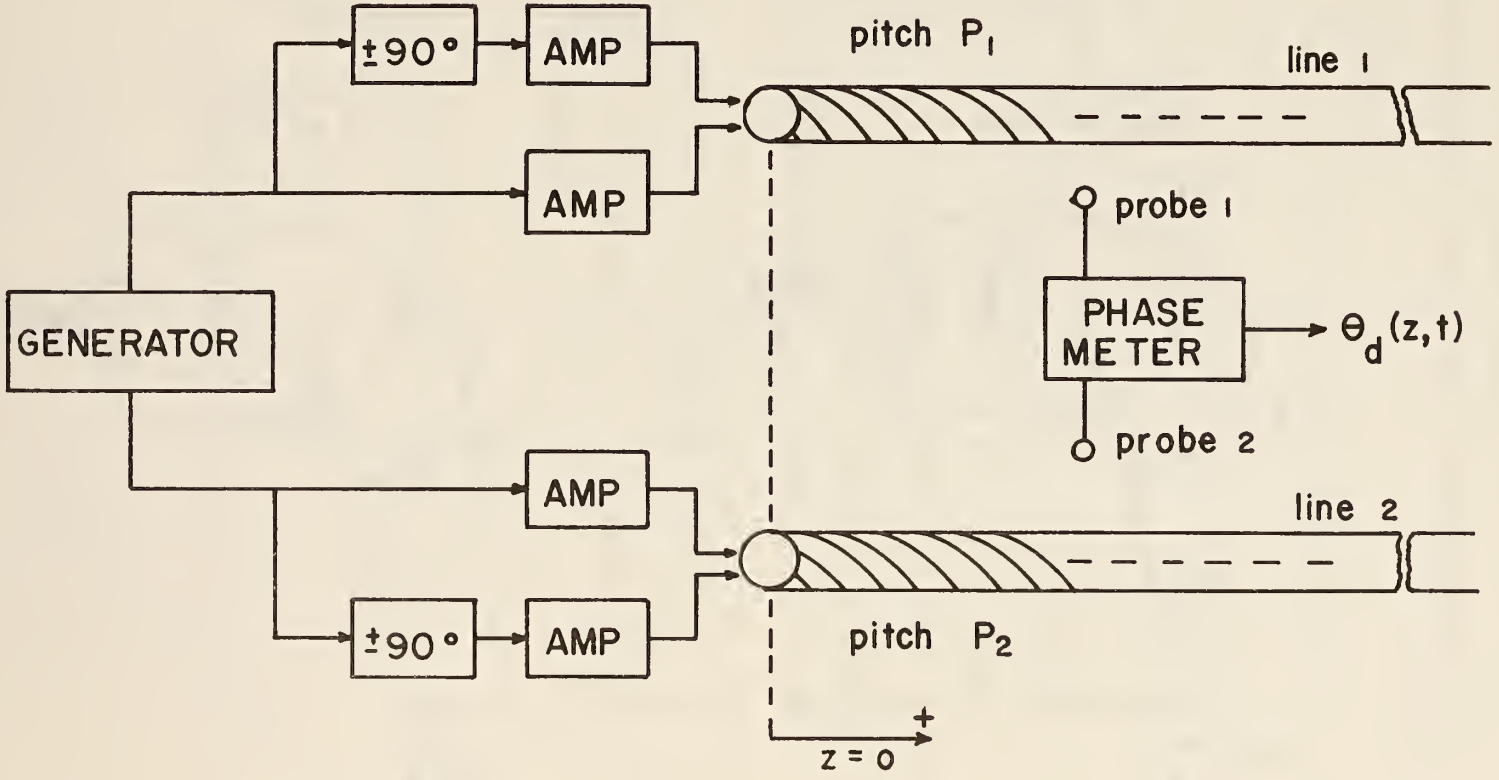

Fig. B-3 Proposed longitudinal reference system using two helically wound transmission lines.

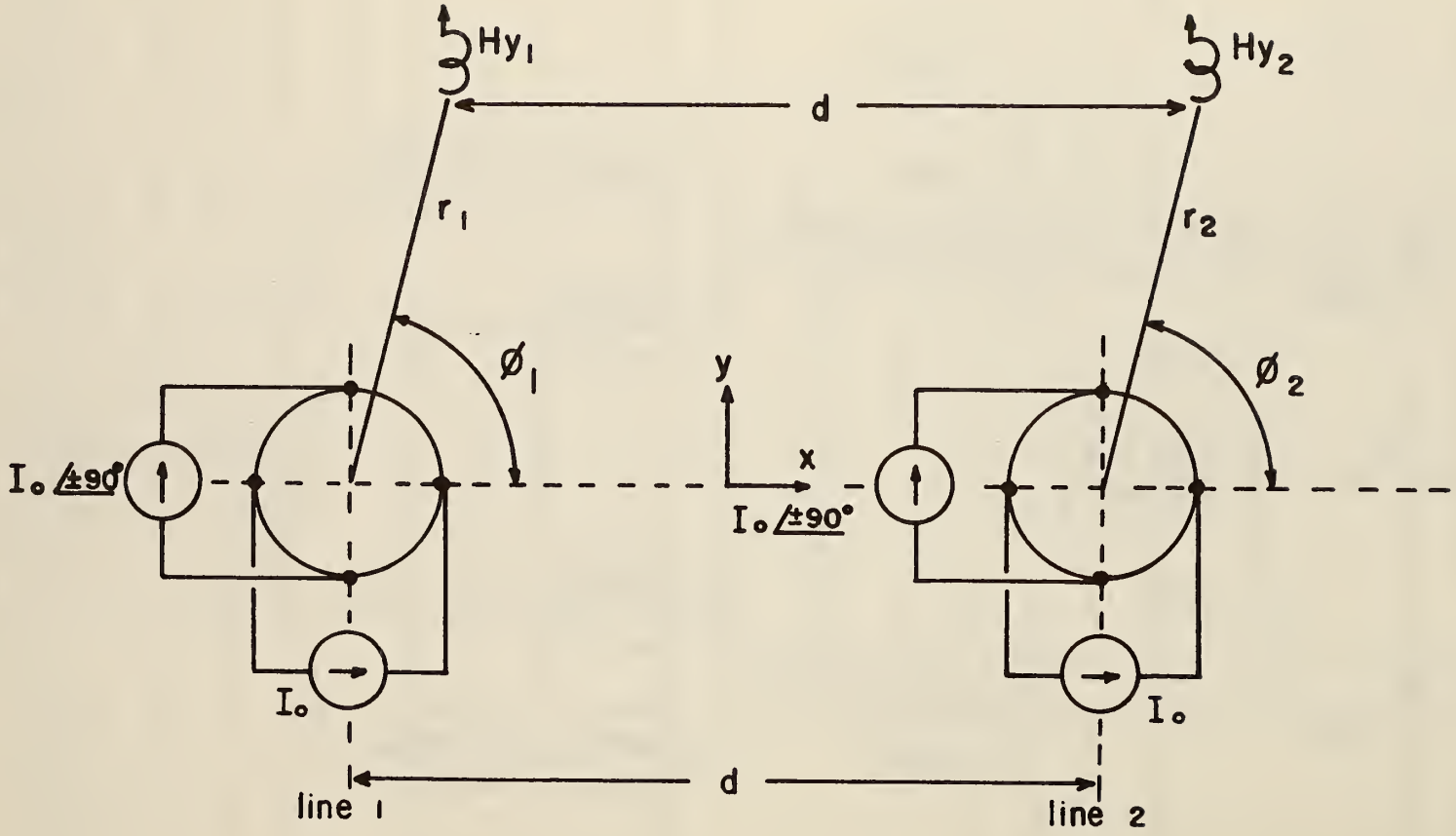

Fig. B-4 Coordinate system, probe location, and excitation for system shown in Figure B-3.

and probe placement is shown in Fig. B-4. The probe spacing, d, was chosen to equal the line spacing, and the probes are assumed to measure H_y (The results would be similar if H_x were measured).

Using (B-6) for Lines 1 and 2, the phase difference as measured by a phase meter would be

$$\theta_d(z) = \arg\,(H_{y2}) - \arg\,(H_{y1}).$$

This reduces to

$$\theta_{d+}\,(z) = 2(\phi_2 - \phi_1) - 2\pi z(\frac{1}{P_2} - \frac{1}{P_1}) \qquad \text{(B-7)}$$

for a choice of $+90^0$ for I_2 on both lines, and

$$\phi_{d-}(z) = 2(\phi_2 + \phi_1) - 2\pi z\,(\frac{1}{P_2} + \frac{1}{P_1}) \qquad \text{(B-8)}$$

for a choice of $+90^0$ for I_2 on Line 2 and -90^0 on Line 1.

In each of the preceeding equations, the phase difference is a spatially periodic function of z, and a typical waveform is shown in Fig. B-5. Here, P_e, the "effective pitch length", is given by

$$\frac{1}{P_e} = \frac{1}{P_2} \mp \frac{1}{P_1}\,. \qquad \text{(B-9)}$$

Any desired value of P_e (both positive and negative) can be achieved via the selection of P_1 and P_2.

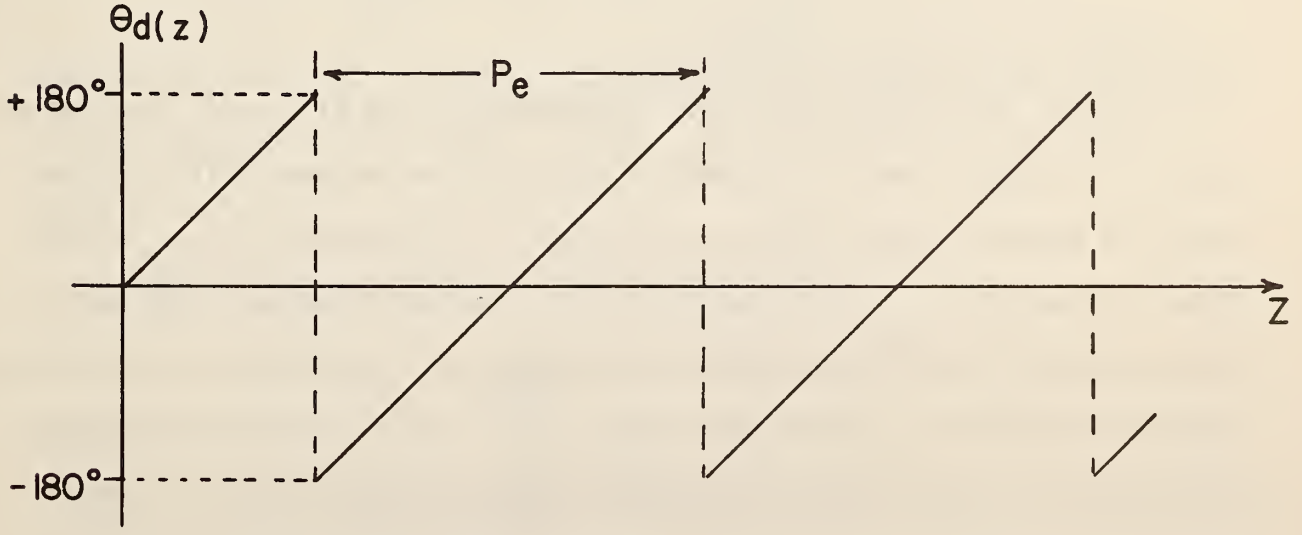

Fig. B-5 Theoretical phase-difference versus the longitudinal coordinate.

Thus, the longitudinal position of a vehicle could be determined if it were equipped with appropriate probes and a phase meter. For absolute position measurement, a counter would be needed to indicate the number of 360^0 phase traversals made by the signal. This would be a "coarse indication" of position. The measured phase within a period of the waveform would be a "fine indication" of position.

Additional versatility, which may be useful, would result if the two lines were operated at slightly different frequencies. If $f_1 = f_o$ and $f_2 = f_o + \Delta f$, and the frequency difference were viewed as a time-changing phase shift $\alpha = \Delta\omega t$, then (B-6) would contain an extra factor of $e^{+j\Delta\omega t}$ for Line 2. Then (B-7) and (B-8) would become

$$\theta_{d+}(z, t) = 2(\phi_2 - \phi_1) - \frac{2\pi z}{P_e} + \Delta\omega t$$

and

$$\theta_{d-}(z, t) = 2(\phi_2 + \phi_1) - \frac{2\pi z}{P_e} + \Delta\omega t.$$

The waveform would still be periodic in z, but the wave would move at a velocity V_H. This can be found by setting $d\theta_d/dt = 0$, with the result

$$V_H = P_e \Delta f. \qquad \text{(B-10)}$$

B. Deviations From Ideal Operation

In the implementation of this configuration (see Fig. B-3), the measured phase will deviate from the theoretical value for two reasons: First, since the field equations were derived on the basis of four-parallel wires, deviations will occur if P is not greater than r. Second, since each line and its probe cannot be entirely isolated from the other pair, deviations due to cross-coupling will occur. These factors would cause a simple bias on the phase if the probes were maintained at a constant cross-sectional point (r = const,

ϕ = const) during longitudinal travel. However, due to the expected lateral and vertical motions of the vehicle, deviations in the measured phase would occur and be interperted as erroneous longitudinal position changes.

The effect of a finite pitch length is difficult to treat analytically. However, from the numerous laboratory experiments conducted, it was surmised that for $P_1 > 2ft$ and $P_2 > 2ft$, the corresponding phase-errors, should be inconsequential.

The effect due to cross coupling was treated both analytically and experimentally. In both cases, parallel wires (infinite pitch length) were used so that the effects could be isolated from the pitch-length factor.

Consider the configuration of Fig. B-6 wherein the probes are shown at positions ($x = \Delta x$, $y = yo + \Delta y$) deviating from the desired positions ($x = 0$, $y = yo$). The magnetic field detected by Probe 1 would be

$$H_{y1} = - \frac{I_o h}{2\pi r^2} e^{\pm j2\phi_1} e^{\mp j \frac{2\pi}{P_1} z} - \frac{I_o h}{2\pi a^2} e^{\pm j2\phi_1'} e^{\mp j \frac{2\pi}{P_2} z}$$

and that by Probe 2

$$H_{y2} = - \frac{I_o h}{2\pi r^2} e^{\pm j2\phi_2} e^{\mp j \frac{2\pi}{P_2} z} - \frac{I_o h}{2\pi r^2} e^{\pm j2\phi_2'} e^{\mp j \frac{2\pi}{P_1} z}$$

Here ϕ_1, ϕ_1', ϕ_2, ϕ_2', a, and b are defined in the figure. The leading term in both equations is the ideal signal. The second term is the undesired signal.

After rearrangement of terms, there results

$$H_{y1} = - \frac{I_o h}{2\pi r^2} e^{\pm j2\phi_1} e^{\mp j \frac{2\pi}{P_1} z} m_1 e^{\pm j\delta 1} \qquad \text{(B-11)}$$

and

$$H_{y2} = - \frac{I_o h}{2\pi r^2} e^{\pm j2\phi_2} e^{\mp j \frac{2\pi}{P_2} z} m_2 e^{\pm j\delta 2} , \qquad \text{(B-12)}$$

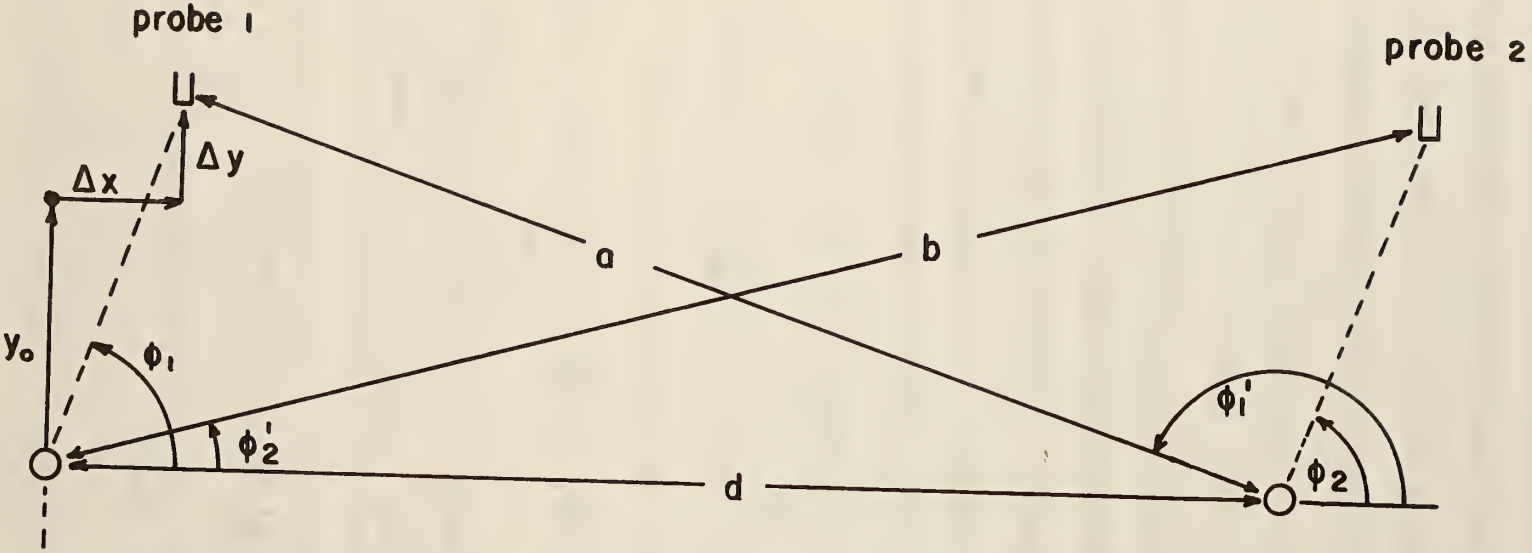

Fig. B-6 Geometry for the probe locations shifted Δx and Δy from the desired location.

where

$$m_1 e^{\pm j\delta_1} = 1 + \frac{r^2}{a^2} e^{\pm j(2\phi_1' \mp 2\phi_1 \mp (2\pi/P_2)z \pm (2\pi/P_1)z)} \quad \text{(B-13)}$$

and

$$m_2 e^{j\delta_2} = 1 + \frac{r^2}{b^2} e^{\pm j(2\phi_2' \mp 2\phi_2 \mp (2\pi/P_1)z \pm (2\pi/P_2)z)} \quad \text{(B-14)}$$

Equations (B-7) and (B-8) become

$$\theta_{d_+} = -2\pi z \left(\frac{1}{P_2} - \frac{1}{P_1}\right) + 2(\phi_2 - \phi_1) + (\delta_2 - \delta_1) \quad \text{(B-15)}$$

and

$$\theta_{d_-} = -2\pi z \left(\frac{1}{P_2} + \frac{1}{P_1}\right) + 2(\phi_2 + \phi_1) + (\delta_2 + \delta_1). \quad \text{(B-16)}$$

The leading term in each equation is the theoretically desired one while the last two terms represent phase-errors.

An obvious means of reducing the phase-error is to use the excitation* which yields θ_{d+}. For simple vertical and lateral vehicle motions with no tilt, $\phi_1 = \phi_2$ and the phase-error (θ_e) would be

$$\theta_e = \delta_2 - \delta_1. \quad \text{(B-17)}$$

From an examination of (B-13) and (B-14), it is apparent that δ_1 and δ_2 are phase angles which result from the addition of two phasors--one of which is unity and a second a small phasor of arbitrary angle as shown in Fig. B-7. If $r^2/a^2 << 1$, then the maximum value of δ_1 will occur when the phasor representing r^2/a^2 is at a 90^0 angle; then $\delta_{1m} = \sin^{-1} r^2/a^2$. A similar argument yields $\delta_{2m} = \sin^{-1} r^2/b^2$. Since, in general, the two angles could be equal but of opposite sign, then

$$\theta_e \leq \sin^{-1} r^2/a^2 + \sin^{-1} r^2/b^2, \quad \text{(B-18)}$$

where from the geometry of Fig. B-6,

---

* To use this mode, one must insist that $P_1 \neq P_2$ so that P_e is finite. Either non-equal pitches of the same sense or arbitrary (equal or nonequal) pitches of opposite sense would suffice. Thus, any value of P_e could still be achieved--at least in theory.

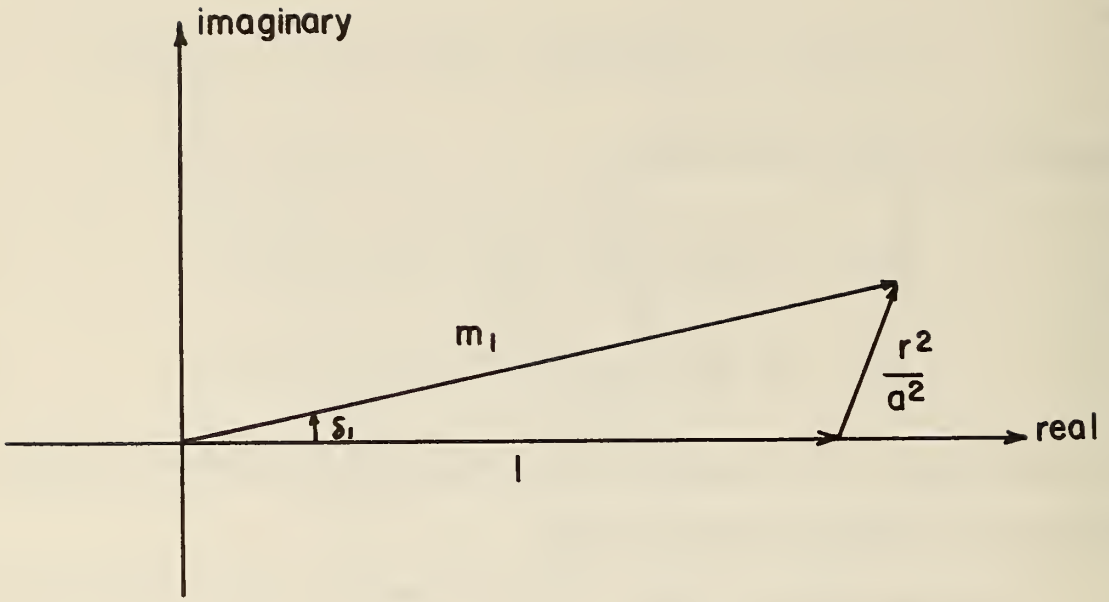

Fig. B-7 Phase angle δ_1 which results from the addition of two phasors.

$$r^2 = (y + \Delta y)^2 + (\Delta x)^2,$$

$$a^2 = (d - \Delta x)^2 + (yo + \Delta y)^2$$

and

$$b^2 = (d + \Delta x)^2 + (yo + \Delta y)^2$$

C. Experimental Verification

The theory of a helical-line information source, as developed here, is based on (B-6). Note from this equation that H_x and H_y have a similar form; therefore, an experimental measurement of one component (H_y) should suffice to validate the theory.

First, H_y vs. r was measured for single lines of various diameters (1/4, 1/2, and 1 in). The results are shown in Fig. B-8 for $I_0h = 0.5$ (The units are peak-to-peak amperes x inches) together with the theoretical $1/r^2$ variation. Within reasonable limits, the signal from the lines varies as $1/r^2$.

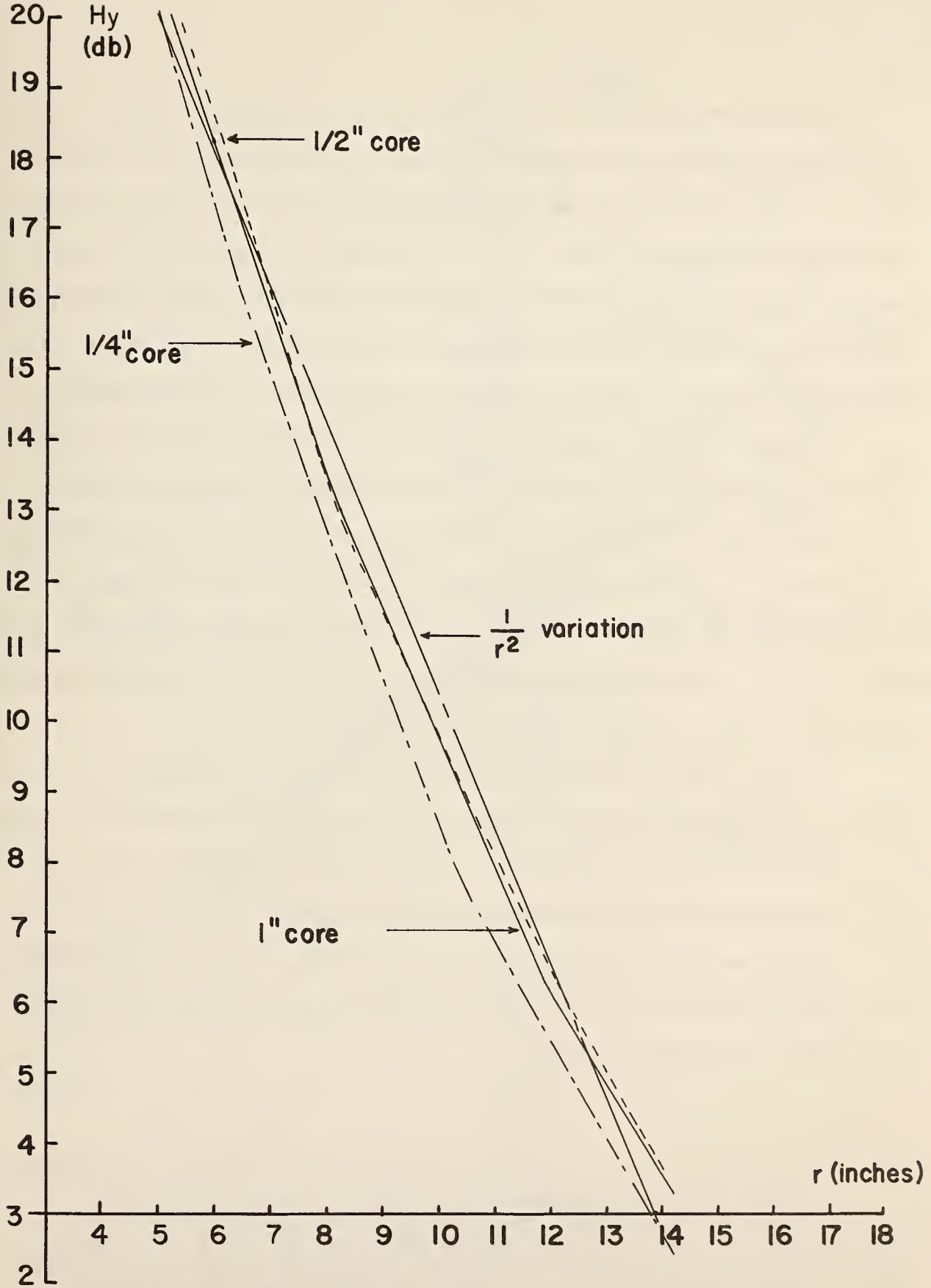

Fig. B-8 Amplitude of Hy versus distance from the line. (I_0h = 0.5).

Second, the variation in the phase of H_y, as the probe was moved over a wide cross-sectional region, was measured (The coordinates are defined in Fig. B-2). The results for the 1" diameter line are shown in Fig. B-9 and the theoretical results in Fig. B-10. (The results for the other lines were similar and are not presented here). Note the generally close agreement between the two; however some distortion exists on one side of the line.* It was concluded that an accurate model for line behavior has been developed.

Lastly, a detailed study of the phase-errors which would be incurred due to lateral and vertical motions of the vehicle was conducted to verify (B-17) and (B-18). Three different line sizes were used but only the results from the 1/2 in. diameter line are shown for brevity. These are shown in Fig. B-11 and the theoretical results, per (B-13), (B-14) and (B-17) are shown in Fig. B-12. A reasonable agreement exists for $y \leq 15$ in., and these equations may be used with confidence in the design process.

An upper bound on θ_e, which was given by (B-18), is plotted in Fig. B-13. While this deviates considerably from both the measured and theoretical results, it provides a very conservative but easily calculated estimate. Thus, this upper bound was employed in the calculations of Chapter IV.

While the tests reported were conducted using 30 in. line separations, the results indicate that calculated values for other separations should be satisfactory for design purposes.

---

* This distortion was due to the presence of steel-reinforcing material which was placed under the lines for all tests. This material also caused the asymmetry of the phase-error curves of Fig. B -11. All results given in this appendix include the effects of reinforcing material and are thereby more realistic than those that could have been obtained without it.

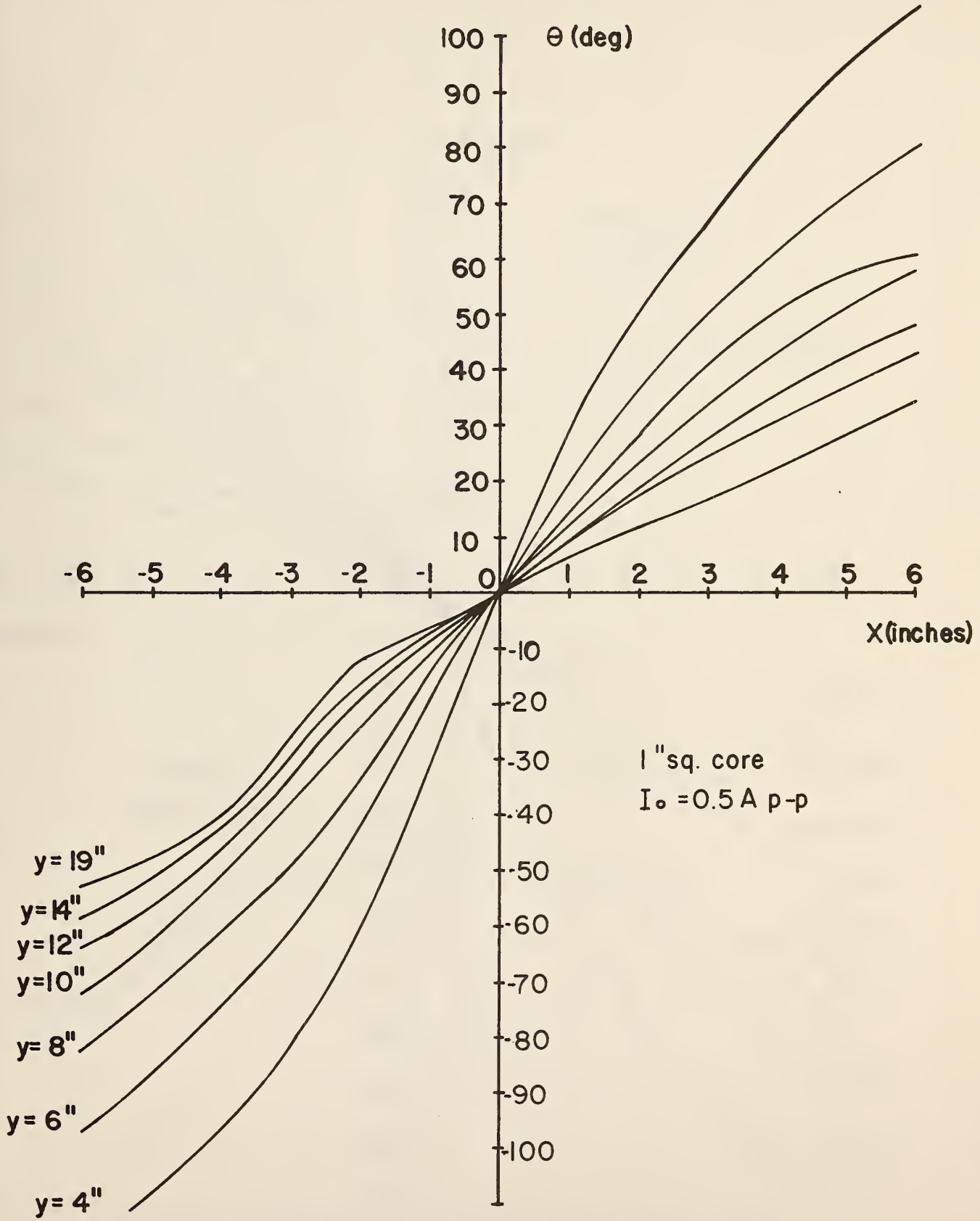

Fig. B-9 Variation in the phase of H_y for various positions in the cross-sectional plane. (Experimental results).

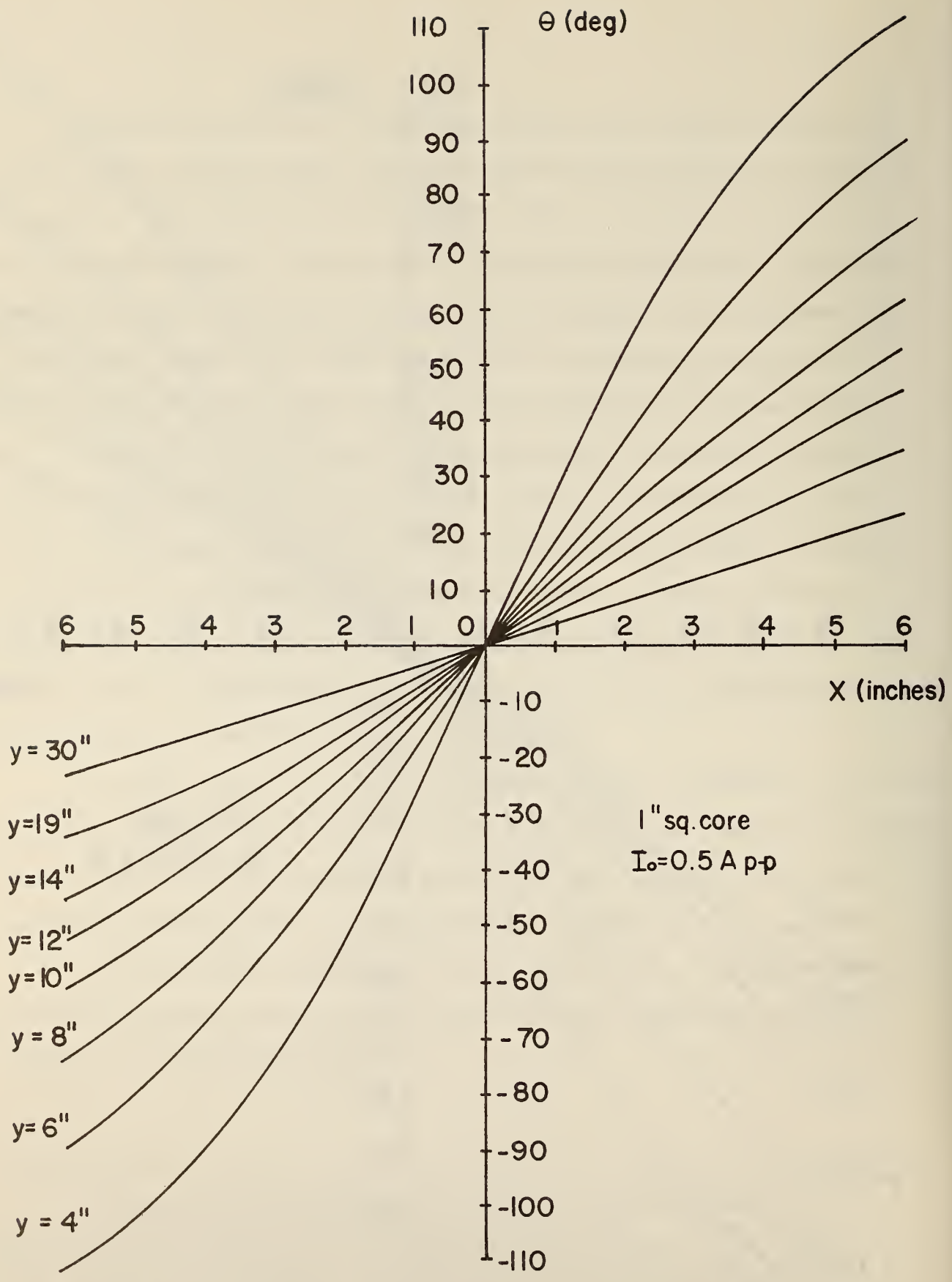

Fig. B-10 Variation in the phase of H_y for various positions in the cross-sectional plane. (Theoretical results).

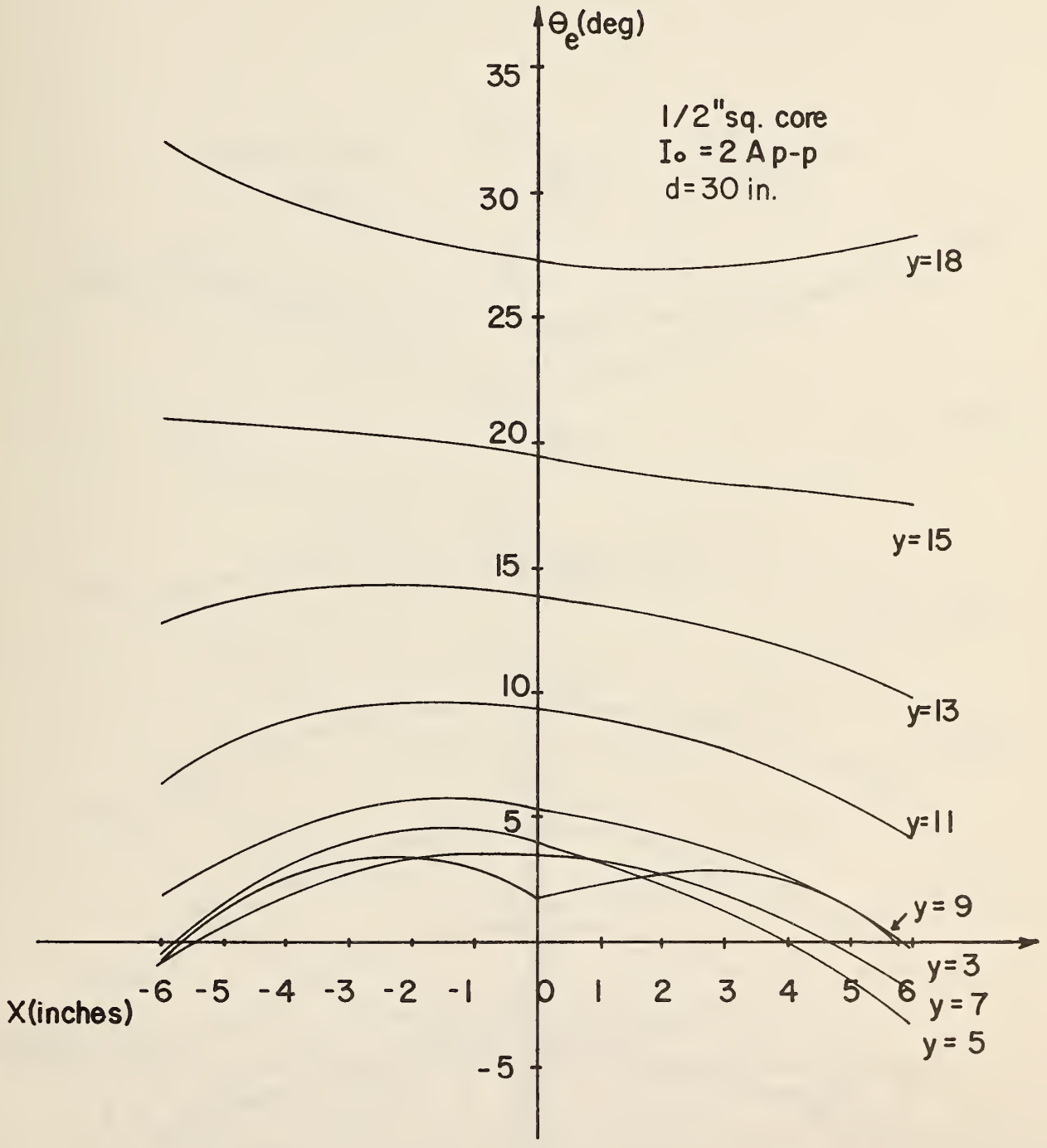

Fig. B-11 Phase-error (θ_e) for various positions of the probes in the cross-sectional plane. (Experimental results.)

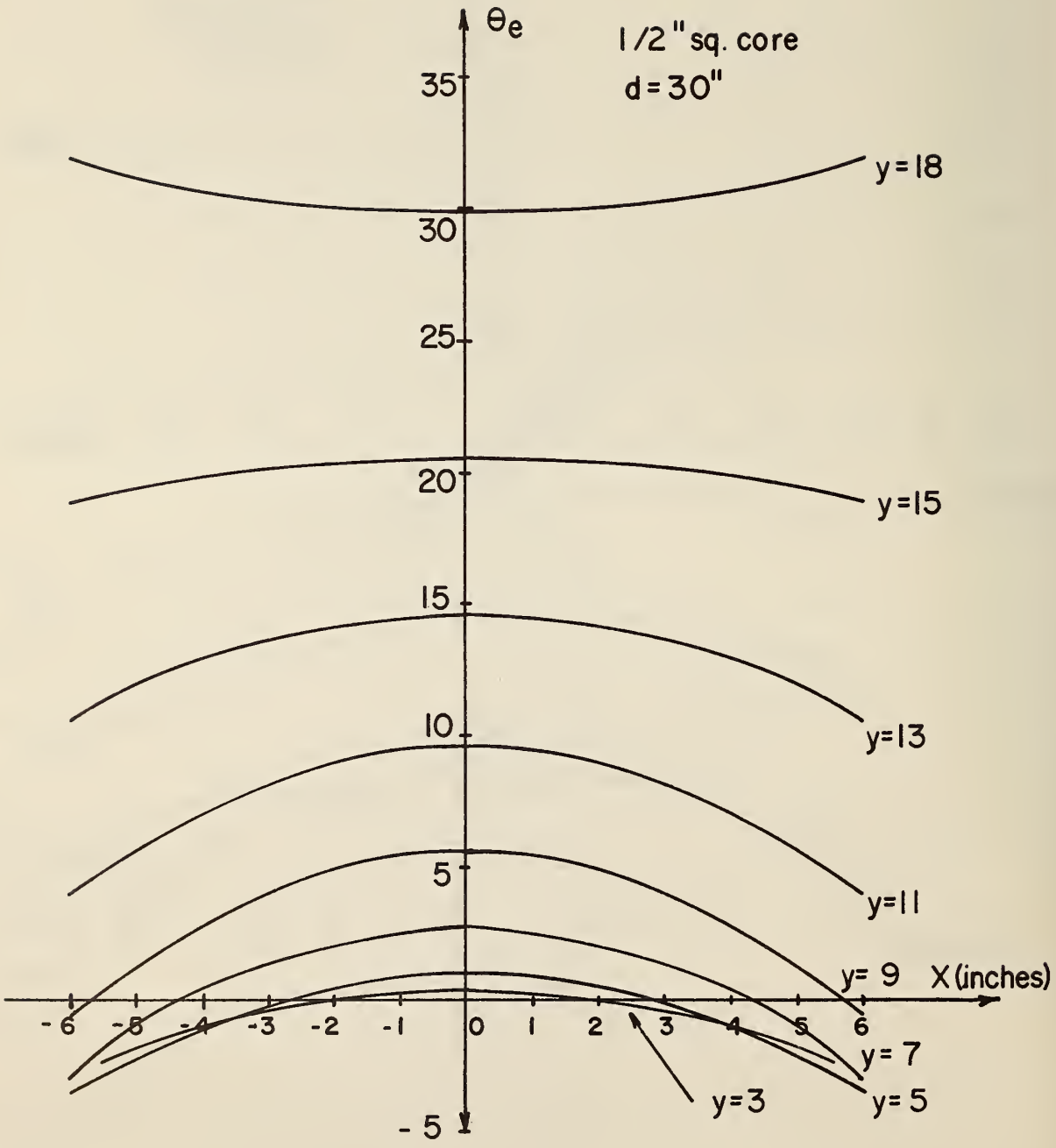

Fig. B-12 Phase-error (θ_e) for various positions of the probes in the cross-sectional plane. (Theoretical Results).

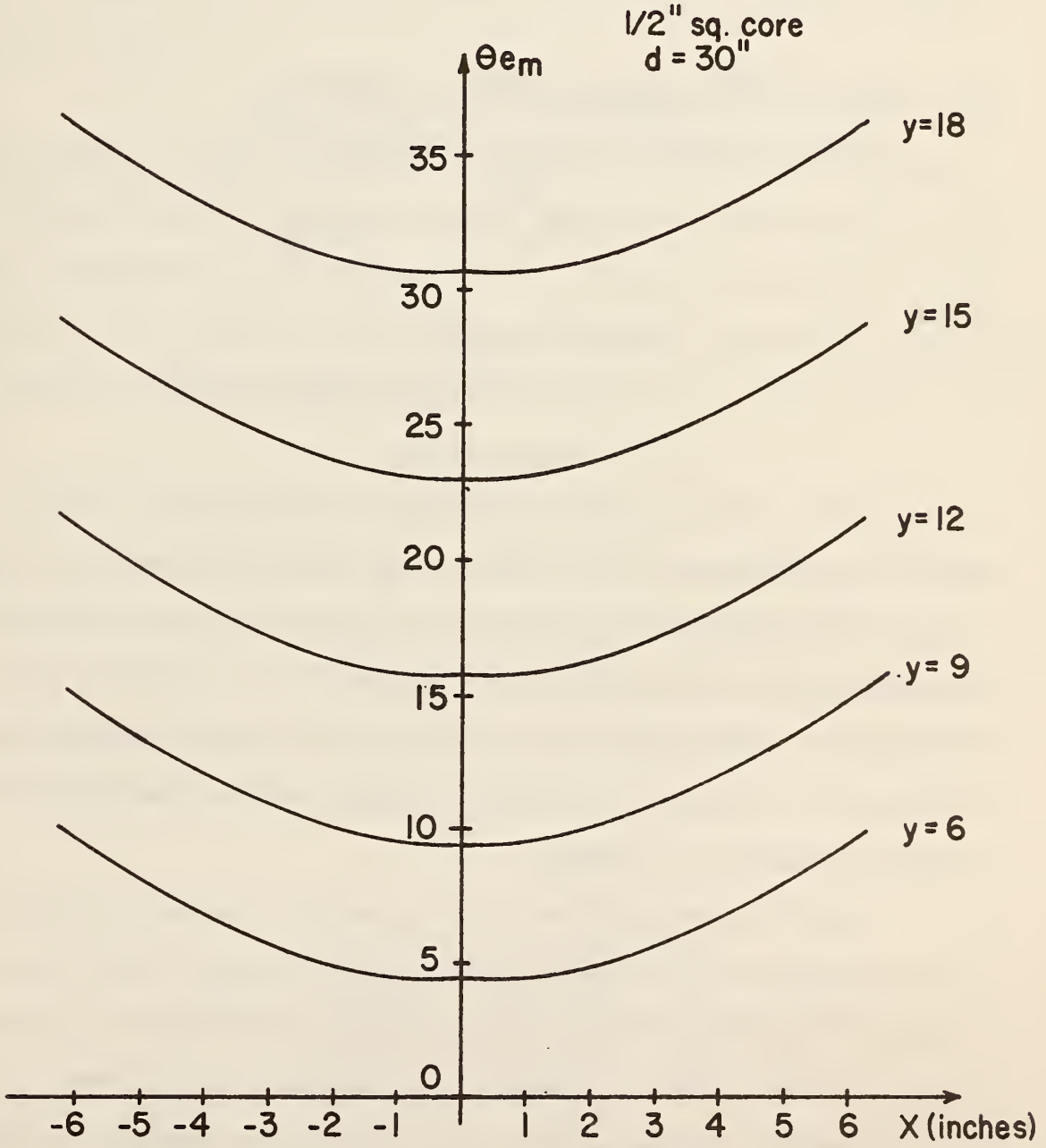

Fig. B-13 An upper bound on the phase error (θ_e) for various positions of the probes in the cross-sectional plane.

APPENDIX C
ON THE IDENTIFICATION OF BRAKING DYNAMICS

A. A Model of Braking/Roadway Interface Dynamics

Braking dynamics are generally represented by

$$V = \frac{K_e^{-\tau p}}{p} V_i \qquad (p \equiv \frac{d}{dt}) \tag{C-1}$$

where

V is vehicle speed,

V_i is the input to the braking system,

K_e is a fixed gain, and

τ is the braking system time delay.

The primary advantage of this model is its simplicity; however, it results in a poor approximation of the behavior of a braking vehicle in many practical situations, and its use could result in unrealistic performance predictions. This would be highly undesirable in view of the exacting braking requirements which would be imposed on an automated ground vehicle operating in a high-speed, small time-headway environment.

The relationship between V and V_i would be dependent on such factors as the condition of the brakes, the properties of the tire/road interface, and a vehicle's deceleration rate (A). This relationship would be nonlinear and probably quite complex. As the goal of the effort reported here is the design of a closed-loop braking system, it is probably not necessary to employ such a complex form, and a much simpler one, involving an input-output relationship for an expected range of vehicle speeds and deceleration rates, could be

adequate. This model would be a nonlinear differential equation whose parameters were dependent on V, A and V_i. A further simplification would result if it were assumed that nearly linear operation were obtained for a prescribed set of conditions (i.e., a fixed command deceleration rate from an initial speed (V_o). Then

$$p^n V = g[p^{n-1} V, \ldots A, V, V_i], \qquad (C\text{-}2)$$

where g defines a linear relationship among the variables in its argument. This relationship would contain quantities which changed with condition, thus partially accounting for the nonlinearities in the braking dynamics. A disadvantage of this approach, which was the one adopted here, would be the failure of a specified model to predict some critical events (e.g., the onset of wheel lock).

It was hypothesized that the braking/roadway interface dynamics of a typical U.S. passenger sedan could be represented, at least for the purpose of designing a closed-loop braking system, by the model shown in Fig. C-1. This model contains 5 quantities K_B, α, β, δ, and τ, which were assumed to be dependent on both V_o and A_c, and its form was specified after an examination of data obtained from braking tests.

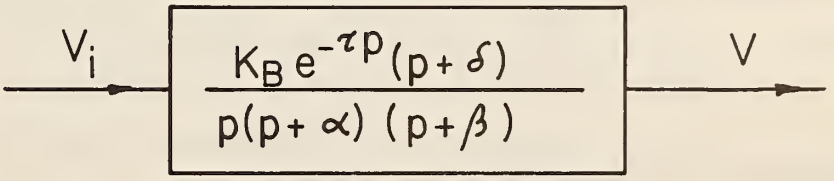

Fig. C-1 A simple model of braking/roadway-interface dynamics.

B. Identification of Model Parameters

One approach toward obtaining the model parameters is via open-loop testing. This would involve driving a test vehicle at a fixed speed V_o, applying a braking command (A_c), obtaining the resultant response, and then estimating the parameters corresponding to V_o and A_c. Unfortunately, this approach is of limited value because of the inevitable presence of both small unwanted disturbances and higher-order effects (not considered here) which result in highly inconsistent and nonrepeatable results.[29] However, this approach could be, and was, employed to obtain a value of some 150 m sec for τ--a value which was somewhat independent of both V_o and A_c.

More consistent results may be obtained by using a closed-loop configuration, and this approach was adopted here. The quantities K_B, δ, α and β were specified via a model-matching technique in which the response of the closed-loop model, shown in Fig. C-2, was matched to that obtained from a corresponding full-scale implementation. The model input is the command velocity (V_c), the braking system input is V_i*, and the output is V.

The compensator (G_c) should be selected so that low-error performance (e.g., $\Delta V = V_c - V_w$ small) is obtained, as this would be a requirement on a system intended for operation in a high-speed, small time-headway environment. Several compensators were evaluated including two proportional-plus-integral units and a gain-only unit; here only the latter with

$$G_c = 1.0$$

was employed in the identification process.

---

* In a full-scale situation, V_i would be the voltage input to an electrohydraulic actuator which would control brakeline pressure.

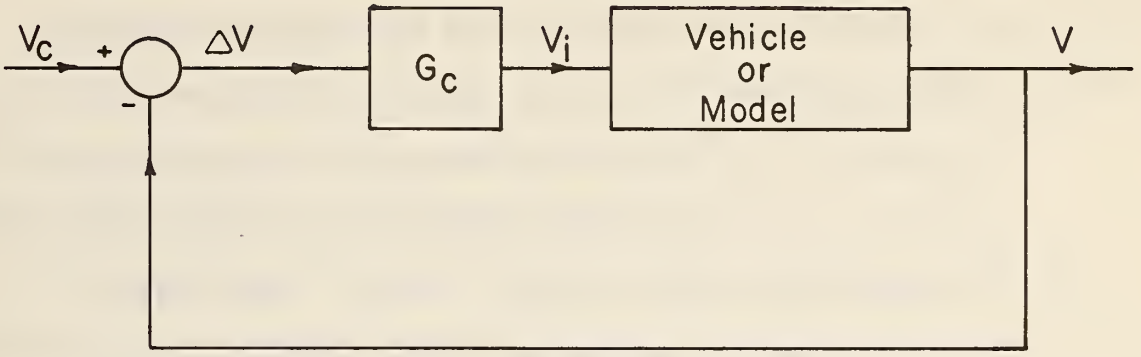

Fig. C-2 Closed-loop system employed in the parameter-identification process.

The model parameters were obtained via the following procedure:

The large-signal command input

$$V_c = V_o - A_c t \qquad [0, t_s] \tag{C-3}$$

was applied to a test vehicle which was traveling at a fixed speed V_o on a nearly level, concrete pavement and the signal ΔV was recorded. Here $t = 0$ is the time the brakes were applied, and t_s is the time the vehicle speed was zero. This procedure was applied for both dry-road and wet-road conditions. For the former, tests were conducted for each of five speeds (20, 40, 60, 80 and 90 ft/sec) and four deceleration (6.44, 9.66, 12.88, and 14.5 ft/sec^2) combinations, while in the latter tests were conducted for each of five speeds (20, 40, 60, 80 and 90 ft/sec) and three deceleration (6.44, 9.66, and 12.88 ft/sec^2) combinations. Here, running water to a depth of $\frac{1}{16} - \frac{1}{8}$ in was present on the surface of the concrete roadway. This condition resulted in a very unfavorable environment for effective braking action.

The full-scale conditions were subsequently replicated in the laboratory. The closed-loop model was excited with an input (Eqn. (C-3) and ΔV was recorded. This was matched with the ΔV obtained in the corresponding full-scale test by appropriately adjusting K_B, α, β and δ. Thus, these quantities were assigned values for each speed-deceleration condition.*

C. Experimental Apparatus

A 1969 Plymouth sedan was employed for the full-scale testing. The braking and accelerating functions were accomplished via electrohydraulic control systems and the actuator, which controlled the brake-line pressure, was characterized by a corner frequency of some 7 rad/sec. This vehicle had drum brakes with the two front and two rear brakes independently operated via a dual-master cylinder.

A computer, consisting of 20 operational amplifiers, 18 potentiometers, and other necessary components was installed over the back seat. The computing elements were used for system compensation and data collection. All data collected were recorded on a six-channel, strip-chart recorder located next to the driving position. In some tests, vehicle speed was measured via a calibrated tachometer connected to the drive shaft. The resulting signal was denoted by V_T and thus, in these cases, $V = V_T$ and $\Delta V = V_C - V_T$. In all other tests, V was obtained via a fifth wheel whose measured output was denoted by V_5. Then, $V = V_5$ and $\Delta V = V_C = V_5$.**

---

* The time delay was neglected in this identification procedure.

** Both of these approaches result in an approximate value of V; however, in view of the 5th wheel data presented in Chap IV, and some braking data reported in this chapter, this approximation seems reasonable.

All testing was conducted on the linear section of the skid pad at the Transportation Research Center of Ohio. The grading of this 8000-ft section varied from .44% at one end to -.50% at the other.

D. Experimental Results--Dry-Pavement Conditions

Typical full-scale and model responses (ΔV vs. t) for dry pavement conditions, A_c = 6.44 ft/sec^2 and V_o = 20, 60 and 90 ft/sec are shown in Figs. C-3(a), (b) and (c), respectively, and similar responses for A_c=14.5 ft/sec^2 are shown in Figs. C-4(a), (b) and (c).* In these cases, $V = V_T$ and $\Delta V = V_c - V_T$.

The following should be noted from an examination of the full-scale responses:

1) The response changes with V_o(e.g., the time at which the peak value (ΔV_m) occurs increases with increasing V_o);
2) The magnitude of the response does not increase linearly with increasing A_c (e.g., for V_o = 90 ft/sec, $\frac{\Delta V_m}{A_c}$ = 0.81 for A_c=6.44 ft/sec^2 while $\frac{\Delta V_m}{A_c}$ = 0.45 for A_c = 14.5 ft/sec^2); and
3) The form of the response changes with V_o and/or A_c.

In essence, the braking dynamics are a nonlinear function of at least V_o and A_c, and this property must be explicit in the specified model.

Additional full-scale data, which were collected on a different day than that presented above, are shown in Fig. C-5 for V_o = 20, 60, and 90 ft/sec and A_c = 14.5 ft/sec^2. The responses on the left were obtained for $V = V_T$ while

---

* The full-scale responses presented in this chapter were copied from the original records so that these responses could easily be compared with those from a model.

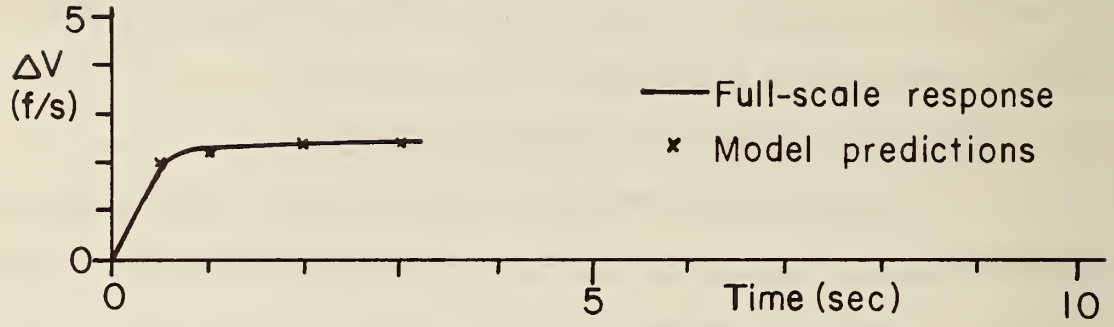

a) V_0 = 20 ft/sec.

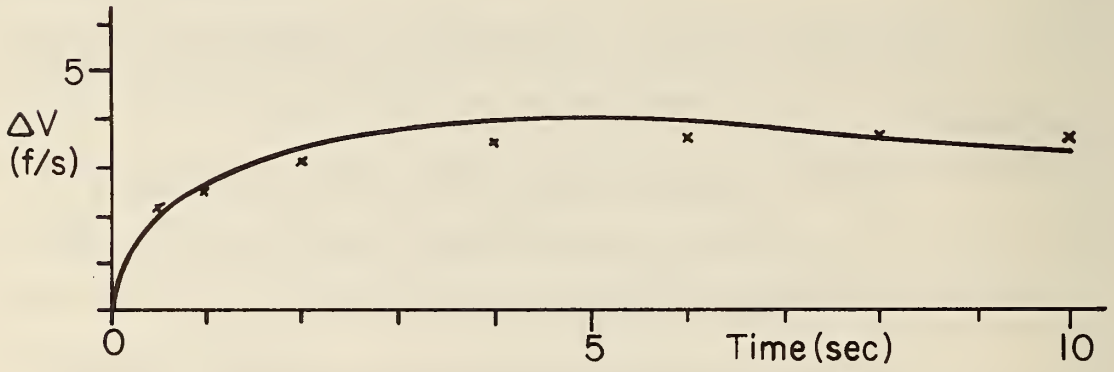

b) V_0 = 60 ft/sec.

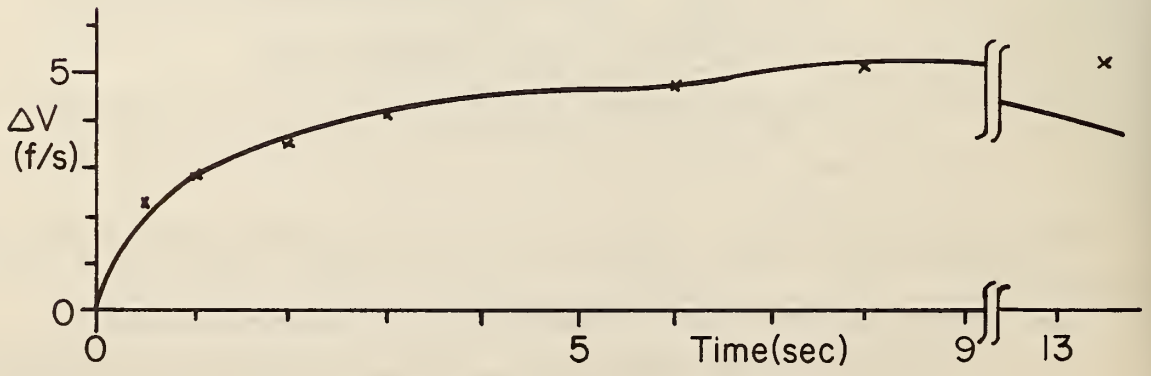

c) V_0 = 90 ft/sec.

Fig. C-3 Comparison of vehicle response and model response for 3 selected initial speeds and A_C = 6.44 ft/sec^2(Dry-pavement conditions).

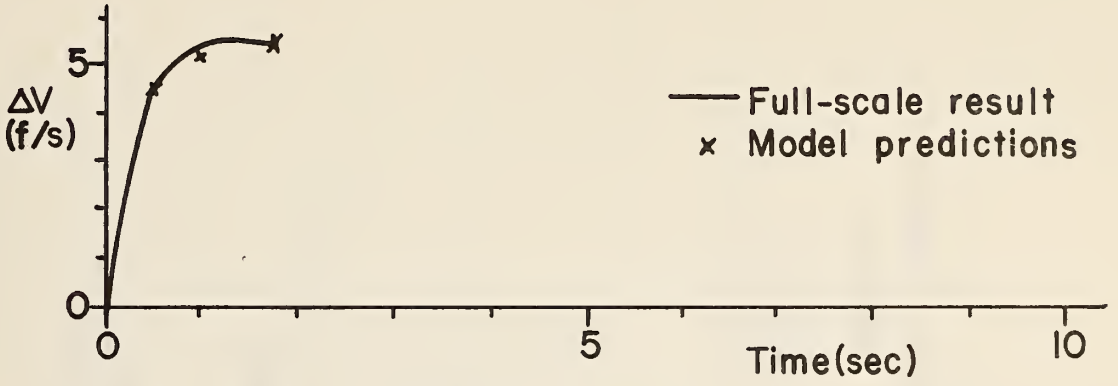

a) V_o = 20 ft/sec.

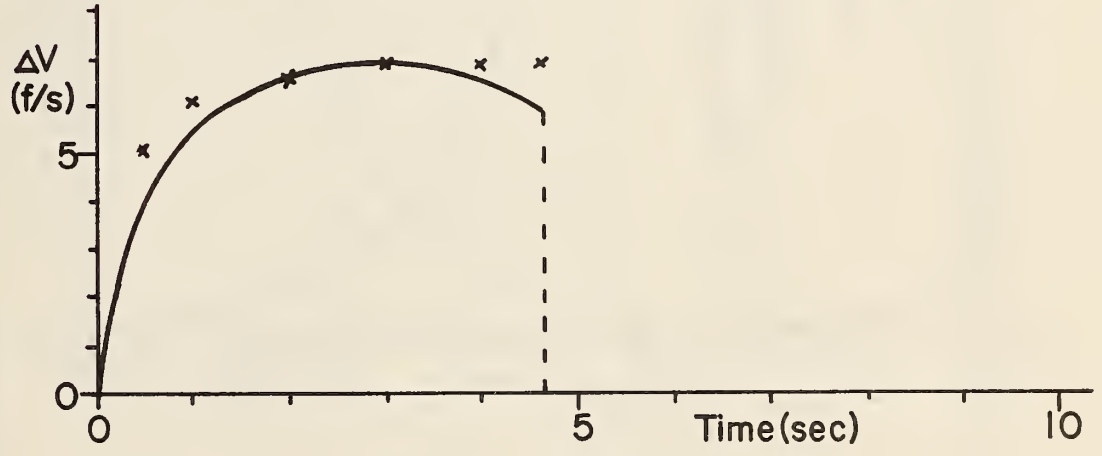

b) V_o = 60 ft/sec.

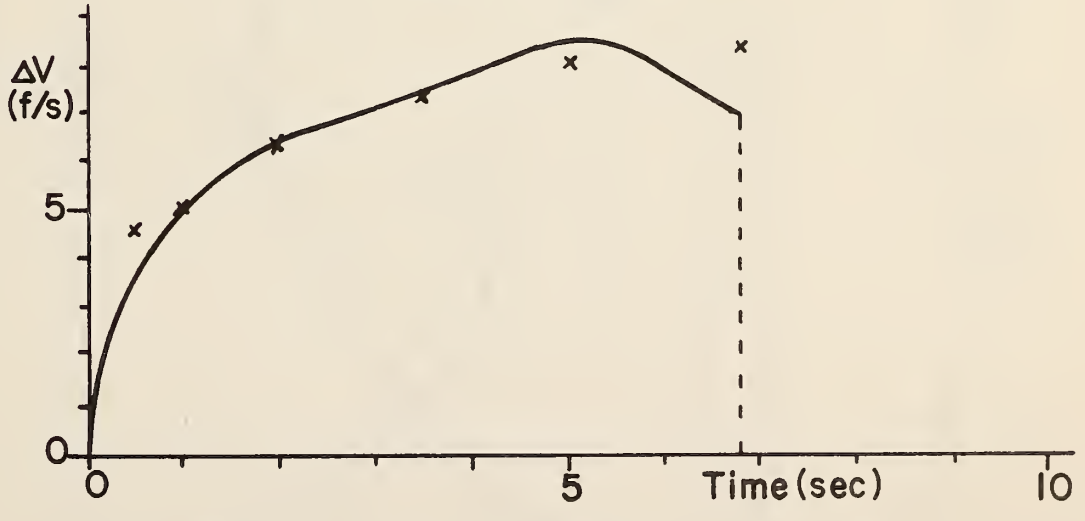

c) V_o = 90 ft/sec.

Fig. C-4 Comparison of vehicle response and model response for 3 selected initial speeds and A_c = 14.5 ft/sec^2 (Dry-pavement conditions).

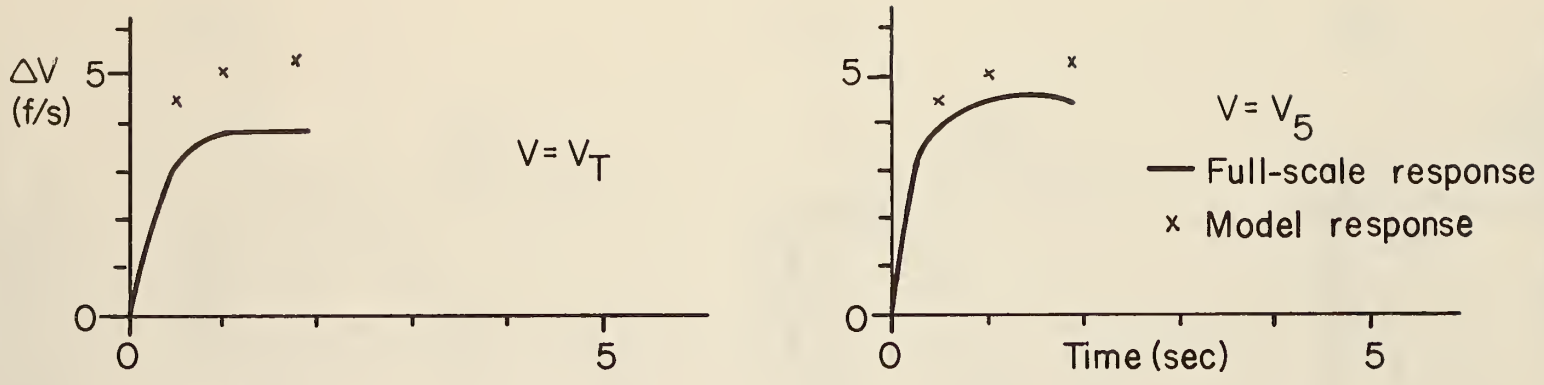

a) V_o = 20 ft/sec.

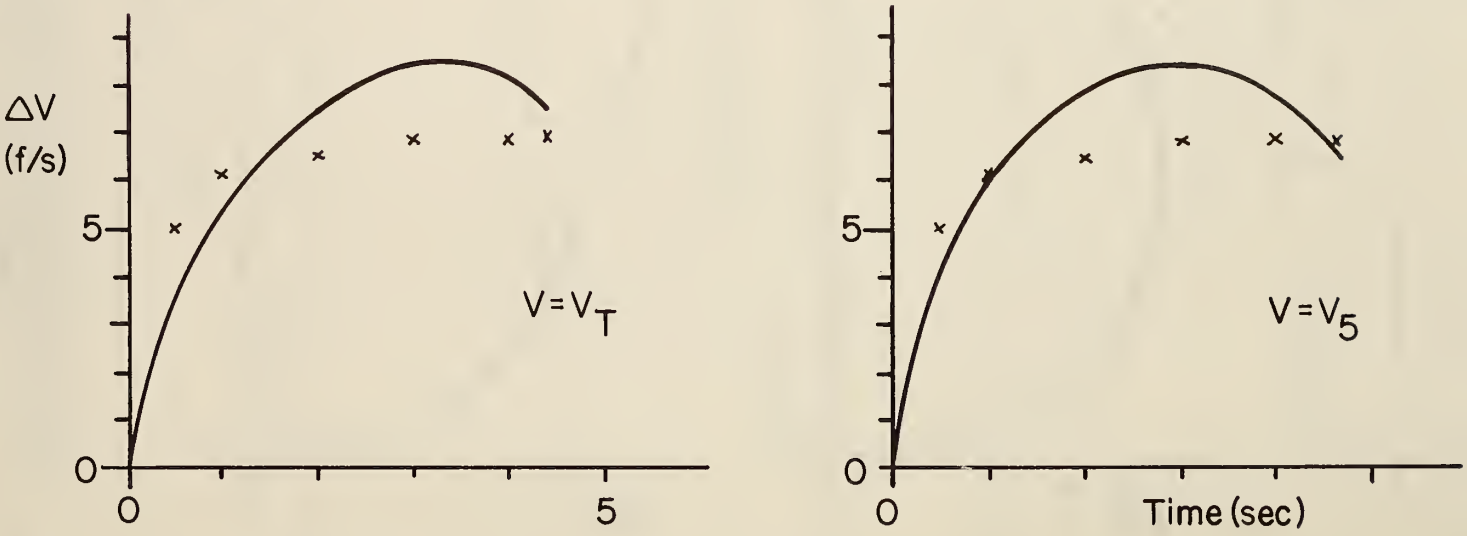

b) V_o = 60 ft/sec.

Fig. C-5 Comparison of vehicle response and model response for $V = V_T$ and $V = V_5$ (A_c = 14.5 ft/sec^2 and dry-pavement conditions). (Fig. C-5(c) is contained on the following page).

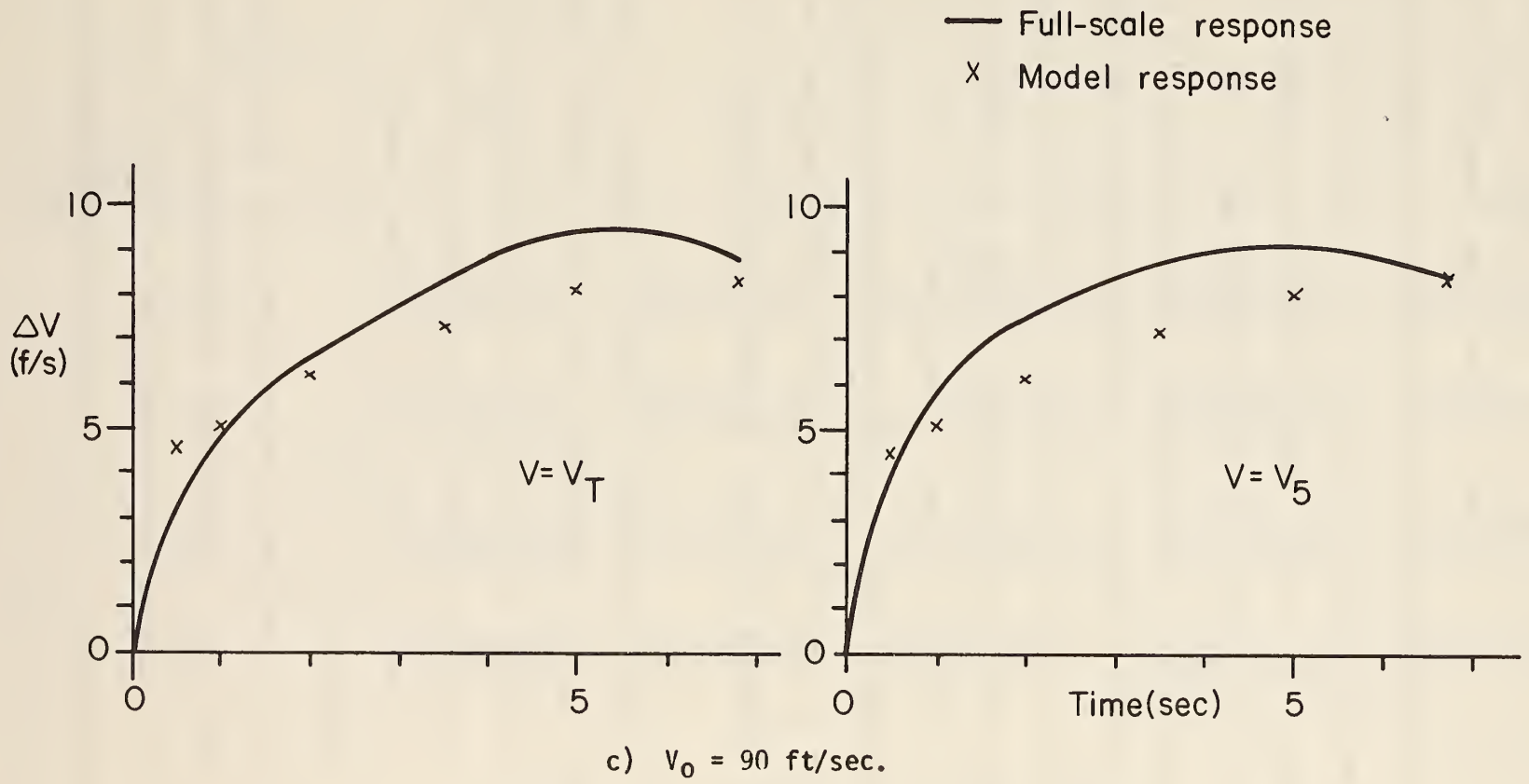

c) V_o = 90 ft/sec.

Fig. C-5 Comparison of vehicle response and model response for $V = V_T$ and $V = V_5$ (A_c = 14.5 ft/sec^2 and dry-pavement conditions).

those on the right were obtained for $V = V_5$. Compare those of the left with those presented in Fig. C-4, which were obtained under identical conditions. The shapes of the corresponding curves are the same for each common speed; however, the maximum amplitudes differ (e.g., ΔV_m = 7 ft/sec in Fig. C-4(b) vs. ΔV_m = 8.5 ft/sec in Fig. C-5(b). These differences are typical of the variability which was observed in all of the collected data.

Given this variability, a model cannot be specified that will precisely match all of the observed responses for a given condition, and an approximation must be employed. Thus, the model for each V_o - A_c condition was selected so as to be consistent with the median magnitude response (as obtained from 5 trials conducted on different days over a 3-month period) for that condition. It is these model responses which are superimposed on the full-scale (median magnitude) responses of Fig. C-4 and those of Fig. C-5. Note that the correlation between the model-and full-scale responses is much better in the former than the latter.

The composite model is presented in Table C-I where K_B, α, β, and δ are specified for various V_o - A_c combinations. The change in model parameters as a function of both V_o and A_c is shown in Fig. C-6 where the quantity $\frac{K_B\delta}{\alpha\beta}$ is plotted versus V_o with A_c as a parameter. If the model were linear, this quantity would be invariant with respect to both of these quantities; instead it varies over a range from 2.63 to 1.25.

The variability in performance can be accounted for by specifying a range of K_B for a given V_o - A_c combination. Correspondingly, one would have a range on $\frac{K_B\delta}{\alpha\beta}$ such as is shown by the dashed lines in Fig. C-6. These correspond to observed changes in K_B of some ±20%, which encompasses the range observed from the collected data.

A_c (ft/sec^2) \ V_o (ft/sec)	20	40	60	80	90
6.44	$\frac{18.045(p+1.75)}{p(p+3)(p+4)}$	$\frac{16.0\,(p+1.75)}{p(p+3)(p+4)}$	$\frac{15.57(p+1)}{p(p+2.5)(p+3.5)}$	$\frac{11.25(p+.5)}{p(p+1.5)(p+3)}$	$\frac{11.25(p+.5)}{p(p+1,5)(p+3)}$
9.66	$\frac{18.045(p+1.75)}{p(p+3)(p+4)}$	$\frac{13.82(p+1.75)}{p(p+3)(p+4)}$	$\frac{14.71(p+1)}{p(p+2.5)(p+3.5)}$	$\frac{12.15(p+.5)}{p(p+1.5)(p+3)}$	$\frac{12.15(p+.5)}{p(p+1.5)(p+3)}$
12.88	$\frac{18.045(p+1.75)}{p(p+3)(p+4)}$	$\frac{15.5(p+1.75)}{p(p+3)(p+4)}$	$\frac{16.1(p+1)}{p(p+2.5)(p+3.5)}$	$\frac{13.45(p+.5)}{p(p+1.5)(p+3)}$	$\frac{13.45(p+.5)}{p(p+1.5)(p+3)}$
14.50	$\frac{18.045(p+1.75)}{p(p+3)(p+4)}$	$\frac{15.5(p+1.75)}{p(p+3)(p+4)}$	$\frac{14.3(p+1.75)}{p(p+3)(p+4)}$	$\frac{15(p+.5)}{p(p+1.5)(p+3)}$	$\frac{15(p+.5)}{p(p+1.5)(p+3)}$

NOTE: $\tau \doteq 150$ m sec for all conditions.

TABLE C-I

MODEL PARAMETERS FOR $\frac{V_w}{V_i} = \frac{K_B(p+\delta)}{p(p+\alpha)(p+\beta)}$

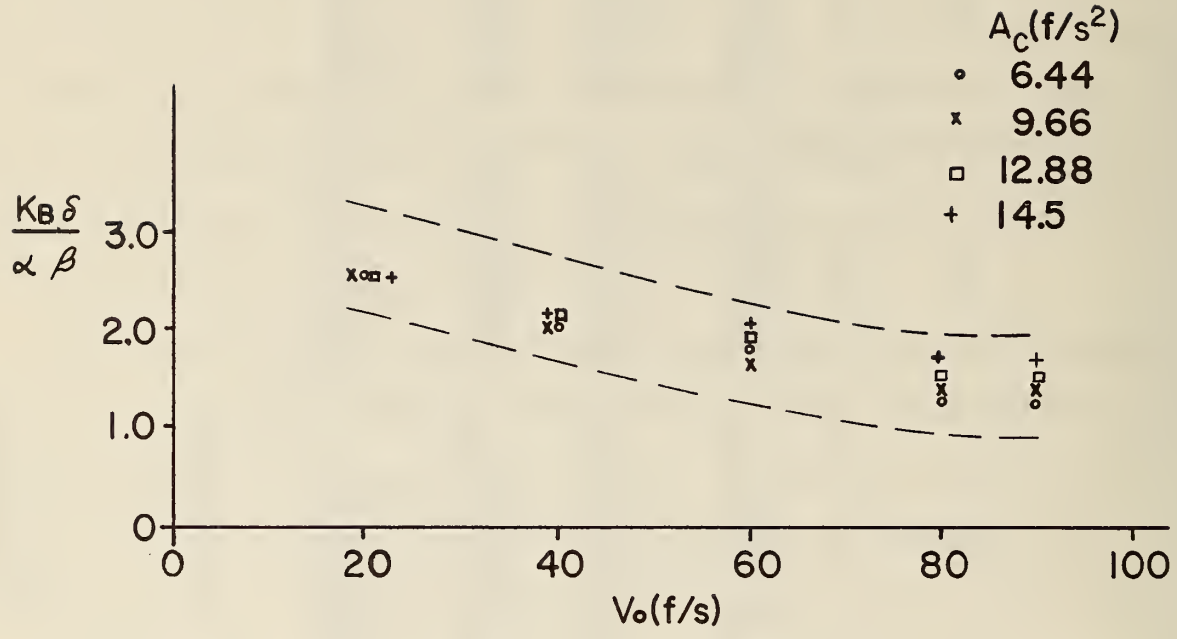

Fig. C-6 $\frac{K_B\delta}{\alpha\beta}$ vs. V_o with A_c as a parameter.

Next compare the responses on the left-hand side of Fig. C-5 with the corresponding responses on the right. In each case (e.g., V_o = 40 ft/sec), the responses are approximately the same differing only in the greater amount of noise present when $V = V_5$ (The primary source of this noise was the bouncing of the 5th wheel).* In view of the similarities here, as well in other collected data, it was concluded that $V_T \doteq V_5$ under dry-pavement conditions, and thus the same model could be employed for the two cases.

The magnitude of G_c cannot be too large or the model is not valid--especially under high-speed conditions. Thus, when G_c = 2 and tests were conducted at a moderate initial speed (e.g., V_o = 60 ft/sec) and A_c = 14.5 ft/sec^2,

---

* This noise was not included in the redrawn full-scale responses of Fig. C-5.

the model and full-scale responses are generally consistent as is shown in Fig. C-7. However, when tests were conducted at higher speeds (V_o = 80 ft/sec) and A_c = 14.5 ft/sec^2, good correlation was not obtained as wheel lock occurred as shown in Fig. C-8. The closed-loop system then responded in an anti-skid mode and thus prevented the loss of vehicle lateral control. The resulting response was highly oscillatory and a very jerky ride resulted. It appears clear that high gains, and corresponding small errors in the controlled variable, should only be employed in conjunction with a more effective anti-skid system than was employed here.*

E. Experimental Results--Wet Pavement

Typical full-scale and model responses (ΔV vs. t) for wet-pavement conditions, A_c = 6.44 ft/sec^2, V_o = 20, 60 and 90 ft/sec, and $V = V_T$ are shown in Fig. C-9. The model responses are those obtained from the parameters specified in Table C-I. As good correlation exists between these responses, it was concluded that the model specified for A_c = 6.44 ft/sec^2 was also adequate for the wet-pavement case. This is also true for A_c = 9.66 ft/sec^2; however not for $A_c \geq$ 12.88 ft/sec^2 and $V = V_T$. This may be seen in Fig. C-10 where ΔV vs. t is plotted for two cases--V_o = 20 ft/sec and V_o = 40 ft/sec. In the former, good agreement exists between the model and the full-scale result whereas in the latter, the correlation is poor. Wheel lock occurred, and the braking system responded in an antiskid mode. The resulting response was, as shown, highly oscillatory, and quite different from the predicted response. However, if a more efficient anti-skid mode (one that would have resulted in minimal amplitude oscillations and a more comfortable stop) had been employed, the model response would have been a fair approximation of the full-scale response.

---

* If such a system were employed, then the model response would be a good approximation to the full-scale response as is subsequently discussed.

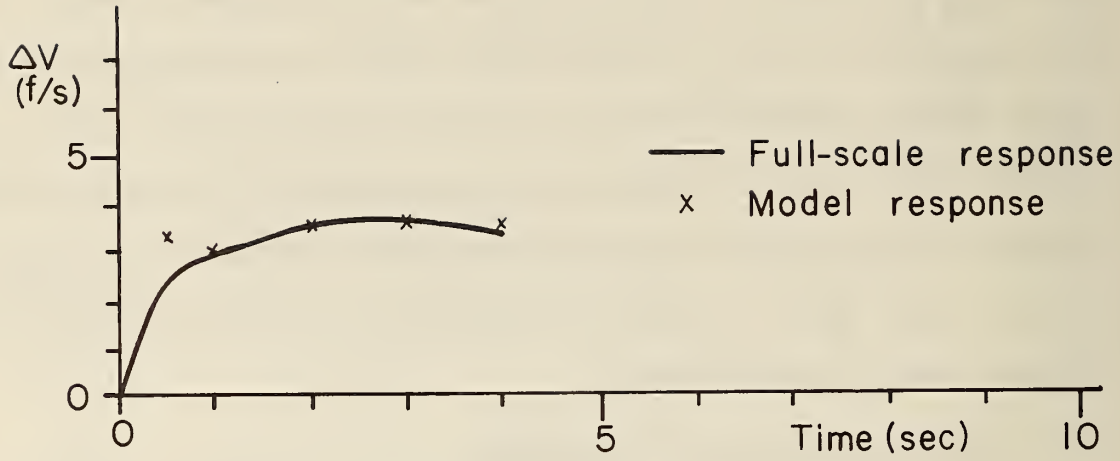

Fig. C-7 Comparison of vehicle and model responses for a high-gain control configuration (V_0 = 60 ft/sec, A_c = 14.5 ft/sec^2, G_c = 2.0 and dry pavement).

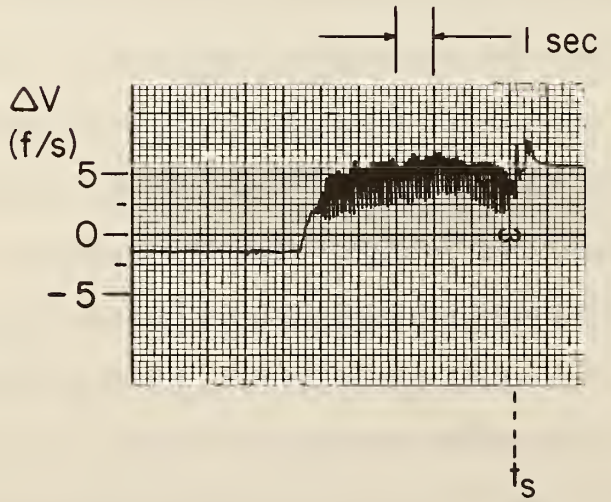

Fig. C-8 Vehicle response under anti-skid conditions (V_0 = 80 ft/sec, A_c = 14.5 ft/sec^2, G_c = 2 and dry pavement).

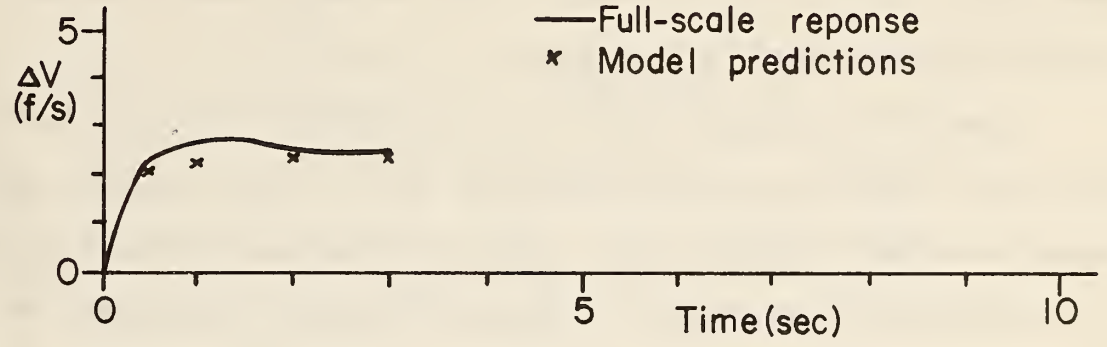

a) V_0 = 20 f/s.

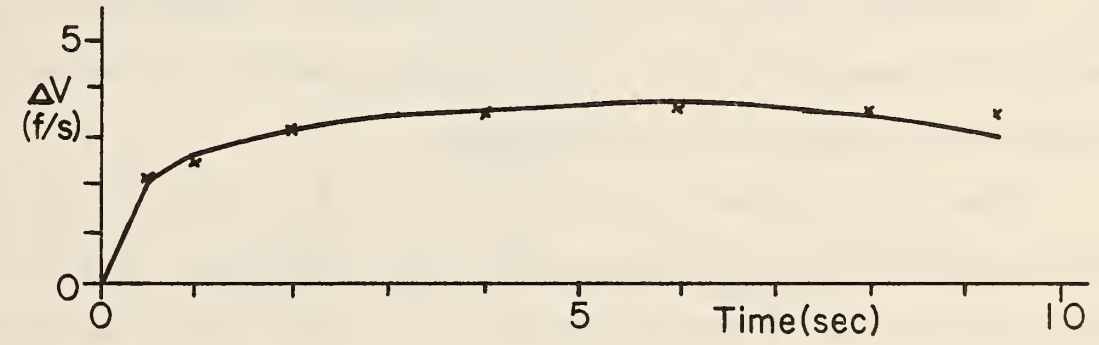

b) V_0 = 60 f/s.

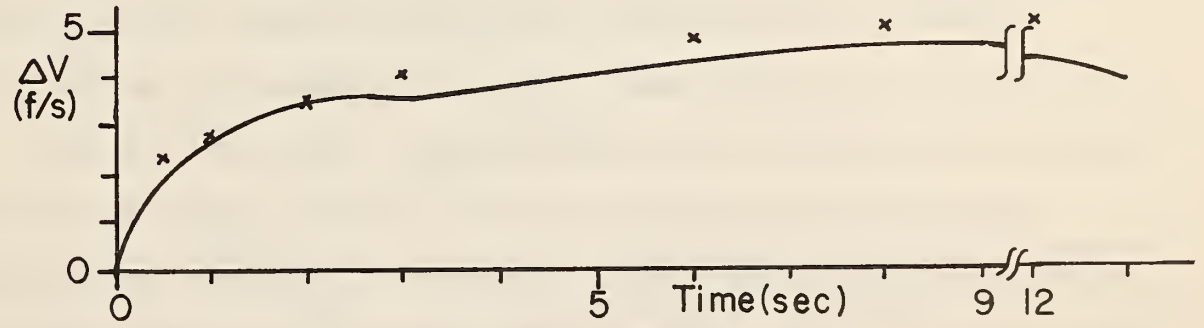

c) V_0 = 90 f/s.

Fig. C-9 Comparison of vehicle response and model response for 3 selected initial speeds and A_c = 6.44 f/s^2 (Wet-pavement conditions and $V = V_T$).

Thus, if the large oscillations of Fig. C-10(b) were greatly reduced, the response shown in Fig. C-11 would result. This response compared favorably with the model response which is also shown.

Essentially the same results were obtained when $V = V_5$ the main difference being a smaller magnitude response for $V_0 \geq 40$ ft/sec (such as could be caused by a slight increase in K_B). This is illustrated in Fig. C-12 where full-scale and model responses (as obtained from Table I) are shown for V_0 = 20, 40 and 80 ft/sec and A_c = 9.66 ft/sec^2. Note that the responses presented here have the same form as those in Fig. C-3; however, the peak amplitudes ΔV_m are markedly lower than the model predictions. In addition, the drive shaft "locked"momentarily during the first two seconds of the test at 80 ft/sec causing the initial oscillatory behavior.

Wheel slip occurred for $V_0 \geq 40$ ft/sec and $A_c \geq 12.88$ ft/sec^2, and the resulting anti-skid mode of response was highly oscillatory. Again, if a more efficient anti-skid mode had been employed, the model response would have been a reasonable approximation to the full-scale response.

F. Conclusions

A model has been specified for the braking/roadway interface dynamics of a typical U.S. passenger sedan. The model parameters are functions of both velocity and acceleration rate, and the model is thus a nonlinear one.

The responses obtained from this model, for the speed range 20-90 ft/sec and the acceleration range 6.44-14.5 ft/sec^2, are reasonable approximations to corresponding full-scale responses under both wet- and dry-road conditions. However, as considerable variability was observed in the full-scale responses, and thus in the correlation between these and the model responses, the model should be employed with care. This variability can be accounted for via a change in gain, and thus when designing a closed-loop braking controller, one

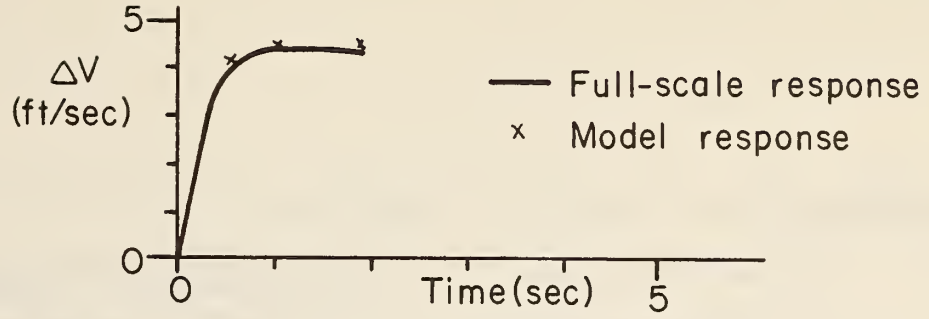

a) V_0 = 20 ft/sec.

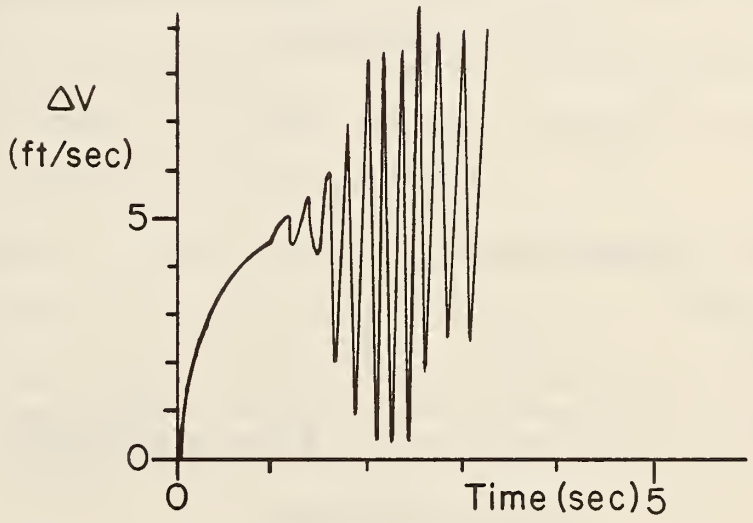

b) V_0 = 40 ft/sec.

Fig. C-10 Vehicle response for two selected initial speeds, A_C = 12.88 ft/sec^2, V = V_5 and wet-pavement conditions.

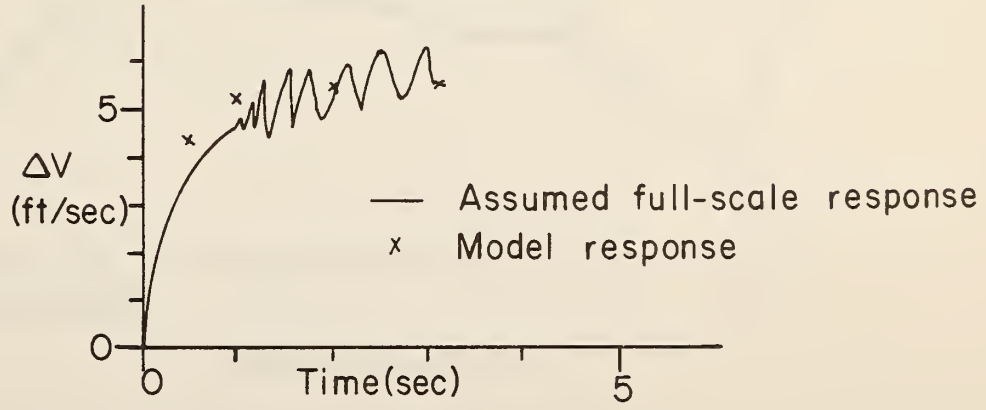

Fig. C-11 Assumed full-scale response with an efficient anti-skid mode (V_0 = 40 ft/sec, A_C = 12.88 ft/sec^2 amd wet-pavement conditions.

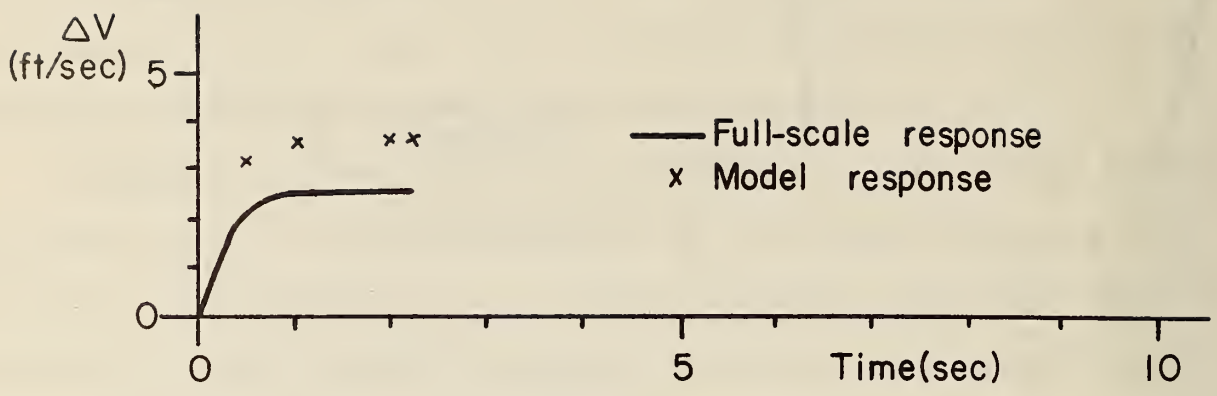

a) V_0 = 20 ft/sec.

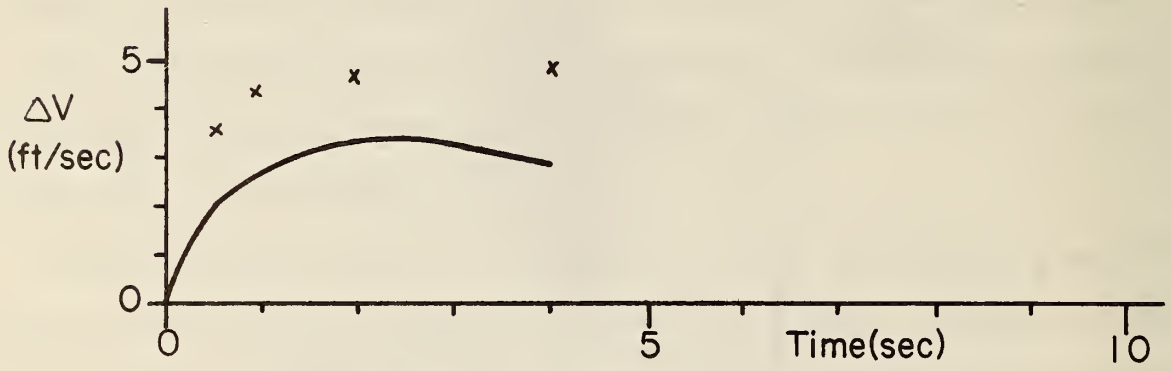

b) V_0 = 40 ft/sec.

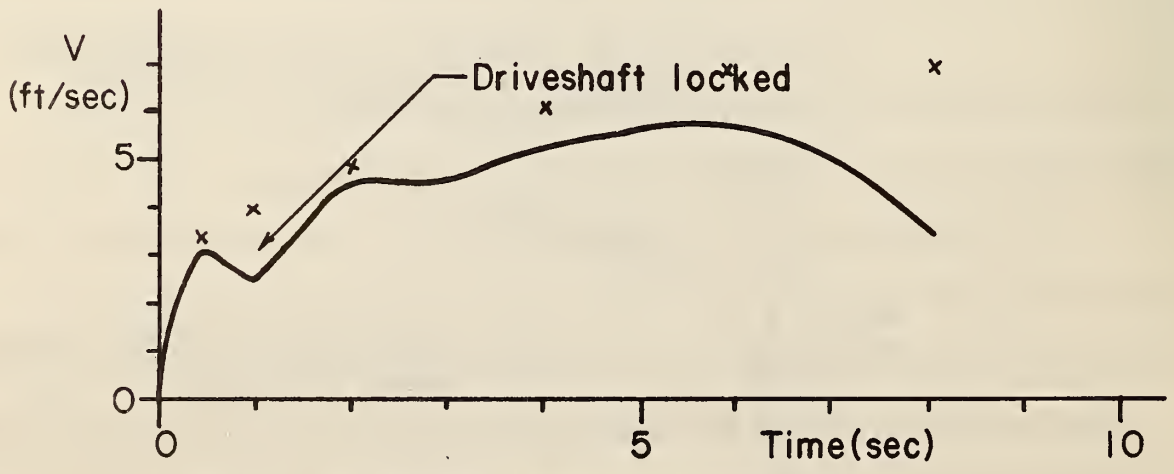

c) V_0 = 80 ft/sec.

Fig. C-12 Comparison between full-scale and model responses for V = V_5, A_c = 9.66 ft/sec^2, and wet-pavement.

one should insure that its performance is relatively insensitive to this change. The observed changes under full-scale conditions were some ±20% of the nominal value specified in Table C-I; thus, for a conservative choice one might design to accomodate changes of up to ±50%.

An efficient anti-skid mode should be incorporated into the design so that adequate braking performance at rates up to 12.88 ft/sec^2 could be achieved on both wet and dry pavement. The specified model could be employed in this part of the design, as it should provide a reasonable approximation to the response in a well-controlled anti-skid mode.

Finally, it should be emphasized that the model presented here was selected because of its simplicity and potential for use in the braking controller design process. Another model, with more accurate predictive properties, may readily be found; however, it seems certain that the latter will be characterized by a fairly complex, nonlinear differential equation.

APPENDIX D

DIGITAL COMMAND GENERATION

A. Introduction

In an operational system, the command state (A_c, V_c and X_c) for a controlled vehicle would only be available at discrete times $t = nT_s$, where T_s is the sampling instant. In one attractive approach, which was described in Chapter II, $V_c(nT_s)$ and $X_c(nT_s)$ would be derived from $A_c(nT_s)$ by appropriate processing onboard a controlled vehicle.

The actual states (A, V, and X) could be continuously available, as was described in Chapter IV and, in terms of the position control of a vehicle, one would have the situation depicted in Fig. D-1. Here, to obtain a good approximation (ΔX^*) to $\Delta X(t) = X_c(t) - X(t)$, the switch S_1 would be synchronized with the processing of $X_c(nT_s)$ so that

$$\Delta X^* = [X_c(t) - X(t)]_{t=nT_s}.$$

This quantity, after processing by a hold circuit, would be the primary input to the vehicle controller. In general, controller performance would be improved by also employing input(s) related to $A_c(nT_s)$ and $V_c(nT_s)$ as shown.

One realization of this configuration, which was intended for use with a crossed-wire information source, is discussed in this appendix.

B. A Command Generator

The command states $A_c(nT_s)$, $V_c(nT_s)$ and $X(nT_s)$ could be computed by a general-purpose computer at either the sector or the vehicle level. However, the numerical computation of V_c and X_c from a given acceleration-command profile is a time-consuming operation which could tie up most of a general-purpose

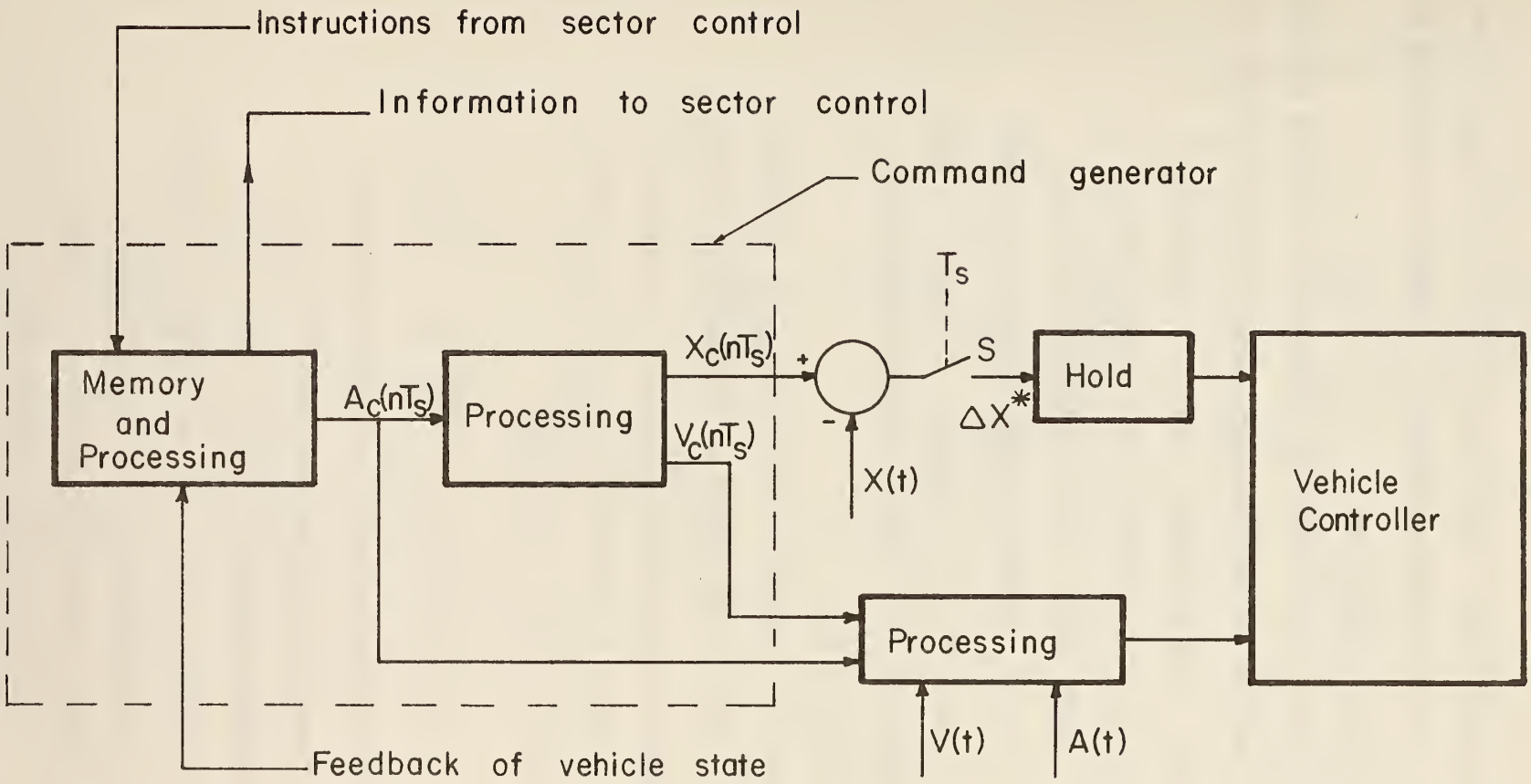

Fig. D-1 Computer and control operations onboard a controlled vehicle.

computer's processing capability. In many applications involving routine repetitive operations, special-purpose hardware, or possibly a dedicated microcomputer, would be a viable alternative.

In the current study, special-purpose hardware was the most practical choice; thus, it was employed in the design and construction of a vehicle-borne command generator. This generator functions as follows:

> Command acceleration profiles are stored in memory as a block of binary words. The weighting of the least significant bit is q_{A_c} ft/sec^2, and the words are accessed from memory at intervals of T_s seconds. The resulting quantized acceleration profile is the basis for velocity and displacement computations.
>
> The integral of the typical quantized $A_c(t)$ function shown in Fig. D-2(a) is the series of dashed straight-line segments, identified as $V_c(t)$ in Fig. D-2(b). Here $A_c(t)$ over the ith interval is denoted by A_{ci} and $V_c(t)$ at the end of this interval by V_{ci}. Note that
>
> $$V_{cn} = T_s \sum_{i=1}^{n} A_{ci} \qquad \text{(ft/sec)} \qquad \text{(D-1)}$$
>
> The second integral of $A_c(t)$ is the continuous position function shown as a dashed line in Fig. D-2(c). A discrete displacement command ($X_c(nT_s) = X_{cn}$), which is equal to this function at the sampling instants, is readily obtained via a 3-part process: First, the area under the V_{cn} function (shown by the solid line in Fig. D-2(b)) is obtained as

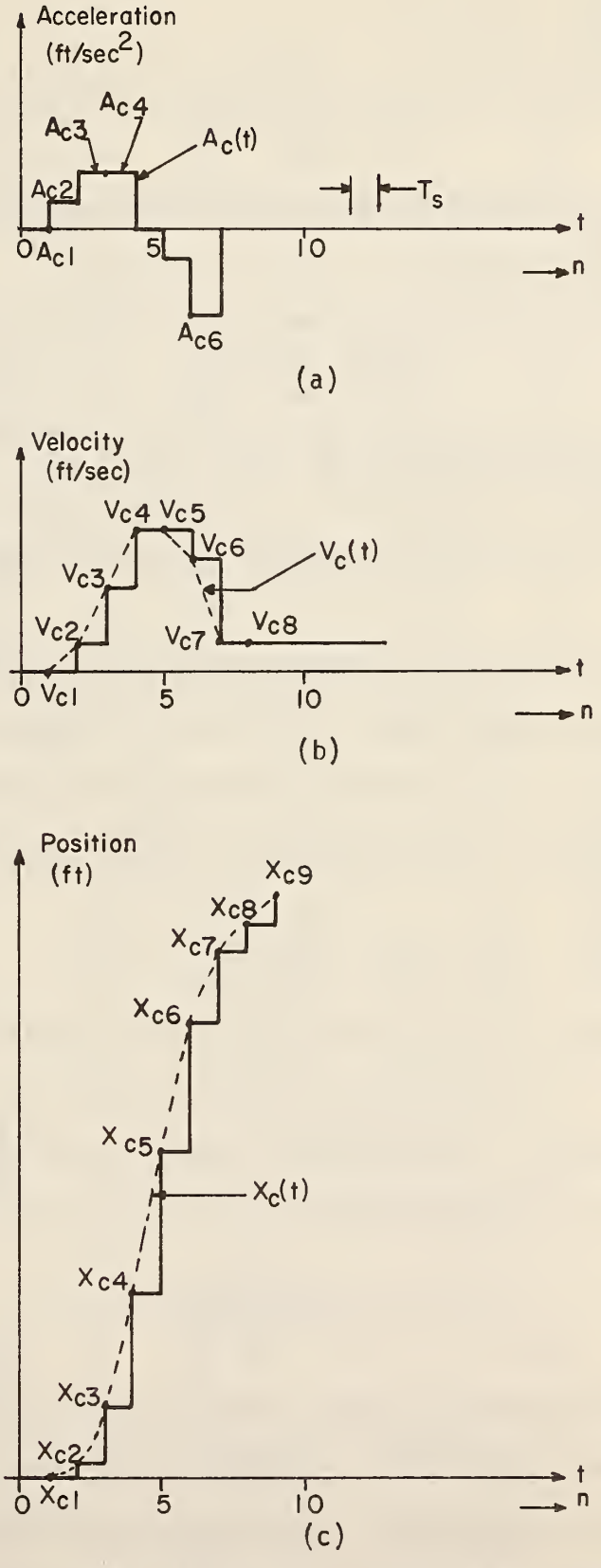

Fig. D-2 A command acceleration profile and corresponding velocity and position profiles.

$$T_s \sum_{i=0}^{n-1} V_{ci};$$

Second, the "triangular" areas between the $V_c(t)$ and V_n curves is computed as

$$\frac{1}{2} T_s^2 \sum_{i=1}^{n} A_{ci};$$

and third, X_{cn} is obtained via

$$X_{cn} = T_s \sum_{i=0}^{n-1} V_{ci} + \frac{1}{2} T_s^2 \sum_{i=0}^{n} A_{ci} \quad \text{(ft)} \quad \text{(D-2)}$$

One hardware realization of these operations is depicted in Fig. D-3. The accelerations are binary coded, using the 2's complement representation for negative values. The weighting of the least significant acceleration bit is q_{A_c}, and the number of bits required to represent acceleration is

$$N_a = \log_2 \frac{||A||}{q_{A_c}},$$

where $||A||$ is the sum of the maximum magnitudes of positive and negative acceleration.

The quantity V_{cn} is obtained from the A_{ci} via an arithmatic accumulator, where the number of required bits is

$$N_v = \log_2 \frac{(V_c)_{max}}{q_{A_c} T_s}.$$

Here, $(V_c)_{max}$ is the maximum required command velocity in ft/sec.

The implementation of the X_{cn} computation consists of an accumulator summing two inputs simultaneously. The derived velocity word is one input and, since the weighting factor (q_{V_c}) of the x <0> bit is $q_{A_c} T_s$ ft/sec,

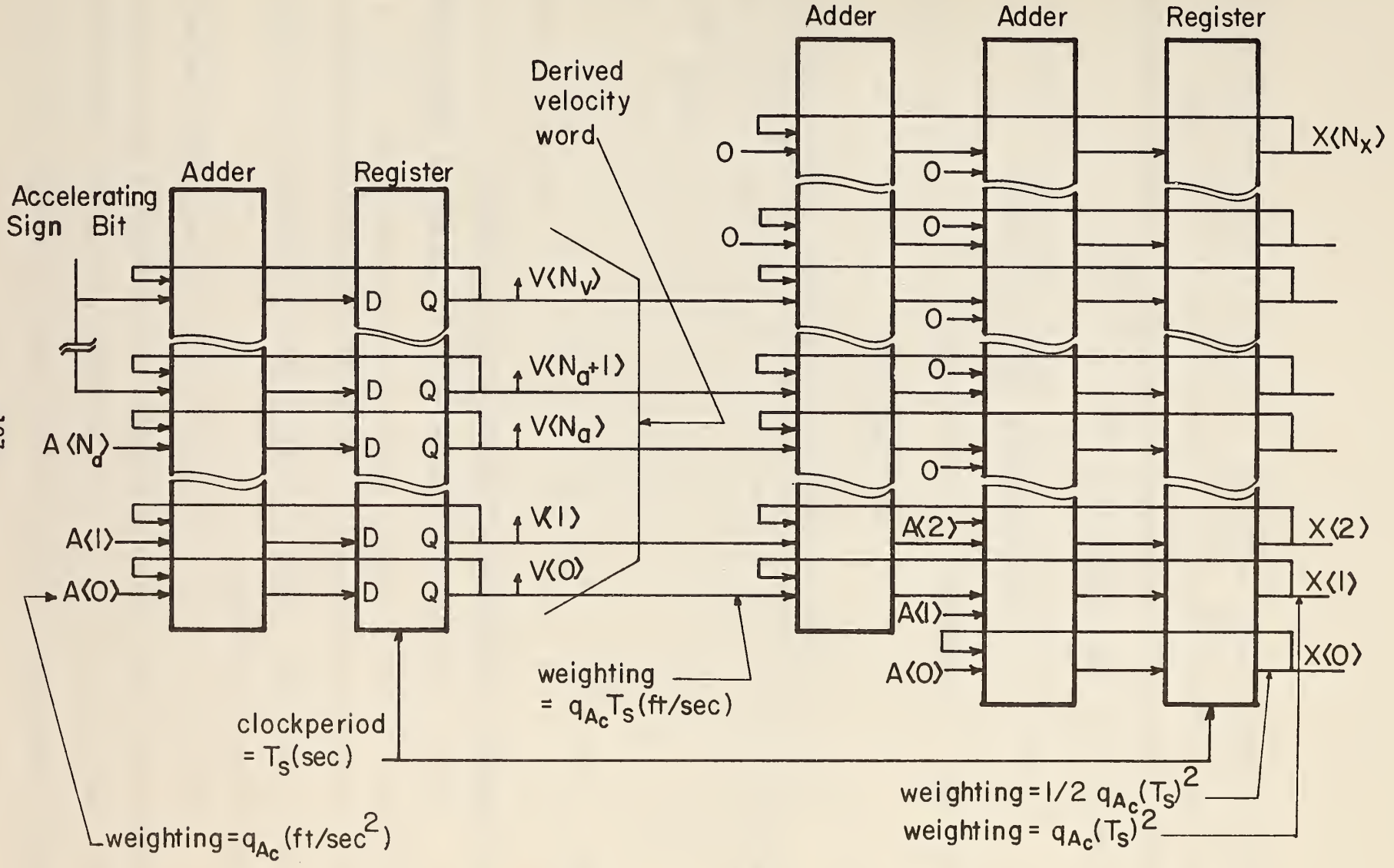

Fig. D-3 One implementation of the $V_c(nT_s)$ and $X_c(nT_s)$ computations.

the first term of (D-2) is realized. The second input is derived from the acceleration word, shifted one bit-position toward the least significant end, thereby halving the effective acceleration input. The number of bits required to implement the X_{cn} accumulator is

$$N_X = \log_2 \frac{X_{max}}{q_{X_c}},$$

where X_{max} is the maximum command distance and

$$q_{X_c} = \frac{1}{2} q_{A_c} T_s^2.$$

It is of interest to specify the required word sizes for a choice of parameters which might be expected in practice. For $A_{max} = 25$ ft/sec^2, $V_{max} = 160$ ft/sec, $X_{max} = 4096$ ft, $q_{A_c} = 0.39$ ft/sec^2 and $T_s = 0.1$ sec, then

$$N_a = 7 \text{ bits},$$

$$N_v = 12 \text{ bits},$$

and

$$N_x = 21 \text{ bits}.$$

C. Integration of Command and Information Source Signals

When a crossed-wire information source is employed to obtain vehicle position, a discrete position signal X_w is available each time a wire is crossed. The use of a position interpolator yields $\hat{\hat{X}}$, an estimate of the distance traveled between wires. Then $X_w + \hat{\hat{X}}$, when properly interpreted, is a continuously available position signal.

Since $X_c(t) = X_{cn}$ at the command updating instant, ΔX^* is derived by sampling and holding ΔX at this instant as is symbolically shown in Fig. D-4. Here, both $X_c(nT_s)$ and X_w are in digital form (and both are capable of representing displacements ranging from zero to some large number such as 4096 ft).

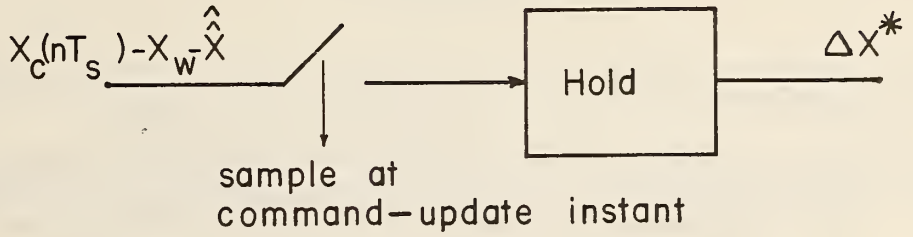

Fig. D-4 Implementation of ΔX^* for a crossed-wire information source with position interpolation.

The only feasible means of obtaining

$$X_c(nT_s) - X_w$$

is by using a binary subtractor. The result in a binary number, which even under extreme conditions, represents less than ±16 ft of position error (It is assumed that position errors larger than approximately 10 ft would represent an abnormal condition and would require a sector shutdown). A binary number in this range can easily and economically be converted to a bipolar, analog voltage; $\hat{\hat{X}}$ is then subtracted and the result is sampled and held. This approach was employed in a preliminary field evaluation of the crossed-wire information source/vehicle controller combination, which was conducted in the summer of 1976.

REFERENCES

1. Elias, S.E.G., "The West Virginia University--Morgantown Personal Rapid Transit System," in Personal Rapid Transit II, J.E. Anderson, Ed., University of Minnesota, Minneapolis, Minn., Dec. 1973.

2. Anon, Proceedings of the First International Conference on Dual-Mode Transportation, Washington, D.C., May 29-31, 1974.

3. Gardels, K., "Automatic Car Controls for Electronic Highways," General Motors Research Laboratories, General Motors Corporation, Warren, Michigan, GMR-276, June 1960.

4. TRW Systems Group, "Study of Synchronous Longitudinal Guidance as Applied to Intercity Automated Highway Networks," Final Report prepared for the Office of High Speed Transportation, Department of Transportation, September 1969.

5. Stefanik, R.G., and Kiselewich, S.J., "Evaluation of the Operating Conditions of a Detriot Dual-Mode Vehicle Network," presented at the 1972 SAE Automotive Engr. Congress, Jan. 1972, SAE Paper 720272.

6. Wilson, D.G., Ed., "Automated Guideway Transportation Between and Within Cities," Urban Systems Laboratory Rpt. No. FRA-RT-72-14, Mass. Institute of Technology, Cambridge, Mass., Feb. 1971(PB 206-269).

7. Giles, G.C., and Martin, J.A., "Cable Installation for Vehicle Guidance Investigations in the New Research Track at Crowthorne," JAM Road Research Lab., Crowthorne, England, Rpt. RN/40 57/CGG.

8. Oshima, Y., Kikuchi, E., Kimura, M., and Matsumoto, S., "Control System for Automobile Driving," Proceedings Tokyo IFAC Symposium, 1965, pp. 347-357.

9. Fenton, R.E., et al, "One Approach to Highway Automation," Proceedings of the IEEE, Vol. 46, No. 4, April 1968, pp. 556-566.

10. Fenton, R.E., et al., "Advances Toward the Automatic Highway," Highway Research Record, No. 344, Washington, D.C., Jan. 1971, pp. 1-20.

11. Fenton, R.E., and Olson, K.W., "An Investigation of Highway Automation," Rpt. EES 276-6, Dept. of Elec. Engr., The Ohio State University, Columbus, Ohio, March 1969.

12. Anon., "An Investigation of Highway Automation," Rpt. EES 276A-12 Dept. of Elec. Engr., The Ohio State University, Cols., Ohio, April 1971.

References (Cont.)

13. Fenton, R.E., Ed., "An Investigation of Highway Automation," Rept. No. 276A-15, Dept. of Elec. Engr., The Ohio State University, Columbus, Ohio, September 1974.

14. "Practicality of Automated Highway Systems," Research Project with Calspan Corp., Contract DOT-FH-11-8903, March 1976.

15. Olson, K.W., et al., "Studies in Vehicle Automatic Lateral Control--Theory and Experiment," Appendix I to "An Investigation of Highway Automation," Rpt. 276A-16, Dept of Elec. Engr., The Ohio State University, Columbus, Ohio, September 1974.

16. Fenton, R.E., Ed., "Fundamental Studies in the Automatic Longitudinal Control of Vehicles," Final Report on DOT-OS-40100, Transportation Control Laboratory, The Ohio State University, Cols., Ohio 43210, July 1975 (Available from NTIS).

17. Fenton, R.E. et al., "Studies in Synchronous Longitudinal Control," Transportation Control Laboratory Rpt. EES 276A-17, Dept. of Elec. Engr., The Ohio State University, Cols., Ohio 43210, September 1974.

18. Ries, Edward and Cuccia, Louis C. "Status Report: Communications in Mass Transit Guided-Roadway Systems," Microwave Systems News (MSN), Vol. 4, No. 6, Dec./Jan. 1975, pp. 34-42.

19. Friedmann, W. and Peltzer N., "Linear Transmission of Information Between Track and Train by Means of High Frequency," Brown-Boveri Review, Sept./Oct. 1965, pp. 752-760.

20. Hahn, H.J., "Automatic Operation of Urban Rapid Transit and Underground Railways," Brown-Boveri Review, Dec. 1971, pp. 553-565.

21. Takahashi, K., et al., "New Induction Radio System," Sumitomo Electric Technical Review, No. 13, Jan. 1970, pp. 29-33.

22. Schwartz, M., Information Transmission, Modulation, and Noise (2nd Ed.), McGraw-Hill, Inc., New York, 1970.

23. Peterson, W.W. and Weldon, E.J., Jr., Error-Correcting Codes, MIT Press, Cambridge, Massachusetts, 1972.

24. Stiffler, J.J., Theory of Synchronous Communications, Prentice-Hall, Inc., Englewood Cliffs, New Jersey, 1971.

25. Gelb, A.G., et al., Applied Optimal Estimation, MIT Press, Cambridge, Massachusetts, 1974.

References (Cont.)

26. Tsypkin, I.Z., Adaption and Learning in Automatic Systems, Academic Press, New York, 1971.

27. D'Azzo, J.J., and Houpis, C.H., Feedback Control Systems Analysis and Synthesis, Second Edition, McGraw-Hill, New York, 1966.

28. Mayhan, R.J., et al., "The Use of Enhancement Plates for Improved Doppler Radar Performance for Ground Transport Systems," Proceedings of the IEEE, Vol. 64, No. 11, November 1976, pp. 1644-1645.

29. Bender, J.G., and Fenton, R.E., "On Vehicle Longitudinal Dynamics," in Traffic Flow and Transportation," G.F. Newell, Ed., American Elsevier Publ. Co., Inc., New York, 1972, pp. 33-46.

☆U.S. GOVERNMENT PRINTING OFFICE: 1977 727-511/1068 1-3